# Geoarchaeology:
## exploration, environments, resources

edited by A. M. Pollard

Geological Society
Special Publication
No. 165

Published by The Geological Society

# Geoarchaeology:
## exploration, environments, resources

edited by A. M. Pollard

Geological Society
Special Publication
No. 165

Published by The Geological Society

Geoarchaeology: exploration, environments, resources

Geological Society Special Publications
*Series Editors*
A. J. HARTLEY
R. E. HOLDSWORTH
A. C. MORTON
M. S. STOKER

It is recommended that reference to all or part of this book should be made in one of the following ways:

POLLARD, A. M. (ed.) 1999. *Geoarchaeology: exploration, environments, resources.* Geological Society, London, Special Publications, **165**.

VERNON, R. W., MCDONNELL, J. G. & SCHMIDT, A. 1999. Medieval iron and lead smelting works: a geophysical comparison. *In:* POLLARD, A. M. (ed.) *Geoarchaeology: exploration, environments, resources.* Geological Society, London, Special Publications, **165,** 15–34.

GEOLOGICAL SOCIETY SPECIAL PUBLICATION NO. 165

# Geoarchaeology: exploration, environments, resources

EDITED BY

A. MARK POLLARD
Department of Archaeological Sciences
University of Bradford, UK

1999
Published by
The Geological Society
London

# THE GEOLOGICAL SOCIETY

The Geological Society of London was founded in 1807 and is the oldest geological society in the world. It received its Royal Charter in 1825 for the purpose of 'investigating the mineral structure of the Earth' and is now Britain's national society for geology.

Both a learned society and a professional body, the Geological Society is recognized by the Department of Trade and Industry (DTI) as the chartering authority for geoscience, able to award Chartered Geologist status upon appropriately qualified Fellows. The Society has a membership of 8600, of whom about 1500 live outside the UK.

Fellowship of the Society is open to persons holding a recognized honours degree in geology or a cognate subject and who have at least two years' relevant postgraduate experience, or not less than six years' relevant experience in geology or a cognate subject. A Fellow with a minimum of five years' relevant postgraduate experience in the practice of geology may apply for chartered status. Successful applicants are entitled to use the designatory postnominal CGeol (Chartered Geologist). Fellows of the Society may use the letters FGS. Other grades of membership are available to members not yet qualifying for Fellowship.

The Society has its own Publishing House based in Bath, UK. It produces the Society's international journals, books and maps, and is the European distributor for publications of the American Association of Petroleum Geologists (AAPG), the Society for Sedimentary Geology (SEPM) and the Geological Society of America (GSA). Members of the Society can buy books at considerable discounts. The Publishing House has an online bookshop (*http://bookshop.geolsoc.org.uk* ).

Further information on Society membership may be obtained from the Membership Services Manager, The Geological Society, Burlington House, Piccadilly, London W1V 0JU (Email: *enquiries@geolsoc.org.uk*; tel: +44 (0)171 434 9944).

The Society's Web Site can be found at *http://www.geolsoc.org.uk/*.The Society is a Registered Charity, number 210161.

Published by The Geological Society from:
The Geological Society Publishing House
Unit 7, Brassmill Enterprise Centre
Brassmill Lane
Bath BA1 3JN, UK
(*Orders*: Tel. +44 (0)1225 445046
Fax +44 (0)1225 442836)
Online bookshop: *http://bookshop.geolsoc.org.uk*

First published 1999



**British Library Cataloguing in Publication Data**
A catalogue record for this book is available from the British Library.

ISBN 1-86239-053-3
ISSN 0305-8719

Typeset by Wyvern 21 Ltd, Bristol, UK

Printed by Anthony Rowe, Chippenham, UK

**Distributors**

*USA*
AAPG Bookstore
PO Box 979
Tulsa
OK 74101-0979
USA
*Orders*: Tel. +1 918 584-2555
Fax +1 918 560-2652
Email *bookstore@aapg.org*

*Australia*
Australian Mineral Foundation Bookshop
63 Conyngham Street
Glenside
South Australia 5065
Australia
*Orders*: Tel. +61 88 379-0444
Fax +61 88 379-4634
Email *bookshop@amf.com.au*

*India*
Affiliated East-West Press PVT Ltd
G-1/16 Ansari Road, Daryaganj,
New Delhi 110 002
India
*Orders*: Tel. +91 11 327-9113
Fax +91 11 326-0538

*Japan*
Kanda Book Trading Co.
Cityhouse Tama 204
Tsurumaki 1-3-10
Tama-shi
Tokyo 206-0034
Japan
*Orders*: Tel. +81 (0)423 57-7650
Fax +81 (0)423 57-7651

# Contents

# Geoarchaeology: an introduction

A. MARK POLLARD
*Department of Archaeological Sciences, University of Bradford, Bradford BD7 1DP, UK*

Of all of the sciences utilized in modern archaeological research, that of geology has the longest history of association with archaeology. Surprisingly, perhaps, geoarchaeology as a recognized sub-discipline has taken slightly longer to establish itself than others such as bioarchaeology. There is still some uncertainty about what exactly geoarchaeology encompasses, and some differences of usage of the term between Europe and North America. This brief introduction explores some of these issues, and attempts to place the other contributions to this volume in a slightly broader context.

Geoarchaeology here is used to describe the application of the geosciences to solve research problems in archaeology. The interaction between the sciences of geology and archaeology has a long and honourable history, going back to the early 19th century, when geology and prehistoric archaeology developed substantially in parallel. Conventionally, it is usual to consider primarily a subset of the geosciences as included within the term 'geoarchaeology', particularly geomorphology, sedimentology, pedology and stratigraphy. This priority perhaps reflects an observation made by Renfrew in 1976, in his introduction to one of the earliest volumes to use the term geoarchaeology (Davidson & Shackley 1976), that 'since archaeology, or at least prehistoric archaeology, recovers almost all its basic data by excavation, every archaeological problem starts as a problem in geoarchaeology' (Renfrew 1976). It also reflects the intensity of interest during the 1980s in the subject of site formation processes, to which these techniques have made a considerable contribution (e.g. Schiffer 1987). Chronology, although central to both archaeology and geology, is usually considered to be a separate sub-discipline.

Opinions differ as to whether chemical analysis (of raw materials and artefacts) and geophysics should be included within the term geoarchaeology. The former, particularly in the United States, is often termed 'archaeometry', and forms a significant subset of the emerging sub-discipline known as 'archaeological chemistry' (e.g. Pollard & Heron 1996). The latter is often incorporated in the wider field of study known as remote sensing or archaeological prospection. We have taken a broad view of the word geoarchaeology here, and, as signified by the sub-title, have included a wider spectrum of geoscience techniques applied to problems in archaeology. The papers presented here are a sub-set of those presented at the Geoarchaeology session of the Geosciences '98 Conference, held at Keele University on 14–16 April 1998.

## Archaeology, geology, geoarchaeology and archaeological geology

The beginnings of scientific archaeology in the 19th century are intimately tied to the parallel development of geology. This approach is personified by Sir Charles Lyell

*From:* POLLARD, A. M. (ed.) 1999. *Geoarchaeology: exploration, environments, resources.* Geological Society, London, Special Publications, **165**, 7–14. 1-86239-053-3/99/$15.00

(1797–1875), who not only wrote *Principles of Geology* (published 1830–1833, and widely regarded as one of the foundations of modern geology), but also *The Geological Evidences of the Antiquity of Man* (1863). The intellectual ferment during the 19th century regarding the age of the earth, the mechanism of evolution and the antiquity of humankind is well documented (e.g. Trigger 1989). Increasing attention was paid during the first half of the 19th century to the commingling of the bones of extinct animals with handaxes as evidence of human activity in either cave deposits or the gravel terraces of major European rivers. As a result of careful stratigraphic observation of such deposits, the widely accepted biblical interpretation — that these deposits reflected the remnants of Noah's flood, and that the Earth had been created in 4004 BC — gradually gave way to an evolutionary model, requiring considerably longer time periods. Lyell's work established the principle of uniformitarianism in geology, thereby establishing a long chronological framework for the evolution of the Earth, and in 1859 Charles Darwin populated this framework with his evolutionary model for the origin of the human species with the publication of *On the Origin of Species*. The need to provide a chronological framework for such evolutionary development against the background of the advance and retreat of the great Ice Ages lead directly to the development of palaeolithic archaeology as a scientific discipline, intimately associated with geology and palaeontology.

Towards the latter half of the 19th century popular imagination was caught by the spectacular finds emerging from the great excavations in Egypt and Mesopotamia (such as Layard's publication of Nineveh and Babylon in 1853). Not only did this shift attention away from the palaeolithic, but it also rekindled the debate about the veracity of the biblical account of the Flood. In the longer term it gave rise to what might be called the European version of the debate for the 'soul' of archaeology. Crudely this might be characterized as the scientific approach building upon the geological and palaeontological derivation of part of the subject versus a more classical, humanities-based view of archaeology arising from its origins in antiquarianism and the growth of classical archaeology at the end of the 19th century. Such debate continues today.

The development of archaeology and its relationship with geology took a different trajectory in the United States, as has been documented by Waters (1992) and Rapp & Hill (1998). The survival into the 20th century of native North American cultures in many areas of the USA and Canada caused the disciplines of archaeology and anthropology to develop together, to such an extent that the majority of academic archaeologists in US institutions form components of larger Departments of Anthropology. Perhaps surprisingly, therefore, the term 'geoarchaeology' has greater currency in the USA than in Europe. This arises from one of the fundamental research questions in New World Archaeology - when, and how, did humans come to colonize the American continent (see, for example, Pollard & Heron 1996; chapter 8). Such questions have been vigorously debated for at least a hundred years, with the issues polarizing around the presence or absence of humans before the last deglaciation and the opening of the so-called 'ice-free corridor'. Culturally the issue centres on whether the people known by their distinctive stone tools (Clovis) were the first occupants of the continent, conventionally dated at around 11 000–11 500 uncalibrated radiocarbon years BP (but see, for example, Batt & Pollard (1996) for a discussion of the importance of radiocarbon calibration on such issues).

The ephemeral nature of the archaeology of crucial early palaeoindian sites has created the necessity for close collaboration between geologists and archaeologists in order to interpret the evidence. It is in this context in particular that the skills of geomorphologists and sedimentologists have been essential to understanding the archaeological record. The earliest evidence for the New World presence of humans in the Pleistocene came from the finding of fluted stone tools with the bones of extinct bison during excavations in New Mexico in the late 1920s (Waters 1992). The stratigraphic studies required to prove the Pleistocene nature of these deposits were carried out by a geologist (Kirk Bryan), and the results were presented at a Geological Society of America meeting in 1929, thus symbolically establishing the close connection between geology and archaeology in North America. This has continued to this day, with the bulk of the academic texts in the field being published there. In one of the most recent of these, Rapp & Hill (1998) discuss extensively the nature of the interaction between geology and archaeology, and define two levels of interaction: geoarchaeology itself, approximately as defined above, and archaeological geology, which, in their view, is geological research that has direct relevance to archaeology. The former is part of archaeology itself. The latter is research carried out for geological reasons, but (perhaps incidentally, but often by design) has implications for archaeology. As an example, Rapp & Hill cite studies of coastal landforms and sea level changes around the Mediterranean, which of course have important repercussions for our interpretation of the development of society and trade in the region.

Rather than get bogged down with further close analysis of the definitions of these highly interrelated activities, we should perhaps take the lead set by the journal *Geoarchaeology*, which, in its first editorial, declared that 'it is *not* the purpose of this journal to define, circumscribe, or attempt to explain what geoarchaeology is or, still less, should be' (Donahue 1986). Furthermore, the editorial points to one of the features of interdisciplinary research that is often forgotten: 'an interface involves two-way interaction, so that research making use of archaeologic data to expand geologic interpretation and understanding is just as valuable as the reverse'. It is in this spirit that this volume has been put together.

## Exploration

Of all of the scientific advances in archaeology, undoubtedly one of the most significant has been the development of remote sensing techniques designed to locate and identify buried features prior to (or indeed, without) excavation. Aerial photography has for many years provided the mainstay of remote sensing applied to archaeology (Riley & Bewley 1996), but in the past decade or so there has been increasing awareness of the potential use of airborne and satellite multispectral data (Shennan & Donoghue 1992). Most remote sensing, however, is carried out on the ground using techniques developed and modified from exploration geophysics. These include resistivity and magnetometry-based techniques (Clark 1990), but the spectrum has broadened considerably over the past few years to include georadar and shallow seismic work. A new journal (*Archaeological Prospection*) was launched in 1994 specifically to promote this aspect of archaeological research. Mostly these surveys are carried out in advance of building or infrastructure development in accordance with planning guidance, but a recent popular TV series has done

much to publicise the potential for remote sensing in a wide range of archaeological settings!

Two of the biggest problems in archaeological remote sensing are discussed in papers in this volume. One is the use of geophysics in urban areas. Most electrical and magnetic techniques used conventionally in archaeological prospection are of little value in urban areas: a setting of increasing significance because of the political importance attached to the re-development of so-called 'brownfield sites'. **Cuss & Styles** show how high-resolution microgravity measurements can be used to locate 150 year old tunnels beneath inner city Liverpool, thus adding considerably to our knowledge derived from imperfect contemporary maps of the features. A second important goal in archaeological prospection is the ability to produce vertical sections of buried features, in order to estimate their depths and stratigraphical relationships. **Murdie *et al.*** report the use of Euler deconvolution on magnetic gradiometry data from a Roman-British villa at Wroxeter in order to produce such profiles. These sections are compared with georadar data across the same features. The value of this work is that gradiometry is relatively quick and cheap, and can be done by a number of specialist archaeological contractors, whereas georadar is still regarded within archaeology as an expensive and sometimes difficult to interpret technique. Thus if depth profile data can be obtained from standard magnetometry datasets, it will have an immediate impact on field archaeology.

In order to illustrate the value of archaeological geophysics within an integrated research programme, **Vernon *et al.*** present some data taken from a relatively unpromising (geophysically speaking!) context — the slag heaps surrounding archaeological iron and lead smelting sites in Yorkshire. Not only do these data help to delineate the extent of these ancient industrial sites, but they also serve to locate areas of smelting activity within the sites in order to constrain the requirements for further excavation or scheduling of such monuments. This study shows that conventional ground-based survey techniques can be applied in a wider range of contexts than has hitherto been considered, and have yet to reach their full potential.

## Environments

Environmental reconstruction from archaeological evidence has long been one of the most productive and intensively studied of the interfaces between the geosciences and archaeology (e.g. Butzer 1964, 1982). One of the most powerful tools in this respect is palynology. **Tipping *et al.*** elegantly present a study showing the input of non-native tree pollen into the soil profile at a known date as a result of the establishment of an arboretum about 1840 AD in southern Scotland. The results show rapid mixing of the pollen in the near-surface horizons, suggesting severe limits on the temporal resolutions available from such palaeoecological studies.

On a completely different timescale, **Latham *et al.*** address the complex issues of stratigraphy within an important cave site in southern Africa: that of Makapansgat, which contained a number of Australopithecine fossils. The dating of the cave has been by magnetostratigraphy, and this paper suggests that the cave environment at the time of deposition was not as simple as had been previously thought. They hypothesise that the bone-rich layer containing these fossils was not the result of flood activity, but may represent a hyena den. They call for a more careful re-examination of the cave

stratigraphy, in order to obtain a better estimate for the age of this important fossil material.

One of the biggest issues in modern day environmental science is the impact of mining activity on the environment. In some parts of the world humans have been mining for raw materials for many millennia, and have left a distinctive mark on the landscape. One such area is likely to have been Dartmoor in the southwest of England, which was a major producer of tin and copper during the Medieval and later periods. It has been speculated that southwest England must have been one of the major sources of tin during the European Bronze Age, since tin is relatively abundant there and is such a scarce commodity elsewhere (see, e.g. Franklin *et al.* 1978). There is, however, virtually no archaeological evidence for prehistoric mining on Dartmoor: a fact which is often attributed to the destruction of earlier evidence by later industrial-scale mining. (It should be noted, however, that even in the most heavily re-worked mining areas such as Parys Mountain, Anglesey, evidence for prehistoric mining does survive: Timberlake 1990.) Using the techniques of environmental geochemistry, **Thorndycraft *et al.*** have attempted to identify increases in tin concentrations in fluvial sediments on Dartmoor as markers of increased prehistoric mining activity. To date, the earliest geochemical evidence appears to be $1280 \pm 45$ AD in the Erme Valley, which is consistent with the documentary evidence, but still some way short of solving the problem of the source of the tin used to supply the rapid demand for bronze nearly 4000 years ago.

## Resources

The use of geochemical analysis as an aid to identifying the provenance of the source of a particular raw materials has been one of the cornerstones of the expansion of scientific archaeology over the past 40 years (e.g. Pollard & Heron 1996). Many of the earlier studies are analytically highly sophisticated, but ultimately fall somewhat short of their purpose (aiding the interpretation of the archaeological evidence) because they hesitate at the final step in the process — the integration of the analytical evidence with archaeological models of trading or circulation patterns established by other techniques. In a particularly incisive study, **Young & Thomas** show how careful mineralogical and textural analysis, when combined with trace element data, can provide an extremely detailed picture of the Medieval trade in iron ore around the Bristol Channel Orefield. The study is particularly noteworthy because the findings appear at first sight to contradict logic. It is suggested that ore was in fact being shipped towards the major part of the orefield when the boat from which the ore was recovered foundered. Examination of the documentary evidence, however, suggests that this might be the result of changing patterns of land ownership across the ore field. This study not only illustrates how documentary and material evidence can be integrated to give a more complete picture, but also highlights one of the important points to be remembered when undertaking any geoarchaeological study - not all human behaviour is predicated on simple laws of nature! **Lazareth & Mercier** have also used geochemical knowledge to identify maritime trade links during a similar historical period. By studying the mineralogy of large boulders carried by ships as ballast, and dumped at a port when loading, they have shown connections between Brittany, Cornwall and Ireland in a novel and perhaps unexpected way. One other aspect of this work worth mentioning is that they have used the geological

age of the granite as a further constraint on the viability of their model. This is something which is perhaps second nature to a geologist, but is unlikely to occur immediately to an archaeologist, and could be more widely applied.

The vast majority of geochemical studies in archaeology have undoubtedly focused on a narrow range of raw materials — lithics, obsidians, clays, glassmaking sands, and (more rarely) organic-rich materials such as jets and shale. One of the most important industries throughout antiquity has been that of textile manufacture, and the associated chemical process of dyeing. One of the important raw materials for this is alum, and yet surprisingly little has been done to study the processing and supply of this raw material. A preliminary study of the 17th and 18th century AD alum industry in North Yorkshire is provided by **Millard**. Given the increasing interest in our industrial heritage, and the resulting pressures to extend the scheduling of its monuments, it is becoming more important to improve our understanding of the chemical processes involved. Experience has shown that contemporary literary and patent evidence cannot always be taken as reliable evidence, as has been shown, for example, by our efforts to understand the development of the post-Medieval European brass industry. Here it has been shown that the British patent to manufacture brass by direct mixing of copper and zinc was taken out in 1738, long after the actual introduction of the process, probably around 1650 (Pollard & Heron 1996; chapter 6).

The paper by **Budd *et al.*** stems directly from the need to use sources of evidence other than total zinc content in order to predict how a particular piece of brass was manufactured. It has long been argued that brass made by the original cementation process introduced by the Romans could not contain more than 28% zinc because of thermodynamic limitations imposed by the nature of the process. Thus any metal shown by analysis to contain more than this amount must have been made by the direct process. Consequently it must date from after the introduction of this process in Europe (an important consideration when judging the authenticity of potentially valuable brass objects, but note above certain discrepencies in the actual dates involved). This rather crude test is somewhat unsatisfactory, and Budd *et al.* demonstrate for the first time that anthropogenic processes in brass manufacture might introduce sufficient differential isotopic fractionation of the zinc to allow the processing methodology to be distinguished. If verified by higher precision measurements, this observation has not only archaeological significance, but also wider implications for environmental geochemical monitoring.

**Thomas & Young** provide a second theoretical paper showing how geochemical modelling can be used to elucidate the behaviour of particular elements in high temperature processes. They study the chemical interaction between the ores, furnace lining and fuel ash in the charge of a bloomery iron furnace, and use these predictions to improve the quality of provenancing information derived from chemical analysis of the remaining slag. They successfully test their model on data from a Romano-British iron bloomery near Ross-on-Wye.

The final contribution by **Zaykov *et al.*** is a rare insight into the huge strides made in understanding the prehistory of parts of the Former Soviet Union during the past 50 years or so. The Southern Urals are important for many reasons, not least of which is that they may have been an important raw material source for western Europe during the Bronze Age. This paper discusses the results of recent research into the exploitation of gold, copper and lead in this region, as well as studying the trade in lithic raw materials between the Bronze Age settlements in the area.

## Summary

The papers presented here exemplify the many and varied ways in which the geosciences and archaeology have come to mutually support each other when the subject of study is one of the most interesting periods in geological history: that in which mankind has played an ever-increasing role in shaping the Earth's environment.

We can look forward to ever-increasing interaction between archaeology and the geosciences, in these and other areas. The benefits to archaeology will be the vast technical expertise in the geosciences. For geoscientists, the benefit will be the input of a knowledge of past human behaviour, which is of increasing importance through the Quaternary. The future agenda of geosciences undoubtedly requires an improved understanding of the two-way relationship between humans and the environment.

The editor would like to acknowledge the help of many people in preparing this volume. In particular, I would like to thank Dr Andrew David, Mr Paul Linford and Dr David Starley (English Heritage), Dr C. Gaffney and Dr Sue Ovenden (Geophysical Surveys of Bradford), Dr Armin Schmidt, Dr Arnold Aspinall and Dr Gerry McDonnell (University of Bradford), Professor Philip Tobias and Professor Tim Partridge (University of Witwatersrand), Professor Kevin Edwards (University of Sheffield), Dr Keith Bennett (University of Cambridge), Dr Ian Freestone and Dr Paul Craddock (British Museum), Dr Olwen Williams-Thorpe (Open University), Dr Barbara Barreiro (NERC Isotope Geosciences Laboratory) and Dr Kate Brodie (University of Manchester). Thanks also go to Roger Nathan, who helped in the editorial process. I would also like to thank the staff at the Geological Society for helping to organize the meeting (especially Amanda Harrison and Judi Lakin), and also the staff in the Geological Society Publishing House, especially David Ogden and Angharad Hills, for their forbearance during the production of this volume. I would like to dedicate the outcome to my mother, who sadly died at the time of the conference.

## References

BATT, C. M. & POLLARD, A. M. 1996. Radiocarbon calibration and the peopling of North America. *In:* ORNA M. V. (ed) *Archaeological Chemistry V*, American Chemical Society Symposium Series 625, Washington D.C., 415–433.

BUTZER, K. W. 1964. *Environment and Archaeology: an Ecological Approach to Prehistory*. Aldine Press, Chicago.

—— 1982. *Archaeology as Human Ecology: Method and Theory for a Contextual Approach*. Cambridge University Press

CLARK, A. J. 1990. *Seeing Beneath the Soil: Techniques in Archaeological Prospecting*. Batsford, Braintree.

DARWIN, C. 1859. *The Origin of Species by means of Natural Selection, or the Preservation of Favoured Races in the Struggle for Life*. John Murray, London.

DAVIDSON, D. A. & SHACKLEY, M. L. 1976. *Geoarchaeology: Earth Science and the Past*. Duckworth, London.

DONAHUE, J. 1986. Editorial. *Geoarchaology*, **1**, 1.

FRANKLIN, A. D., OLIN, J. S. & WERTIME, T. A. 1978. *The Search for Ancient Tin*. Smithsonian Institution, Washington D.C.

LAYARD, A. H. 1853. *Discoveries in the Ruins of Nineveh and Babylon, with Travels in Armenia, Kurdistan, and the Desert*. John Murray, London.

LYELL, C. 1830–1833. *Principles of Geology: being an attempt to explain the former changes of the earth's surface, by reference to causes now in operation*. John Murray, London (3 vols).

—— 1863. *The Geological Evidences of the Antiquity of Man with remarks on Theories of the Origin of Species by Variation*. John Murray, London.

POLLARD, A. M. & HERON, C. 1996. *Archaeological Chemistry*. Royal Society of Chemistry, Cambridge.

RAPP, G. JR. & HILL, C. L. 1998. *Geoarchaeology*. Yale University Press, New Haven.

RENFREW, A. C. 1976. Introduction. *In:* DAVIDSON, D. A. & SHACKLEY, M. L. (eds) *Geoarchaeology: Earth Science and the Past*. Duckworth, London.

RILEY, D. N. & BEWLEY, R. H. 1996. *Aerial Archaeology in Britain*. Shire Archaeology, Princes Risborough.

SCHIFFER, M. B. 1987. *Formation Processes of the Archaeological Record*. University of New Mexico Press, Albuquerque.

SHENNAN, I. & DONOGHUE, D. N. M. 1992. Remote sensing in archaeological research. *In:* POLLARD, A. M. (ed.) *New Developments in Archaeological Science*. Proceedings of the British Academy 77, Oxford University Press, 223–232.

TIMBERLAKE, S. 1990. Excavations at Parys Mountain and Nantyreira. *In:* CREW, P. & CREW, S. (eds) *Early Mining in the British Isles*. Occasional Paper No 1., Plas Tan y Bwlch, 15–21.

TRIGGER, B. G. 1989. *A History of Archaeological Thought*. Cambridge University Press, Cambridge.

WATERS, M. R. 1992. *Principles of Geoarchaeology: a North American Perspective*. University of Arizona Press, Tucson.

# Medieval iron and lead smelting works: a geophysical comparison

ROBERT W. VERNON, J. GERRY McDONNELL & ARMIN SCHMIDT

*Department of Archaeological Sciences, University of Bradford, Bradford, West Yorkshire BD7 1DP, UK*

**Abstract:** Geophysical techniques (fluxgate gradiometry and magnetic susceptibility) have been applied to ten iron and two lead smelting sites in the North Yorkshire Moors National Park and the Pennines, respectively. These geophysical techniques, particularly magnetometry, are often regarded as having little application on such sites. Large quantities of iron slag, for example, can mask structures associated with the on-site industrial activity, and this may result in the incomplete or erroneous interpretation of the geophysical data. Geophysical surveys can, however, identify the strong magnetic anomalies associated with iron-smelting furnaces and to a lesser extent those associated with lead smelting. To provide a valid interpretation of such geophysical data it is important to understand the processes that have been conducted on iron and lead smelting sites. This paper compares and contrasts the geophysical responses produced by iron and lead smelting sites and provides examples of the structures that geophysical techniques may reveal on smelting sites.

Metal smelting sites have been geophysically surveyed, mainly with proton and fluxgate magnetometers, since the late 1960s. Some of the earliest surveys in England were conducted on medieval iron-working sites in West Yorkshire (Bartlett 1971). In continental Europe, many of the early surveys were conducted on slag pit furnaces, mainly in Denmark and Germany (Smekalova *et al.* 1993). This early work concentrated on iron-smelting sites and was only capable of identifying the positive magnetic anomalies produced by furnaces and associated slag deposits. This trend continued through to the 1980s with magnetometer surveys on iron, lead and copper working sites, with Fluck (1990) and Goldenberg (1990) conducting surveys in the Vosges and Black Forest, respectively. Further limited experiments were being conducted on smelting sites using a variety of geophysical techniques, including earth resistance and magnetic susceptibility (Hesse *et al.* 1986; Crew 1985). The application of these new techniques produced mixed results, but provided an assessment of their suitability. The 1990s saw a growing trend to precisely relate and understand the nature of the geophysical responses to buried metal-working features. Crew (1989) in Snowdonia, North Wales was equating magnetic susceptibility data with the spread of iron slag and more recently to the quantity of slag (Crew, pers. comm.). Elsewhere, a magnetic susceptibility survey of a smithy floor at Burton Dassett, Warwickshire by the Ancient Monument Laboratory, English Heritage, was precisely correlated with the distribution by weight of magnetic material (primarily hammerscale) in the floor deposits (Mills & McDonnell 1992). In Germany, Al-Mussawy (1990)

*From:* POLLARD, A. M. (ed.) 1999. *Geoarchaeology: exploration, environments, resources.* Geological Society, London, Special Publications, **165,** 15–34. 1-86239-053-3/99/$15.00

identified a direct relationship between magnetic anomalies and the thickness of iron slag deposits and Panitzki (1994) compared the detailed magnetic characteristics of iron slag pit furnaces with the variations of proton and fluxgate magnetometer data.

In Britain most metal working sites over which geophysical surveys have been conducted are associated with iron. There are several exceptions. An inconclusive survey was conducted in 1992 over lead slag deposits at Grinton, North Yorkshire (McDonnell *et al.* 1992). In the same year, fluxgate gradiometer, pulsed induction (EM) and earth resistance techniques were applied to a tin processing site at Crift Farm, Lanlivery, Cornwall (McDonnell 1993). More recently, gamma-ray spectroscopy techniques have been used to examine a lead-working site in Ireland (Ruffell & Wilson 1998).

The current geophysical research project in the Department of Archaeological Sciences, University of Bradford, which aims to examine the geophysical responses produced by metal-working sites, commenced in 1995. Initially three diverse iron-working sites were geophysically surveyed in Bilsdale and Rievaulx, in the North Yorkshire Moors National Park (Vernon 1995). This work has continued in subsequent years. The surveyed sites are representative of a variety of iron-working activities, ranging from a simple bloomery through to a blast furnace, with a finery/chafery complex (Vernon *et al.* 1998). In addition, the interpretation of one site as a bloomery (Kyloe Cow Beck), geophysically surveyed in 1996, was confirmed by subsequent excavation. During 1997, a variety of magnetometer surveys were conducted at Lock Farm, Humberside across a bloomery furnace that had been reburied in a magnetically inert medium (Schmidt *et al.* 1998). This experimental work was the first step in precisely equating geophysical responses with a buried furnace at different orientations.

The research project has now been extended to examine geophysically the responses produced by lead smelting sites. During 1997 surveys on a site at Dacre, northwest of Harrogate, North Yorkshire have enabled several features to be identified which are associated with lead-production processes.

The research has understandably produced a large amount of geophysical data from both iron and lead smelting sites, making it possible to draw some comparisons between responses and to characterize buried features, as will be outlined below.

## Geophysical techniques and methodology

The strong positive magnetic anomalies produced by furnace remains and iron slags are generated in two ways. Firstly, induced magnetism produced by the earth's local magnetic field passing through the material; secondly permanent or remanent magnetism is acquired by firing (Clark 1990). The response from the thermoremanent magnetism originates from a combination of free iron oxides (FeO and $Fe_3O_4$) and iron inclusions, becoming fixed when the temperature, on cooling, falls within the range of $600° \pm 100°C$. The magnitude of the positive magnetic response is therefore a function of both slag composition and volume (Vernon 1995). The re-orientated slag in a tipped deposit may also result in random magnetic reinforcement or opposition, contrasting with a furnace, where the thermoremanent magnetism is coherent over the whole volume (Vernon 1995).

This work compares the results derived from magnetic susceptibility measurements of selected samples and fluxgate gradiometer (magnetometer) surveys. In addition,

earth resistance, magnetic susceptibility and pulse induction surveys were conducted over many of the sites (Vernon *et al.* 1998). All magnetometer surveys have been completed using the Geoscan FM range of fluxgate gradiometers. The fluxgate sensors have a separation of 0.5 m and only record the vertical magnetic component. All fluxgate gradiometer data is recorded in nanoteslas (nT), the unit of magnetic flux density.

The authors adopted the following approach for surveying smelting sites: surveys were usually conducted in 20 m, 10 m or 5 m square grids, which, at 400 readings per grid, gives resolutions of 1 m, 0.5 m and 0.25 m respectively. The 20 m grid surveys were conducted for general reconnaissance work. Once the limits of the metal-working site were known, the metal-working area was resurveyed using 10 m grids. This provided enough data for the site components to be defined. Furnace features were then resurveyed using 5 m grids that enabled the characteristics of the furnace to be identified.

The mass specific magnetic susceptibility (the degree to which material responds to a magnetic field) of weighed samples of slag and furnace material was measured in the laboratory using a balanced AC bridge.

## The surveys

The geophysical surveys have all been conducted on sites in northern England (see Fig. 1 for site locations). All the iron smelting sites are located on the western side

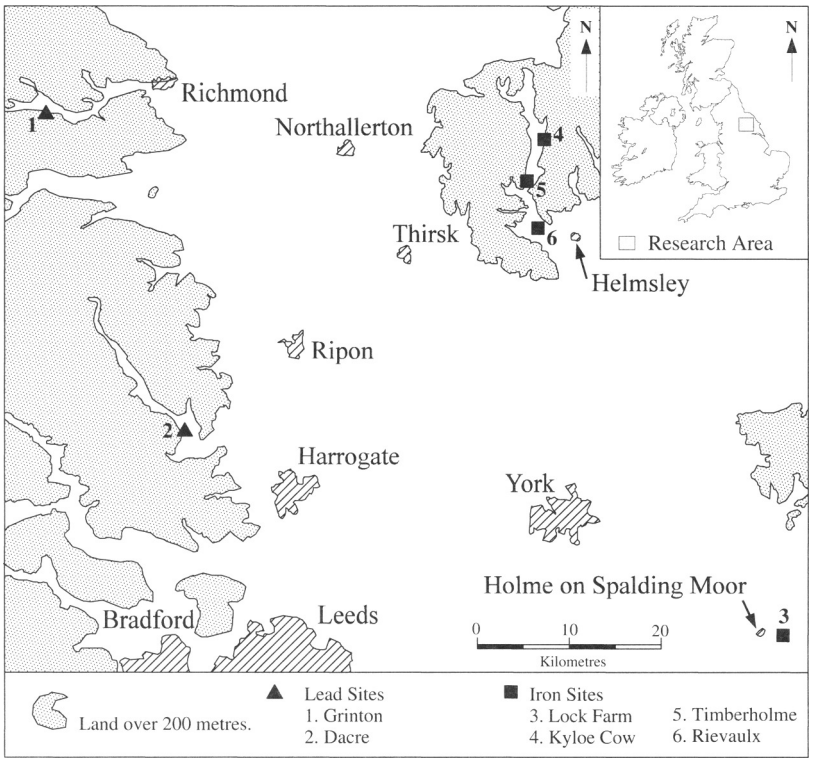


**Fig. 1.** Map showing the locations of geophysically surveyed smelting sites.

of the North Yorkshire Moors National Park in Bilsdale and Rievalux, to the north-west of Helmsley. Sites surveyed up to 1998 range chronologically from middle to late-medieval bloomeries as well as a post-medieval charcoal blast furnace operation with an associated finery/chafery (Vernon *et al.* 1998). To supplement this research programme, experimental work was undertaken at Lock Farm, Humberside that examined the geophysical responses from a reburied iron smelting furnace.

The geophysical surveying of lead smelting sites at present is confined to two sites in the Northern Pennine Orefield. The first is at Grinton, Swaledale, North Yorkshire (McDonnell *et al.* 1992). Current work has involved the re-examination of fluxgate gradiometer data and further slag sampling has been carried out. A fluxgate gradiometer survey has also been conducted at the second site at Dacre, together with examination of slag samples.

It is appropriate to briefly describe the processes employed to smelt both iron and lead in order to appreciate site characterizations.

## Iron-smelting technology

Iron-smelting technology has been subdivided into two distinct processes. The *direct process* or the bloomery process produces a malleable iron (often mistakenly described as wrought iron). In Britain, the bloomery shaft furnace (see Fig. 2) is generally cylindrical, probably not more than 2.0 m in height and with an internal diameter in the order of 0.3 m. A mixture of charcoal and iron ore is fired within the furnace. The highest temperatures (≈1500°C) occur towards the base near the

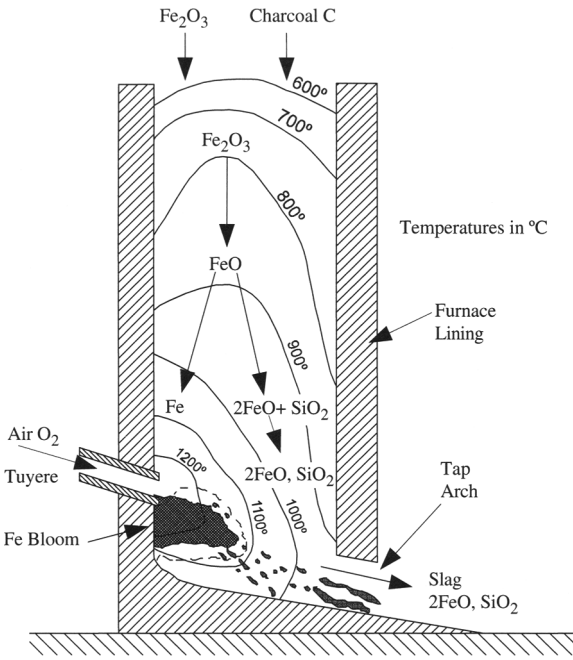


**Fig. 2.** Simplified section through a shaft (bloomery) furnace showing the main components and the products at different stages of the process (after McDonnell 1995).

tuyere, where air is blown into the furnace. The waste material from the process either remains within the furnace or is frequently removed via the tap arch. The iron does not melt but is reduced to form a 'bloom', a mixture of iron and slag which adheres to the furnace wall (Crew 1991). When extracted the bloom has to be continuously re-heated and hammered to clean it and produce a malleable iron billet.

The *indirect process* utilizes a blast furnace to produce a cast iron. It then undergoes further processing at a finery to produce a malleable iron that is then converted to bar iron at the chafery. The high bloomery, an intermediate technology between a bloomery and a blast furnace, could operate in either mode. An essential requirement of the high bloomery and blast furnace was water power to operate bellows. These bloomeries, high bloomeries and early blast furnaces were all fired by charcoal.

The furnaces and the slags from all the processes generally produce high positive responses on magnetometer surveys. Bloomery slags generally have a higher iron content than blast furnace slags, an average of 60% FeO compared to about 5% FeO, respectively (Vernon 1995).

## The Lock Farm experiment

The Lock Farm experiment was conducted in 1997 as part of a NERC-funded project to study advanced magnetometry (Schmidt *et al.* 1998). Essentially an iron-smelting shaft furnace previously excavated at Castleshaw, Greater Manchester, was reburied in a magnetically inert environment. A series of surveys using a variety of magnetometers (caesium, three-component and vertical fluxgate gradiometers) were then carried out across the furnace (Schmidt *et al.* 1998).

When excavated, the clay furnace had internal and external diameters of 0.4 m and 0.75 m, respectively. The tap arch was intact. The recovered furnace consisted of five large side pieces and about half the base, including part of the tapping channel, a total of six pieces. A fibreglass mould of the *in situ* furnace's interior enabled the pieces to be orientated accurately and fitted together.

The site chosen for the experiment was Lock Farm, Holme on Spalding Moor, Humberside. The area is flat and composed of sandy soil underlain by thick deposits of sand. Figure 3 details the section and magnetic susceptibility of the soil/sub-soil profile. The bulk of the furnace was buried in sand with a mean magnetic susceptibility of $2.5 \times 10^{-8}$ kg/m$^3$, whilst the fired clay furnace lining had a magnetic susceptibility between $1.24 \times 10^{-6}$ kg/m$^3$ and $1.13 \times 10^{-5}$ kg/m$^3$.

Only the six larger furnace pieces were used for the experiment. The circular reburied furnace's diameter was similar to the *in situ* furnace. The reburied furnace was placed so that its position relative to magnetic north corresponded to its original orientation. On reburial, the top of the furnace was 0.3 m below the surface. The experiment could not exactly replicate the furnace as found, due to the different surface geology (Namurian sandstone and shales at Castleshaw, glacial sands at Lock Farm), slag spread and loss of some fragments of the clay furnace lining.

The survey work was carried out in five stages as detailed in Fig. 4. At each stage, two fluxgate gradiometer surveys were conducted at 0.5 m and 0.25 m resolution, respectively.

*Stage 1* was the initial survey of the site to establish that the location was magnetically inert. The variations of the data had a standard deviation of less than 1 nT.

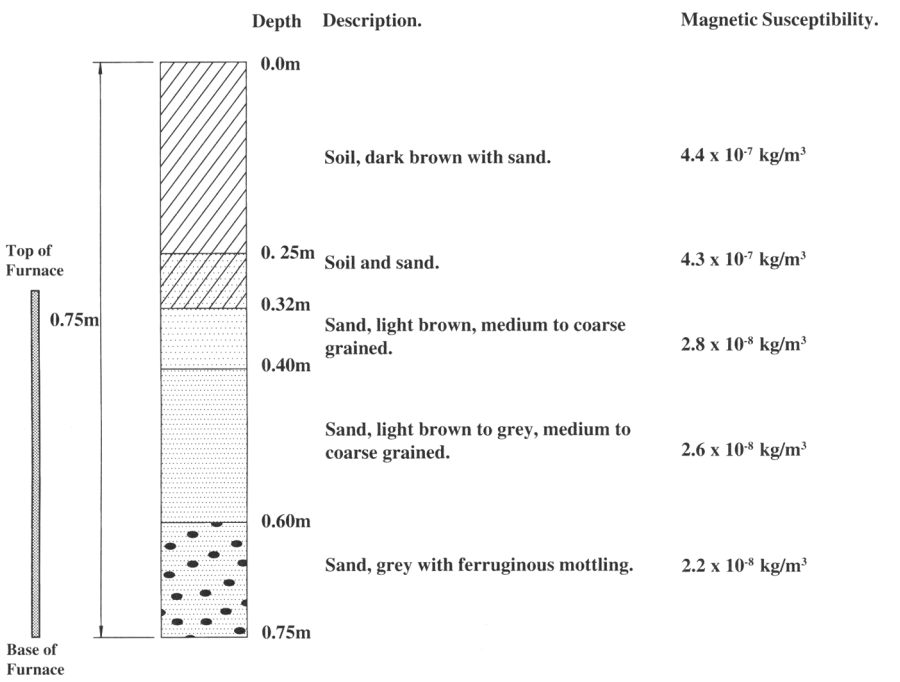


**Fig. 3.** Lock Farm: soil profile through furnace reburial pit.

*Stage 2* was conducted after the furnace was reburied. Figure 5 shows the fluxgate gradiometer reading recorded over and around the furnace for 0.5 m and the 0.25 m resolution surveys. The highest positive value recorded (221 nT) is lower than those recorded on other surveyed furnaces. At Kyloe Cow Beck (see Fig. 6), for example, the highest recorded value at a resolution of 0.25 m was 869 nT. These differences in fluxgate response may be a function of the depth of burial (the top of the Kyloe Cow Beck furnace only varied from 0.15 m to 0.2 m deep), type of furnace infill (slag or soil) and the composition of the furnace lining. It was noted during this stage of the experiment that a slight bulge on the southwest side of the positive anomaly corresponded to the position of the tapping arch.

At *Stage 3*, bags of randomly orientated iron-slag were buried against the southwest edge of the furnace. Despite being built up to the full height of the furnace, the slag alone did not produce readings above 20 nT. This probably results from the totally random disposition of the remanently magnetized slag pieces. (*In situ* slag tips may be less random. Slag may still be above its Curie temperature after tipping.)

At *Stage 4*, the slag was removed and the furnace rotated clockwise through 90°. This resulted in a corresponding rotation of the negative halo on the north side of the anomaly, indicating a pronounced remanent magnetism. In addition there was a slight reduction in the negative response. This is attributed to the interaction of both the remanent and induced magnetization in the furnace. At *Stage 2* they reinforce each other, whilst in *Stage 4* they are partially acting in opposition.

*Stage 5* was the survey of the site after the furnace had been removed.

Some significant observations could be made from the Lock Farm experiment:

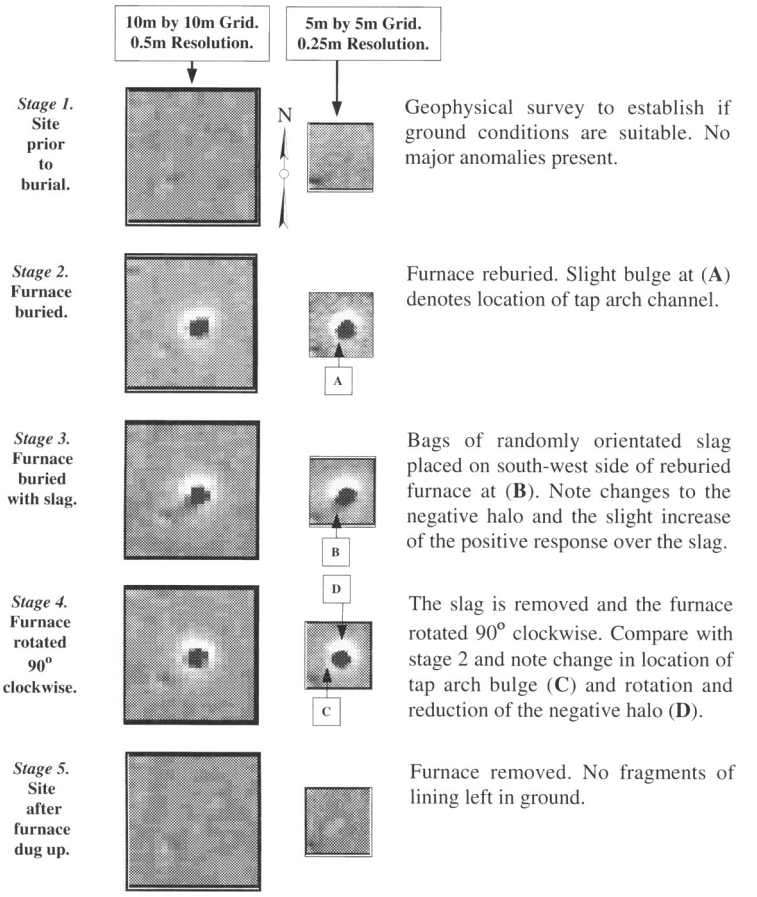


**Fig. 4.** Lock Farm experiment: clipped fluxgate gradiometer plots of surveys recorded at each stage of the experiment. Data clipped to −10 nT (white) to +10 nT (black).

- The positive data formed a well defined cluster surrounded by negative values. The positive data approximated the furnace's location.
- A slight bulge on the circumference of the positive data corresponded to the lip of the tapping channel still attached to the furnace bottom.
- The random orientation of dumped slag greatly reduces its overall remanent magnetic signal.
- The magnetic anomaly of the furnace is mainly due to remanent and only to a much lesser degree induced magnetization.

## North Yorkshire Moors Surveys

A total of ten iron-smelting sites have been surveyed: four in Bilsdale and six in the vicinity of Rievaulx within the North Yorkshire Moors National Park. In Bilsdale, two sites, Kyloe Cow Beck (bloomery) and Timberholme (high bloomery), have been singled out for more detailed survey work. See Fig. 1 for locations. This was followed up with a partial excavation of the bloomery site.

| | | | | |
|---|---|---|---|---|
| -7 | -17 | -27 | -24 | -12 |
| -10 | -12 | **23** | **38** | -6 |
| -10 | **18** | **126** | **51** | 0 |
| -7 | -6 | **25** | **9** | -2 |
| -4 | -6 | -5 | -5 | -5 |

10m Grid.
(0.5m resolution)
Centre area around
furnace.

7 positive values.

All units in nanoTesla

| | | | | | | | |
|---|---|---|---|---|---|---|---|
| -13 | -15 | -20 | -30 | -33 | -23 | -17 | -12 |
| -15 | -22 | -16 | -6 | **18** | -5 | -7 | -13 |
| -16 | -20 | -6 | **74** | **98** | **24** | **-2** | -12 |
| -16 | -5 | **67** | **221** | **176** | **68** | **11** | -2 |
| -13 | **31** | **96** | **174** | **123** | **47** | **4** | -7 |
| -9 | **5** | **33** | **60** | **57** | **26** | **13** | -1 |
| -9 | -2 | **19** | **14** | **16** | **9** | **1** | -7 |
| -7 | -6 | -1 | -2 | -3 | -3 | -2 | -2 |

5m Grid.
(0.25m resolution)
Centre area around
furnace.

26 positive values.

**Fig. 5.** Lock Farm: furnace prior to rotation. Raw fluxgate gradiometer data for a 10 m (0.5 m resolution) and 5 m grid (0.25 m resolution).

## *Kyloe Cow Beck*

The Kyloe Cow Beck site was discovered in 1996 by field walking. The site is located in Smiddale ('Valley of the Smiths' in Scandinavian) on the east side of Bilsdale. The site also lies near to the outcrop of the Dogger ironstone. A 1.0 m resolution fluxgate gradiometer reconnaissance survey revealed the site to contain an extensive spread of slag. Two areas of high positive data, presumed to be furnaces, with maximum values of 321 nT and 469 nT, were noted on the west and east sides of the slag spread, respectively.

The principles derived from the detailed Lock Farm experiment survey work were applied to the Kyloe Cow Beck site. The area of slag was resurveyed at 0.5 m resolution and the eastern furnace was also surveyed at 0.25 m resolution. The latter survey produced a higher response (869 nT) than the1.0 m resolution survey. The positions of the survey grids, together with data plots and the actual data for the eastern furnace, are shown on Fig. 6.

During 1997 the Kyloe Cow Beck eastern furnace was excavated and the position of the furnace was confirmed to correspond to the large positive anomaly that occurred on all three surveys. The external dimensions of the furnace were 1.8 m and 1.4 m on the north/south and east/west axis, respectively. Adjacent areas of lower readings correlated with thin (<0.5 m) spreads of slag.

Similar to Lock Farm, data from Kyloe Cow Beck showed a slight bulge on the northwest side of the positive data that corresponded to the excavated tapping channel. The grouping of high positive values on the north side of the furnace coincides with the location of the tuyere. This is the first time that this phenomenon has been noted and it is considered to be a significant discovery. Reference to Fig. 2 indicates

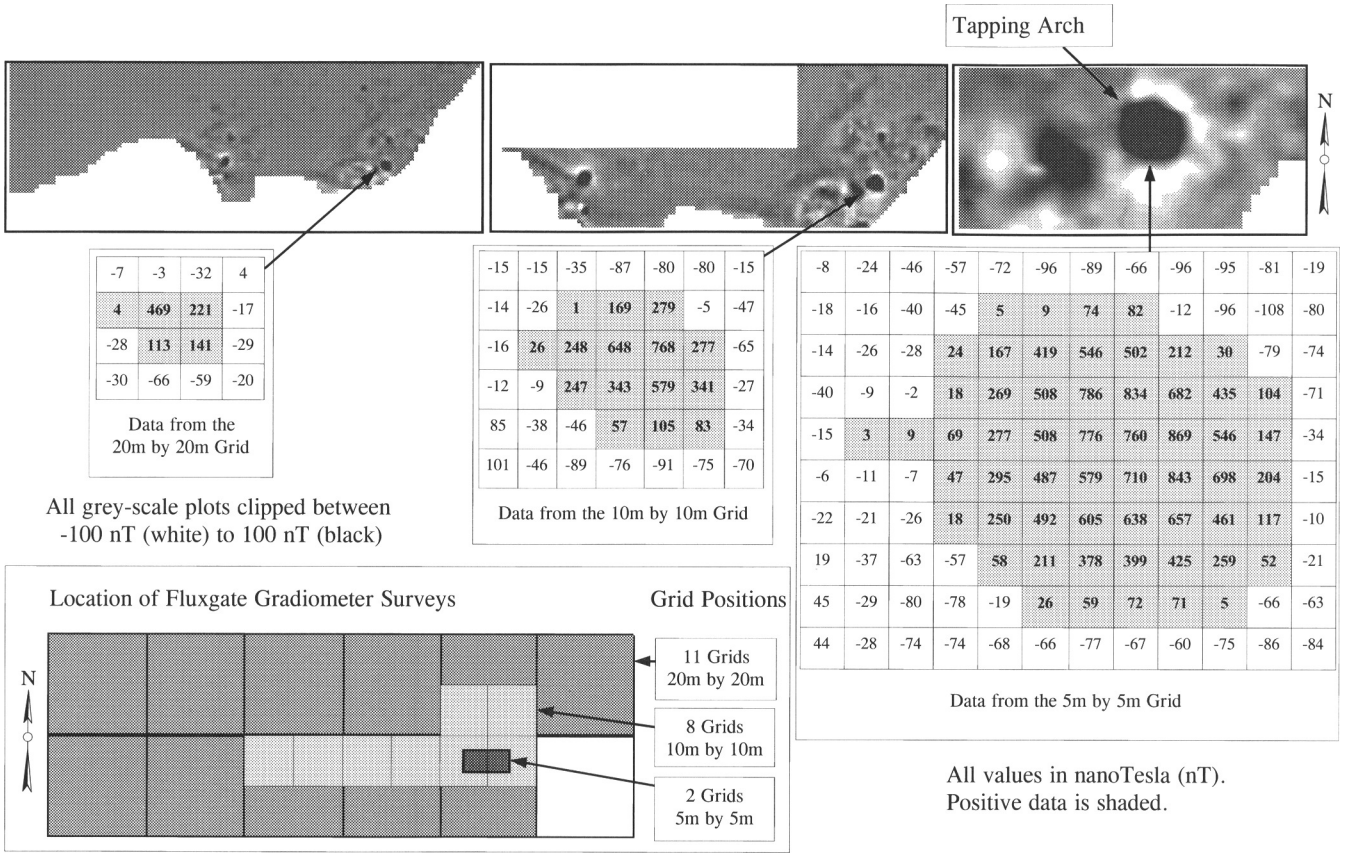


**Fig. 6.** Kyloe Cow Beck: fluxgate gradiometer data recorded at different resolutions over the eastern furnace.

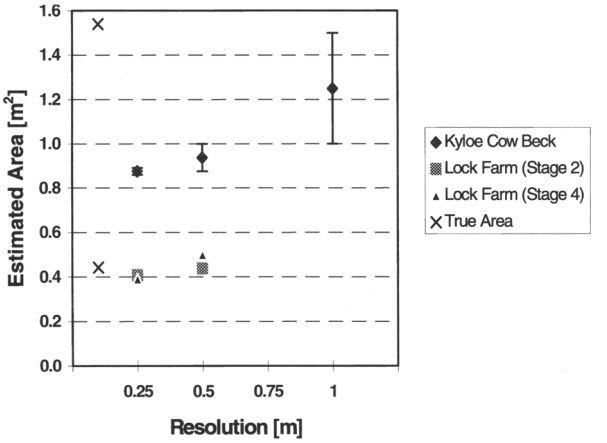


**Fig. 7.** Graph comparing the areas of positive data from the Lock Farm and Kyloe Cow Beck fluxgate gradiometer surveys with the true area.

that the highest temperature occurs around the tuyere thereby providing the opportunity for free iron oxide to form in this area. With removal of the iron and slag bloom it is inevitable that some of the iron oxide will remain attached to the furnace lining. Successive removal and reconstruction of the furnace lining around the tuyere area will inevitably lead to a build-up of iron oxide in this area. High temperatures around the tuyere also result in lining erosion. In the case of Kyloe Cow Beck, excavation has shown that the furnace was relined at least five times in the tuyere area.

Since the negative halo in magnetometer data is just the consequence of the geophysical nature of the response (Clark 1990), by examining the positive data it may be possible to approximate some simple properties about each furnace.

The graph in Fig. 7 suggests how the groupings of high positive readings can be utilized to estimate the area of the Kyloe Cow Beck and the Lock Farm (stages 2 and 4) furnaces. The approximate area of the furnace was calculated using the following formula:

$$\text{Area of Furnace} = (\text{number of positive readings}) \times (\text{resolution/scaling factor})^2.$$

As shown before (Schmidt & Marshall 1997, Fig. 1b), a scaling factor close to 2 has to be introduced in order to relate anomaly width to one-dimensional feature width. The error of the calculated area can be estimated as $\pm 0.5 \times (\text{resolution/scaling factor})^2$. As the error bars on the graph show, a higher degree of accuracy is achieved when calculating furnace area with the data from higher resolutions (0.25 m). The graph shows that:

- for the measurements at Lock Farm, this estimated cross-sectional area is close to its true value
- for the shallower furnace at Kyloe Cow Beck, the area was underestimated showing the limitations of a constant scaling factor

Whilst this idea is rudimentary in both concept and application, it is hoped that eventually with enough geophysical data and physical evidence derived from excavation, it may be possible to increase the accuracy of this method. It may eventually be possible to accurately derive furnace diameters from the geophysical data.

## *Timberholme*

An initial fluxgate gradiometer survey of 20 m reconnaissance grids at Timberholme identified a well defined furnace area and an associated slag tip covered by approximately 0.3 m of river alluvium. The visible remains of a leat that once fed water to a water wheel traverse the site. The results and the interpretation of the fluxgate gradiometer survey are shown in Fig. 8. Slag analyses indicate that the Timberholme

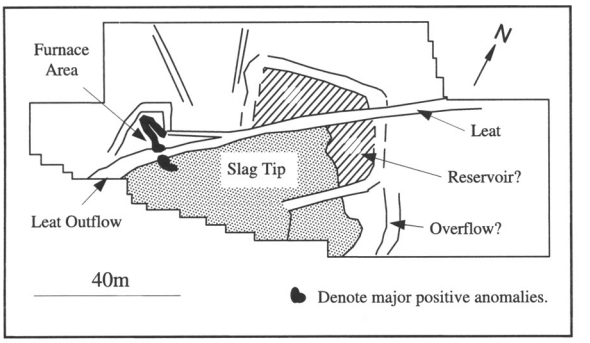


Interpretation of the Fluxgate Gradiometer Data.

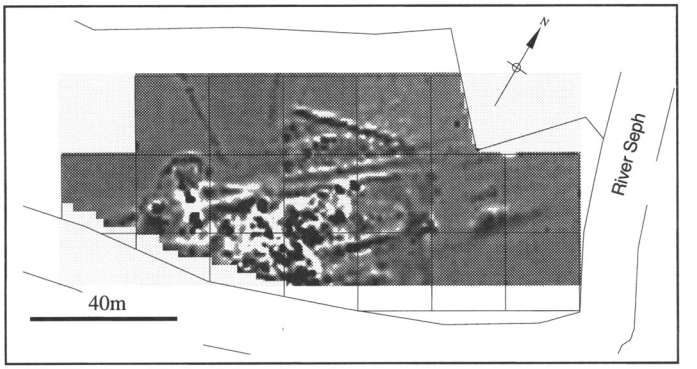


Complete Site. (1.0m resolution)
Clipped Range -44 nT (white) to 50 nT (black)

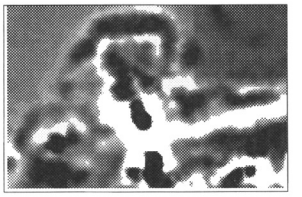

Furnace Area.
(0.5m resolution)
Clipped Range -40 nT
(white) to 40 nT (black)

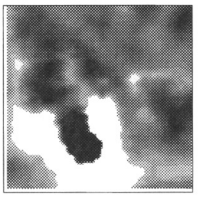

Collapsed Furnace.
(0.25m resolution)
Clipped Range -75 nT (white)
to 75 nT (black)

**Fig. 8.** Timberholme: a monastic water powered bloomery operation. The site contains the remains of a leat and slag tip. The furnace area is covered by river alluvium. The fluxgate gradiometer surveys suggest the furnace collapsed across the water leat.

furnace produced a slag that ranged in composition from a bloomery to blast furnace type (Vernon 1995; Finney 1997). Fluxgate gradiometer readings varied between −197 nT to 1391 nT over the slag tip. In the vicinity of the furnace, two areas of positive readings up to 2014 nT were recorded. Compared to data recorded at other iron-smelting furnaces, e.g. Kyloe Cow Beck, these readings are high. These high readings, together with slag analyses that are comparable with those generated by blast furnaces (5% FeO), support the hypothesis that the Timberholme furnace was a high bloomery. The high positive fluxgate gradiometer readings are exceptional. The only other site where similar values have been recorded is at the Forge Farm finery/chafery complex associated with the Rievaulx Blast Furnace. The very high positive values probably relate to the presence of free iron in the slag. The 0.5 m and 0.25 m resolution surveys (see Fig. 8) over the Timberholme High Bloomery furnace would suggest that it was probably a square (up to 5 $m^2$) structure. Unlike the Kyloe Cow Beck surveys, the positive data do not form a distinct circular cluster that would be a characteristic of the furnace. The reason for this may be that after abandonment, the furnace, which would probably have been taller than a simple shaft furnace, collapsed in a southerly direction across the leat.

Magnetic susceptibility measurements taken on the Timberholme slags range between $0.7 \times 10^{-7}$ kg/$m^3$ to $4.0 \times 10^{-6}$ kg/$m^3$.

## Lead-smelting technology

Very little is known about the early history of lead-smelting technology. Unlike iron smelting, very few lead smelting sites have been excavated (Cranstone 1992). Most researchers regard medieval lead smelting as a two-stage process. Gill (1992) describes the various methods as follows.

The first stage involved heating the ore in an oxygen-rich environment. Two basic methods appear to have been used: either the bale (or bole) or the ore-hearth. The bale was usually constructed on high land to catch the wind. It was essentially a wood bonfire on which the lead ore was placed. The ore-hearth was probably smaller. Air was introduced by bellows. The lead ore was mixed with fuel (coal, wood or peat) (Gill 1992). Temperatures between 600° and 800°C are achieved, giving a recovery of between 40% to 70% lead. The residue is a lead-rich 'grey' slag.

The second stage involved re-heating the 'grey' slag at higher temperatures (1100° and 1200°C) in a slag hearth. This produced molten lead. The molten slag generally floated on the metal. Such secondary slag is generally referred to as 'black' slag. This latter phase would have utilized bellows, either operated manually or by a water wheel, to provide air to raise the temperature. Manually operated bellows were also occasionally used at the bole stage (Tyson *et al.* 1995).

## Surveyed lead-working sites

### *Grinton*

The first published geophysical survey of a lead-smelting site in England is recorded as recently as 1992, at Grinton, North Yorkshire (see Fig. 1 for location) (McDonnell *et al.* 1992). Eight 20 m grids were surveyed with a fluxgate gradiometer. The results from this survey were inconclusive and it is unclear whether the survey was conducted over the site of a bale or slag furnace. It was, however, suggested that furnace fragments may

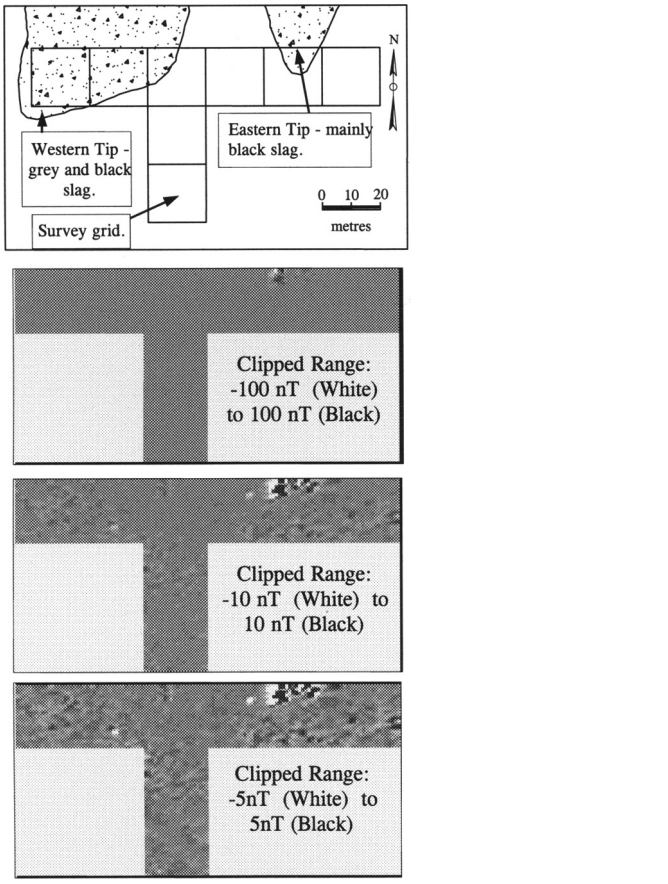


**Fig. 9.** Grinton: site plan and clipped fluxgate gradiometer plots (after McDonnell *et al.* 1992).

have generated some of the anomalies noted on the survey. A recent (1998) visit to the site for sampling confirms the presence of two low-lying tips (see Fig. 9). The western tip is predominantly grey slag with furnace material whilst the eastern tip is composed of black slag which is generally spread about the site. A re-examination of the Grinton data has yielded very little additional information. It confirms that spreads of lead slag have negligible magnetic properties. Most of the fluxgate gradiometer data fell between −4 nT and 4 nT, the range of data produced by non-fired archaeological targets. Two anomalies generated data between 15 nT and 30 nT. It was thought that they could relate to disturbed furnaces or hearths. Another area on the eastern tip produced positive responses of 100 nT generated by modern iron-rich debris. Measurement of the magnetic susceptibility of both slag types confirms that the slag has low magnetic properties. Values for the slags varied between $6.5 \times 10^{-8}$ kg/m$^3$ and $3.2 \times 10^{-7}$ kg/m$^3$.

## *Dacre*

More recent surveys (1997 and 1998) at Dacre, northwest of Harrogate, North Yorkshire enabled several features to be identified which could be associated with

lead-production. The site is on low-lying grazing land on the west side of the River Nidd. The site was first noted during a historical investigation of iron production in Nidderdale. Blacker *et al.* (1996) described the site as lying close to Smelt Maria Beck with the outline of a two-roomed building defined by summer scorch markings. Grey lead slag and slag-rich sediments are also exposed about 0.3 m below the surface in the side of the adjacent beck. The age of the site is not known but it certainly predates the 19th century (Blacker, pers. comm.).

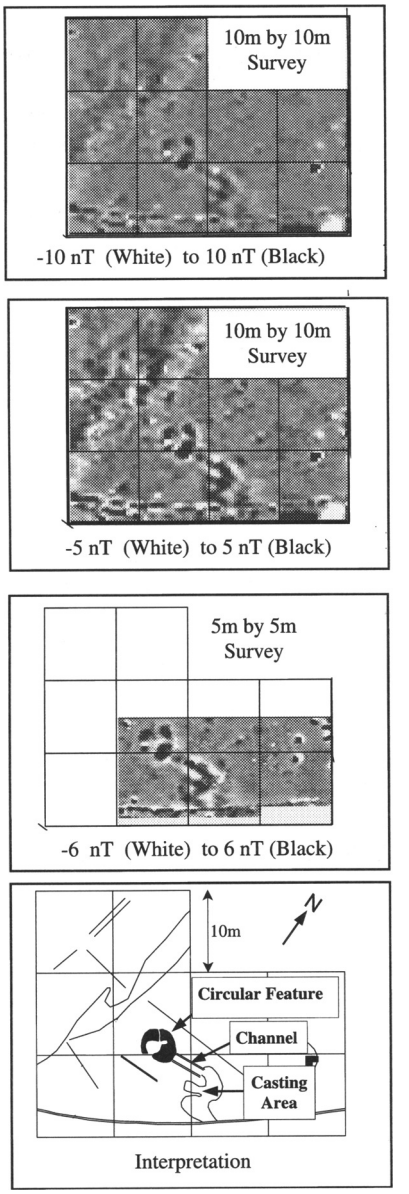


**Fig. 10.** Dacre: clipped fluxgate gradiometer data plots and interpretation.

Prior examination of the land surface enabled the limits of the Dacre site to be defined. An initial survey of ten fluxgate gradiometer 10 m grids covered most of the site and also examined the possibility of water being conducted onto the site to work a water wheel. Once the main structure was identified a survey of eighteen 5 m grids was conducted over it. The results and interpretation of the survey are shown in Fig. 10. In common with the Grinton survey, the range of values (−10 nT to 10 nT) at Dacre were generally low. The plots shown in Fig. 10 have been clipped to this and lower ranges. It has been possible to identify on the survey a roughly circular feature about 5 m in diameter composed of clusters of positive values (see Fig. 10). This feature is interpreted as a smelting hearth. The presence of grey lead slag would suggest that this is a bale-type structure. However, the dimensions of the hearth are larger than those for previously recorded bales. Raistrick (1926/27) recorded a diameter of 1.5 m on a bale at Winterings near Gunnerside, North Yorkshire. However, as there appear to be large differences in the dimensions and design of these early smelting sites (Willies & Cranstone 1992) it is perfectly plausible to regard Dacre as a bale site. A narrow linear anomaly interpreted as a channel (up to 1 m wide) runs east from the hearth towards an irregular area of positive data. The latter area lies close to the exposed slag in the beckside. It is presumed that, in common with other lead smelting hearths, the linear feature is a casting channel terminating at a small casting floor.

Figure 11 shows the data associated with the hearth on the 10 m grid survey. The circular hearth feature is defined by the clusters of positive values. The values vary between 0 nT and 97 nT with the majority of data less than 10 nT. Compared with data from iron-working sites the values are considerably lower. This also applies to magnetic susceptibility results. Dacre grey slag produced values between 4.3 and $9.1 \times 10^{-8}$ kg/m$^3$.

## Discussion

Unlike iron-smelting technology, lead smelting processes and the layout and organization of lead-smelting sites are not fully understood. Topographic surveys and limited archaeological excavations of both lead and iron smelting sites have been conducted since the early part of this century. For example, Raistrick (1926/27) describes a lead bale at Gunnerside, North Yorkshire and Cowper (1898) excavated an iron smelting site, near Coniston, Cumbria. While iron technology can be grouped into the direct and indirect phases, representing pre-blast furnace and blast furnace technology, respectively, this is not entirely true for the lead-smelting process. The limited evidence available from medieval lead smelting sites would suggest that both techniques and structures exhibit some regional variations in this period (see Willies & Cranstone 1992). This results in a chrono-technological overlap making it difficult to assign specific lead-smelting structures to an exact period of time.

Usage of geophysical surveying methods has enabled both iron and lead smelting sites to be assessed rapidly. However, if the on-site smelting processes are not fully understood, interpretation may be difficult. With iron-smelting sites a combination of geophysical surveying techniques may provide more answers. It is even possible in some instances to identify charcoal storage areas employing earth resistance methods (Vernon *et al.* 1998). The shaft or bloomery technology has

| | | | | | | | | | | | | | | | | |
|---|---|---|---|---|---|---|---|---|---|---|---|---|---|---|---|---|
| -3 | -3 | 0 | -3 | 0 | -2 | -1 | -2 | -2 | -1 | -3 | -3 | -2 | -2 | -2 | -2 | -1 |
| -5 | -11 | -5 | -4 | -2 | -1 | -2 | -3 | -4 | -2 | -3 | -4 | -6 | -3 | 0 | -1 | -1 |
| 13 | -3 | 0 | -2 | -2 | -3 | -2 | -1 | **0** | -5 | -1 | **0** | **1** | -5 | -1 | -1 | 0 |
| -1 | -2 | -3 | -4 | -4 | -1 | **1** | **0** | -2 | -3 | **5** | **7** | **1** | -5 | -4 | -3 | -1 |
| -2 | 0 | -3 | -3 | **4** | **10** | **8** | **4** | **1** | -2 | **5** | **14** | **10** | -2 | -3 | -1 | 0 |
| -3 | -2 | -3 | -4 | **4** | **11** | **1** | **2** | **2** | -4 | -5 | **4** | **7** | **0** | -5 | -2 | -1 |
| 0 | -2 | -2 | -3 | **3** | **4** | **2** | -3 | -2 | -5 | -6 | -4 | **0** | **0** | -7 | -3 | -2 |
| -1 | 3 | -3 | -3 | -3 | -39 | -13 | -7 | -5 | -7 | **1** | -1 | **2** | -5 | -8 | -4 | -3 |
| 1 | -1 | -5 | -3 | -3 | **97** | **4** | -5 | -5 | **0** | **12** | **10** | **7** | -2 | -6 | -4 | -4 |
| -1 | -2 | -3 | -3 | **0** | **6** | -2 | -6 | -6 | **11** | **21** | **6** | **1** | -2 | -2 | -2 | -3 |
| -3 | -2 | -2 | -2 | -3 | -2 | -4 | -4 | **7** | **12** | **22** | **11** | -1 | -4 | -2 | -1 | -4 |
| -2 | -1 | 0 | -1 | -4 | -4 | -2 | -3 | **5** | **8** | **22** | -3 | -5 | 2 | 4 | 3 | -2 |
| -3 | -1 | -1 | -2 | -2 | -2 | -4 | -4 | -5 | -2 | -4 | -8 | -6 | -3 | 2 | 2 | -3 |
| -2 | -2 | -2 | -2 | -1 | -2 | -1 | -3 | -6 | -4 | -4 | -4 | -3 | -4 | -4 | -5 | -3 |
| -1 | -1 | -3 | 0 | -1 | 1 | -1 | -2 | -3 | -2 | -3 | -2 | -2 | -3 | -4 | -6 | -6 |

**Fig. 11.** Dacre: data from part of the 10 m by 10 m grid survey over the circular feature. The recorded values are much lower than those found on iron-working sites. Further, negative data is found in the central area of the feature. By shading the positive data it is possible to see the roughly circular feature. However, this outline is broken by areas of negative data. Compare the data with the plots of the circular feature in Fig. 10.

remained virtually unchanged from the late Iron Age (100 BC) to the late-medieval period (*c.* 1450 AD) although there are regional and diachronic variations in furnace construction. Major changes in iron smelting furnaces only occurred with the development of pseudo-blast furnace technology, represented by the high bloomery. Sites became more elaborate with the introduction of water power, for example, at Timberholme. Iron-working sites all tend to contain a wide spread of slag, sometimes several metres in thickness. Furnaces can be identified by distinctive positive magnetic anomalies that often produce magnetic responses approaching 1000 nT. Occasionally, sites like that at Castleshaw will contain multiple furnaces sometimes constructed on top of each other (Redhead 1993).

In principle, all iron smelting sites are similar. At a basic level they contain a furnace and slag dump. However, the geophysical surveys conducted at higher resolutions have shown that it may also be possible to identify furnace specific features, e.g. tap arch and tuyere locations. In addition, further comparisons between positive data and measurements taken from excavations may allow the furnace diameter to be

estimated from the geophysical data. Both the Lock Farm experiments and the detailed comparisons made at Kyloe Cow Beck, suggest that this may be possible. The advent of cast iron production presented greater opportunity for free iron to be present in both furnace linings and slags, as iron prills. This increases the possibility for clusters of values, in excess of 2000 nT, to be encountered on surveys, for example at Timberholme.

Compared to iron, the geophysical study of lead-smelting sites, and indeed other non-ferrous metal smelting sites, is still in its infancy. Nevertheless from the limited work completed, it has been possible to draw some fundamental comparisons. The Grinton data clearly demonstrates the low responses that lead slag produces. Even within the −10 nT to 10 nT range very few features stand out. In principle, the data is comparable to that obtained from surveys of non-industrial sites.

In contrast, the Dacre survey is much more encouraging. It shows a possible smelting hearth, although how it actually functioned is not fully understood. There is a lack of documentary records and excavation work on this site but it may be medieval, of monastic origin. Despite its location next to a beck no evidence, either topographical or geophysical, has been found for water-power on the site. Further, as it is not located on a hillside, the traditional site for a bale, it is presumed to be a smelting or slag hearth with air introduced by hand bellows. Other features tentatively identified at Dacre include a likely tapping channel and casting area.

The dominant factor that governs the geophysical responses from both iron and lead smelting operations is the presence of iron and iron oxides. The data in Fig. 12 demonstrate this point clearly by comparing the magnetic susceptibility of the various slags and furnace material.

In Fig. 12, sample 2 has the lowest magnetic susceptibility. This is the value for the sand in which the Lock Farm experiment took place. Sample 1, the sandy soil at Lock Farm is higher, reflecting a higher iron content. However, both soil and sand are much lower than the values obtained for the Lock Farm furnace (Samples 3, 4 and 5). Most of the Timberholme slags (Samples 6 7 and 8) also fall within a similar range to the Lock Farm furnace. However, sample 9 has a much lower value. This particular sample is from High Bloomery tap slag that contained 5.3% FeO compared to 34.7% to 74.8% FeO for samples 6 to 8. The Kyloe Cow Beck data (samples 10, 11 and 12) are generally higher and probably result from the higher amounts of iron oxides in the slag, compared to different technology that operated at Timberholme. The data from the lead smelting sites (Samples 13 to 20) all exhibit lower values than those for iron. Most of the values are similar to that derived for the Lock Farm sand. Sample 20 is an exception. It is a mixture of slag fragments and soil taken from the lead slag rich layer in the beckside. It has a higher value than the large pieces of grey slag found in the same horizon and is probably contaminated with either iron-rich soil or sediment mobilized by the beck. It is interesting to note from the data presented in Fig. 12 that iron smelting operations produce magnetic susceptibility values higher than $1.0 \times 10^{-6}$ kg/m$^3$, whilst those from lead smelting sites are below this value.

Iron and lead smelting sites therefore all produce distinct signatures on geophysical surveys. Although is possible to objectively compare the data so that valid geophysical interpretations can be made, it must be stressed that the interpretation usually needs support from other sources, for example, topographical mapping, excavation and historical documentation.

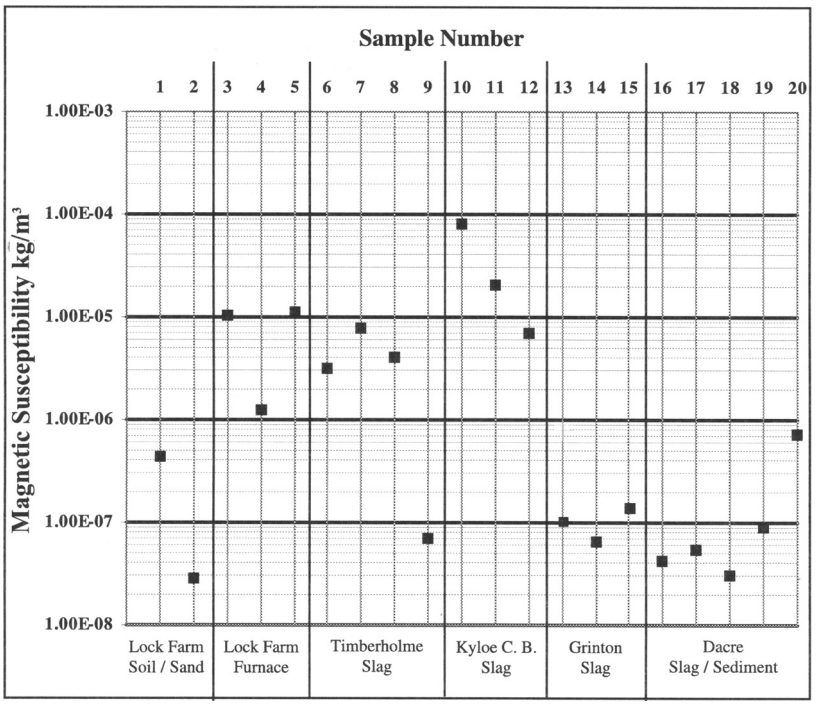


**Fig. 12.** Comparison of the magnetic susceptibility values.

## Conclusions

The significance of iron being present when comparing geophysical data from iron and lead smelting sites is irrefutable. From the limited data available it has been possible to show that by understanding the geophysical properties and the technological changes valid interpretations can be drawn for the surveys. Additional surveys of iron-smelting sites will allow the rudimentary principles that have been outlined to be honed further so that features that are important to the interpretation of iron-working sites can be determined without excavation and placed within their archaeological context.

Lead smelting sites appear to produce a range of magnetic responses that are weaker but identified on most magnetometer surveys. This is fortunate as it provides a geophysical distinction between the iron and lead smelting processes. In addition, lead-smelting techniques and associated structures are not as readily understood as those associated with iron. Bearing this point in mind, it is anticipated that future geophysical surveys of lead-smelting sites should make significant contributions in the furthering of our understanding of how these sites functioned.

We would like to acknowledge the following organizations and individuals. Firstly we would like to acknowledge the financial support from the Natural Environment Research Council, the University of Bradford, the British Academy and the North Yorkshire Moors National Park Authority which enabled the research to proceed. Secondly we would like to thank the residents and landowners who have given access to sites, particularly in North Yorkshire. Mr Richardson of Arden Estates, Mr Stoney at Kyloe Cow Beck and Mrs and Mr Dowkes of Timberholme have shown a continuing interest in our research work. A special thank you

to N. Redhead who provided the Castleshaw furnace and also to Mr. Payne who allowed the Lock Farm experiment to take place on his land. We are also indebted to Dr Kamei and Mr Marukawa for their assistance at Lock Farm. Lastly we would also like to thank P. Halkon, M. Gill, G. Blacker, C. Heron and M. Vernon who assisted at various stages of the research and the anonymous referees for their constructive comments.

## References

AL-MUSSAWY, S. N. 1990. Magnetic study of some slag sites located in Stumpf-forest, West Germany. *Archaeo-physika Naturwissenschaftliche Beitrage zur Archaologie*, **12**, 409–427.

BARTLETT, K. S. 1971. 70/49 Middlestown, West Riding. *Yorkshire Archaeological Register.*

BLACKER, G., BARLEY, M. & MOOREHOUSE, S. 1996. Post Medieval iron production in Nidderdale and an association with the Ingilby and Yorke Families. *In: Memoirs 1996.* British Mining No. 57. Northern Mine Research Society, Sheffield, 134–149.

CLARK, A. 1990. *Seeing Beneath the Soil.* Batsford, London.

COWPER, H. S. 1898. Excavations at Springs Bloomery (iron smelting-hearth) near Coniston Hall, Lancashire, with notes on the probable age of the Furness bloomeries. *Archaeological Journal,* **55**, 88–104.

CRANSTONE, D. 1992. Conclusion: the way forward. *In:* WILLIES, L. & CRANSTONE, D. (eds) *Boles and Smeltmills.* Historical Metallurgy Society, Matlock Bath.

CREW, P. 1985. Bryn y Castell Hillfort, Ffestiniog: a late prehistoric ironworking centre in North Wales. *Journal of the Historical Metallurgy Society* **19**, 142.

—— 1989. Excavations at Crawcwellt, Trawsfynydd, North Wales. *Journal of the Historical Metallurgy Society*, **23**, 124.

—— 1991. The experimental production of prehistoric bar iron. *Journal of the Historical Metallurgy Society*, **25**, 21–36.

FINNEY, T. 1997. *The Investigation and Characterisation of the Rievaulx Ironworks through Slag Analysis.* Undergraduate Dissertation, Department of Archaeological Sciences, University of Bradford.

FLUCK, P. 1990. Le Samson: ateliers et habitats d'une mine d'argent du XVIeme siecle. In: *Pierres et Terre*, 34, Federation Patrimoine Minier, Ste. Marie-aux-Mines, 116–119.

GILL, M. C. 1992. An outline of the chemistry of lead smelting. *In:* WILLIES, L. & CRANSTONE, D. (eds) *Boles and Smeltmills.* Historical Metallurgy Society, Matlock Bath.

GOLDENBERG, G. 1990. Die montanarchaologische prospektion – methoden und ergebnisse. *Freiburger Universitatsblatter*, **109**, 85–113.

HESSE, A., BOSSUET, G. & CHOQUIER, A. 1986. Reconnaissance electrique et electro-magnetique de sites et de structures de metallurgie ancienne. *Prospezioni Archeologiche*, **10**, 71–77.

MCDONNELL, G. 1993. Further investigations at Crift Farm, Lanlivery. *Journal of the Trevithick Society*, **20**, 48–50.

—— 1995. Ore, slag, iron and steel. *In:* Abstracts for *Iron for Archaeologists Workshop*, Occasional Paper No. 2. Plas Tan y Bwlch, Snowdonia National Park Study Centre, 3.

——, DOCKRILL, S., HERON, C., STARLEY, D. & TIRPAK, J. 1992. Geophysics and slag analysis at Grinton smeltings. *In:* WILLIES, L. & CRANSTONE, D. (eds) *Boles and Smeltmills.* Historical Metallurgy Society, Matlock Bath, 48–50.

MILLS, A. & MCDONNELL, J. G. 1992. The identification and analysis of the hammerscale from Burton Dassett, Warwickshire. *Ancient Monuments Laboratory Report No.* **47/92**. English Heritage, London.

PANITZKI, M. 1994. *Eine Hochauflosende magnetische Kartierung eines Eisenverhuttungsplatzes in Gohlen (Sudwestmecklenburg).* Diplomarbeit, Institut fur Geophysik der Christian-Albrechts-Universitat zu Kiel.

RAISTRICK, A. 1926/27. Notes on lead mining and smelting in West Yorkshire. *Transactions of the Newcomen Society,* **7**, 81–96.

REDHEAD, N. 1993. *Spa Clough, Castleshaw: second interim excavation report.* The Greater Manchester Archaeological Unit, Manchester.

RUFFELL, A. & WILSON, J. 1997. Near-surface investigation of ground chemistry using radiometric measurements and special gamma-ray data. *Archaeological Prospection,* **5**, 203–215.

SCHMIDT, A. & MARSHALL, A. 1997. Impact of resolution on the interpretation of archaeological prospection data. *In:* SINCLAIR, A., SLATER, E. & GOWLETT, J. (eds) *Archaeological Sciences 1995*. Oxbow Monograph 64. Oxbow, Oxford, 343–348.

——, MCDONNELL, G. & VERNON, R. 1998. Advanced magnetometry for the characterisation of early iron-working sites. *Annales Geophysicae*, **16**, Supplement I, C228.

SMEKALOVA, T., VOSS, O. & ABRAHAMSEN, N. 1993. Magnetic investigation of iron-smelting centres at Snorup, Denmark. *Archaeologia Polona*, **31**, 83–103.

TYSON, L. O., SPENSLEY, I. M. & WHITE, R. F. 1995. *The Grinton Mines*. British Mining No. 51. Northern Mine Research Society, Sheffield.

VERNON, R. W. 1995. *Development of Geophysical Techniques for Studying Early Iron Smelting Sites*. MSc Dissertation, Department of Archaeological Sciences, University of Bradford.

——, MCDONNELL, G. & SCHMIDT, A. 1998. The geophysical evaluation of an iron-working complex: Rievaulx and environs. *Archaeological Prospection,* **5**, 181–201.

WILLIES, L. & CRANSTONE, D. (eds) 1992. *Boles and Smeltmills*. Historical Metallurgy Society, Matlock Bath.

# Euler deconvolution methods used to determine the depth to archaeological features

RUTH E. MURDIE[1], PETER STYLES[2], PAULA UPTON[1], PHIL EARDLEY[1] & NIGEL J. CASSIDY[1]

[1]*Department of Earth Sciences, Keele University, Keele, Staffordshire ST5 5BG, UK*

[2]*Department of Earth Sciences, Liverpool University, Brownlow Street, P.O. Box 147, Liverpool L69 3BX, UK*

**Abstract:** Field techniques, instrumentation and data processing for geophysical location of archaeological remains are now at such a standard that clear maps of the subsurface detail are readily obtainable. Magnetic gradiometry and resistivity plots are widely used to locate diverse features such as walls, ditches and burial areas. However, information concerning the depth to these features is not often extracted from such plots and would be useful in planning any following excavation. Here we use Euler deconvolution methods, on a reasonably high-resolution magnetic gradiometer data set, to determine the depth to a buried Romano-British villa at the Wroxeter archaeological site. The interpretation of these depth estimates is compared to GPR sections taken over the same site.

The Wroxeter archaeological site in Shropshire has been the subject of recent intense geophysical investigation (Barker *et al.* 1997; Wroxeter Hinterland Project, University of Birmingham). Although the remains of the Romano-British city of Viroconium Cornoviorum have been the focus for much archaeological exploration over the last hundred years, a large proportion of the area within the still extant city ramparts remains unexcavated. Some 90% of this land is now covered by grazing pasture and parch marks evident in dry summers, indicated that extensive wall footings survive beneath much of the area. Detailed magnetometry and resistivity surveys, conducted as part of the Wroxeter Hinterland project, have produced an extensive and detailed street plan of the whole Roman town (Gaffney & Linford 1997).

The field work carried out for this exercise was completed on a University final year student field weekend over a specific target. The task was to survey an area using a Geoscan fluxgate gradiometer. The survey was completed in six grids of 10 m × 10 m with a point spacing of 0.25 m along each line, a line spacing of 0.5 m and at 0.1 nT resolution. Data processing only included spike, mean and trend removal for each grid. Despite the inexperience of the operators, the final plot of this 20 m by 30 m area clearly shows the outline of a building (Fig. 1a) which is interpreted as shown in Fig. 1b. The walls appear as negative magnetic anomalies compared to the positive anomalies of the more magnetic soils as has been noted in this area of the city by other authors (Tabbagh *et al.* 1997). These authors have

*From:* POLLARD, A. M. (ed.) 1999. *Geoarchaeology: exploration, environments, resources.* Geological Society, London, Special Publications, **165,** 35–40. 1-86239-053-3/99/$15.00

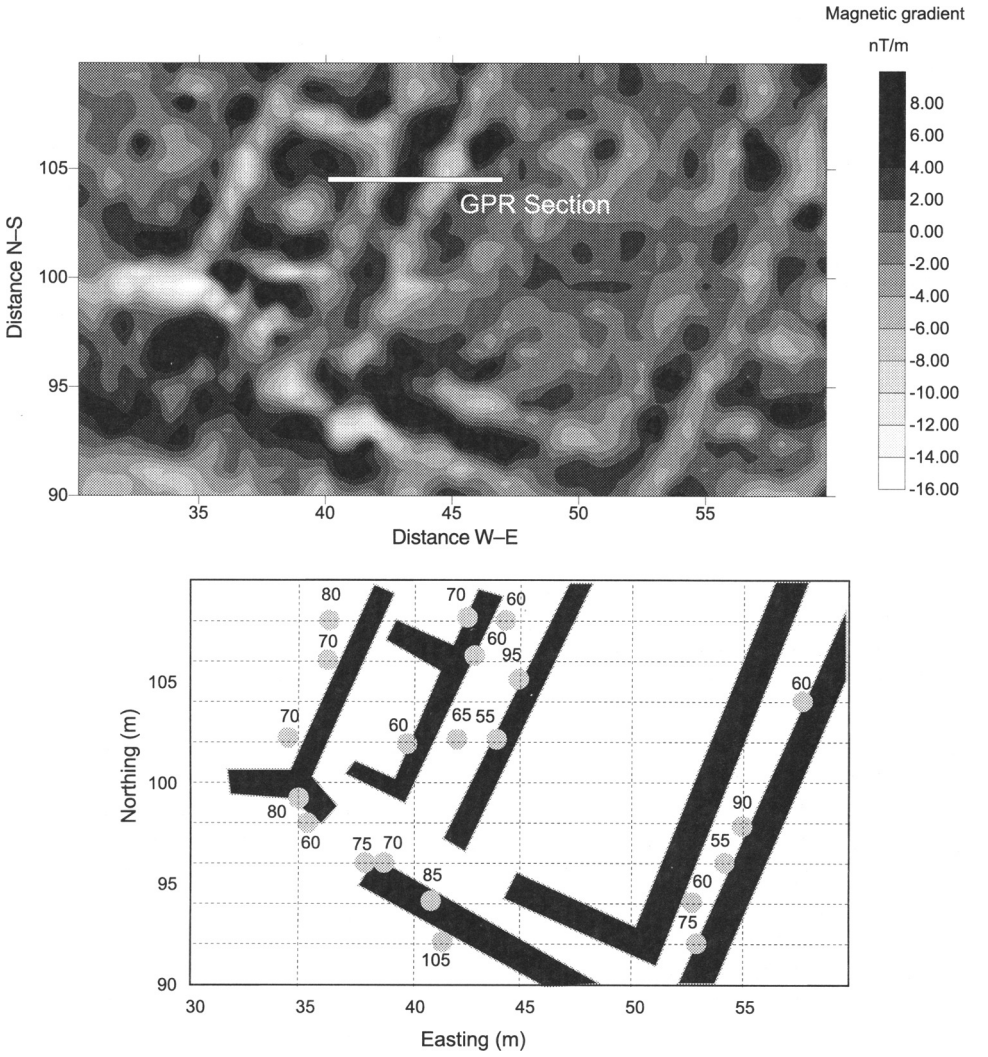


**Fig. 1.** (**a**) Magnetic gradiometer map over the site of a Romano-British Villa at Wroxeter. (**b**) Interpretation of the magnetic gradient map (Fig. 1a) showing the inferred positions of the walls of the villa. The dashed lines are those profiles selected for deconvolution and the grey spots are the depths to the features as deduced by Euler deconvolution.

had some success in using spectral analysis methods, including the analytical signal to enhance the delineation of the position of features, but have not extended their analysis to the determination of their depth.

This particular site was a good area to study as the underlying building had been partially excavated in 1952–1953 and the trenches had subsequently been filled in. From Kenyon (1975), it is possible to correlate the features seen on the trench sections to the results found by the Euler deconvolution methods and GPR (Ground Penetrating Radar). The digs found several episodes of habitation evident in the layers of building and associated rubble.

## Euler deconvolution theory

Euler deconvolution is a method for locating the sources of potential fields based on both their amplitudes and gradients and estimates the probable geometry of the causative body. Previous theoretical and actual examples used to test Euler deconvolution have been on the larger geological scale (Thompson 1982; Reid *et al.* 1990) to look at the depth of sedimentary basins and their bounding faults, dykes and intrusions. However, it has been recently used for microgravity studies of abandoned stope workings in Gold Mines (Styles pers. comm.). The method has been successful in determining the depth to the edges of the features. The theory is exactly the same for archaeological purposes, except on a sub-metre scale.

Potential fields such as gravity, magnetism and their spatial derivatives are solutions of Laplace's equation and also satisfy Euler's equation of inhomogeneity

$$(x - x_0)\frac{\partial V}{\partial x} + (y - y_0)\frac{\partial V}{\partial y} + (z - z_0)\frac{\partial V}{\partial z} = -nV$$

The derivatives of the continuous field $V$ satisfy the above homogeneous equation of degree $n$, where $n$ is known as the structural index. This is an indicator of the fall-off rate of the field with distance $r$ and depends on the geometry of the suspected body (e.g. line, point, sphere or any combination thereof) and the particular field type (Thompson 1982). Hence, for a field which is measured at point $(x, y, z)$, the gradients in these directions can be calculated. If one knows or can obtain the values of the derivatives of the field at four or more locations $(x, y, z)$, and can make an estimate for $n$, one can solve for the location of the causative body, $(x_0, y_0, z_0)$ by a least-squared inversion matrix.

In the investigated case, we have the vertical gradient of the vertical component of the magnetic field as our value for V. Usually, for magnetic data, preprocessing is required to separate the local field from the regional field. However, for magnetic gradient data, the regional field is already removed.

Software developed at Liverpool University was used to solve for the depth to an anomaly. The horizontal derivative was calculated from the difference between adjacent values divided by the point separation. We are able to deduce the vertical derivative from the data because the potential field satisfies Laplace's equation. It is calculated via the Fourier domain by multiplying each frequency by $k$, the wave number (where $k = 2\pi/\lambda$). If it can be assumed that the body is $2D$ in shape i.e. a wall, then $d^2y/dx^2 = 0$, so the second derivative of the magnetic gradient equals zero and hence the 2D version of Laplace's applies (in $x$ and $z$). The software as yet only operates in 2D i.e. along a profile line. Profiles were extracted across the area, perpendicular to the main features and also in E–W and N–S lines. A window of 15–20 points (i.e. 7.5–10 m) is moved across the data, and solutions for $(x_0, y_0, z_0)$ are obtained. A window of 15–20 points was chosen as it gave enough solutions to define the body. Too few points give unstable solutions and high least-squares errors; too many points give too few solutions to describe the body. The exact value is chosen iteratively. The structural index used assumed that the anomaly was caused by a vertical tabular body, i.e. $n = 1$.

Only those locations of $(x_0, y_0, z_0)$ which are solutions for several windows are considered real. Figure 2 shows an E–W profile taken across a line 98 m north running from 30 to 60 m E–W. The clustering of circular markers around 6 m indicates a

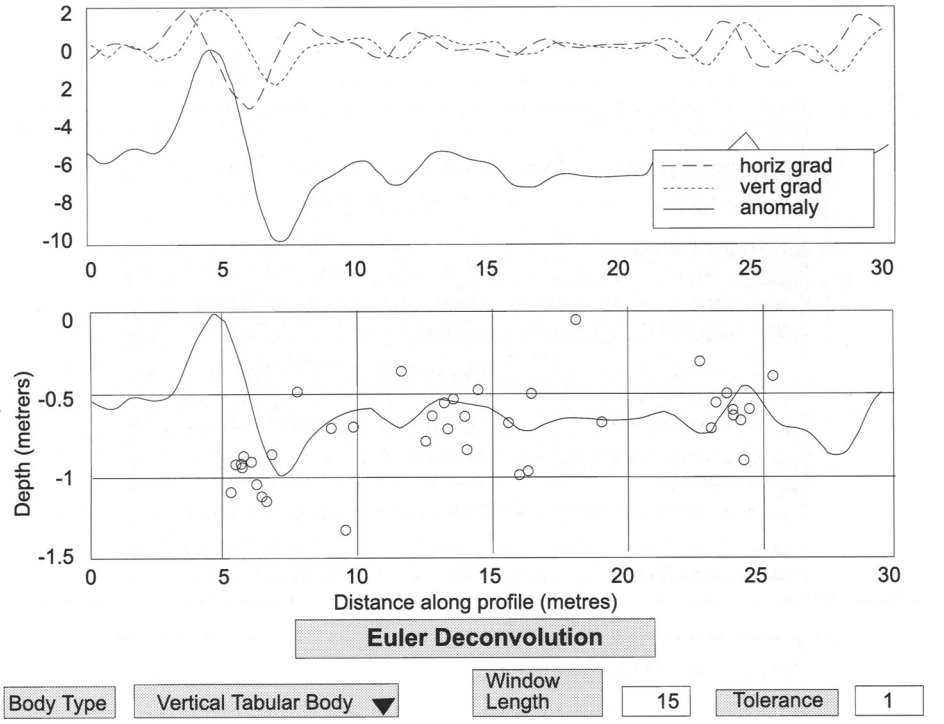


**Fig. 2.** Screen capture of the output from the Euler deconvolution anaylsis program for a profile 98 m north and 30–60 m East. The figure shows the clustering of solutions at about 6 m along the profile at a depth of about 0.9 m. The scattered individual solutions come from a single window position and are not considered to be valid solutions.

good solution to the equations at that point. Single markers are discounted as these are only solutions for only one of the windows and therefore unlikely to be real. A map was then made of the locations and depths indicated by the clusters of markers (Fig. 1b). It can be seen that the clusters lie along the edges of the walls. The depth to these clusters is fairly consistent, being about 0.65–0.95 m deep. It is interpreted that the depth indicated by the Euler deconvolution is the depth to the floor of the building. As seen from the excavated portion of the city, this would have been of bricks or tiles similar to those found else where on the site which would have a greater magnetic signature than the sandstone walls of the building.

## GPR section

To confirm the depths to the floor of the building, a ground penetrating radar was taken over a short section of the area (Fig. 1a) using a Pulse EKKO 1000 system. The section produced is given in Fig. 3a. The two-way travel times are converted into depth using the Sensors and Software program supplied with the radar system using a uniform velocity of $0.08 \times 10^9\ \mathrm{ms}^{-1}$ (the suggested values for a substrate somewhere between silt and sand). The walls of the building are clearly seen as hyperbolic diffraction arcs on the GPR profile at a depth of about 0.6 m at 2 m across and 0.35 m at about 5 m along the section (Fig. 3b). This correlates almost exactly with the

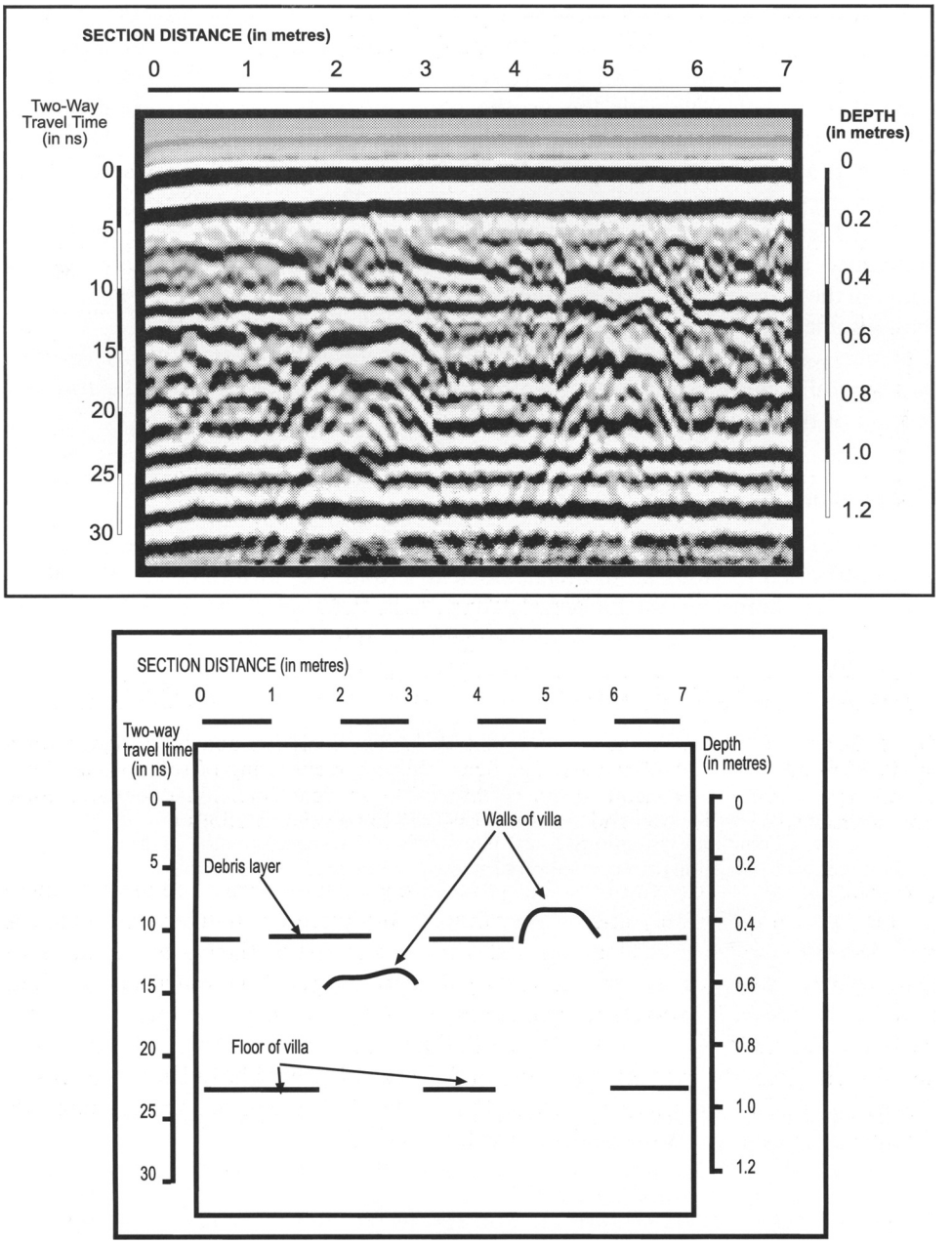


**Fig. 3.** (**a**) GPR section for a 900 MHz antenna taken along the section marked in Fig. 1a. The positions of the walls are clearly seen as diffraction arcs and the intervening floors as flat-lying reflectors at about 1 m depth. (**b**) Interpretation of the GPR section of Fig. 3a.

excavations of Kenyon (1975). The thickness of the walls is seen to be about 1 m wide although it should be remembered that the section was not taken perpendicular to the walls. Standing walls measured at the site range from about 0.5 to 1 m wide. To either side of the walls the next clear reflector is seen at depths of 1 m on either sides of the

two walls and possibly slightly shallower at 0.7 m between them. This reflector is interpreted as the flat floor of the building which was made of mortar and lay at about 3–4 feet (approximately 0.9–1.2 m) deep (Kenyon 1975). These values to the floor of the building correlate well with the depths obtained from the Euler deconvolution methods.

There is a continuous reflector at about 0.5 m depth that also lies at the lower limit of the values obtained by the Euler deconvolution. This reflector is disrupted by the walls and is interpreted as a rubble layer that was found to overlay the ruins during excavation (Kenyon 1975). It is possible that along the GPR profile, the difference between the magnetic properties of the walls and the soil has given a gradient anomaly that is sufficiently large to appear as a solution to the Euler deconvolution.

Hence, we can estimate that there is not much of the walls left standing as we interpret the differences in estimated depths to be the difference between the top and bottom of the walls and the floors of the building.

## Conclusion

The application of the Euler deconvolution method appears to give good estimates of depth of buried features in an archaeological setting. Depth estimates obtained by magnetic gradiometry can be correlated with features seen on the GPR section over same target. These methods of obtaining depth estimates has the advantage over GPR in that it utilises data that has already been collected rather than employing another instrument. This type of estimation can be applied to other potential field methods such as gravity (Cuss & Styles 1999) and the various components of the magnetic field.

We would like to thanks English Heritage for permission to work on the site, the School of Archaeology, Classic and Oriental Studies, University of Liverpool for the loan of a fluxgate gradiometer and two anonymous reviewers for their comments on the script.

## References

BARKER, P. A., WHITE, R. H., PRETTY, K. B., BIRD, H. & CORBISHLEY, M. 1997. *The Baths Basilica Wroxeter: excavations 1966–90*. English Heritage, London.

CUSS, R. J. & STYLES, P. 1999. The application of microgravity in industrial archaeology: an example from the Williamson tunnels, Edge Hill, Liverpool. *This Volume*.

GAFFNEY, C. F. & LINFORD, P. 1997. The application of geophysical techniques at Wroxeter Roman City. *Proceedings of the 1997 CAA Conference*, British Archaeological Reports International Series 750 (1999), 161.

KENYON, K. M. 1975. Excavations at Viroconium in Insula 9 1952–3. *Transactions of the Shropshire Archaeological Society*, **LX**, 5–74.

REID, A. B., ALLSOP, J. M., GARNER, H., MILLETT, A. J. & SOMERTON, I. W. 1990. Magnetic interpretation in three dimensions using Euler deconvolution. *Geophysics*, **55**, 80–91.

TABBAGH, A., DESVIGNES, G. & DABAS, M. 1997. Processing of Z gradiometer magnetic data using linear transforms and analytical signal. *Archaeological Prospection*, **4**, 1–13.

THOMPSON, D. T. 1982. EULDPH: A new technique for making computer-assisted depth estimates from magnetic field data. *Geophysics*, **47**, 31–37.

# The application of microgravity in industrial archaeology: an example from the Williamson tunnels, Edge Hill, Liverpool

ROBERT J. CUSS[1] & PETER STYLES[2]
[1]*Department of Earth Sciences, University of Manchester, Oxford Road, Manchester, M13 9PL, UK*
*(Present address: British Geological Survey, Keyworth, Nottingham NG12 5GG, UK)*
[2]*Department of Earth Sciences, University of Liverpool, Brownlow Street, Liverpool L69 3BX, UK*

**Abstract:** This article presents the results of a high-resolution microgravity survey which was successful in delineating the 150-year old Williamson tunnels beneath inner-city Liverpool, England. The tunnels, which date from the Napoleonic Wars, lie at depths of *c.* 5 to 15 metres, and are poorly mapped because of several phases of later development and subsequent dereliction. The 'brown-field' nature of this site created substantial noise signals which required the application of careful terrain corrections and second derivative and Euler deconvolution methods to isolate and identify the tunnel signatures. Successful delineation was only possible because of a comprehensive initial desk study and prior modelling, which assessed the likely depths and conditions of the impassable tunnels and allowed appropriate techniques and survey parameters to be determined.

Non-intrusive geophysical methods are becoming more commonly applied in archaeological and engineering investigations for the detection of voids such as burial chambers, limestone caverns and abandoned historic mine-workings, as an alternative to traditional methods. Geophysical methods, which rely upon differences in resistivity, conductivity, density, magnetization, and dielectric permittivity between rock and air, have increasingly been used in void detection through the application of resistivity tomography, seismic reflection, ground-penetrating radar, magnetometry, and microgravimetry. However, all geophysical methods have limitations imposed upon them by their inherent resolution thresholds and the noise component of any recorded signal. There is substantial field experience of microgravity for engineering purposes, although archaeological targets in 'brown-field' sites have rarely been surveyed.

After evaluating all the possible geophysical methods, it was concluded that only microgravity had the potential to delineate the 150-year old Williamson tunnels which lie beneath Edge Hill, Liverpool. Although the survey site is small, the terrain is severe with several 5–7 m vertical drops and the site was found to have been seriously affected by redevelopment and dereliction in several areas, leading to a complex interaction between surface and sub-surface gravity sources. However, consideration of the development history and geology of the area allowed the rejection of many features, giving increased confidence in the identification of the other features as tunnels.

*From:* POLLARD, A. M. (ed.) 1999. *Geoarchaeology: exploration, environments, resources.* Geological Society, London, Special Publications, **165,** 41–59. 1-86239-053-3/99/$15.00

Microgravity has not yet been widely applied in extensively redeveloped inner-city urban areas; this investigation demonstrates the applicability of the technique to industrial archaeological studies within such areas.

## Joseph Williamson and the construction of his tunnels

Joseph Williamson (1769–1840), a Liverpool philanthropist known as 'The King of Edge Hill', was born into a poor Warrington family, and at the age of eleven moved to Liverpool to find employment. After apprenticeship with the tobacco merchant Richard Tate he married Tate's daughter Elizabeth in 1802 and ran the company until 1818. Williamson then retired from the company to his Mason Street mansions after amassing considerable wealth.

Williamson employed local men to construct a number of mansions on land he had purchased at Long Broom Field, Mason Street in 1806 under the Waste Lands Commission. After their completion, he continued to employ the men to construct a tunnel system under his land with a Norman-arch brick-lined roof geometry, probably initially from the low western side of his land. Although vaulting of the tunnels was unnecessary due to the strength of the rock, spectacular brick arches were produced. Construction occurred randomly, with pits, wells and blind passages creating a tunnel-system many miles long 1–15 m below the surface, 1–12 m wide, and up to 15 m high (Hand 1916, 1927). The quarried rock was utilized in the construction of the houses, walls, and ornate archways, some of which are still evident.

Williamson left little money as his tunnels had cost an estimated £100 000 (the equivalent of around £25 million at today's value) and his estate valued at £39 000 fell into disrepair and the location of the tunnels became lost.

## Redevelopment of the site

Williamson's land remained untouched until the council assumed control in 1858, and the area was divided up, developed and then redeveloped over time. The Army used the main upper terrace including Williamson's mansion houses (Fig. 1, area 1) as store houses until 1902 when most of the larger buildings were demolished and the majority of the tunnel system bricked-up for security reasons. The army retained control until the 1950s when small industrial units were constructed, one of which incorporates Williamson's original house frontage. The tunnels can be accessed from this now derelict site.

The council kept the lower terrace of the estate (Fig. 1, area 2), constructing the City Stables in 1860 which still stand. Complaints of odours in this area (Anon 1867) were attributed to the local residents using the tunnels as a sewer system, and so many tunnels were destroyed or covered up, although three tunnel entrances are still accessible.

The 1898 OS map shows the houses Williamson built upon Grindfield Hill wastelands (Fig. 1, area 3) to be still standing but surrounded by densely populated terraces along Grindfield Street and Congress Street. Since then these houses have been demolished and the area has been resurfaced and has become a wasteland.

The Army survey suggests that Williamson constructed tunnels outside of the northern boundary of his land (Fig. 1, area 4). By 1898 this area was also densely populated with terraced housing, most of which was demolished during the development of the Archbishop Blanche School in the 1960s. Although several boreholes were drilled during the construction of this school, no tunnel discoveries were documented.

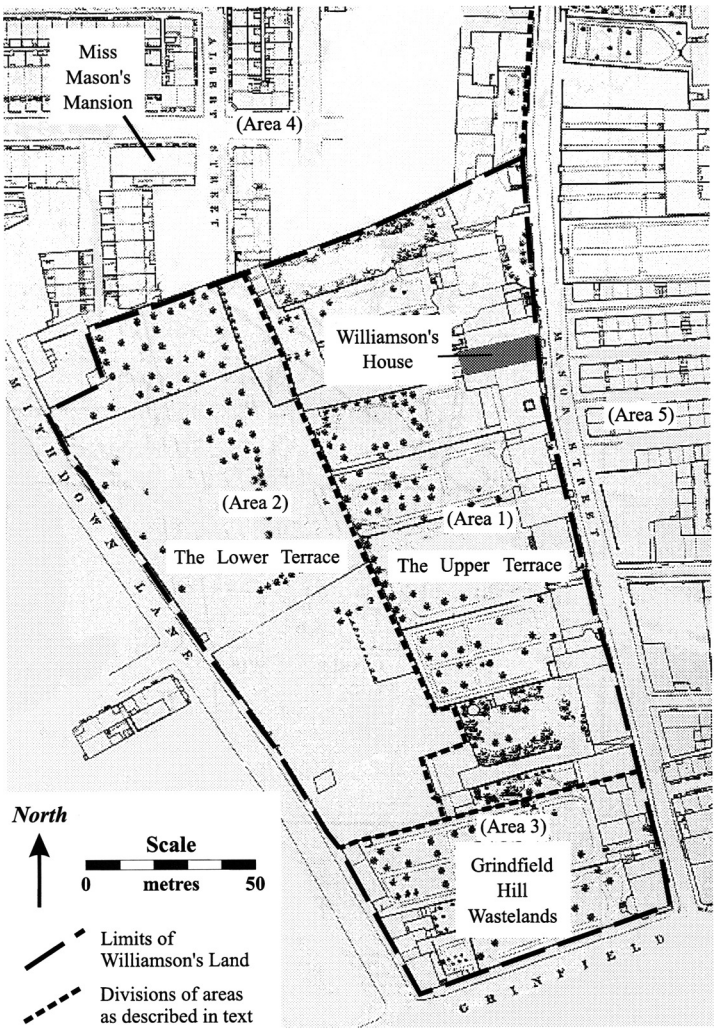


**Fig. 1.** 1847 Ordnance Survey map of Williamson's land soon after his death showing the location of his houses and gardens.

By 1898, Williamson's houses on the eastern side of Mason Street (Fig. 1, area 5) were intermingled with terrace developments. Part of this site was developed in the 1930s with the construction of tenement flats to ease the problem of inner-city crowding: these flats are now derelict. Tunnels were discovered during their construction but were not fully documented and were probably destroyed. Council houses, which are still inhabited, replaced the terracing between Helsby Street and Shimmin Street.

## Previous investigations of the survey site

A 1903 Army survey provides a map and cross-section of the system, displaying what was assumed to be both a typical and a maximal tunnel. The typical tunnel is a $1.8 \times 2.4$ m Norman-arch structure, with the largest feature being the

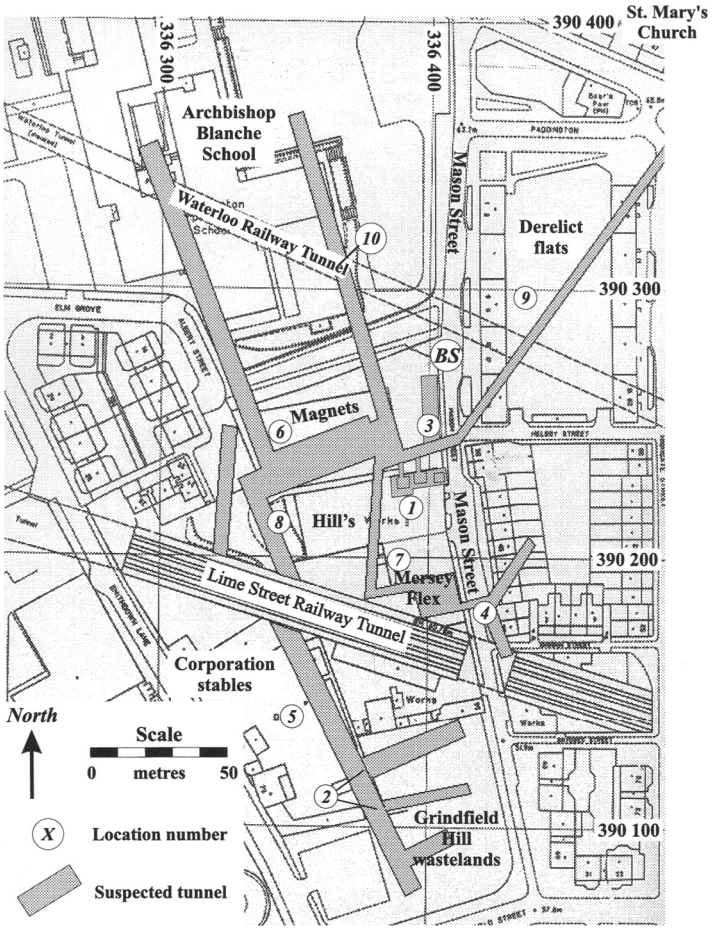


**Fig. 2.** Map showing the survey site, with a summary of the tunnel-system as described by previous surveys, and features noted during site reconnaissance as described in text.

45 × 18 × 12 m Great Hall at 4.5 m depth. This survey shows several tunnels within Williamson's land, and has been incorporated into Fig. 2 which summarizes previous surveys.

## Techniques for void detection

In engineering terms, the presence of voids within the rock mass lead to restrictions in development and may result in collapse which can seriously damage building infrastructure. Prior to re-development the most common method used to identify and define the spatial extent of cavities has been to drill a detailed borehole grid over the target area. The zone of sampling of a borehole is extremely small and can compromise the integrity of the very structure it is meant to sample. There are many physical properties that are significantly different for rock and air which geophysical methods can detect, including conductivity, density, dielectric permittivity,

magnetization, and resistivity. Thus, the application of seismic reflection, gravimetry, ground-probing radar (GPR), magnetometry, and resistivity tomography surveying techniques all offer the potential for void detection (Owen 1983). However, these methods have limitations imposed upon them by the ambient and cultural noise component of the recorded signal which may be too great for the different techniques within this area. Seismic reflection was not possible because of the difficult terrain and high ambient noise levels present in the area. Although magnetometry can be utilized in the search for man-made archaeological features, such as mine workings (Clarke 1986), it has rarely been reported. In 1959, Dr C. D. V. Wilson of the University of Liverpool conducted an unpublished feasibility study for the City Architect's Department into the possible detection of the tunnel system using geophysical methods. He concluded that resistivity would be adversely affected by noise, and that detection would be too difficult by this technique. His calculations showed that the tunnels could only be detected by magnetometry if they were filled with iron, while gravimetry and seismic techniques at that time were inadequate to detect the expected small features. Wilson thus concluded that currently available geophysics techniques were unlikely to delineate the system.

While resistivity tomography can be effective in detecting voids (Noel & Xu 1991), the difficulties of access and the limited resolution for this depth range made it inappropriate for this site. GPR can be very effective for cavity detection in materials of low conductivity like sandstones (Davis & Annan 1989) and would be an appropriate technique as part of a follow-up study in targeted areas identified by microgravimetry.

## Microgravimetry

The microgravity technique in the context of archaeology consists of measuring minute variations in the gravitational pull of the Earth created by variations in density and interpreting the presence of voids and cavities, which are generically termed targets, from these readings. The most common natural targets are solution cavities such as swallow holes and sinkholes in limestone, whilst man-made cavities include mine-workings, tunnels and archaeological tumuli. The value of the Earth's gravity is approximately $9.81\,\mathrm{m\,s^{-2}}$ in units of gravitational acceleration but microgravity anomalies are quoted as microgals (μgal), where 1 gal is $0.01\,\mathrm{m\,s^{-2}}$. Thus, the Earth's gravity is about 980 000 000 μgal, whilst variations of significance in cavity detection are generally between 5 and 200 μgal. For example, Williamson's Great Hall would create a 550 μgal gravity anomaly, which is half of the expected anomaly for the 26 m deep and 18 m wide Lime Street railway tunnel.

In order to detect subsurface voids there needs to be a contrast in density (termed $\mathrm{d}\rho$) between the target and the surrounding bedrock. Air-filled cavities offer the largest anomaly condition ($\mathrm{d}\rho = -2.5\,\mathrm{g\,cm^{-3}}$) because of the complete absence of dense material in the target. Water-filled and rubble-filled cavities have a lower contrast ($\mathrm{d}\rho = -1.5\,\mathrm{g\,cm^{-3}}$ and $\mathrm{d}\rho = -1.0\,\mathrm{g\,cm^{-3}}$ respectively), resulting in gravity anomalies 60% and 40% respectively of that of an air-filled feature. However, as a consequence of the formation of a void, fractures develop which may extend for two or more diameters away from the cavity (Daniels 1988). The size of a target is thus dependent not only on the strict volume of the cavity, but also on this secondary halo effect, which increases the apparent target size, ensuring that a cavity can be indirectly sensed (Chamon & Dobereiner 1988; Bishop *et al.* 1997, Patterson *et al.* 1995).

Microgravity surveying has improved considerably over the last ten years with the development of high-resolution equipment, and, allied with careful field acquisition techniques and sophisticated reduction and analysis methods, these anomalies can be detected and interpreted. The method is becoming widely used in engineering investigations, having the advantage of leaving the ground undisturbed. This allows not only the determination of the location of features, but also provides information on their depths and geometries. Target location depends upon the ratio of noise to the anomaly of interest, with resolution decreasing with depth, and upon the ratio of survey-point spacing to target dimension. Multiple traverses with closely spaced gravity stations, or the collection of data on a regular grid, result in improved data accuracy that can be used to separate the cavity's localized effect, from the predictable long-wavelength field created by topography, latitude and regional geological variations. Although, numerous microgravity case studies exist (see following section), microgravity has not been used extensively in 'brown-field' sites; however, it represents the only viable field-method in this area.

## Previous microgravity surveys

The literature records some early examples of the application of microgravity techniques to detect cavities (Fajklewicz 1956, 1976; Colley 1963; Neumann 1967; Arzi 1975; Butler 1984). The success of these studies in delineating and modelling subsurface geometries led to the development of field methods and development of data processing techniques. Fajklewicz (1976) and Butler (1984) both investigated the vertical gravity field to enhance feature recognition and modelling. Estimates of anomalous 'missing-mass' can be obtained using Gauss' theorem and proved by repeat surveying (Arzi 1975).

Ferguson & Styles (1992), Emsley *et al.* (1992), Bishop *et al.* (1994, 1997) all describe the utilization of the microgravity technique using gridded maps of data in the detection of both karstic and man-made cavities. The papers also describe how the resulting data can be enhanced by image-processing to better define the anomalies associated with the targets. Patterson *et al.* (1995) used the method in detection of dissolution subsidence in gypsiferous Permo-Triassic strata in Yorkshire. They calculated their accuracy to be *c.* 4 μgal, and postulated that voids as small as 4 m in diameter might be detected in the right circumstances to 12 m depth.

Microgravity has the potential to delineate natural or man-made void systems in an effective non-destructive manner, with accuracy dependent upon survey-point spacing and site coverage. Bishop *et al.* (1997) concluded that the technique should be coupled with the results of a comprehensive desk study, including knowledge of the site geology and topography, and followed up by specifically targeted borehole investigations. Using all this information, anomalous ground conditions can be accurately described, delineated and where necessary, successfully treated.

## Survey design

Preceding the acquisition of gravity data, a comprehensive desk study, modelling, and site reconnaissance is necessary to determine the nature of the target and to design the survey specifically for this target. Existing data were studied to establish target size, allowing survey point separation to be determined, and the location of desirable

survey sites was determined from maps with the position of surveyable points determined by their accessibility.

Survey point separation was determined by consideration of the dimensions of the targets which were obtained from the Army survey and field observations. A typical sized tunnel was assumed to be a $1.8 \times 2.4$ m Norman-arch feature, and this was mathematically modelled over a range of depths with density contrasts of $-2.0\,\mathrm{g\,cm^{-3}}$, $-1\,\mathrm{g\,cm^{-3}}$, $-0.5\,\mathrm{g\,cm^{-3}}$ to simulate air-filled, water-filled, and rubble-filled tunnels within sandstone. The detectability of the calculated gravity anomaly deteriorated as point-spacing increased within the range 0.5 to 10 m, with feature recognition dependent upon whether a point was taken directly over a tunnel for spacings larger than 5 m. A 3 m spacing was optimal for target detection and the number of survey lines required to cover the survey site. However, it was logistically impossible, partly because of terrain, but also because of resources and time available within the scope of this investigation, to cover the whole area on a regular 3 m by 3 m grid. It was decided to have the best coverage, at 3 m by 3 m , in areas like the suspected Great Hall and to compromise with an along-line spacing of 3 m with profiles at variable spacing oriented on the basis of the strikes and position of suspected features in the other areas. We appreciate that this will necessarily have implications for the frequency resolution because of the effects of aliasing as we have produced a detailed gridded model from a variable spacing data set but even with this spacing some 1200 data points were collected which constitutes a very considerable microgravity survey. We would always recommend a regular grid as the optimum configuration for microgravity surveys but would point out that this is almost never the case in reconnaissance gravity investigations where irregularly spaced data sets are the rule rather than the exception.

Detection becomes dependent on gravimeter accuracy as features broaden and decrease in amplitude with depth. The largest expected target, the Great Hall, had dimensions of $45 \times 18 \times 12$ m at a depth of 4.5 m which should create a 550 μgal anomaly: the Lime Street railway tunnel, which is 18 m wide and 26 m deep, should create a 1000 μgal anomaly.

Two types of gravimeter were available for use during surveying; the LaCoste-Romberg G and Worden type gravimeters. While neither is ideal for the highest-resolution work, they can achieve good accuracies with careful field procedure. Results from the different instruments were consistent, with no adjustment needed and both were able to delineate the tunnel system satisfactorily. Ideally a LaCoste-Romberg D-meter or a Scintrex CG3-M should be used for microgravity surveys but careful field procedure is as much the key to accurate delineation of features as intrinsic resolution of the instrument.

Several old maps were acquired which displayed possible tunnel locations, as summarized in Fig. 2, which shows the tunnel system to be mainly centred around the original mansion houses, within Williamson's land, with only a few tunnels extending outside the area which were assumed to lead to local landmarks. Hand (1927) suggests that tunnels were built to St. Mary's church and an unidentified Public House: the survey was therefore extended to investigate this. Tunnelling probably began from the lower side of the site into the hill, thus it was assumed that tunnels do not exist on the low ground west of Smithdown Lane. As the larger, more elaborate, constructions are likely to be close to Williamson's house, surveying was concentrated within this area. The tunnel system may have interconnected

several of Williamson's houses, so original maps were acquired to locate these properties.

The site reconnaissance identified several features suggestive of the presence of voids within the field area, as summarized in Fig. 2. Tunnel entrances were found at locations 1 and 2, with tunnels still accessible. Collapse features were noted at location 3 with the concrete surface displaying 1–2 m subsidence, while more subtle subsidence was identified by a curvature in the brickwork of a council house at location 4. Within the factory units at locations 6 and 7, considerable subsidence had occurred, and since surveying a major collapse has occurred at location 8. The uneven-cobbled surface at location 5 showed linear trends possibly caused by the tunnel system.

## Data acquisition

Between June and December 1994, 1243 data-points were collected during 21 field days. The base station was located as a secure corner-curb at location BS (Fig. 2) central to the survey site. This point was repeated at hourly intervals with at least five gravity readings recorded to remove the effect of drift and Earth tides. Due to logistic difficulties in achieving base stations at hourly intervals, it was necessary to establish a series of temporary base stations which were later adjusted to the main base station.

Survey lines were marked out with a 3 m point spacing on all accessible land, with location identified by clear markers on the OS map. In open-areas, a regular pattern of survey points was adopted, with a line spacing of 12 m (see Fig. 3). At every survey-point, at least three gravity readings were taken, along with a time reading, and notes

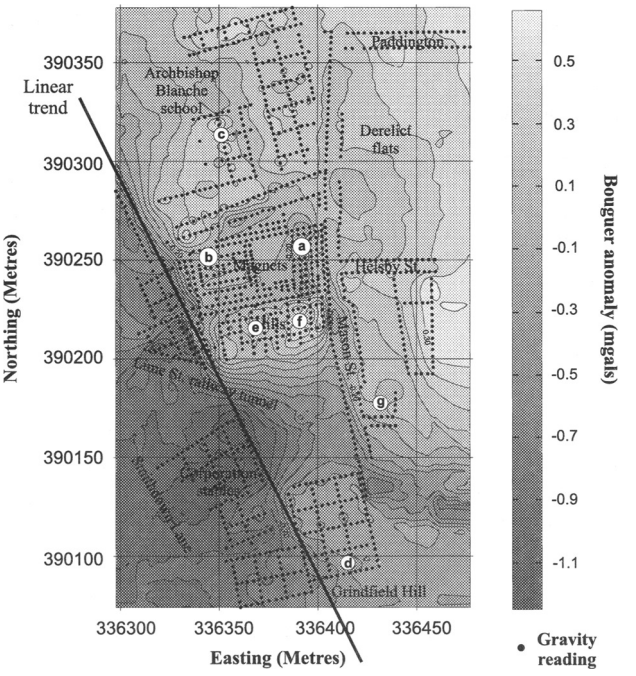


**Fig. 3.** Bouguer anomaly map of the survey site, showing all survey points.

on the condition of the location; including wind strength, amount of traffic vibration, and surface stability to explain any discrepancies. Points were marked out using surveying chalk or spray, allowing height readings to be taken after a few gravity-surveying days using conventional levelling.

With slopes of up to 45° on site, the levelling of the gravimeter becomes difficult. The levelling dish and feet of the gravimeter can compensate for some of this slope, but terraces needed to be dug to lower slope angle in steeper areas. Many of the old walls are unstable and survey points could not be taken too near to these due to the danger of collapse. Survey coverage was also limited by occupied housing as it was not practical to survey within private residences. The derelict buildings at locations 5 and 1 were surveyable but not those at locality 9 which were dangerous and the rubble surface was unsuitable for surveying.

Figure 3 shows the high number of survey points and good coverage within a significant proportion of the area of interest which resulted in a high degree of confidence in the results although some inaccessible areas resulted in locally sparse coverage.

## Data reduction

Data were reduced by computer spreadsheet which applied corrections for instrumental and Earth tides, Bouguer and Free Air effects. In some surveys it is necessary to make correction for latitude and terrain and to convert readings into absolute gravity. Small surveys of less than a kilometre in size generally do not require a latitude correction as this will be removed as part of the regional field. A terrain correction is usually calculated for individual points, this correction was made later using an interpolated data-set. Microgravity surveys are not generally concerned with absolute values of gravity, only with relative variations in the local gravity field, thus the conversion to absolute gravity was unnecessary.

Profiles were checked regularly to monitor survey progress and to ensure that anomalies were consistent with the earlier modelled results: initial checks showed a 'text-book' anomaly of $-300\,\mu$gals over the suspected position of a tunnel. The Bouguer anomaly data were interpolated onto a regular $1\,m^2$ grid which aids identification of linear features and facilitates the application of frequency domain techniques such as filtering and derivative methods. Figure 3 shows the raw Bouguer anomaly map of the surveyed area.

## Data enhancement

Although many features can be identified on the Bouguer anomaly map (Fig. 3), it is vital to process the data to aid feature recognition. The strong regional trend and effect of terrain significantly mask the smaller features created by the targets, and their removal will enhance the data. The identification of the tunnels will be simplified by calculating the second horizontal derivative of the data-set to enhance subtle linear trends created by the tunnels.

Figure 4 shows the adverse terrain within the area as interpolated using the recorded height data, spot height readings, and wall locations from an OS map. This terrain creates distinct anomalous gravity effects which may approach $500\,\mu$gals anomaly and have a significant effect over a distance of *c.* 10 m. Smaller

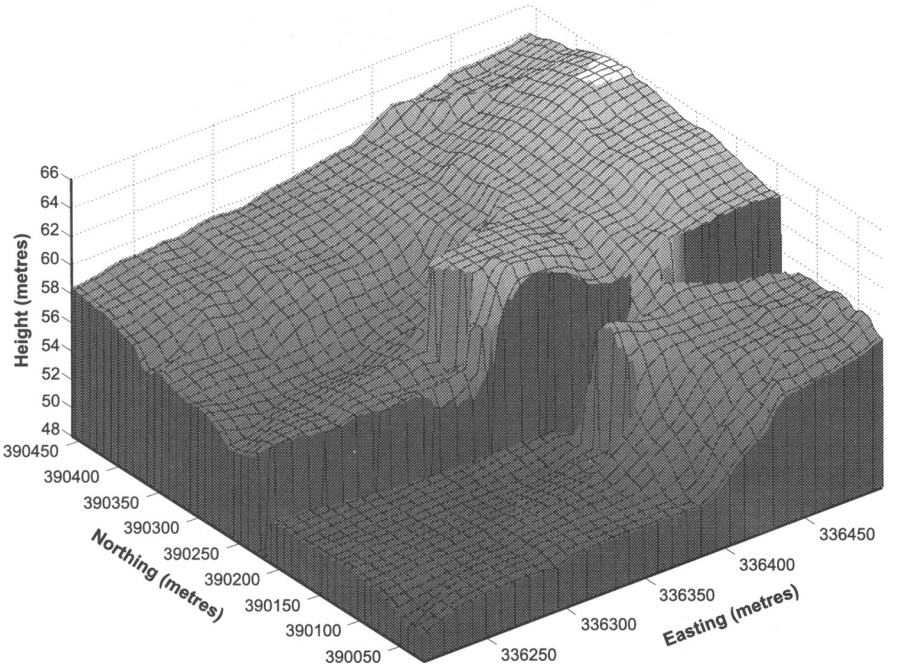


**Fig. 4.** 3-D Topographic surface of the Mason Street area, highlighting the severe terrain of the site.

features are masked by this terrain effect, necessitating the terrain correction. The circular graticule methods of Hemmer (1939) and Ballina-Lopez (1990) were found to be inapplicable as they are designed for regional scale surveys.

Ketelaar (1976) developed a method for use with regularly sampled terrain surfaces which are approximated by a $21 \times 21$ grid of square prisms with upper surfaces that slope toward the grid centre. The effect of each prism within the grid is calculated and summed to give a value of terrain correction of the centre point. Ketelaar showed that, although for moderate terrain the difference in accuracy between a $5 \times 5$ and a $17 \times 17$ grid was insignificant, severe terrain created a significant error. A slope of $7^\circ$ creates an error of 1%, with a $30^\circ$ slope creating nearly 25% error. A FORTRAN computer program was written and fully tested on simple geometric shapes, giving results which are consistent with two-dimensional modelling.

Spot heights were added to the height data to avoid edge-effects, and once the terrain correction had been calculated the border was removed. The terrain correction method fails in the proximity of the railway tunnel which has a prism slope of approximately $90^\circ$. This high-frequency error was removed by filtering the terrain correction which was applied to the raw-Bouguer anomaly results to create a terrain-corrected Bouguer anomaly map. Some residual features follow the topography and may be either due to uncorrected terrain, or geological features controlling the relief within the area. However, the removal of the terrain effect significantly improved the data-set.

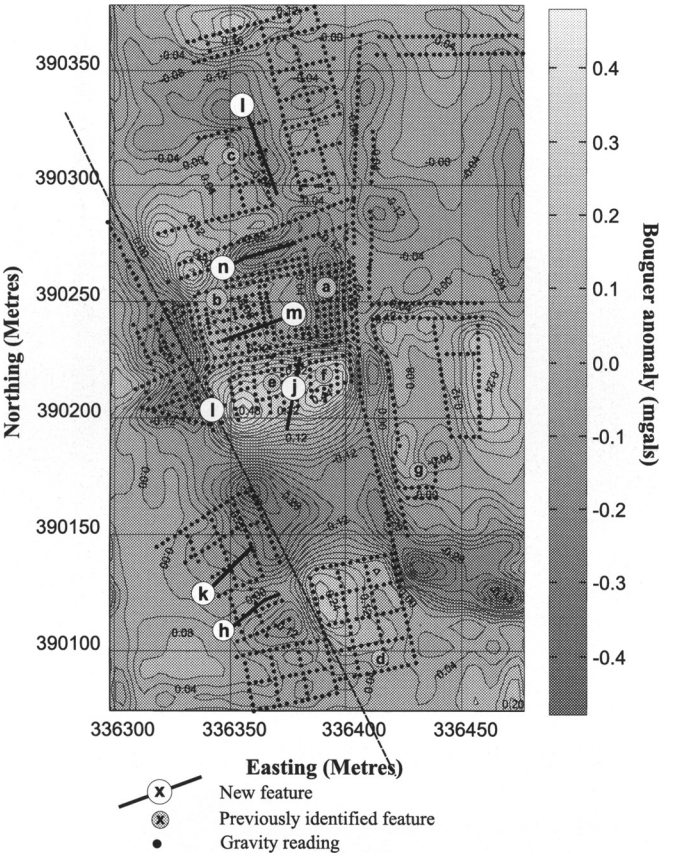


**Fig. 5.** Final Bouguer anomaly map of the Williamson tunnels site after filtered terrain correction and the removal of the regional surface.

Bouguer anomaly fields are often characterized by long-wavelength regional anomalies which are created by deeper variations in density, superimposed upon which are higher wavenumber local variations. By removing the regional anomaly it is hoped to only have the residual local anomaly which is created by shallow features of interest. The regional field can be removed by either surface fitting or upward-continuation of the data by a distance equal to the grid separation. Most commonly a low-order polynomial surface is removed from the data; in this case a third-order polynomial was removed by fitting the data in a least-squares sense (Fig. 5).

The detection of target edges can be enhanced by examining the gradients of the gravity field, as these show marked changes at boundaries. The second horizontal derivative is commonly applied for this purpose as it can be calculated very readily for gridded data using Fourier techniques (Fig. 6). The method can help to determine the nature of buried geological features, and with linear targets, should delineate the tunnel-system aiding feature recognition. In two dimensions the second derivative creates a characteristic distinct peak feature for a tunnel, which is flanked by subsidiary negatives.

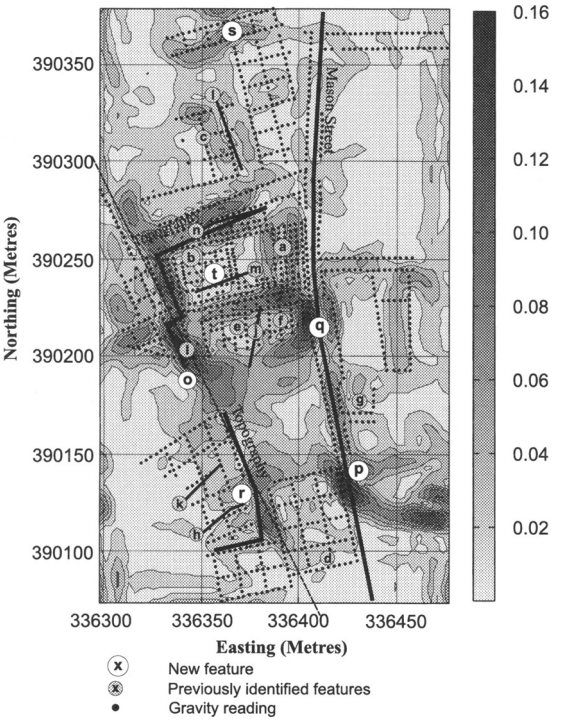


**Fig. 6.** Second horizontal derivative map of the area.

## Identification of 'noise' sources

The gravity anomaly is a complex superimposition of signals from many sources. The difficulty of extraction of the 'signal' for the cavity from the 'noise' from all of these other effects is the major limitation of geophysical surveying. To enable confident target identification all other anomaly sources need to be identified. Both natural and man-made features can create background 'noise' which mask the target anomalies. The natural sources derive from geological features including faults and glacial drift, and tend to be unpredictable unless significant geological data are available.

The Permo-Triassic sediments of the Cheshire Basin are generally poorly-exposed due to extensive Quaternary to recent cover, but have good exposure on Edge Hill. Many cross-sections of the area have been constructed using the extensive exposures created by the Lime Street railway tunnel (Morton 1863), and show a faulted half-graben feature within the Bunter, Muschelkalk, and Keuper facies (Evans *et al.* 1993). Throws of up to 200 m are seen within the Sherwood Group sandstone, although no faults seem to cut the survey site. Water levels in the area should be low due to the high aspect of the site, and the proximity of the Lime Street tunnel which is still pumped and is deeper than the Williamson tunnels, implying that the system will be dry. Therefore, the apparent absence of both glacial-drift and faulting predicts that the effect of geology upon the results will be simple, and the dry-nature of the tunnels implies that the main affect on the gravity anomaly strength will be the presence of rubble fill.

Man-made noise sources within the survey site are created by the redevelopment of the land, which as outlined earlier, has been substantial. Developments have modified the ground-surface with large areas being filled with a variable thickness of low-density rubble which can create a complex and unpredictable anomaly of up to 40 μgals. The study of development in the area was vital to explain which anomalous features were due to man-made noise. Grindfield Hill will be the most affected area as subsequent developments have left the area refinished using a thick and highly variable depth of rubble fill. Lesser thicknesses of rubble are expected at locality 5 (Fig. 2). Many of the tunnels are suspected to have been modified during development. The army sealed many of the tunnels close to Williamson's house; it is uncertain whether any were destroyed. Tunnels would also have been destroyed, filled with debris or sealed during the construction of the city stables, and the developments on Paddington and Grindfield Hill. The filling of debris will reduce the density contrast and hence the anomaly amplitude but not affect the intrinsic anomaly shape and wavelength.

The 24 m deep open Lime Street tunnel and the deeper enclosed Waterloo tunnel will create a significant yet predictable noise signal and were modelled from dimensions determined from the OS map. These tunnels will have accompanying smaller air-shafts that are not documented which creates a possible confusion over the source of anomalous linear-features in the proximity of the railway tunnels. The Waterloo tunnel has a number of large air-shafts (locality 10) creating predictable localized anomalies.

## Data interpretation

The Bouguer anomaly map (Fig. 3) shows many high-frequency anomalies superimposed upon a complex long-wavelength regional feature which slopes from the northeast to the southwest. A linear feature trends through the survey site, as highlighted in Fig. 3, which coincides with the topographic terracing of the area and may be explained as either an effect of terrain or by the presence of a geological fault. The fault would explain the terraced nature of the area but the geological cross sections show no faults within the site (Morton 1863). The survey points displayed on Fig. 3 shows the dense coverage in some areas, but also identify areas of sparse coverage within which the interpolation process has created features indicative of tunnels; these were identified and rejected. Other features were identified as created by terrain, especially along the topographic terracing and around the periphery of the Lime Street tunnel. These features complicate target identification as they mask the smaller features created by the tunnels. No effect was evident from the building infrastructure, as recognized in Kuwait by Bishop *et al.* (1997). Although the regional and terrain effects are substantial, linear features can be seen around the site of Williamson's house where coverage is high, with the largest anomaly sub-parallel to Mason Street representing a previously unidentified feature (Fig. 3 locality a). A large rectangular anomaly at location b is of similar dimension to the Great Hall, with smaller features at locations c–f. Many of these features correspond to those of Fig. 2 with an anomaly at location g corresponding to the subsidence at location d (Fig. 2) confirming void collapse.

The removal of the terrain effect and regional trend created the final Bouguer anomaly map (Fig. 5) and increased the number of identifiable targets, particularly features h–n which were previously unidentified.

The second derivative map shows many of the expected 'spike-like' lineations indicative of tunnels as shown in Fig. 6. The main feature delineates the Lime Street tunnel (o) and is an artefact of the limitations of the terrain correction program, as is the feature at locality p. Unexpectedly, the road is clearly delineated (q) as a weak anomaly is created by the difference in density between the road-stone and surroundings. After the elimination of noise features, many targets were identified around Williamson's house, the school grounds, and Grindfield Hill, some of which were previously undetermined, localities r–t. The application of the second derivative method aided target identification and represents a valuable method for the delineation of void features associated with industrial archaeology.

To aid final feature interpretation the results were divided into four smaller maps covering Williamson's house, Grindfield Hill, Archbishop Blanche School, and Paddington. Using all the available information, including the full- and small-scale

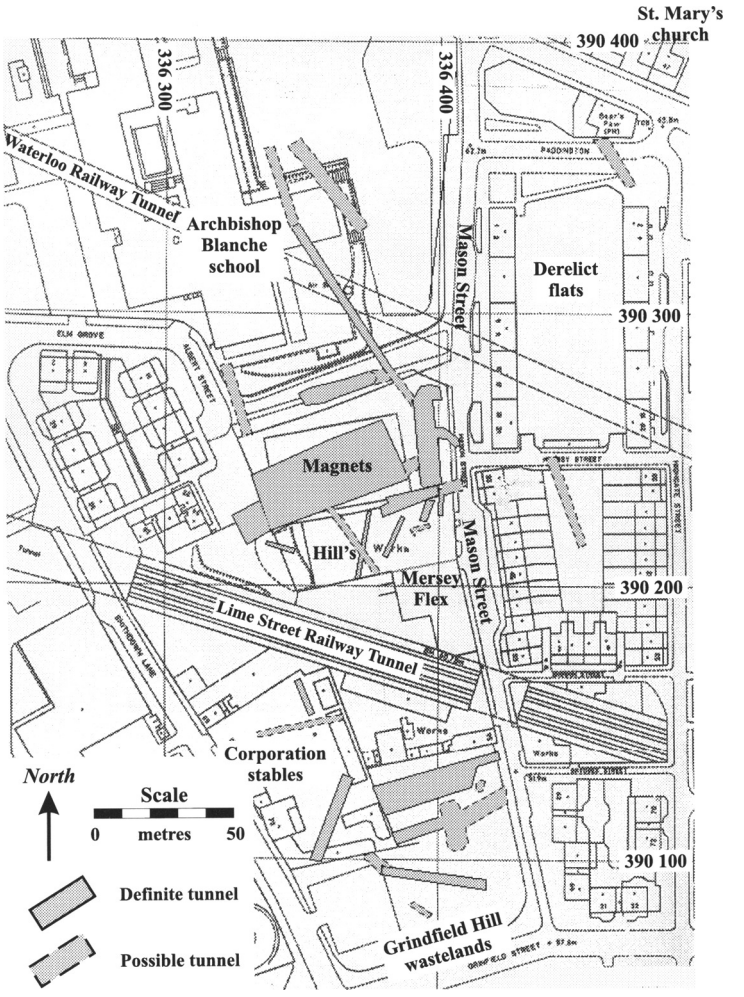


**Fig. 7.** Map of the Williamson tunnels as determined from microgravity.

Bouguer maps, second-derivative map, historical documentation, noise survey, field evidence, and desk study, the tunnel system was delineated as summarized in Fig. 7. All previously known accessible tunnels were located successfully, but no evidence for the suspected tunnel running to St. Mary's church was obtained. The survey identified many known and previously unknown tunnels, and was successful at delineating the tunnel system. Although the adverse terrain and the complex regional feature, complicated data-interpretation, the application of a terrain correction and the removal of the polynomial surface enhanced feature recognition.

## Gravity analysis and modelling

The delineation of the tunnel system, although successful, only gives a two-dimensional plan of target geometry. Two methods are available for the determination of the depth of the targets; forward gravity modelling or inversion methods such as Euler deconvolution. Gravity modelling has the potential to determine the depth and the nature of the identified targets through the construction of geological cross sections. Seven transects of interest were obtained from the interpolated gravity-grid and were modelled using the GRAVMAG program which calculates the gravity effect of geometrical bodies of different density within a constant density background. The geometry and density of these bodies are adjusted to match the recorded field-results. Accurate geological cross sections can be achieved within the limitation of the intrinsic non-uniqueness that affects gravity modelling. Models can be constrained using additional information, such as surface lithology in the modelling of regional transects to reduce the ambiguity.

The numerous surface tunnel expressions help to determine the depth of the features with respect to land surface, tunnels at locality 1 (Fig. 2) were 0.2–3 m depth, with previous surveys showing tunnels to a 5 m depth. Additional depth estimates using the half-width and gradient-amplitude methods were obtained from the anomalous curves, but these showed large errors due to the shallow depth range of the tunnels. Tunnel location along each transect were determined using the second-horizontal derivative to identify the 'central sharp peak and flanking negative' signature of a tunnel.

In order to determine the position of the targets in three dimensions we have used the technique of Euler Deconvolution. Euler Deconvolution is a method for locating the sources of potential fields based on both their amplitudes and gradients and an estimate of the probable geometry of the causative body (Thompson 1982; Reid *et al.* 1990). The technique is very appropriate for use in microgravity surveys where high-quality, closely spaced data are available.

Potential fields such as gravity, magnetism and their spatial derivatives satisfy Euler's equation of homogeneity:

$$(x - x_0)\frac{\partial V}{\partial x} + (y - y_0)\frac{\partial V}{\partial y} + (z - z_0)\frac{\partial V}{\partial z} = -nV.$$

The derivative of the continuous field $V$ satisfies the above homogeneous equation of degree $n$ where $n$ is known as the structural index. This is an indicator of the fall-off rate of the field with distance $r$ and depends on the geometry of the suspected body, e.g. line, point, sphere or any combination, and the particular potential field type. Hence, from a field which is measured at point $(x, y, z)$, the gradients in these

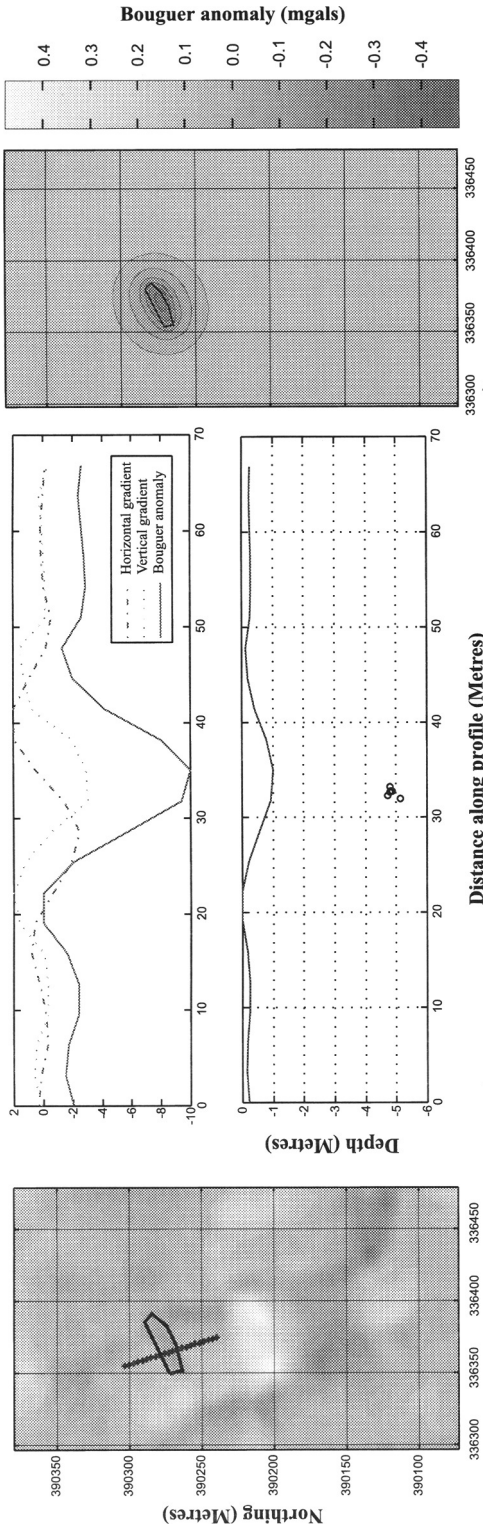


**Fig. 8.** Modelling of the Great Hall using automated depth analysis and 3D gravity modelling using Fourier techniques. Figure 8b shows the calculated depth for a tunnel from the gravity profile shown in Fig. 8a. Figure 8c shows a 3D gravity model using dimensions for the Great Hall from the Army survey giving a good fit as seen in the observed anomaly.

directions can either be measured or calculated. If we have the values $(x, y, z)$ and their derivatives at more than four points, and an estimate of $n$, we can solve for the location of the causative body, $(x_0, y_0, z_0)$, by a least-squares matrix inversion.

In this case, we have microgravity as our value for $V$. A window is moved across the data, and solutions for $(x_0, y_0, z_0)$ are obtained. Only those locations of $(x_0, y_0, z_0)$ which cluster as solutions from several window positions are considered real.

The program was used to solve for the position and depth to an anomaly in 2D, i.e. along a profile line shown on Fig. 8a. Figure 8b shows the Bouguer Gravity, and its vertical and horizontal derivatives and the solutions for the target position derived from them. The clustering of circles around 5 m depth at a position of 32 m along the profile indicates a good solution to the equations at that point. This agrees very well with the depth and position of the Great Hall which is modelled as Fig. 8c. This is a full 3-D gravity model implemented using Fourier techniques for a void representing the Great Hall and the anomaly amplitude of more than 400 μgal agrees well with the observed amplitude of the anomaly.

## Conclusions

The microgravity survey successfully produced a map of the Williamson tunnels in an accurate and reliable manner, demonstrating the validity of applying the method to industrial archaeology even in 'brown-field' sites. With careful field acquisition, Worden and LaCoste-Romberg gravimeters were shown to be adequate, if not ideal, for target location for air-, water-, or rubble-filled conditions using a 3 m point-spacing which was optimal for these features. The 1243 survey-point readings gave a high coverage in most of the site, especially around the location of Williamson's house, but restrictions in access resulted in several sparsely covered areas. We appreciate that this limits the confidence which can be placed in the identification of features in these sparsely covered areas and recommend that wherever access and cost allow a regularly spaced grid at an appropriate spacing is to be preferred. This does not detract from the conclusion that microgravity has been extremely useful in the identification of features in this area and should be considered as a valuable additional tool in industrial archaeological investigations.

The Bouguer anomaly map showed many features that were consistent with previous surveys, but a strong regional gradient and terrain effects masked some of the smaller tunnel features. Removal of the gradient allowed some previously unrecognized targets to be identified once noise sources were recognized and eliminated through a comprehensive desk study of the history of land use. The second-horizontal derivative significantly aided feature recognition by enhancing smaller anomalies and clearly delineated the Lime Street tunnel and Mason Street as well as identifying previously unrecognized tunnels. Euler deconvolution provided positions and depths to the anomaly sources. The theoretical cross sections produced show that even with a difficult data-set it is possible to model expected features. The success of these methods highlighted their potential for the delineation in three dimensions of cavities associated with both industrial archaeological and geological features.

A full appraisal of the system required a comprehensive desk study which examined historical documentation and field evidence. The accessibility of some of the tunnels confirmed identification, allowing many new tunnels to be identified. Using this

information and all available gravity data, many known and unknown tunnels were successfully identified.

The authors would like to acknowledge the following people for their invaluable contribution during this survey. J. Harvey and J. Hakes for general assistance, K. Helps, D. G. Cuss and P. D. Cuss for assistance during levelling, G. Muies, D. Hartley (Magnets Showrooms) and J. M. Venn (Archbishop Blanche School) for allowing access to land. We are very grateful to Sam Toon for his assistance with the computer graphics.

## References

ANON 1867. A gigantic nuisance and the Edge Hill caverns. *Porcupine*, **9**, August 31, p. 216.

ARZI, A. A. 1975. Microgravity for engineering applications. *Geophysical Prospecting*, **23**, 408–425.

BALLINA-LOPEZ, H. R. 1990. FORTRAN program for automatic terrain correction of gravity measurements. *Computers & Geosciences*, **16**, 237–244.

BISHOP, I., STYLES, P., EMSLEY, S. J. & FERGUSON, N. S. 1997. The detection of cavities using the microgravity technique: case histories from mining and karstic environments. *In*: MCCANN, D. M., EDDELSTON, M., FENNING, P. J. & REEVES, G. M. (eds) *Modern Geophysics in Engineering Geology*, Geological Society, London, Special Publications, **12**, 155–168.

BUTLER, D. K. 1984. Microgravimetric and gravity gradient techniques for the detection of subsurface cavities. *Geophysics*, **49**, 1084–1096.

CHAMON, N. & DOBEREINER, L. 1988. An example of the uses of geophysical methods for the investigation of a cavern in sandstones. *Bulletin of the International Association of Engineering Geology*, **38**, 37–43.

CLARKE, A. J. 1986. Archaeological geophysics in Britain. *Geophysics*, **51**, 1404–1413.

COLLEY, G. C. 1963. The detection of caves by gravity measurements. *Geophysical Prospecting*, **11**, 1–10.

DANIELS, J. 1988. Locating caves, tunnels and mines. *Geophysics: The Leading Edge of Exploration*, **7**, 32–37.

DAVIS, J. L. & ANNAN, A. P. 1989. Ground-penetrating radar for high-resolution mapping of soil and rock stratigraphy. *Geophysical Prospecting*, **37**, 531–551.

EMSLEY, S. J., SUMMERS, J. W. & STYLES, P. 1992. The detection of sub-surface mining related cavities using the micro-gravity technique. *Proceedings of a Conference on Construction over Mined Areas, Pretoria, South Africa*, May 11–12, 1992, 27–35.

EVANS, D. J., REES, J. G. & HOLLOWAY, S. 1993. The Permian to Jurassic stratigraphy and structural evolution of the central Cheshire Basin. *Journal of the Geological Society, London*, **150**, 857–870.

FAJKLEWICZ, Z. 1956. Underground gravity measurements as applied to coal mining. Results of investigations in Miechowice Colliery. *Archiwum Goimictwa*, tI, no. 4, 345–355.

—— 1976. Gravity vertical gradient measurements for the detection of small geologic and anthropogenic forms. *Geophysics*, **41**, 1016–1030.

FERGUSON, N. S. & STYLES, P. 1992. The detection and delineation of subterranean cavities by the microgravity method and subsequent image enhancement. *Annales Geophysicae*, **10**, 120.

HAMMER, S 1939. Terrain corrections for gravimeter stations. *Geophysics*, **4**, 184–194.

HAND, C. R. 1916. Joseph Williamson: 'The King of Edge Hill'. *Transactions of the Historical Society of Lancashire & Cheshire*, **68**, 1–23.

—— 1927. Joseph Williamson: 'The King of Edge Hill II'. *Transactions of the Historical Society of Lancashire & Cheshire*, **79**, 86–111.

KETELAAR, A. C. R. 1976. A system for computer-calculation of the terrain correction in gravity surveying. *Geoexploration*, **14**, 57–65.

MORTON, G. H. 1863. *The Geology of the Country around Liverpool*, revised edition. Geo. Smith, Watts & Co., Liverpool.

NEUMANN, R. 1967. La gravimetrie de haute precision – application aux recherches de cavities. *Geophysical Prospecting*, **15**, 116–134.

NOEL, M. & XU, B. W. 1991. Archaeological investigation by electrical resistivity tomography: a preliminary study. *Geophysics Journal International*, **107**, 95–102.

OWEN, T. E. 1983. Detection and mapping of tunnels and caves. *In:* FITCH, A. A. (ed.) *Developments in Geophysical Exploration Methods, Volume 5*. Applied Science, London, 161–258.

PATTERSON, D. A, DAVEY, J. C., COOPER, A. H. & FERRIS, J. K. 1995. The investigation of dissolution subsidence incorporating microgravity geophysics at Ripon, Yorkshire. *Quarterly Journal of Engineering Geology*, **28**, 83–94.

REID, A. B., ALLSOP J. M., GARNER, H., MILLETT, A. J. & SOMERTON I. W. 1990. Magnetic interpretation in three dimensions using Euler deconvolution. *Geophysics*, **55**, 80–91.

THOMPSON D. T. 1982. EULDPH: A new technique for making computer-assisted depth estimates from magnetic field data. *Geophysics*, **47**, 31–37.

WILSON, C. D. V. 1959. *Feasibility Study of the Application of Geophysics to the Detection of the Williamson Tunnels*. Unpublished, University of Liverpool.

# The Makapansgat Australopithecine site from a speleological perspective

ALF G. LATHAM[1], ANDREW HERRIES[1], PATRICK QUINNEY[1], ANTHONY SINCLAIR[1] & KEVIN KUYKENDALL[2]

[1]*Archaeology Department, Liverpool University, Liverpool, L69 3BX, UK*

[2]*Department of Anatomical Sciences, University of Witwatersrand, Johannesburg, South Africa*

**Abstract:** Remains of *Australopithecus africanus* from the Limeworks Cave, Makapansgat, South Africa, are believed to belong mainly to a metre-thick, bone-rich, speleothem layer. The flowstone is one stratum among a sequence of speleothems, muds, silts, sands and fine and coarse breccias, the study of which has evoked some disagreement. The limeworkers' excavations revealed some stratigraphic relationships but they have obscured others. Partly because of this, controversy surrounds the supposition about whether there are separated depositional basins within the overall site and, if so, whether strata can be securely correlated. This is important because a reconstruction of an overall stratigraphic sequence was used as a basis for a magnetostratigraphic reversal record and by which the site has been tentatively dated. There is qualification and disagreement about the origin of the various flowstones and the actual depositional environment of the muds and silts. Evidence is presented which rules out some previous interpretations. From the point of view of the Australopithecine fossils themselves, it can be said that the calcite matrix in which they were provenanced was a low-energy environment and that the dense bone accumulation of this layer almost certainly did not arise by the action of floods, as previously supposed. The most likely main cause of the dense accumulation was hyena denning activity. It is clear that further work is needed to see how a reliable overall sequence can be established and that closer sampling is required for magnetostratigraphy.

The Limeworks Cave in the Makapansgat Valley, Transvaal, South Africa (Fig. 1) is well known for its remains of *Australopithecus africanus* from which there are about 30 specimens, the first finds appearing in 1947 (Mason 1988). Despite more than 50 years of research, neither the finds nor the deposits from which they came have been firmly dated and there is no complete consensus on the origins of the deposits or on whether a complete stratigraphic sequence can be reconstructed.

Based on faunal evidence, the Australopithecine deposit, a kind of bone breccia set in grey-white flowstone, is thought to be no younger than 2.5 Ma and as old as 3 Ma (Vrba 1982). This grey to white speleothem is too old for U-Series dating which, by mass-spectrometry, has an upper limit of about 500 ka. The electron spin resonance (ESR) method has not yet been applied to date the enamel of teeth from the site; ESR studies at Sterkfontein have only been partially successful (Schwarcz *et al.* 1994). Recently, U-Pb methods have been developed to date geologically young

*From:* POLLARD, A. M. (ed.) 1999. *Geoarchaeology: exploration, environments, resources.* Geological Society, London, Special Publications, **165,** 61–77. 1-86239-053-3/99/$15.00

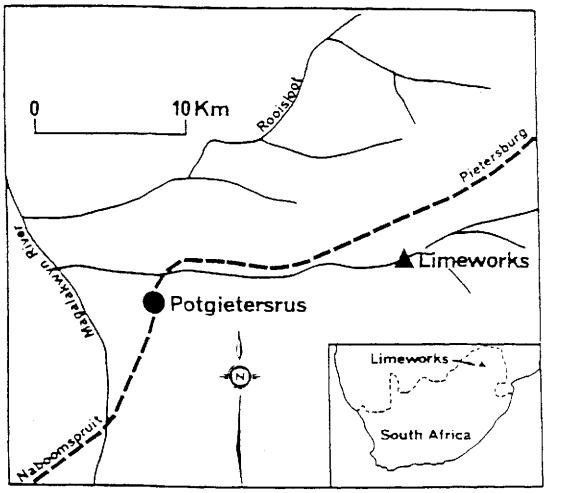


**Fig. 1.** Location map of the Limeworks Cave, Makapansgat Valley, Transvaal (Northern Province, South Africa (after Maguire *et al.* 1980).

rocks (Getty & DePaolo 1995) and it has been used successfully to date speleothems, having high uranium content, as young as 250 ka (R. Cliff, pers. comm. 1998). However, a suite of speleothem pilot samples from the Limeworks Cave showed that uranium content is generally low (<0.5 ppm) and the common lead was comparable to the radiogenic lead (work in progress and details to be reported elsewhere).

Perhaps the most promising method to date the site is to compare the reversal magnetostratigraphy of the various layers with the Global Magnetostratigraphic Timescale, which was attempted by McFadden *et al.* (1979). The potential advantage of this method, bearing in mind the current interest in changes in palaeoclimate linked to changes in palaeofauna (Vrba 1996) is that it can potentially provide ages for the whole sequence. The composite section, from the earliest speleothem to the latest breccia, could be placed somewhere between 3.32 Ma and 2.43 Ma. There are problems, however, with the ages so estimated. Firstly, D. Jones & A. Brock (pers. comm.) believe that the sampling density for palaeomagnetism within each subsection was low, which implies that reversal boundaries might have been misplaced. Secondly, sampling was carried out on widely separated subsections, and as Turner (1980), Maguire (1985) and Maguire *et al.* (1985) have noted, it is not clear that a complete composite section was reconstructed reliably. The latter authors believed that there were four depositional basins within the site, and palynological analysis by Cadman & Rayner (1989) and Zavada & Cadman (1993) showed that the deposition between basins was not uniform or synchronous. Thus it is not known if there is an absence of hiatuses or if similar beds are also time-equivalents, as the composite reconstruction for magnetostratigraphy assumes. Lastly, the upper part of the sequence consists of breccias. As McFadden *et al.* (1979) recognized, the interpretation of the palaeomagnetic record of samples taken from this kind of deposit has its own special problems (see later) and, because of the indeterminate palaeomagnetic directions, the upper part of the breccia was essentially unplaced.

In many places, the deposits show rapid lateral changes on a scale of tens of metres or less. A full assessment of these changes, showing the effect they will have on an overall stratigraphic sequence and upon any overall magnetostratigraphy, can only be made by surveying and correlating vertical sections at close intervals. The extant survey work has included long cross sections of broad stratigraphy, but not vertical sections on individual faces. In preparation for further sectional surveying, palaeomagnetic and radiometric work, and to contribute further to the discussion on stratigraphy, we present a number of observations about the mode of speleothem deposition and early sedimentation at the Limeworks site and also include some observations about speleogenesis at Makapansgat. In the tradition of Brain (1958), but differing from him in a number of details, our observations and interpretations are guided by observations from studies of other caves.

## The Limeworks Cave and its broad stratigraphy

The cave, formed in Precambrian dolomite of the Transvaal Supergroup, was initially worked for its thick speleothem flowstone by limeworkers from about 1908 to 1936. (In the literature, the flowstone at Makapansgat is often referred to as travertine, meaning cave travertine as opposed to hot-spring travertine.) In order to get at the flowstone, the workers had to blast and remove consolidated and unconsolidated breccia; bones are found in clastic sediments, breccias and in all but the earliest speleothem. There do not appear to be any extant mining records which would indicate the original extent of the deposits but there are still remnants of deposits in some areas or, in the case of some flowstones, traces of them left by negative contact surfaces. Broad stratigraphic sequences have been constructed by Wells & Cooke (1956), by Brain (1958) and by Partridge (1979) and they are in rough agreement. The palaeomagnetic sampling followed Partridge's (1979) reconstructed sequence. Those bone remains containing *Australopithecus africanus* were mostly recovered from the limeworker's dumps, rather than *in situ,* and were nearly all assigned to a later grey flowstone called Member 3, in the notation of Partridge (1979). The outline plan of the cave with the limeworkers' quarries and access cuttings is shown in Fig. 2 and the corresponding composite section is shown in Fig. 3. Massive eroded stalagmitic columns above the Cone mouth, on the surface, indicate that the original roof of the cavern was tens of metres above the present surface.

Between the Main Quarry and the Exit Quarry is a 15–20 m thick cemented breccia essentially separating the two excavated halves of the site. The Entrance Quarry, to the west, leads to the Main Quarry which, on the west side, contains the Classic Section. This, in turn contains, unambiguously, deposits now referred to as Members 1, 2 and 3. To the south and between the Main Quarry and the East Quarry is the Cone, a pile of breccia that has resulted from collapse by undermining. The corollary of this is an inverted funnel mouth to daylight, containing speleothem and about 10 m of breccia and stratified red sediment. Around the Cone mouth, the clastic deposits vary laterally, being free of large clasts adjacent to the back wall, and there are non-cemented sections to the east. Behind the Cone there are short cave passages and alcoves containing early phases of speleothem and another entrance to the south-west. The passages open to the east into the Exit Quarry and an exit cutting, to the side and under which is Horse Mandible Cave. The Exit Quarry contains a short

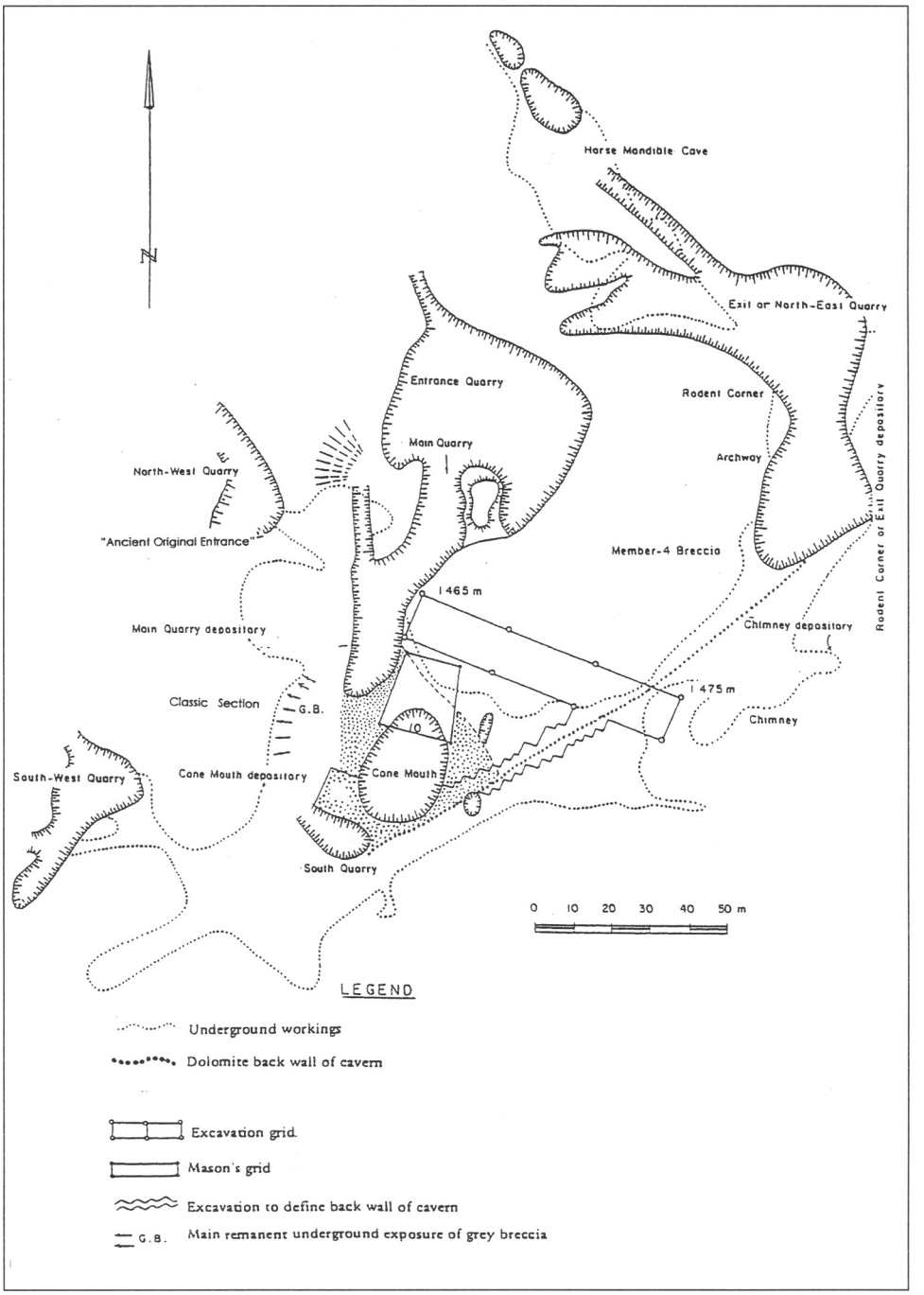


**Fig. 2.** The Limeworks quarries and underground workings (after Maguire *et al.* 1980).

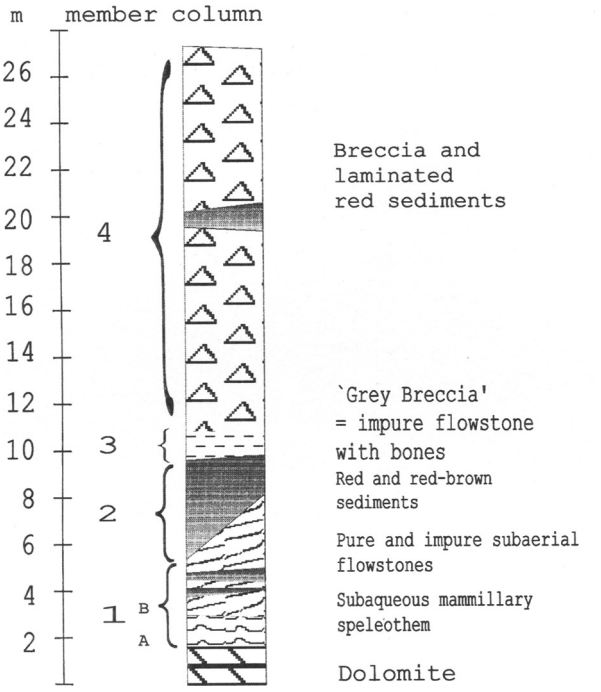


**Fig. 3.** Composite section of the Limeworks Cave stratigraphy (adapted from Partridge 1979), with subdivision of member 1 into Member 1A and Member 1B. Member 4 includes former Member 5.

tunnel above which is a layer of cemented sediment containing many rodent bones. This area is called 'Rodent Corner' (Fig. 4).

## Description of Deposits

### *Member 1 (A and B)*

The first major depositional phase, Member 1, is massive stalagmite. Within this member there are two quite distinctive phases, here designated A and B.

The stalagmitic concretions which coat the floor, walls and roofs are unusual mammillary forms. These bulbous concretions protrude in various directions, mostly up and down, but there are no corresponding stalactite–stalagmite pairs as would be the case for normal subaerial, gravity-dominated, deposition. Where the miners have smashed them, they show even deposition over the various undulations (Fig. 5). This is member 1A and, in its earliest phase, exposures in recesses inside the Exit Quarry cave show radiating aragonitic cores with later calcite layering.

In several of the recesses 1A is the end of deposition. There is no other layer apart from a thin coating of dust.

At the base of the Classic Section, a 7 m long exposure shows red-brown staining within the mammillary speleothem, which implies an input of muddy water into the local pool (Fig. 6).

**Fig. 4.** Looking out from the Exit Quarry to Rodent Corner. The wall to the left consists of collapsed roof slabs and breccia with flowstone which once rested against massive speleothem, leaving a gap. The massive speleothem has been mined out. Behind and above these slabs is Member 4 breccia. The tunnel itself was mined through the rhythmites.

*Origins of Member 1A.* It is known that mammillary speleothems form subaqueously (Hill & Forti 1986). Evidently, at the Limeworks Cave, they formed under, and close to, water surfaces from which $CO_2$ was allowed to outgas to the cave atmosphere. This caused the water to become saturated with respect to aragonite and calcite, which thereby precipitated under water onto available solid surfaces. It is very likely that, by this time, the actual cave forming streams were no longer extant and that these pools owed their existence to more saturated percolation water from the overlying surface. In all likelihood it would have been the same water that formed the massive speleothem formations and Member 1A and 1B may have been, in part, contemporaneous. The outgassing of $CO_2$ from the pools may have been accelerated by the proximal development, to the northwest, of surface collapse and regression. At any rate, an entrance near the Main Quarry is suggested by the red-brown staining within the mammillary forms under the Classic Section. It may well be that, here, regressing collapse was close enough for clastic sediment to enter the underground pools for the first time.

*Member 1B.* This constitutes the bulk of the mined speleothem from the site and probably represented most of the deposition within the interior of the cavern before it became unroofed. Layers of 1B are seen to slope steeply at first and then to lie subhorizontally in and under the Classic section especially around the excavated cavern toward the entrance labelled the 'Ancient Original Entrance'. Undercuts of stalagmitic bosses are seen in the roof. 1B is a light buff to white calcite with thickening

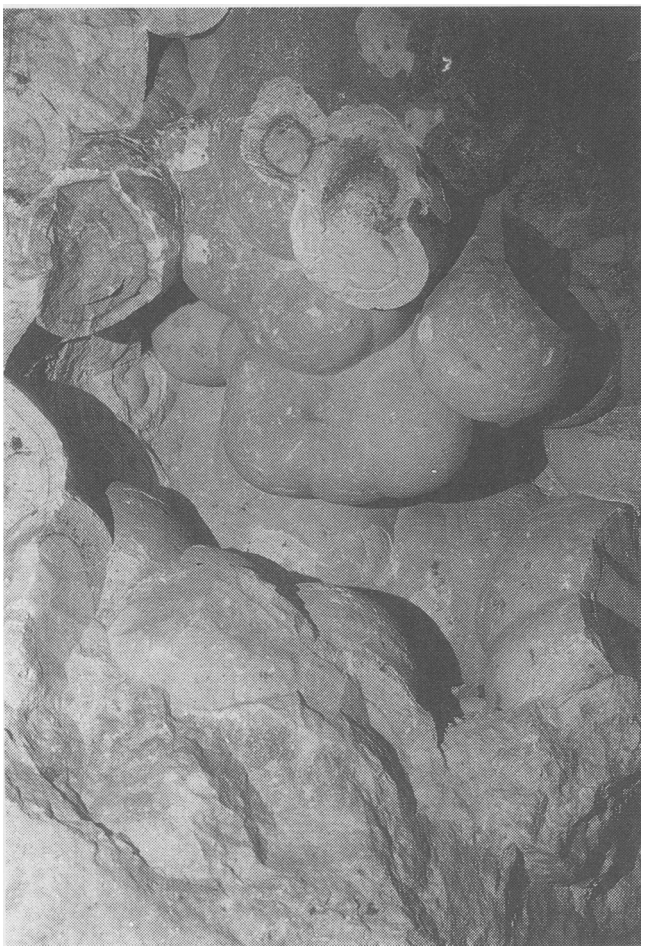

**Fig. 5.** Mammillary speleothems (Member 1A) from the underground workings, viewed from below looking upwards. These forms are about 200–300 mm in diameter.

intercalated series of layers of brown and red-brown sediment. Occasionally the calcite is coloured by this fine sediment. In the roof, within a few metres of the 'Ancient Original Entrance', both precipitated and clastic layering is horizontal, and there are several generations of negatives of mud cracks, with varying sizes of mud crack polygons (Fig. 7).

*The formation of 1B in the Classic Area.* The presence of microgours (small ~10 mm rimstone pools), collapsed layers of calcite, and sheet flows that thicken toward the quarry, demonstrate that 1B was formed subaerially from major feed sources near the quarry. As in other limestone caves, these stalagmitic flowtones were supplied by carbonate rich feedwater from fissures in the former roof. The fact that there are thickening intercalations of layers of fine clastic sediment suggests that an entrance was also opening up in the quarry area at this time by progressive roof collapse.

**Fig. 6.** Mammillary speleothem of 1A, with staining between layers, overlain by 1B, beneath the Classic Section.

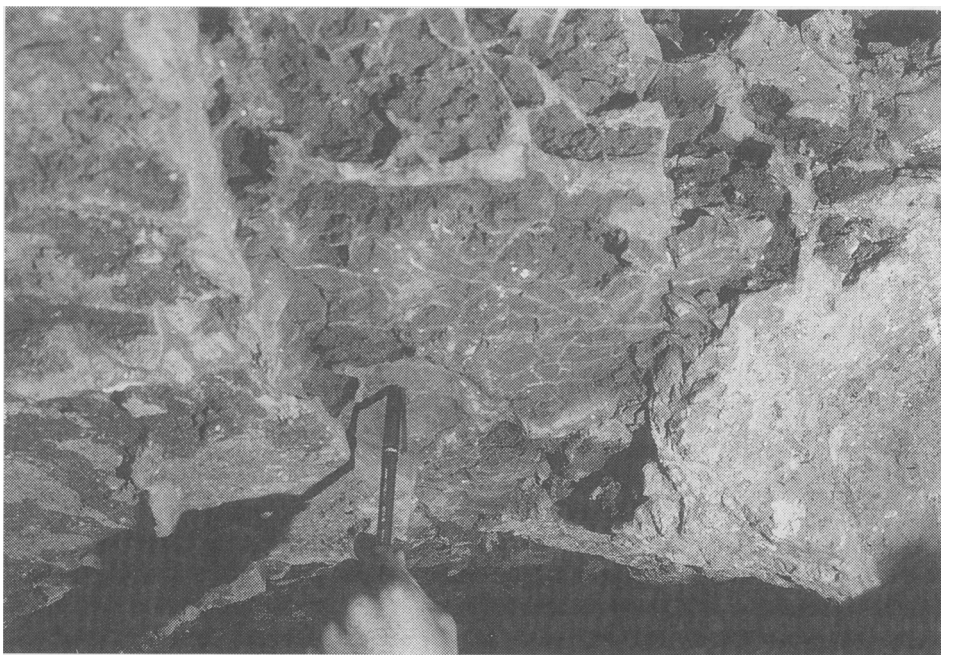

**Fig. 7.** Mud-crack polygons in several layers, near the top of Member 1B, in the 'Ancient Original Entrance'.

According to Partridge (1975) a large stalagmitic boss occupied the quarry area, before it was removed by the limeworkers, and it is the lower sloping 1B flows of this which are still extant in the quarry area out to the 'Ancient Original Entrance'.

*Member 1A and B in the East Section.* In the east section there are two 2.5–3 m high pillars of calcite left by the miners as supports for Member 2. The base of the outer pillar sits on the dolomite. Great quantities of both 1A and 1B were removed from this area by the miners. The sequence is: 1A, showing aragonite and calcite mammillary forms, up to about 1m or more in thickness, followed by up to several metres of 1B which becomes increasingly contaminated with fine sediment. Above the second pillar, another contributor to impurities in the calcite is a 1 m thick layer of blue to blue-white collophane, most of it crumbly. Evidently this area acted as a bat roost for a while (Hill & Forti 1986; Partridge 1975). Back toward the centre of the cavern these 1B deposits give way to the breccia of the middle section.

*The formation of 1B in the East Section.* As in the Classic Section, 1B stalagmite was deposited into some kind of basin in such a way that whatever the original depositional surface, the final surface was subhorizontal near the cavern walls. Deposition ceased around the margins of the cavities so these lower recesses tend to have only 1A forms.

The extensive excavations of the miners and the negatives of flowstone layering, left as an imprint on the breccias, suggest that massive flowstone existed in a roughly horseshoe-shaped arc stretching from the Entrance to the Exit Quarries. In places this massive flowstone was in contact with the wall and was cemented to it. This formed a barrier beyond which sediment could not pass. One notable location is under the roof of the Main Quarry and it accounts for the southern limit of the Classic Section.

## *Member 2*

*Member 2 in the Classic Section.* The fine sediments of Member 2 begin to dominate over deposition of Member 1B flowstone layers and, depending on the exact location, this occurs over tens of centimetres to metres. Ten to twenty metres further away from the entrance, toward the interior of the cave, the sediment was deposited horizontally against Member 1B flowstone where the latter was deposited vertically. At that locality, Member 2 consists of almost 5 metres of thinly deposited layers of purple, red-brown and red-yellow clays and silts with occasional thin partings of calcite (Partridge 1979). It contains fragments of bone and broken speleothems.

*Origin of Member 2 in the Classic Section* (Fig. 8). The sediment is colluvium derived from the surface and was washed in through an entrance that was probably caused by continuing retreat of the surface. Rayner *et al.* (1993) supposed that the sediments were laid down in standing water. It is not necessary to invoke a water-table or standing water to explain either the sediments or their textures. From the presence of the mud crack polygons and thin calcite partings, the simpler explanation is that pools caused by rain events simply dried up.

*Member 2 in the Exit Quarry.* In the area of the columns, clastic impurities occur within the calcites at intervals of tens of centimetres. These are overlain in part by

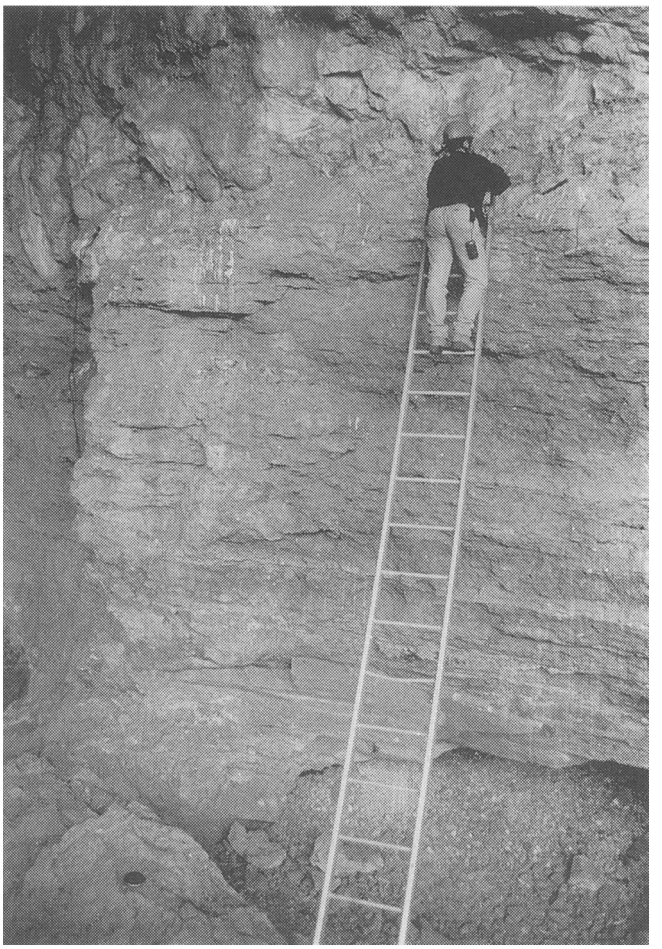

**Fig. 8.** Member 2 in the Classic Section. The ladder is resting on dolomite bedrock (seen to the left of the ladder); at the base is Member 1A with a vertical remnant of 1B attached to the sediments. The person is at the level of Member 3 and above that is the dolomite cave roof. The region between the deposits and the camera position is inferred to be mined speleothem, Member 1B.

about 2 m of Member 2 red sediments. In the roof, the calcites give way to indurated pinkish clastic sediments and finally, the breccias. This is approximately the same sequence as in the Classic Section though without Member 3. The roof is actually excavated breccia in the northwest and dolomite in the east. Behind and below the columns, there are two recesses; one with no red sediments and one packed with them. Evidently the speleothem barrier to flood-lain clastics was incomplete for the latter.

## *Member 3*

From the Limeworks dumps, *Australopithecus* is mainly represented in Member 3. This is a 1 m thick grey to white flowstone with a dense accumulation of bones and

it lies directly on top of Member 2 in the Classic Section (Fig. 8). Member 3 is again visible in the overhanging dolomite roof in another exposure about 10–15 metres further in, among broken stalactites, and where long bones are visible. It is traceable against the dipping dolomite roof to about 1/4 way round the cone to the southwest. There is a 1 m thick stalagmitic deposit containing large bones on the underside of a bulge at the back of the Cone but it appears to lie stratigraphically below the clastic sediments. Member 3 is apparently absent from the Cone round to the Exit Quarry.

In the Classic Section, Member 3 was deposited outside the arc of massive speleothem. According to McFadden *et al.* (1979), the Member 2–Member 3 contact is unconformable, but conformable according to Maguire *et al.* (1985). Member 3 shows sublayers which alternate with vertical stalagmitic wall draperies, as judged by abutment relationships.

The former extent of the whole layer in the area between the Classic Section to the Cone, before the limeworkers undermined and removed it, is unknown, but the existing remnants represent an area of very dense bone accumulation and concentration. From the distinctive damage to bone fragments, Maguire *et al.* (1980) concluded that the bones derive largely from hyena activity and, judging by the sloping disposition of all the deposits in this area, it is very likely that the bones may have rolled into the recesses from dens nearby and higher up. Alternatively, since the layer also contains broken speleothems and sand grains, flowing water has also been invoked as an agent to concentrate the bones against the wall and roof (Brain 1958; Partridge 1979; Maguire *et al.* 1980). This is not easy to reconcile against the observation that the enclosing matrix of the grey breccia throughout is calcitic, consisting of thin (a few mm to several cm) layers of flowstone, which is a low-energy water deposit. In hand sample, the thin calcite layers are separated by air pockets showing that some layers formed as thin rafts on the tops of small gour pools. This kind of formation is common in many caves and is always formed by slow flowing carbonate-rich water. Thus, in comparison with such features in other caves, it is more likely that this area was periodically, perhaps seasonally, wetted, as water seeped down the walls and along the horizontal substrate of Member 2. The precipitation of calcite would form horizontal layers within the bones. Toward the entrance, the uppermost layers of Member 2 and Member 3 abut against vertical stalagmitic flows and wall pillars (half-pillars) which are occasionally seen to be continuous with the horizontal layering, and several generations are represented. Partridge (1979) tended to discount hyena activity as an agent for concentrating the bone so closely against the roof, preferring activity by floods. However, near the Cone, the massive speleothem columns would have provided a rapid change in gradient down which bones might have rolled to lie finally underneath the roof.

## *Member 4*

*The breccias.* The miners' dumps show that bone remains also came from the lower breccias and *Australopithecus* is represented. The breccias, originally subdivided by Partridge (1979) into members 4 and 5, are now all assigned to member 4 (Partridge, pers. comm.). The breccias are coarse pink to red, containing small to large clasts of dolomite and detached flowstone. On the east side of the Cone mouth, the clasts are rounded cobbles while, on the west side and toward the top, the sequence consists of

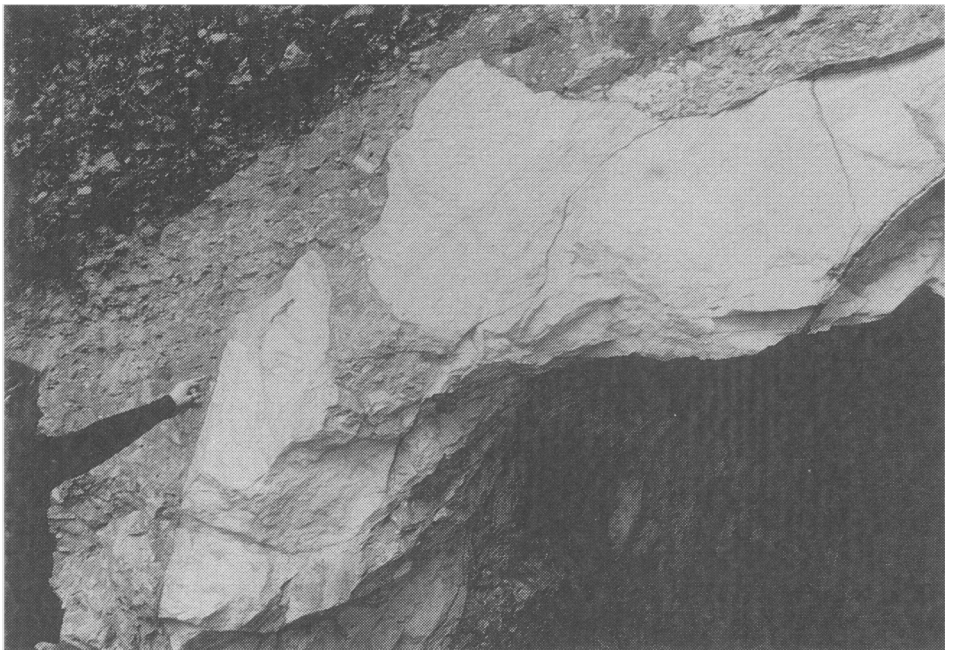

**Fig. 9.** The lower west side of the Cone mouth and eroded parts of Member 1B, the underside of which has been mined out. Member 4 breccia lies above.

both indurated and uncemented stratified clast-free red sediments. Thus the deposits vary laterally from breccias to clast-free equivalents. The clast-free zones imply deposition under a roof. Parts of these layers are cemented by carbonate whereas, a few metres further round, the sediments are unconsolidated. Around the Limeworks site, tree roots have the effect of decalcifying indurated breccia but the effect is restricted to the area of the roots; these are referred to locally as 'mekondos'. In the Cone mouth, however, the unconsolidated strata were probably never cemented. As yet it is not known what the difference the cementation makes to a palaeomagnetic record; most of the samples of McFadden *et al.* (1979) have been taken from cemented sediments.

In the Cone mouth, separated blocks of massive flowstone in the lower part of the breccia exhibit truncated growth layering, indicating that they were partially dissolved before being enclosed in the breccia (Fig. 9). This occurrence was also noted by Maguire *et al.* (1985).

The whole of the area between the two quarries consists of breccia. In the Entrance Quarry, the breccia presents 12 m or more of a negative impression of the former flowstones against which it abutted, and the breccia rests on dolomite. A small section of breccia, referred to as the Partridge Block, can also be found to the west of the Main Quarry between it and the Entrance Quarry. In one or two places some of the subvertical flowstone sheets are still visible (Fig. 10). The ground between the Entrance Quarry to the 'Ancient Original Entrance' is a dolomite 'bridge' which, on the surface, steps down to breccia overlying flowstones and clastics of Members 1 and 2. Apart from this occurrence, most of the breccia was deposited inside the arc of the massive speleothem deposits.

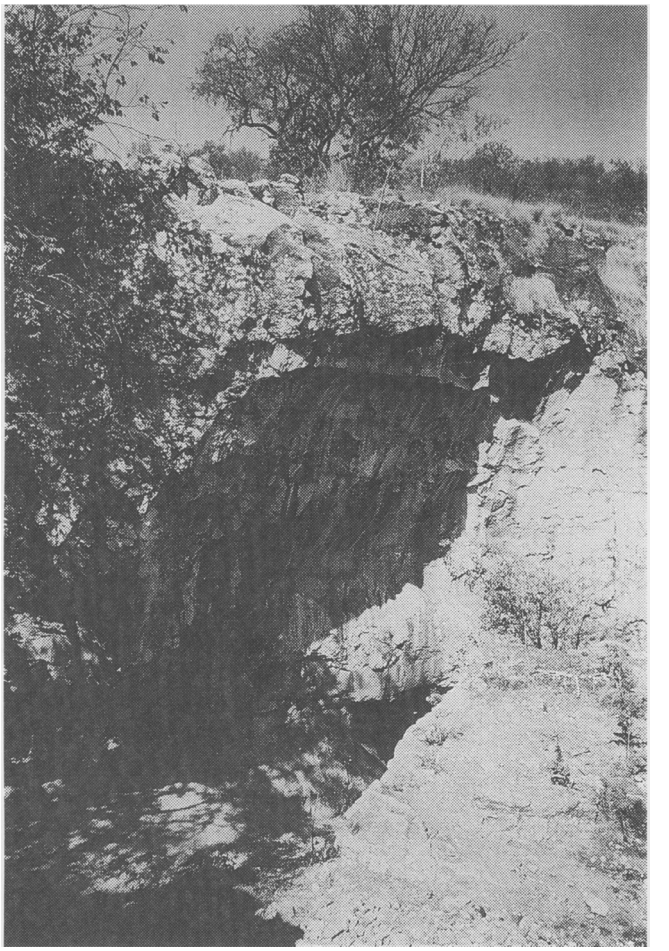

**Fig. 10.** The East Quarry wall showing the negative impression of the flowstone on the breccia, Member 4. The clasts in the breccia can clearly be seen above one extant flowstone layer. The space between the breccia and the camera position was probably occupied by massive flowstone.

*Member 4 at Rodent Corner.* Partway along the Exit Quarry, in an open area known as Rodent Corner, is a short tunnel of about 2 m in height (Fig. 4) which has been created by mining. Partridge (1979) ascribed its cement-indurated red muds and sands to Member 4 and, as such, it was sampled for palaeomagnetism as an aid to completing the magnetostratigraphic sequence. The sediments containing rodent bones are situated above the rhythmites and are probably witness to owl roosts. The rhythmites were later studied by Turner (1980) who believed that the 2 m of cemented sands, silts and clays was an entity separate from the Classic Section. He found that the sequence was made up of about 45 cycles, each about 30–40 mm thick, of coarse sands, fining upwards to sands with mudcracked surfaces. About two-thirds of the way up the sequence, the rhythmites are interrupted by two thin flowstone layers (he refers to this as 'limestone', but this is incorrect), the upper one containing cave pearls, and a layer of coarse sand with granular conglomerate. The different palaeomagnetic directions of sequential

rhythmites suggested, somewhat surprisingly, that they were not annual. From Turner's figures, each cycle appears to represent about a thousand years. The significance of this apparently long periodicity is not known.

The flowstone layers and owl roosts indicate that there was still a roof extant at this time. This is also borne out by the presence of cave pearls as these are known to form only by the drip-water agitation of seed-grains (e.g. of sand particles) and by their concentric growth in pools (e.g. Ford & Williams 1989). It can be clearly seen, in the Rodent Corner arch, that the spaces between calcitic roof layers and stalactites are filled with the fine, red, sandy muds. Preceding both of these, apparently, is breccia Member 4 and it seems likely that the rhythmites were winnowed out of the breccia through the large collapsed blocks seen at the edge of M4 in the Exit Quarry (behind the person in the figure). Thus if the rhythmites are the result of winnowing of the eastern extent of M4, it is uncertain how they fit in the stratigraphy with respect to M4 in the Main Quarry and with sediments in the Classic Section.

## The palaeomagnetism of breccias

Unpublished palaeomagnetic work carried out on borecores from the breccias at the Sterkfontein Australopithecine site by V. Schmidt show that sequentially cored samples gave near-random orientations mainly due to the fact that samples contained rolled detrital titanomagnetite grains. They have not yielded any meaningful sequence for magnetostratigraphic work. Generally, the problems for the palaeomagnetism of breccias are that (i) most breccias consist of a variety of randomly oriented particles and clasts, each one having its own magnetic signal, (ii) the iron-rich matrix gives a signal which may be related to mechanical effects, such as fine-particle rolling, rather than to the influence of the ambient magnetic field and (iii) if later, iron-rich, cement is involved in diagenesis, then there may be a post-depositional signal which corresponds to a time after deposition of the breccia. The question of whether meaningful signals can be recovered from breccias, such as those at the Limeworks Cave, can only be answered by more exhaustive studies that aim to eliminate or minimize the above problems. The work of McFadden *et al.* (1979) and our own preliminary work shows that magnetically cleaned palaeomagnetic directions can be obtained from these deposits. As is usual (Latham *et al.* 1989), the purer speleothem samples are magnetically weaker

## Discussion

Massive subaerial speleothem is forming in many tropical caves today. The main factors are high temperature and humidity, and fast speleothem deposition is the norm (e.g. Ford & Williams 1989). Therefore, does the massive speleothem in the Limeworks Cave bear witness to a much wetter climate at the time? Although the question of palaeoclimate and palaeoecology has preoccupied many researchers working at Makapansgat, we draw attention to the possibility of inferring a more humid earlier climate by the existence of such huge quantities of subaerial flowstone.

On the surface above the cave there is are areas of dolomite stripped of vegetation for research purposes (Fig. 2). The area shows numerous solution holes and hollows, up to a few metres deep, occupied either by hardened red breccia or by shrubs and trees with soil. Thus, it is easy to see how seepage water used this kind of pathway to form

stalactites and other speleothems below. A comparison of the depths of modern caves in the valley, where there is very little runoff and very little modern speleothem formation, leads one to suppose that the conditions at the time of chemical deposition in the Limeworks Cave would have been more humid. But other corroborative evidence would be needed to convert the inference to a firmer conclusion. For one thing, we do not know reliably the duration of deposition. It may also be the case that significant deposition of speleothem could not occur until the surface eroded to a point where sufficient seepage could penetrate to the cavern roof.

## Pools, standing water and water tables

Examination of the Member 2 clastic sediments has not revealed major flow features such as ripple marks or cross-bedding. This has led a few authors to infer that the deposits from Member 1 to Member 3 were laid down under standing water, which has then been called a water table (Maguire *et al.* 1985) and subsequently labelled as a Plio-Pleistocene water table (Cadman & Rayner 1989; Rayner *et al.* 1993). The presence of mud-cracks does not preclude such a hypothesis if water levels have fluctuated, as happens today in the nearby Peppercorns–Ficus aquifer. Mud cracks can be observed in parts of this cave system, even under a few feet of water, and evidently the level can fluctuate by several metres. The following points, however, argue against the notion of water tables.

(i) In compact limestones and dolomites the phrases 'aquifer' and 'water table' need to be qualified considerably. Water tables in the classical sense do not exist since these carbonate rocks have very low porosity. Instead, the hydrology of limestones consists of water flowing slowly in linked, totally filled (phreatic) or partially air-filled (vadose) passages. In Southern Africa, Namibia and Zimbabwe, the carbonate rocks often hold water and act like giant storage tanks. (The tourist cave at Chinhoyi, north of Harare, Zimbabwe, with its deep lake, is a good example.) Classically, a porous sandstone will have a water table and its flow will be Darcian; this is not the case for limestones (Ford & Williams 1989).

(ii) Member 1B flowstones are undoubtedly subaerial, and Member 2 clastic sediments lie on top of them and abut against them. Though not impossible, it would be unusual if standing water, for Member 2, returned to alter conditions that had been water-free, for Member 1B.

(iii) Since there are mud-cracks in Member 1B and Member 2, with interbedded subaerial flowstone, it is better to think of the clastic sedimentation as having occurred in ephemeral pools. The runoff formed the pools and the pools then dried out between rainfall events. Flowstones formed on top of the clastics. A similar situation occurs today in Horse Mandible Cave where the disturbed loose red sediments are being mobilized by ephemeral rivulets coming from a mined opening nearby. The deposits dry out rapidly because there is a good current of air.

Thus, for these deposits, the supposed past existence of a water-table could be misleading for the reconstruction of palaeohydrology and of palaeoenvironment.

## Summary

After the formation of most of the flowstone and stalagmites, most of the deposition occurred on the inside of the massive speleothem arc as breccias, and the sediments at

Rodent Corner were probably winnowed out from them. In the Main Quarry, deposition also occurred on the outside of the arc between the calcite formations and the 'Ancient Original Entrance' and dolomite walls. Later, when the roof receded further upslope the clastic sediments were entrained as alluvium and colluvium into the Cone area. From one local basin to the next, therefore, contemporaneous, diachronous and sequential deposition can be entertained as possibilities for sedimentary members and sub-members. A retreating entrance for clastic infill forces the possibility of a complex sequence stratigraphy. The grey bone breccia is a spatially limited deposit partway through the overall sequence.

Calcite pilot samples from the exit quarry and from Member 3 in the Classic section carry a weak but measurable, stable, magnetic signal. This supports the findings of McFadden *et al.* (1979) that most of the calcites are accessible to palaeomagnetic analysis for reversal stratigraphy. One core sample from Member 3 shows an intermediate direction (D. Heslop, pers. comm. 1998) and this disagrees with the conjecture of McFadden *et al.* (1979) who reckoned that it might be normal. This again points to the necessity for further palaeomagnetic sampling. The interior Exit Quarry calcite sequence could be used to augment the record since, like Classic Section Member 1B, it overlies 1A without a break. The most promising section appears to be in the south of the Cone where, apart from the possible absence of Member 3, deposition appears to be complete from Member 1 to the top of the breccias. In the Main Quarry, it may be possible to connect the sampling directly from Members 2 and 3 to Member 4 of the 'Partridge Block'. Unfortunately, the overhanging nature of all these exposures means that sampling will be difficult.

The British Academy and the University of Liverpool supported this work. P. Quinney acknowledges support from the NERC (UK). R. Cliff, supported by NERC, carried out U-Pb analyses at Leeds. D. Heslop carried out pilot magnetic studies, at the Liverpool Geomagnetic Laboratory, on a small set of samples from the Limeworks Cave. We acknowledge permission to sample through the University of Witwatersrand and the Bernard Price Institute, Johannesburg. Collaboration initiated by T. C. Partridge of the Transvaal Museum, Pretoria on reversal stratigraphy using samples taken from long cores from the Limeworks site is now ongoing and we thank both him and Judy Maguire for all kinds of assistance and discussion.

## References

BRAIN, C. K. 1958. The Transvaal ape-man-bearing cave deposits. *Transvaal Museum Memoir*, **11**, 1–131.

CADMAN, A. & RAYNER, R. J. 1989. Climate change and the appearance of *Australopithecus africanus* in the Makapansgat sediments. *Journal of Human Evolution*, **18**, 107–113.

FORD, D. C. & WILLIAMS, P. 1989. *Karst Geomorphology and Hydrology*. Unwin Hyman, London.

GETTY, S. R. & DEPAOLO, D. J. 1995. Quaternary geochronology using the U-Pb method. *Geochimica et Cosmochimica Acta*, **59**, 3267–3272.

HILL, C. A. & FORTI, P. 1997. *Cave Minerals of the World*. National Speleological Society, Huntsville, Alabama.

LATHAM, A. G., FORD, D. C., SCHWARCZ, H. P. & BIRCHALL, T. 1989. Secular variation from Mexican stalagmites: their potential and problems. *Physics of the Earth and Planetary Interiors*, **56**, 34–48.

MAGUIRE, J. M. 1985. Recent geological, stratigraphic and palaeontological studies at Makapansgat Limeworks. *In:* TOBIAS, P. V. (ed.) *Hominid Evolution: Past, Present and Future*. Liss, New York, 151–164.

——, PEMBERTON, D. & COLLETT, M. H. 1980. The Makapansgat Limeworks grey breccia: hominids, hyaenas, hystricids or hillwash? *Palaeontologia Africana*, **23**, 75–98.

MAGUIRE, J. M., SCHRENK, F. & STANNISTREET, I. G. 1985. The lithostratigraphy of the Makapansgat Limeworks Australopithecine site: some matters arising. *Annals of the Geological Survey of South Africa*, **19**, 37–51.

MASON, R. 1988. *The Cave of Hearths, Makapansgat, Transvaal.* Archaeological Research Unit Occasional Paper No. 21, University of Witwatersrand Press, Johannesburg, South Africa.

MCFADDEN, P. L., BROCK, A. & PARTRIDGE, T. C. 1979. Palaeomagnetism and the age of the Makapansgat Hominid site. *Earth and Planetary Science Letters*, **44**, 373–382.

PARTRIDGE, T. C. 1975. *Stratigraphic, Geomorphological and Palaeo-Environmental studies of the Makapansgat Limeworks and Sterkfontein Hominid Sites: a progress report on research carried out between 1965 and 1975.* South African Society for Quaternary Research, Cape Town Conference.

—— 1979. Re-appraisal of lithostratigraphy of Makapansgat Limeworks hominid site. *Nature*, **279**, 484–488.

RAYNER, R. J., MOON, B. P. & MASTERS, J. C. 1993. The Makapansgat Australopithecine environment. *Journal of Human Evolution*, **24**, 219–231.

SCHWARCZ, H. P., GRUN, R. & TOBIAS, P. V. 1994. ESR dating studies of the Australopithecine site of Sterkfontein, South Africa. *Journal of Human Evolution*, **26**, 175–181.

TURNER, B. R. 1980. Sedimentological characteristics of the "Red Muds" at Makapansgat Limeworks. *Palaeontologia Africana*, **23**, 51–58.

VRBA, E. S. 1982. Biostratigraphy and chronology, based particularly on Bovidae of southern hominid-associated assemblages: Makapansgat, Sterkfontein, Taung, Kromdraai, Swartkrans and also Elandsfontein Saldanha, Broken Hill (Kabwe) and Cave of Hearths. *Proceedings of the 1st International Congress on Human Palaeontology*, **2**. Paris, CNRS, 707–752.

—— 1996. On the connections between palaeoclimate and evolution. *In:* VRBA, E. S., DENTON, G. H., PARTRIDGE, T. C. & BUCKLE, L. H. (eds) *Palaeoclimate and Evolution, with Emphasis on Human Origins.* Yale University Press, Yale, 24–45.

WELLS, L. H. & COOKE, H. B. S. 1956. Fossil Bovidae from the Limeworks Quarry, Makapansgat, Potgietersrus. *Palaeontologia Africana*, **4**, 1–56.

ZAVADA, M. S. & CADMAN, A. 1993, Palynological investigations at the Makapansgat Limeworks: an Australopithecine site. *Journal of Human Evolution*, **25**, 337–350.

# Testing the potential of soil-stratigraphic palynology in podsols

RICHARD TIPPING[1], DEBORAH LONG[1], STEPHEN CARTER[2], DONALD DAVIDSON[1], ANDREW TYLER[1] & BRIAN BOAG[3]

[1]*Department of Environmental Science, University of Stirling, Stirling FK9 4LA, UK*

[2]*Headland Archaeology, Albion Business Centre, 78 Albion Road, Edinburgh EH7 5QZ, UK*

[3] *Scottish Crop Research Institute, Invergowrie, Dundee DD2 5DA, UK*

**Abstract:** Pedological, palynological, soil-micromorphological, geochemical and soil-faunal data are presented for a weakly developed free-draining ferric podsol soil profile in which three securely dated, known-age inputs (non-native tree pollen, spheroidal carbonaceous particles, $^{137}Cs$) have been added to the soil surface and incorporated over the last *c.* 150 years, from *c.* 1840 AD. We can thus observe the mechanisms of particle incorporation over time-spans appropriate to those of pedogenic processes, and analyse the rates, depth, extent and significance of mixing processes in a soil type that has often been seen as providing secure stratigraphic contexts for subfossil pollen analysis.

Our data indicate that pollen and other particles are thoroughly and completely mixed within the L/F horizon of podsols. Mixing occurs predominantly by ingestion and bioturbation by large near-surface feeding invertebrates. Mixing is also very rapid. Transfer of pollen to lower organic horizons occurs through the liberation of pollen as large invertebrate excrement is itself ingested by enchytraeid populations, but bioturbation in these lower horizons is insufficient to move further the already-mixed pollen assemblages. The absence of earthworm populations in these acid soils means that subsequent vertical transfer to mineral horizons does not occur in any significant way. This ability of organic horizons in podsols to store pollen, the complete mixing of particles in near-surface horizons, and the prolonged time-spans over which these mixing processes can operate, indicate that resultant pollen stratigraphies are normally probably too coarse in temporal resolution to be of value in palaeoecological interpretation.

Pollen contained within soils buried beneath archaeological sites is widely used as a source of palaeoecological information (Dimbleby 1985). Effectively sealed from later contaminants by the construction of archaeological monuments, pollen assemblages within such soils are argued to retain evidence for vegetation cover and land uses immediately prior to burial (e.g. Casparie & Groenman van Waateringe 1980; Andersen 1992; Tipping *et al.* 1994). The use of pollen assemblages within soils to reconstruct vegetation histories over time (Dimbleby 1957; 1961, 1985), rather than simply the 'snapshot' pre-burial approach, has been more controversial since many

*From:* POLLARD, A. M. (ed.) 1999. *Geoarchaeology: exploration, environments, resources.* Geological Society, London, Special Publications, **165,** 79–90. 1-86239-053-3/99/$15.00

soils are biologically active, and the retention of stratigraphically interpretable data is thus questioned (Godwin 1958; Havinga 1967).

The organic surface (mor) horizons of podsol profiles have long been viewed as providing the most secure stratigraphies from which to obtain long-term vegetation histories from soils (Dimbleby 1962; Havinga 1968; Munaut *et al.* 1968; Iversen 1969; Smith & Taylor 1969; O'Sullivan 1973; Stockmarr 1975; Andersen 1979; Cruickshank & Cruickshank 1981; Aaby 1990; Dijkstra & van Mourik 1995). The limited numbers of soil organisms in these acid soils leads to the assumption that 'the fossil mor layer has accumulated like peat or gyttja' (Iversen 1969: 39), more conventional sediment-types for pollen analysis, and thus it retains stratigraphic integrity.

There are difficulties in this assumption, however. Podsols derive from more biologically active soils with mull organic horizons, and the extent to which the mineral horizons of podsols retain an imprint of biologically mixed pollen assemblages has been debated (Munaut *et al.* 1968; Iversen 1969; Havinga 1974). More importantly, mor formation may not result in pollen-stratigraphic resolutions that are any more than very coarse (e.g. capable of temporal resolution at centurial or poorer resolutions). The development of a 'fossil' mor (Iversen 1969; Stockmarr 1975) is gradual, occurring over centuries (Aaby 1990) and passes through stages in which rates of biological activity are slowly reduced (Kendrick 1959; O'Sullivan 1973). Early stages of mor formation are characterized by biological activity, particularly at the soil surface where arthropods digest litter and mix organic matter (Stockmarr 1975). Deeper and more advanced stages are characterized by enchytraeid and fungal organic matter decomposition (Andersen 1979), and it is here that vertical mixing of materials is reduced. A critical issue is, then, to determine over what duration mixing processes in early mor formation occurs.

In 1995 a project commenced to establish whether a range of currently forming soil types, commonly found preserved beneath archaeological monuments, retain interpretable pollen stratigraphies. One of these soil types is a podsol. The project combined the application of both fine-resolution palynological and soil-micromorphological techniques (Tipping *et al.* 1994). In particular, the project was able to monitor over long time-periods (the last *c.* 150 years) the deposition, incorporation, processes of movement, degree of mixing and extent of destruction of known-age 'marker' pollen grains and other dated components in these soils. Other publications discuss in detail our field site in southern Scotland, our methodology and the ways in which we establish the known age of our 'markers' (Tipping *et al.* 1997), the recent ecological and agrarian history of the field site, critical to pedological change (Carter *et al.* 1997), and discussion of the processes of pollen incorporation observed through soil-micromorphology (Davidson *et al.* 1999). Details of the palynological techniques are found in Long *et al.* (in press). We will discuss elsewhere the rates of sediment/pollen mixing in all the soils examined and the important processes of pollen deterioration and destruction in podsols and other soils.

## The field site and methods

The upland rough pasture of Lour lies in the upper Tweed valley in southern Scotland, just south of Peebles (Fig. 1). The treeless grazed grass-heath lies *c.* 1 km downwind of Scotland's oldest arboretum at Dawyck (Bown 1992), which is the

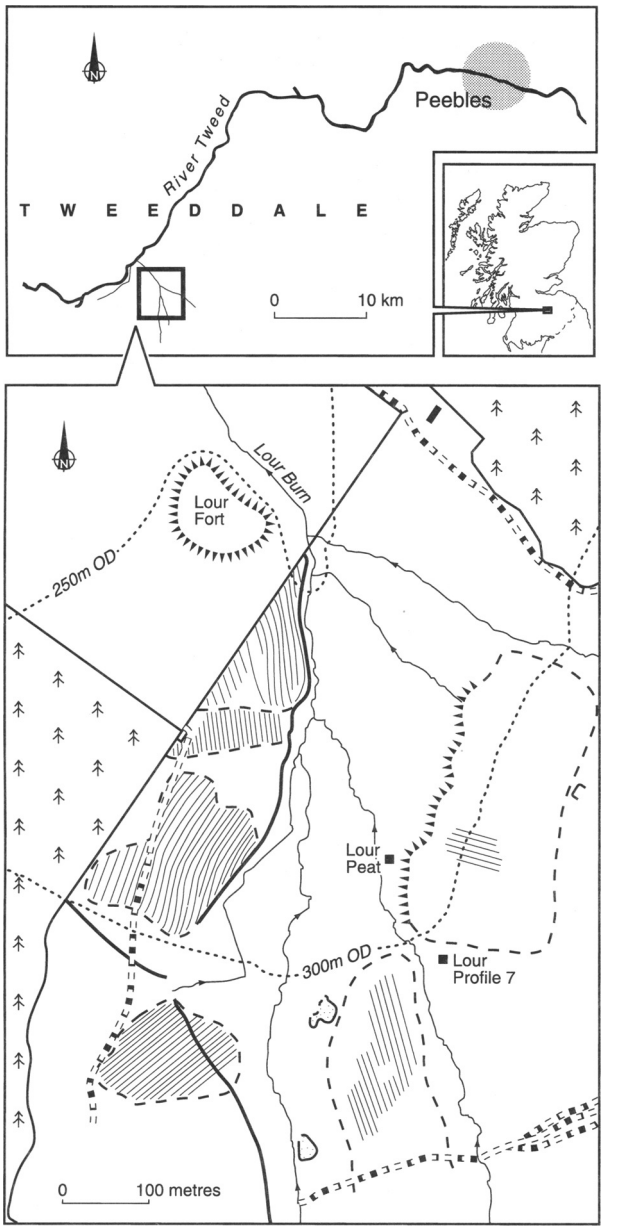


**Fig. 1.** (**a**) The location of Lour in southern Scotland and (**b**) the site-setting of profile 7 (P7) outside the agricultural remains mapped by Carter *et al.* (1997). The location of the Lour Peat Profile (LP) is also shown.

source for much of the known-age non-native tree pollen being incorporated into the soils at Lour (Tipping *et al.* 1997). Three dated inputs to the soils are examined. Non-native tree pollen (Coniferales, *Fagus*, *Pinus* [not native in southern Scotland] and *Ulmus* [native but largely regionally extinct before 18th century AD planting]; Tipping *et al.* 1997) was deposited on the hillside at Lour from *c.* 1840 AD and

dated independently by $^{210}$Pb and spheroidal carbonaceous particle (SCP) dating at a small-diameter peat basin at Lour (Carter *et al.* 1997). SCPs were deposited on soil surfaces after *c.* 1900 AD (Rose *et al.* 1995; Tipping *et al.* 1997). Pollen and SCP's are silt-sized particles.

$^{137}$Cs was deposited after 1963 AD. $^{137}$Cs arrives at the soil surface in solution. It is retained in organic-rich soils through electrostatic bonding (Wauters *et al.* 1994) and is sorbed onto clay particles (Shand *et al.* 1994; Maes *et al.* 1998). The majority of measured $^{137}$Cs is probably attached to clay particles or organic matter complexes, and if so, the distribution of $^{137}$Cs within a soil profile is a measure of the re-distribution of clays and organic matter since 1963 AD. However, our data suggest that a small but measurable proportion of $^{137}$Cs can be translocated in solution down-profile for tens of centimetres before being bonded, so that the vertical distribution of $^{137}$Cs is not entirely accounted for by particle movement. The different dated inputs may, therefore, not behave in exactly the same ways during incorporation into soils (below).

Lour has a mosaic of soil types developed on colluvium from acid Silurian mudstones, with groundwater hydrology representing the dominant soil-forming gradient and acidification representing a secondary gradient (Davidson *et al.* 1999). The different soil types and the dated peat sequence (Fig. 1) are clustered within a few hundred metres, which allows us to assume that sub-aerial inputs of non-native pollen, SCPs and $^{137}$Cs are uniform in timing and concentrations between sites.

Profile 7 is a relatively weakly developed free-draining ferric podsol (Table 1) of the Minchmoor Series. Although dithionite-extractable Fe is not significantly reduced in the L/F and H horizons compared to lower horizons, it is elevated in the E horizon (Table 2). Its immaturity is explained by the late Holocene acidification of the soils; although the onset of podsolization cannot be dated directly, it predates the incorporation of known-age inputs to the soil, after *c.* 1840 AD (below). The expansion of acid heath on the hillside is dated to the mid-18th century from the Lour Peat pollen diagram (Carter *et al.* 1997). The podsol is evolving naturally, and lies outwith areas of post-medieval agrarian disturbance (Fig. 1: Carter *et al.* 1997). Ground cover is 100%; principal taxa and approximate percentages are *Calluna vulgaris* (99%), *Sphagnum* spp. (90%), *Polytrichum* spp. (10%) and *Pteridium* (2%).

The soil profile was excavated to the Bx horizon; Table 1 is the field description. Kubiena tins were inserted in closely adjacent columns for both soil-micromorphological preparation (Murphy 1986; Davidson *et al.* 1999) and palynological subsampling (Tipping *et al.* 1994). Bulk samples 10 mm thick were taken to 130 mm, 20 mm thick samples below 150 mm, for $^{137}$Cs and physical analyses (pH, organic matter by loss-on-ignition, particle size determined by Coulter Counter following disaggregation and removal of organic matter, pyrophosphate-extractable and dithionite-extractable Fe ratios (Avery & Bascomb 1982): Table 1). Larger bulk samples, one per soil horizon, were taken to determine soil faunal populations by hand sorting and, for enchytraeids, using Tullgren funnels (Boag *et al.* 1997). Soil-micromorphological descriptions are described on a web-site (http://www.stir.ac.uk/ envsci/Lour/lour7). Palynological methods are described fully in Long *et al.* (in press). The interpretations are derived from pollen counts of *c.* 3 mm thick slices at 10 mm intervals, with pollen sums of 200 arboreal pollen grains.

**Table 1.** *Field description of the soil profile at Lour 7*

| LOUR 7: PODSOL<br>EXCAVATED 19TH OCTOBER 1994<br>FIELD SAMPLED 19/20/25TH OCTOBER 1994 | |
|---|---|
| Profile description | |
| 0.0–4.0 cm<br>L/F | moist fine fibrous poorly, humified peat, clear smooth boundary to |
| 4.0–10.0 cm<br>H | : 5 YR2.5/1 black loamy well-humified fine fibrous peat, increasingly amorphous in lower part and leading to organic staining of upper part of next horizon in basal 2–3 cm, featuring very weakly developed fine subangular blocky structure, moist, friable, with many fine fibrous and few medium woody (*Calluna*) roots; stoneless, clear wavy (over 2 cm) boundary to |
| 10.0–16.0 cm<br>E | : 10 YR 4/2 dark greyish brown fine sandy silt loam with very weakly developed medium angular blocky structure, slightly, moist, friable, with common fine fibrous roots and few small subrounded Silurian mudstones; clear wavy (over 4–5 cm) boundary to |
| 16.0–16.5 cm<br>B(f) | : 7.5 YR 5/6 fine sandy silt loam with very weakly developed medium angular blocky structure, slightly moist, friable, with common fine fibrous roots and few small subrounded Silurian mudstones with thin discontinuous faint to distinct fe-pan or zone of fe-enrichment; broken boundary to |
| 16.5–25.0 cm<br>B | : 10 YR 5/4 yellowish brown fine sandy, silt loam with weakly developed fine-medium subangular blocky structure, slightly moist, friable, with common fine fibrous roots and common medium subrounded and few large subrounded Silurian mudstones; gradual wavy (over 2–3 cm) boundary to |
| 25.0–41.0 cm<br>Bs | : 10 YR 6/6 brownish yellow fine sandy silt loam with weakly developed fine subangular blocky structure, slightly moist, friable, with few fine fibrous roots and common medium subrounded and few large subrounded Silurian mudstones; clear wavy (over 2 cm) boundary to |
| 41.0–45.0 cm +<br>B(x) | : 10 YR 4/6 dark yellowish brown sandy silt loam with weakly developed fine-medium platy structure, weakly indurated, with no roots but many small, many medium and few large subrounded Silurian mudstones. |
| | base not seen |

## Presentation of data and results

The many and complex data-sets have been reduced or simplified in order to examine the question of stratigraphic integrity, degree and depth of mixing within the surface organic horizons. Table 1 summarizes the field description of the profile. Table 2 summarizes the physical properties of the soil: mean values of these variables for each horizon are presented. Figure 2 presents data on the location of tetrad (*Calluna, Erica, Vaccinium*) pollen grains within soil-structural components derived from soil-micromorphological analysis; these distinctive grains were seen in thin-section using auto-fluorescence techniques (Phillips 1972; Davidson *et al.* 1999). Thin-section descriptions are found on the web-site listed above: the boundaries between horizons are comparable in depth and character between field and soil-micromorphological

**Table 2.** *Physical and soil-faunal data for the soil profile at Lour 7*

| Horizon | Depth (cm) | pH | Organic Content (%) | Di-extractable Fe | Mean Particle Size (μm) | Enchytraeids per $m^2$ * |
|---|---|---|---|---|---|---|
| L/F | 0–4 | 2.70 | 83 | 0.85 | 65.10 | 2500 |
| H | 4–8 | 2.74 | 39 | 1.70 | 66.93 | 938 |
| E | 8–19 | 3.46 | 10 | 1.93 | 54.19 | none recorded |
| Bf | 19 | n.d. | n.d. | 1.90 | n.d. | n.d. |
| Bw | 19–27 | 3.59 | 6.5 | 1.70 | 57.16 | 4700 |
| Bw/Bx | 27–31 | 3.72 | 5.5 | 1.87 | 69.21 | none recorded |
| Bx | 31+ | 3.97 | 2.5 | 1.28 | 88.63 | none recorded |

* estimated from 40 g bulk sample and assuming soil bulk density of 1.25
n.d. not determined

descriptions except the L/F–H boundary (Tables 1, 2). Figure 3 depicts the fine-resolution stratigraphic analyses of non-native pollen, SCPs and $^{137}Cs$ concentrations plotted against depth: soil horizon boundaries are also depicted. The pollen data are presented as total concentrations of non-native tree pollen: percentage values of these non-native tree types are low because of the influx of local herb pollen, and this measure is the clearest way to depict the depth of mixing of this dated input. SCPs

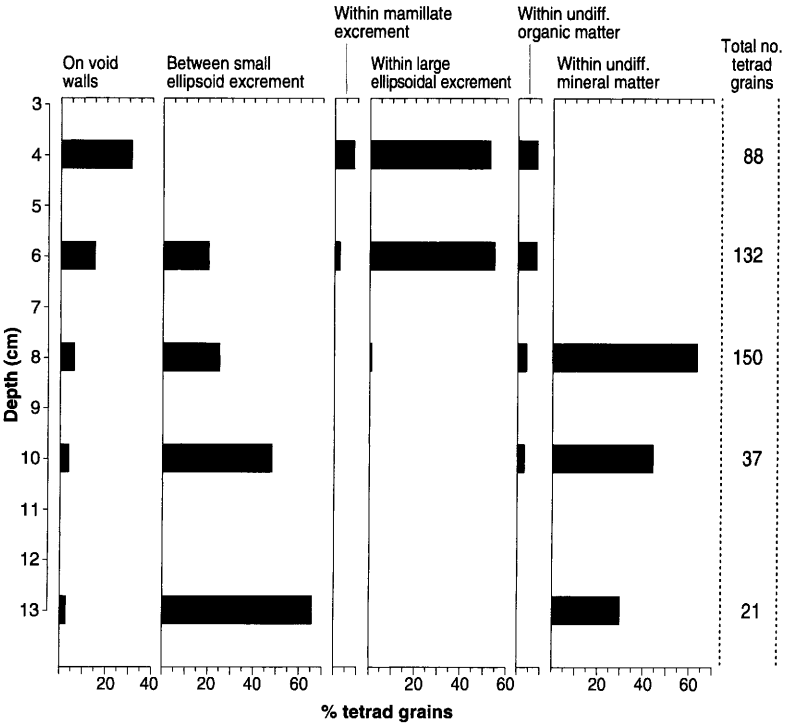


**Fig. 2.** The location of tetrad pollen grains (*Ericaceae* undiff.) within different micro-structural elements of the organic horizons at Lour 7 plotted against depth below ground surface, identified from thin-section fluorescence analysis.

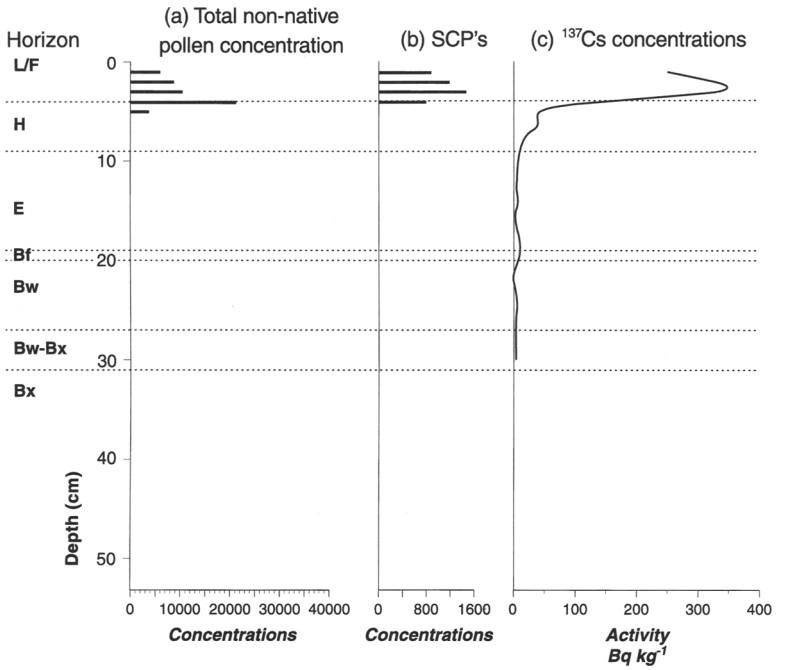


**Fig. 3.** Fine-resolution stratigraphic analyses of (a) non-native pollen concentrations, (b) SCP concentrations and (c) $^{137}$Cs concentrations plotted against depth: soil horizon boundaries are also depicted.

are also depicted as concentrations. $^{137}$Cs concentrations are expressed as Becquerels per kg. Only enchytraeids were identified from faunal samples (Table 2).

pH is throughout the profile strongly acid, and no evidence for earthworms was found either from faunal analyses (Table 2) or thin-section identification of excrement (Lour web-site). L/F and H horizons are highly organic, and from soil-micromorphological description (Lour web-site) these comprise organic excrement containing cellular and amorphous residues. The L/F horizon is significantly richer in recognizable coarse tissue residues (stem, leaf and root tissues), and the H horizon has a much higher amorphous organic component. The crumb/granular micro-structure of both L/F and H horizons is created by invertebrate excrement, principally large ellipsoids, with consequent high porosity. Small ellipsoid excrement, probably produced by enchytraeid populations, are present in the L/F horizon, but are dominant in the H and E horizons where they create a micro-aggregate structure. Enchytraeids are found in faunal analyses throughout the profile (Table 2), although their rarity in Tullgren funnel collections indicates that estimates of density per $m^2$ have large errors, and the non-recording of enchytraeids in certain horizons has no significance.

The distribution of tetrad pollen grains within structural components in thin-section suggests that only in the L/F horizon and uppermost part of the H horizon is a significant proportion of pollen grains found as free elements on void walls, and thus capable of downwashing (Fig. 2). The high proportion of such grains above *c.* 60 mm is probably due to the high porosity produced by faunal excrement. Nevertheless, the majority of grains are contained within large ellipsoid excrement, probably from species of Arthropoda (Stockmarr 1975). Being contained within

excrement, the pollen grains within the topmost *c.* 60 mm are seen to be ingested by large invertebrates, and are subject to mixing by these animals. These near-surface large invertebrates are, from the distribution of large ellipsoidal excrement, confined to the topmost *c.* 60 mm of the profile. Below 60 mm, within the H horizon and mineral horizons, the proportions of tetrad grains on void walls is very small (Fig. 2). Nearly all pollen grains are packed between the micro-aggregates of enchytraeid excrement or, in the E horizon, are bound within mineral matter aggregates. Tetrad grains in thin-section decline in abundance into the E horizon (Fig. 2). Proportions of such grains between enchytraeid excrement increase down-profile; reliable counts were not possible below 130 mm.

The dated inputs show close comparability in the depths to which they have been incorporated (Fig. 3). Non-native pollen, deposited on the soil surface after *c.* 1840 AD, is found only to 50 mm, throughout the L/F horizon and into the top of the H horizon. Concentrations increase from the ground surface within the L/F horizon to a peak at the L/F–H horizon. SCP's are found to 40 mm depth, the L/F–H boundary, and occur at uniform concentrations within the L/F horizon. $^{137}$Cs concentrations, deposited since 1963, decline smoothly from 20 mm to 60 mm; concentrations are largely insignificant below this depth.

## Interpretation

The three dated inputs to the podsol are found to approximately the same depth in the profile. This is not an artefact of sampling because all inputs were monitored at the same 10 mm sampling resolution (Fig. 3). Small and largely insignificant amounts of $^{137}$Cs, probably in solution, are found at greater depths, but the majority of $^{137}$Cs, sorbed onto particles, is locked within the topmost 2–3 cm of the soil. These inputs are found to the same depths despite being added as separate and independent 'injections' at different times within the last *c.* 150 years. It is likely that this pattern represents mixing of these components within the L/F horizon over time. The appearance of SCPs at uniform concentrations to 50 mm suggests that this degree of mixing occurs in much less than a century.

There are differences in the degree to which these dated components are distributed through the L/F horizon. While the older components, non-native pollen and SCPs, are more-or-less uniformly and so completely mixed, $^{137}$Cs concentrations decline down-horizon, suggesting that it takes longer than *c.* 30 years (1963–1997) for complete mixing to occur.

Non-native pollen grains, despite being incorporated into the profile since *c.* 1840 AD, have only been assimilated into the topmost layer of the H horizon. This suggests that transfer of pollen from L/F to H horizons is by no means rapid. There is thus the potential for pollen to continue to accumulate in the L/F horizons for very long periods (discussed below), and that for this duration all vegetation changes will be conflated into one completely mixed and uniform pollen assemblage.

The depth to which these components are mixed at Profile 7 is very largely controlled by horizon-forming pedogenic properties, in particular by the vertical range of near-surface feeding large invertebrates. It is probable that most pollen in the L/F horizon is transferred in small vertical increments through repeated ingestion, because $^{137}$Cs bound to particles is only moved a couple of centimetres and is not completely mixed to the base of the L/F horizon (above). Over a time interval of

less than a century, however, this small-increment mixing is thorough. Enchytraeids liberate pollen grains at and below the L/F–H boundary by ingesting large ellipsoid excrement. Enchytraeids are too small to ingest or to move pollen grains. The liberation of pollen grains in this way does not make pollen grains more susceptible to downwashing because of the densely packed structure of enchytraeid excrement. However, any pollen transferred from L/F to H horizons and to deeper and more humified mor horizons in older podsols, will remain mixed; pollen assemblages in lower organic horizons are no more capable of temporal resolution than those in the surface horizon.

Transfer of pollen does not appear to occur from organic to mineral horizons. Cruickshank & Cruickshank (1981) report a marked increase in pollen concentrations at the organic/mineral horizon boundary, although this is not seen at Lour 7; this may again relate to the age of the podsol and the time taken for pollen to move down and stack against this boundary. In detail this boundary possibly exists due to microstructural changes but in broad terms is through the absence of earthworm activity. The absence of earthworms also suggests that up-profile transfer of pollen (Walch *et al.* 1970) from mineral to organic horizons does not occur, although we cannot demonstrate this. The organic horizons appear, once formed, to be sealed from the addition of older pollen from subsurface horizons.

## Discussion

Vegetation change on a podsol surface will be depicted by changing pollen inputs to the soil (Dijkstra & van Mourik 1995). The mechanisms and rates of incorporation into the surface organic horizons discussed above, however, mean that pollen assemblages cannot be employed in detailed temporal palaeoecological reconstructions of such vegetation changes. It is the length of time the L/F horizon retains a pollen assemblage and so mixes it with earlier assemblages that is critical. O'Sullivan (1973) argued that the time spent in this mixed zone is short compared to that within deeper stratified horizons. The debate focuses on whether the 'broad stratification' of these mixed assemblages allows 'meaningful interpretation' (O'Sullivan 1973: 260). Our data suggest that pollen will remain in the L/F horizon over very long periods, and that pollen assemblages will not be interpretable.

At Lour we statistically compared, using DECORANA, the pollen assemblages at all soil profiles with the more secure pollen stratigraphy at the Lour Peat (for the latter see Carter *et al.* 1997). All soil profiles failed to reproduce the pollen stratigraphy within the peat (Long *et al.* in press). This suggests that mixing is at least partly responsible for a profound reduction in the ability to interpret podsol pollen profiles, as in all soil profiles examined at Lour. Another issue, not discussed in this paper through lack of space, is the loss of information induced through pollen destruction, and this too is thought to be highly significant (Long *et al.* unpublished data).

Our model implies that pollen stratigraphies from deeper mor horizons within podsols should be smoothed by this mixing process. This is seen in other studies (e.g. Iversen 1969; Stockmarr 1975). It is best analysed by Andersen (1979), who illustrated the vertical spreading of a known-age 'injection' of *Calluna* pollen in thin immature podsols compared to a master-profile (H16): Andersen refers to this master-profile, with its extraordinary 'spiky' pollen record, as a soil but we interpret this site as a peat lying within a small depression, biologically inert through, perhaps,

waterlogging. The majority of O'Sullivan's (1973) eight detailed pollen diagrams are also smoothed; exceptions (Profiles 1, 7, 8) are abrupt changes that coincide with pedogenic boundaries between F and H horizons, seen as critical in terms of storage and transfer of pollen (above).

Our findings do not question those of other workers in which sequences of $^{14}C$ dates are obtained in stratigraphic order (O'Sullivan 1973; Cruickshank & Cruickshank 1981; Stockmarr 1975). However, these $^{14}C$ dates represent only the mean age of a mixed organic component (Scharpenseel 1971; Matthews 1993); again it is the duration of mixing that is important. O'Sullivan (1973) recognized the problem of vertical mixing in the explanation of one erroneous near-surface $^{14}C$ date (UB-393), and suggested that organic matter has a prolonged residence time in these shallow horizons, an observation our methodology cannot test. Cruickshank & Cruickshank (1981), with a more intensive dating programme, argued that all $^{14}C$ dates lie in correct stratigraphic order, but this is only so after omitting assays (e.g. UB-2327) argued to be too young, explained through rootlet penetration (despite these being excluded in sample pre-treatment) but perhaps equally explicable through organic matter mixing. Most relevant to our 'known-age marker' approach is the work of Stockmarr (1975). $^{14}C$ dating was not used sufficiently to test interpretations, but two pollen types of, broadly, known age, *Secale cereale* and *Centaurea cyanus*, were found in samples higher and younger than expected, and a third, *Fagopyrum*, was found deeper and earlier than expected. The apparent displacement of *Secale* and *Centaurea* may be explained by local absence until after regional introduction, but down-profile displacement of the Medieval indicator-taxon, *Fagopyrum*, to purportedly Roman horizons, is harder to explain. These 'marker' pollen types suggest that vertical mixing is significant in these profiles, and that pollen of several hundred years age-difference, greater than observed at Lour 7, is possible.

## Conclusions

The study has developed techniques able to trace particle incorporation in soils over long time-spans of centuries and longer, durations over which slow pedogenic processes operate. These techniques confirm earlier studies in identifying that mixing of pollen and other particles occurs in the uppermost organic horizon, the L/F horizon. Mixing occurs through large near-surface feeding invertebrates; the taxa remain unidentified although species of Arthropoda are perhaps most likely. Mixing takes place through ingestion of pollen, and subsequent defecation, by these large invertebrates. Physical downwashing through pores is not a significant process.

What this study demonstrates is the completeness of mixing, and the rapidity of mixing. Although the three known-age inputs are separated in time by over 100 years, all three occur to all depths within the L/F horizon, showing thorough mixing in, probably, much less than a century. It has also been shown that there has been no measurable transfer of known-age particles from organic to mineral horizons over the last *c.* 150 years, probably through the absence of earthworms in this acid profile. We assume that upward movement of older pollen from mineral horizons is also insignificant. Pollen within the organic horizons, although thoroughly mixed, is thus trapped. This is disadvantageous for palaeoecological reconstruction from such soils because the near-surface organic horizons can potentially recruit

and then mix pollen for very long periods; re-interpretations of Stockmarr's (1975) data suggest that pollen of many centuries may be integrated into uniform pollen assemblages. Earlier studies have suggested that pollen stratigraphies in podsols are 'broadly' capable of temporal interpretation. However, although the definition of 'broad' is open to interpretation, our data suggest that the temporal resolution of pollen stratigraphies in podsol profiles is so crude as to be effectively meaningless.

We would like to thank A. Hipkin for identifying Profile 7 at Lour, and assisting in its excavation and field description. R. Kynoch produced the pollen samples and undertook most physical analyses. M. McCleoud manufactured the thin-sections and assisted with fluorescence techniques. L. Donaldson generated the Fe data, A. Mennim the particle-size data and S. Bradley the $^{137}Cs$ counts. The project was funded by a NERC grant (GR/J73421).

## References

AABY, B. 1990. Forest vegetation and podzol soil development. *Quaternary Studies in Poland,* **10**, 13–20.

ANDERSEN, S. TH. 1979. Brown earth and podzol: soil genesis illuminated by microfossil analysis. *Boreas,* **8**, 59–73.

—— 1992. Early- and middle-Neolithic agriculture in Denmark: pollen spectra from soils in burial mounds of the Funnel Beaker Culture. *Journal of European Archaeology,* **1**, 153–180.

AVERY, B. W. & BASCOMB, C. L. 1982. *Soil Survey Laboratory Methods.* Soil Survey Technical Monograph 6. Soil Survey of Great Britain (England and Wales), Harpenden.

BOAG, B., PALMER, L. F., NEILSON, R., LEGG, R. & CHAMBERS, S. J. 1997. Distribution, prevalence and intensity of earthworm populations in arable land and grassland in Scotland. *Annals of Applied Biology,* **130**, 153–165.

BOWN, D. 1992. *Four Gardens In One.* HMSO, Edinburgh.

CARTER, S. TIPPING, R., DAVIDSON, D., LONG, D. & TYLER, A. 1997. A multiproxy approach to the function of postmedieval ridge-and-furrow cultivation in upland northern Britain. *The Holocene,* **7**, 447–456.

CASPARIE, W. A. & GROENMAN VAN WAATERINGE, W. 1980. Palynological analysis of Dutch barrows. *Palaeohistoria,* **22**, 7–65.

CRUICKSHANK, J. G. & CRUICKSHANK, M. M. 1981. The development of humus-iron podsol profiles, linked by radiocarbon dating and pollen analysis to vegetation history. *Oikos,* **36**, 238–253.

DAVIDSON, D. A., CARTER, S., BOAG, B., LONG, D., TIPPING, R. & TYLER, A. Analysis of pollen in soils: processes of incorporation of pollen in five soil profile types. *Soil Biology and Biochemistry,* **31**, 643–653.

DIJKSTRA, E. F. & VAN MOURIK, J. M. 1995. Palynology of young acid forest soils in the Netherlands. *Mededelingen Rijks Geologische Dienst,* **52**, 283–296.

DIMBLEBY, G. W. 1957. Pollen analysis of terrestrial soils. *New Phytologist,* **56**, 12–28.

—— 1961. Soil pollen analysis. *Journal of Soil Science,* **12**, 1–11.

—— 1962. *The Development of British Heathlands and their Soils.* Clarendon Press, Oxford, Oxford Forestry Memoirs 23.

—— 1985. *Palynology of Archaeological Sites.* Academic Press, London.

GODWIN, H. E. 1958. Pollen-analysis in mineral soil: an interpretation of a podzol pollen-analysis by Dr. G. W. Dimbleby. *Flora,* **146**, 321–327.

HAVINGA, A. J. 1967. Palynology and pollen preservation. *Review of Palaeobotany and Palynology,* **2**, 81–98.

—— 1968. Some remarks on the interpretation of a pollen diagram of a podsol profile. *Acta Botanica Neerlandica,* **17**, 1–4.

—— 1974. Problems in the interpretation of pollen diagrams of mineral soils. *Geologie en Mijnbouw,* **53**, 449–553.

IVERSEN, J. 1969. Retrogressive development of a forest ecosysytem demonstrated by pollen diagrams from forest mor. *Oikos Supplement,* **12**, 35–49.

KENDRICK, W. B. 1959. The time factor in the decomposition of coniferous leaf litter. *Canadian Journal of Botany,* **37**, 907–912.

LONG, D. J., CARTER, S., DAVIDSON, D., TIPPING, R., BOAG, B. & TYLER, A. Testing the assumptions of stratigraphic integrity in soil pollen analysis: extent and rates of particle incorporation. *Journal of Archaeological Science.* In press.

MAES, E., DELVAUX, B. & THIRY, Y. 1998. Fixation of radiocaesium in an acid brown forest soil. *European Journal of Soil Science,* **49**, 133–140.

MATTHEWS, J. A. 1993. Radiocarbon dating of arctic-alpine palaeosols and the reconstruction of Holocene palaeoenvironmental change. *In*: CHAMBERS, F. M. (ed.) *Climate Change and Human Impact on the Landscape.* Chapman & Hall, London, 83–100.

MUNAUT, A. V., DURIN, L. & EVRARD, J. C. 1968. Récherches paleoécologiques et pédologiques en fôret d'Andigny (Aisne-France). *Bulletin de Société Botanique du Nord France,* **21**, 105–133.

MURPHY, C. P. 1986. *Thin Section Preparation of Soils and Sediments.* AB Academic Publishers, Berkhamsted.

O'SULLIVAN, P. E. 1973. Pollen analysis of Mor humus layers from a native Scots pine ecosystem, interpreted with surface samples. *Oikos,* **24**, 259–272.

PHILLIPS, L. 1972. An application of fluorescence microscopy to the problem of derived pollen in British Pleistocene deposits. *New Phytologist,* **71**, 755–762.

ROSE, N. L., HARLOCK, S., APPLEBY, P. G. & BATTARBEE, R. W. 1995. Dating of recent lake sediments in the United Kingdom using spheroidal carbonaceous particle (SCP) concentration profiles. *The Holocene,* **5**, 328–335.

SCHARPENSEEL, H. W. 1971. Radiocarbon dating of soils. *Soviet Soil Science,* **3**, 76–83.

SHAND, C. A., CHESHIRE, M. V., SMITH, S., VIDAL, M. & RAURET, G. 1994. Distribution of radiocaesium in organic soils. *Journal of Environmental Radioactivity,* **23**, 285–302.

SMITH, R. T. & TAYLOR, J. A. 1969. The Post-glacial development of vegetation and soils in northern Cardiganshire. *Transactions of the Institute of British Geographers,* **48**, 75–96.

STOCKMARR, J. 1975. Retrogressive forest development, as reflected in a mor pollen diagram from Mantingerbos, Drenthe, The Netherlands. *Palaeohistoria,* **17**, 38–51.

TIPPING, R., CARTER, S. & JOHNSTON, D. 1994. Soil pollen and soil micromorphological analyses of old ground surfaces on Biggar Common, Borders Region, Scotland. *Journal of Archaeological Science,* **21**, 387–401.

——, CARTER, S., DAVIDSON, D. A., LONG, D. & TYLER, A. 1997. Soil pollen analysis: a new approach to understanding the stratigraphic integrity of data. *In*: SINCLAIR, A., SLATER, E. & GOWLETT, J. (eds) *Archaeological Sciences 1995.* Oxbow, Oxford, Oxbow Monograph 64, 221–232.

WALCH, K. M., ROWLEY, J. R. & NORTON, N. J. 1970. Displacement of pollen grains by earthworms. *Pollen et Spores,* **12**, 39–44.

WAUTERS, J., SWEECK, L., VALCKE, E., ELSEM, A. & CREMERS, A. 1994. Availability of radiocaesium in soils: a new methodology. *Science of the Total Environment,* **157**, 239–248.

# Tracing the record of early alluvial tin mining on Dartmoor, UK

VARYL R. THORNDYCRAFT[1,2], DUNCAN PIRRIE[1] & ANTHONY G. BROWN[2]

[1]*Camborne School of Mines, University of Exeter, Redruth, Cornwall TR15 3SE, UK*

[2]*Wetland Research Centre, School of Geography and Archaeology, University of Exeter, Amory Building, Rennes Drive, Exeter EX4 4RJ, UK*

**Abstract:** Although there has been considerable speculation, there is as yet no conclusive evidence to confirm Dartmoor as a tin producing region in prehistory. This is in part due to extensive tin mining on the moor during the Medieval period destroying evidence of earlier mining activity. This paper presents the preliminary results of an integrated mineralogical and geochemical geoarchaeological approach to identifying the record of early mining activity. Floodplain sedimentary successions, that have not themselves been mined, and are downstream of known areas of tin streaming, retain a geochemical record of the mining activities because the early tin streaming released large quantities of mine waste tailings. Where these successions can be dated, they provide an indirect means of testing the record of mining activity on Dartmoor. Geochemical and mineralogical analyses of datable fluvial sediments aimed to (a) distinguish between natural and mine contaminated sediments, and (b) to date the onset of sediment aggradation caused by tin mining activity in the headwaters. Results from the Avon Valley show negligible Sn concentrations in basal silts that are dated to pre-2845 $\pm$ 45 yrs BP. Overlying silts are enriched in Sn and were deposited after 1560 $\pm$ 40 AD, suggesting that the Sn enrichment corresponds with tin streaming in the 16th century. In the Erme Valley, significant Sn enrichment post-dates an organic-rich silt dated at 1280 $\pm$ 45 AD. At both sites there is sediment aggradation coupled with an enhancement in Sn concentration consistent with mine waste contamination as a result of Medieval tin streaming.

The mineralogy and geochemistry of alluvial sediments reflects the geology, land use history and mining history within a river's catchment. Mining activity, and the release of mine waste products can have a major effect on both the rate of sedimentation within catchments, and in addition can significantly affect the sediment geochemistry and mineralogy. In recent years, geochemical studies of heavy metal contamination from historical mining operations, have been used to date alluvial sediments and determine sedimentation rates with reference to the known contaminant production record (e.g. Macklin 1985; Macklin *et al.* 1994, 1997). In the same way geochemical and mineralogical studies of datable sedimentary systems can be used to recognize the environmental impact of previous mining activity (e.g. Pirrie *et al.* 1997). On Dartmoor, there is a direct documentary record of tin mining from the 12th century onwards, and there has been considerable speculation that the record of tin mining on

*From:* POLLARD, A. M. (ed.) 1999. *Geoarchaeology: exploration, environments, resources.* Geological Society, London, Special Publications, **165,** 91–102. 1-86239-053-3/99/$15.00

Dartmoor may date back to the Bronze age. However, there is little direct evidence to prove local extraction of tin in the Bronze Age (Penhallurick 1986; Pearce 1979). It is possible that the fluvial systems draining the moor retain that evidence.

In this paper we utilize the contaminant record contained within datable fluvial sediments in order to identify periods of past tin mining on Dartmoor. In particular, we consider whether this approach can be used to identify prehistoric mining activity on the moor. The first tin (Sn) deposits likely to have been exploited were alluvial placer deposits of cassiterite in valley fills, believed to have been formed under periglacial conditions during the Pleistocene (Hosking & Camm 1982; Camm & Croot 1994). These alluvial tin deposits were extracted using hydraulic mining techniques (termed tin streaming) which would have had a significant effect on the sediment discharge downstream from the mining site. The destructive nature of tin streaming coupled with subsequent late Medieval reworking of the Sn-bearing alluvium has probably resulted in the destruction of earlier prehistoric and early Medieval mine remains, hence the need for this geoarchaeological approach.

## Tin mining on Dartmoor

Documentary evidence first records tin mining on Dartmoor during the 12th century (Greeves 1981; Penhallurick 1986; Harris 1992). Despite theoretical reasons suggesting the likelihood of prehistoric mining, there is, as yet, no unequivocal evidence for earlier mining on the moor (Pearce 1979; Sharpe 1992). The only physical evidence that has been cited in the literature is the discovery of a cassiterite pebble and one fragment of tin slag from an excavated Bronze Age hut on Dean Moor, in the River Avon catchment (Fox 1957). More recently, tin ingots (of late or post Roman age) have been recovered from a wreck in Bigbury Bay, near the mouth of the River Erme (Fox 1995), but these may have originated in Cornwall where there is evidence for tin mining as early as 3600 years BP (Miles 1975). The significance of tin slag deposits at a possible early Christian site, at Week Ford in the Dart Valley, is also contentious, as it is only constrained by a single radiocarbon date (570–890 AD) (Gerrard 1997).

The documented peak periods of tin production on the moor, during the 12th, 13th and 16th centuries (Harris 1992), were associated with the tin streaming of high grade alluvial tin deposits which typically contained 0.45–3 kg (0.022–0.15%) cassiterite per cubic metre (Beer & Scrivener 1982). The largest annual production was 252 tons of processed tin metal in 1524 (Harris 1992). There followed a decline in mining with production largely ceasing in the late 17th century. A small resurgence, in the 18th and early 19th centuries, brought about by increased tin demand, was associated with the reworking of previously mined reaches and the extraction of poorer quality lode tin by shaft and adit mining (Gerrard 1997).

The major environmental impact of tin streaming was an increase in sediment supply to local stream systems (Knighton 1989). Streaming involved the removal of the Holocene overburden of peats and fine-grained alluvial sediments to gain access to the placer gravels. The dense cassiterite was separated from the lighter gangue minerals using a controlled flow of river water through diverted channels or leats (Hitchens & Drew 1824; Gerrard 1992). The quartz dominated gangue, cassiterite locked within larger silicate grains, along with unrecoverable cassiterite in the silt and clay grain size fractions (Bradley 1990), was washed into the local

river systems affecting downstream channel geomorphology and floodplain sedimentation rates. The effect of this type of mining can be seen elsewhere, for example in the Ringarooma River in Tasmania (Knighton 1989). In response to tin streaming in the Ringarooma catchment, aggradation of the river bed of up to 5 m occurred, the channel widened by up to 300% and braided reaches commonly replaced the natural single channel pattern (Knighton 1989). Increased sedimentation rates were evident in Devon in the Medieval period. Siltation of important harbours, such as Plymouth and Teignmouth, resulted in 1531 in an Act of Parliament to implement pollution legislation, to curb the quantity of sediment released into the river systems by the tinners (Greeves 1981).

## Field methodology

### *Field sites*

In order to differentiate between natural and contaminated fluvial sediments, a variety of sites of different ages and lithologies were sampled. A site at Taw Marsh, on northern Dartmoor (Fig. 1), was chosen to represent natural upland sediments, owing to the exposure of a remnant fluvial terrace, with no evidence for mining by tin streaming. Although the terrace cannot be considered typical of those exploited, as it was unmined, the gravels at the base of the terrace provide a good opportunity to characterize the likely geochemistry and mineralogy of Dartmoor placer deposits. A lowland site in the middle reaches of the Teign Valley, near Chudleigh (Fig. 1), was chosen to characterize fine-grained, downstream alluvium of pre-mining age, in order to compare with downstream, fine-grained mining-contaminated sediments. An exposure of the upper (and therefore oldest) terrace of this floodplain consisted of a thick sequence of gravel and boulder deposits, suggesting deposition under the periglacial conditions of the late Pleistocene, and overlain by a silty-clay unit of probable early–mid-Holocene age.

The floodplain sites chosen for the characterization of mine waste contaminated sediments required the following criteria:

- The need to be downstream of any known tin mining activity so that the fluvial stratigraphy at the sample site was itself undisturbed by alluvial mining.
- The potential for dating at the site. This was either in the form of river terrace sequences, for relative dating, or peat deposits for radiocarbon ('absolute') dating.

A suitable series of terrace exposures was located in the Teign Valley, and palaeochannels with datable organic deposits were studied from the Erme Valley and the Avon Valley (Fig. 1).

### *Sediment sampling*

Monolith tins were used to collect samples from terrace exposures. There were no exposures of the palaeochannel deposits so these were cored using a 50 mm diameter gouge auger to sample the inorganic sediments for subsequent geochemical analysis. Peat deposits, for radiocarbon dating, were sampled using a 50 mm diameter Russian corer. The stratigraphy was described using a modified Troels–Smith scheme (Aaby

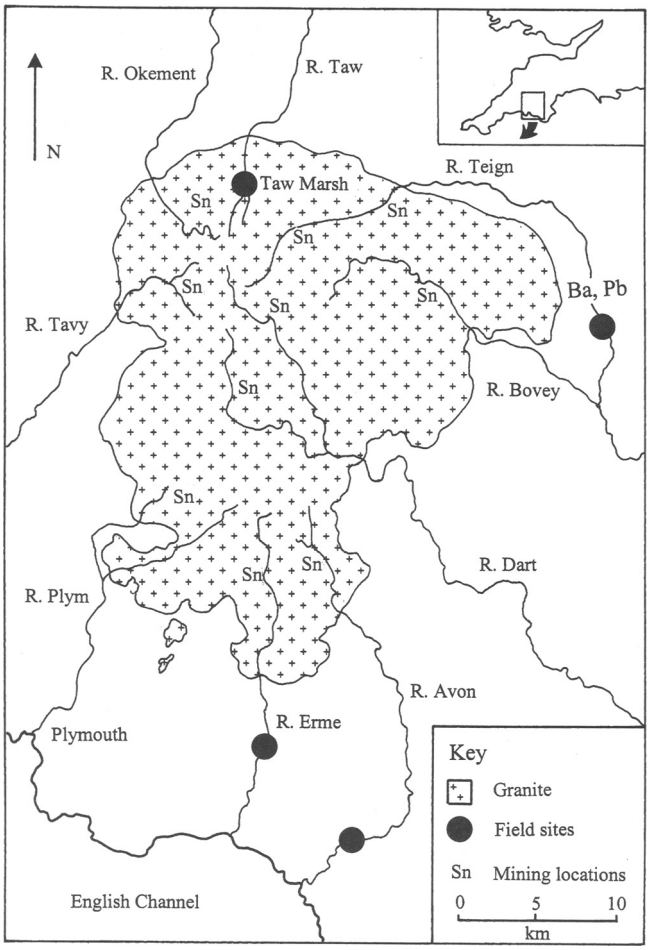


**Fig. 1.** Sketch map of Dartmoor showing sample locations and areas of documented mining activity.

1986). Sub-samples were taken at intervals of 50 mm to provide a sufficient sample size for the analytical techniques used.

## Laboratory methods

### *XRF analysis*

The sediment geochemistry was determined by X-ray fluorescence (XRF) using a Phillips PW 1400 analyser. The sample was dried overnight at 40°C, then riffled to obtain 20 g of sediment. This was then ground in a chrome steel tema mill for 90 seconds. Pressed disks of the ground sample were prepared using a boric acid jacket and a binding agent of 4% elvacite in acetone solution. Each sample was analysed for Sn, As, Cu, Pb, Zn and W using internally calibrated standards and data are reported as mg/kg (equivalent to ppm). The error limit for the metal concentrations determined was ±10 mg/kg.

### *Particle size distribution analysis*

Particle size distribution analysis was carried out using the procedures outlined by the British Standards Institution (1975, 36). Concentrated (30–40%) hydrogen peroxide ($H_2O_2$) was added to air-dried samples to remove organic matter. The samples were left for several days, with occasional gentle warming in order to speed up the oxidation reaction. The remaining sample was sieved at 2 mm and 600 μm, then dried and weighed. The <600 μm fraction was centrifuged for 30 minutes, washed with methylated spirit, re-centrifuged and dried overnight at 40°C. The dried sample was weighed before addition of 0.4% sodium hexametaphosphate ($NaPO_3$) and sodium carbonate ($Na_2CO_3$) dispersant solution. The samples were then stirred in an ultrasonic bath and analysed using a Malvern Mastersizer MS20 laser particle sizer. The Mastersizer had a measuring range of 1.2–600 μm.

### *Sample sieving*

Selected samples were prepared for geochemical analysis of the separate particle size fractions in order to show which sediment fractions were metal-dominated. The grain size fractions examined were: <63 μm, 63–125 μm, 125–180 μm, 180–250 μm, 250–500 μm, 500–2000 μm, 2–4 mm. In order to obtain 20 g of each size fraction, as required for XRF analysis, a bulk sample of 0.5–1 kg of sediment was usually required. Initial screening was carried out by dry sieving the sample on a shaker for 20–30 minutes followed by wet sieving.

### *Scanning Electron Microscopy analysis*

Scanning Electron Microscopy (SEM) studies were used to determine the mineralogy, in particular whether cassiterite occurred as liberated grains or in association with other host minerals and the nature of the heavy mineral assemblage. As the concentrations of the heavy metals in the sediments were generally low, density separation was performed using a shaking-table to obtain a heavy mineral concentrate in preparation for SEM analysis. SEM analysis was carried out on a polished mount of the sample using a JEOL 840 with Link (Oxford Instruments) AN10000 energy dispersive spectrometer (EDS). Digiscan and Digimap software linked to the SEM allowed grain measurements and chemical classifications to be determined.

### *Radiocarbon dating*

Eleven samples were submitted for radiocarbon dating at the NERC radiocarbon laboratory at East Kilbride. Nine were conventional dates on bulk samples and the remaining two were AMS-$^{14}$C dated due to insufficient carbon content of the samples for conventional dating.

## Results

### *Natural Sn-bearing sediments: Taw Marsh terrace*

For the Taw Marsh terrace sequence the highest Sn concentrations, which range from 93 to 114 mg/kg, occur in the basal (placer) gravels (Fig. 2). This is consistent with

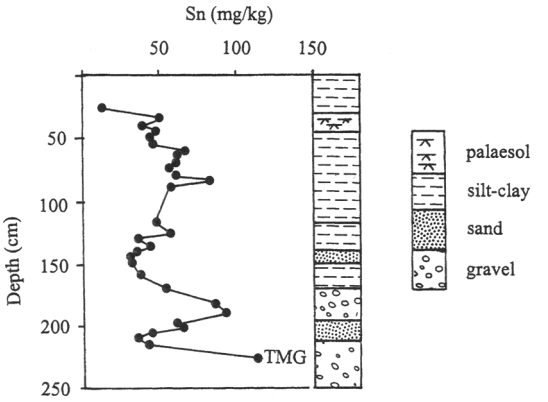


**Fig. 2.** Stratigraphy vs Sn profile for the uncontaminated Taw Marsh terrace. Note the elevated Sn concentration in the basal gravels. Particle size vs Sn concentration for sample TMG is shown in Fig. 3.

previous sedimentological studies of heavy mineral transport mechanisms which show the highest concentrations of cassiterite in the gravel bed load (Fletcher & Loh 1996). The fining upwards sedimentary sequence is associated with a decreasing trend in Sn concentration. The particle size geochemical distribution from the basal gravels (Fig. 3) clearly shows a peak Sn concentration of 1379 mg/kg in the 125–250 μm grain size fraction; this is coarser than that expected in mine waste contaminated sediments as the coarser grained cassiterite can be more easily extracted by simple mineral processing (Bradley 1990). In addition, the abundance of Sn in this grain size fraction is comparable to previously described Cornish placer deposits (Camm & Croot 1994; Camm 1999). In comparison to these upland gravel deposits, the lowland fine grained sediments sampled from the upper terrace deposits, of pre-mining age from the Teign Valley floodplain, contain negligible (<5 mg/kg) Sn concentrations.

## *Contaminated sediments (1): the Teign Valley middle terrace*

The Teign Valley middle terrace shows three distinct sedimentary units (Fig. 4), with two phases of contaminated sediment deposition separated by a unit consisting of

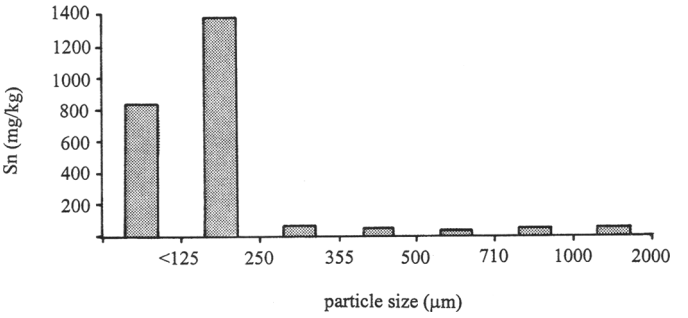


**Fig. 3.** Particle size vs Sn concentration for the basal gravels of the Taw Marsh terrace (sample TMG). Note the concentration within the 125–250 μm fraction.

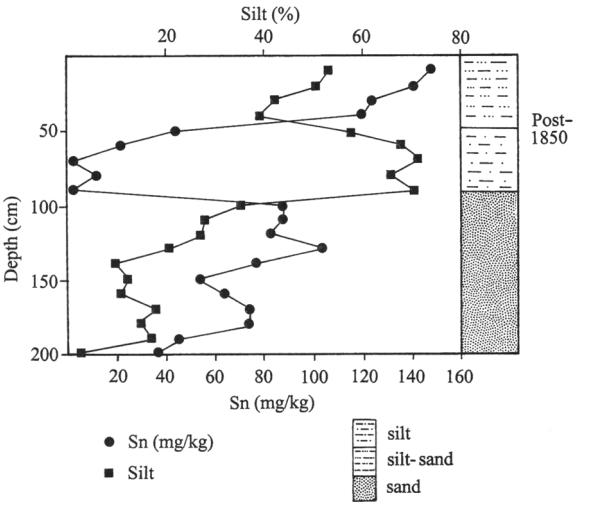


**Fig. 4.** Diagram showing Sn concentration and percentage silt vs stratigraphy for the Teign Valley middle terrace. Note the clear correlation between percentage silt and Sn concentration except in the uncontaminated silt-dominated interval 500–900 mm (see text for interpretation). The upper unit contains elevated levels of Pb and Ba, suggesting that it post-dates 1850.

uncontaminated, overbank, fine grained sediments. Despite the lack of organic deposits for radiocarbon dating, the geochemistry and mineralogy of the upper silty-sand unit gives a good indication of the age of the terrace, and when used in conjunction with mining history evidence allows a reconstruction of the depositional history of the terrace to be postulated. This unit shows increased abundance of barytes (from SEM studies) and enhancement in Pb (up to 372 mg/kg) which suggests sediment deposition after 1850 AD, the date of the onset of barytes and galena mining in the middle Teign Valley (Cheshire 1969). It is likely, therefore, that the basal sand deposits which pre-date 1850 were deposited as a consequence of late Medieval tin mining. The coarse sand grain size of these deposits suggests that they were deposited within the river channel and would have resulted in the aggradation of the river bed, as observed in the Ringrooma River this century (Knighton 1989). When the supply of sand to the river was reduced following the decline of the tin mining industry during the seventeenth century (Harris 1992) the sand deposits would have been incised by the River Teign, a common occurrence in river systems recovering from mine waste contamination (Knighton 1989; James 1991). As the river incised its bed sediment deposition on the floodplain would only occur during overbank flood events resulting in the deposition of fine-grained alluvium and accounting for the middle silt unit of the terrace. With the onset of local barytes and galena mining in 1850 (Cheshire 1969) and the brief resurgence of the tin industry in the mid-19th century (Harris 1992), the supply of mine waste sediment once again increased causing aggradation of the river bed and allowing the deposition of the coarser grained silty-sand unit.

In contrast to the negligible Sn concentrations in the natural upper terrace of the River Teign floodplain (noted in the previous section), the values in the middle terrace are higher, reaching 148 mg/kg (Fig. 4). There is also a correlation, within

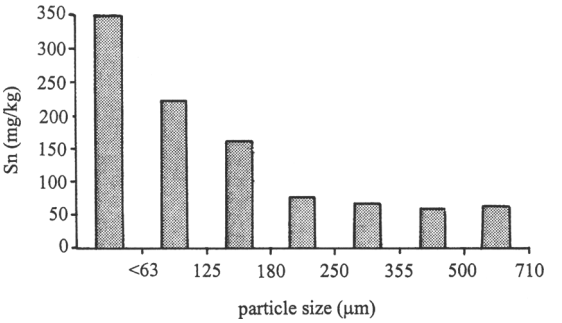


**Fig. 5.** Particle size vs Sn concentration for the 100–300 mm interval from the Teign Valley middle terrace. Note the significant enrichment of Sn in the <63 μm fraction.

the contaminated units, between percentage silt and Sn concentration ($r^2 = 0.91$), suggesting the enhancement of Sn in the <63 μm fraction as found by Bradley (1990). The enhancement is confirmed by the Sn concentration distribution in the different particle size fractions. For both this site (Fig. 5) and others, including the River Erme (see Fig. 8), Sn concentration is highest in the <63 μm fraction. The increase in Sn concentration towards the top of the profile, within both the contaminated units, is a consequence of the fining upwards sedimentary sequence and the deposition of greater quantities of silt containing unrecoverable cassiterite.

The mine waste contaminated sediments show a mineralogy typical of those derived from a granitic lithology. Quartz is abundant and the heavy mineral assemblage is dominated by zircon, monazite and various Fe-minerals, these being typical accessory minerals of the Dartmoor granite (Edmonds *et al.* 1968; Alderton 1992). Zircon and monazite occur in a wide range of particle sizes in both the natural and contaminated sediments. By contrast, cassiterite grains in the mine waste contaminated sediments are predominantly found in the <63 μm fraction and where cassiterite does occur in the sand grain size fraction it is usually locked within a quartz host (Fig. 6). The mineralogy, therefore, confirms that cassiterite is concentrated in the fines of mine contaminated sediments and the deficiency of Sn in the sand fractions is a result of efficient recovery during tin streaming and processing.

## *Contaminated sediments (2): River Erme palaeochannel*

The River Erme palaeochannel sequence is shown in Fig. 7. An increase in Sn concentration from 11 to 136 mg/kg occurs in a unit of silty-sand grain size at 150 cm below the sediment surface and is radiocarbon dated as post 1280 ± 45 AD (laboratory code SRR-6226) based on the underlying organic rich silt. The aggradation of Sn enhanced sediment at approximately 1.50 m below the sediment surface is also evident in two nearby exposures of the terrace. The particle size Sn distribution data from these exposures (Fig. 8) once again shows the highest Sn concentration in the silt fraction, consistent with the mine waste contaminated sediments of the Teign Valley.

## *Contaminated sediments (3): River Avon palaeochannel*

The River Avon palaeochannel shows negligible Sn values (<5 mg/kg) in the lower silt unit (Fig. 9), which is dated to pre-2845 ± 45 year BP (laboratory code SRR-6225)

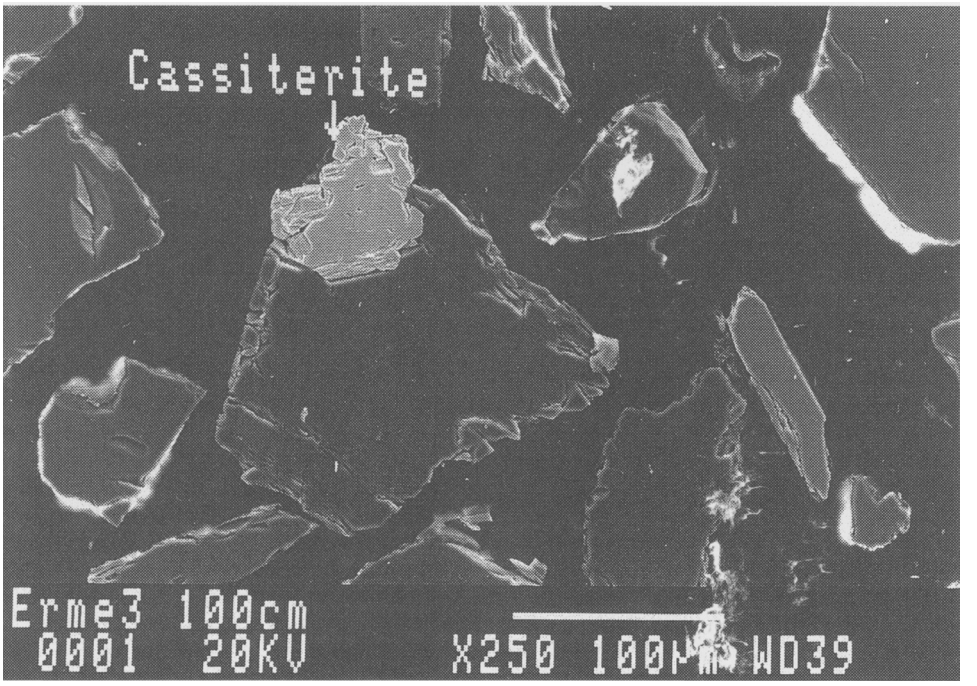


**Fig. 6.** Scanning electron microscope image showing a large cassiterite grain locked within a silicate host (River Erme floodplain, contaminated sediments).

from a radiocarbon date from the base of the overlying peat. The upper silt layer shows Sn enhancement. The values of enhancement are low (around 20 mg/kg) in comparison to the Erme and Teign sites, but this is a reflection of the lower energy depositional environment of this site at the back of the floodplain. The age of the

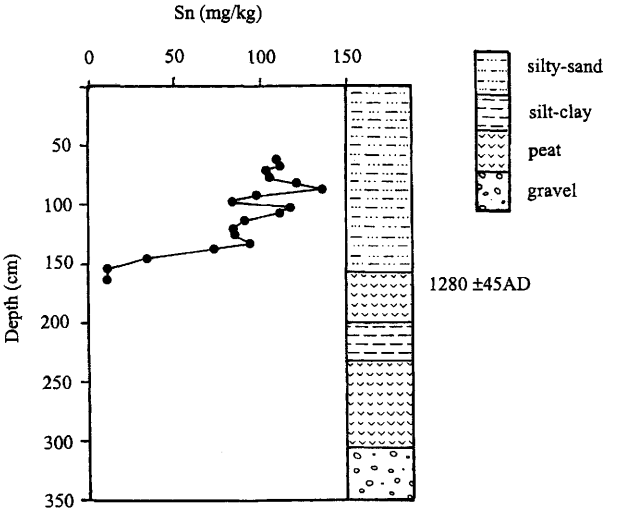


**Fig. 7.** Stratigraphy, Sn concentration and radiocarbon date for the Erme palaeochannel. Note the prominent increase in Sn concentration post dating the organic silt horizon dated at 1280 ± 45 AD.

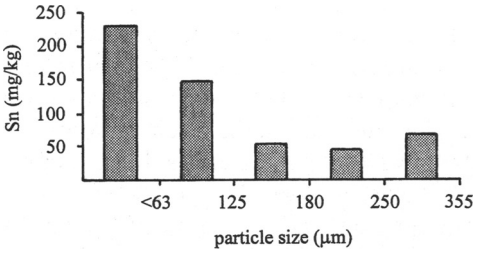


**Fig. 8.** Particle size vs Sn concentration for the 500–60 mm interval from the River Erme floodplain stratigraphy. Note the concentration of Sn in the <63 μm fraction.

upper boundary of the peat deposit is 1560 ± 40 AD (laboratory code SRR-6224) thus suggesting these sediments were deposited in response to the peak period of Medieval tin streaming in the 16th century (Harris 1992).

## Conclusions

It is possible to distinguish between historical mine waste contaminated sediments and natural sediments using a combination of geochemistry, mineralogy and particle size analysis. Indeed the skewed nature of the particle-size Sn fractionation data would appear to differentiate between contaminated and natural sediments. The initial dating suggests that aggradation of Sn-enhanced sediment seen in the valleys draining Dartmoor is of Medieval age and no earlier than pre-12th century AD. The signal of enhanced metal contamination by the release of the fine sediment fraction in to the rivers, appears to clearly mirror the documentary evidence of mining activity. Aggradation occurs in the River Erme valley in the latter half of the 13th century, and correlates with the first peak period of mining identified in

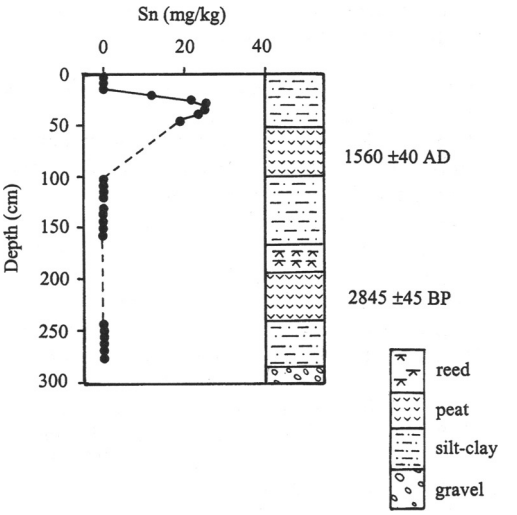


**Fig. 9.** Stratigraphy, Sn concentration and radiocarbon dates for the Avon Valley palaeochannel. Note the Sn enrichment post dating the peat dated at 1560 ± 45 AD.

the documentary record (Harris 1992). In the River Avon palaeochannel aggradation of Sn-enhanced sediment occurred in the 16th century following both the highest Sn production period and the introduction of pollution legislation (1531 AD) to reduce the quantity of sediment released into the river systems (Greeves 1981). It must also be noted, however, that the changes in sedimentation occurring at this time may also be influenced by climatic change, such as the instability of the late Medieval climatic deterioration, the Little Ice Age (Brown 1998).

As yet, no prehistoric contamination has been identified on Dartmoor. Any prehistoric mining may have been on a very small, local scale, hence would have a minimal downstream impact. In addition, subsequent reworking by Medieval tin streaming may have destroyed the earlier record, or may be masking prehistoric sediments with a lower level of enrichment. However, this paper clearly shows that the combined mineralogical–geochemical approach adopted has the potential to identify past mining activity on the moor, even in quite distal sites. The search is now on for critical sections where the record of prehistoric mining may be retained.

The research was supported by a NERC research studentship (VRT). Radiocarbon dates were provided through NERC Scientific Services at the NERC Radiocarbon Laboratory, East Kilbride. Gerard Aalbersberg provided fieldwork assistance. Many archaeologists have helped with advice and information, including Debbie Griffiths and other staff of the Dartmoor National Park, and Tom Greeves and members of the Dartmoor Tin Research Group. Thanks are also due to local landowners for access. The technical support of the analytical laboratories at the Camborne School of Mines is gratefully acknowledged.

## References

AABY, B. 1986. Palaeoecological studies of mires. *In*: BERGLUND, B. (ed.) *Handbook of Holocene Palaeoecology and Palaeohydrology*. Wiley, Chichester, 231–246.

ALDERTON, D. H. M. 1992. Mineralization associated with the Cornubian Granite Batholith. *In*: PATTRICK, R. A. D. & POLYA, D. A. (eds) *Mineralization in the British Isles*. Chapman & Hall, London, 270–354.

BEER, K. E. & SCRIVENER, R. C. 1982. Metalliferous mineralisation. *In*: DURRANCE, E. M. & LAMING, D. J. C. (eds) *The Geology of Devon*. University of Exeter Press, Exeter, 117–147.

BRADLEY, S. B. 1990. Characteristics of tin-streaming channels on Dartmoor, UK. *Geoarchaeology*, **5**, 29–41.

BRITISH STANDARDS INSTITUTION 1975. *Methods of Tests for Soils for Civil Engineering Purposes*. British Standards Institution, BS1377.

BROWN, A. G. 1998. Fluvial evidence of the Medieval warm period and the Late Medieval deterioration in Europe. *In*: BENITO, G., BAKER, V. R. & GREGORY, K. J. (eds), *Palaeohydrology and Environmental Change*. Wiley, Chichester.

CAMM, G. S. 1999. Review of Cornish stanniferous placers — with special reference to offshore placers of Quaternary age on the south coast. *Transactions of the Royal Geological Society of Cornwall*, **XXIV**, **2**, 57–88.

—— & CROOT, D.G. 1994. Quaternary placer cassiterite deposits in Cornwall: the role of periglacial processes in their development. *Proceedings of the Ussher Society*, **8**, 328–330.

CHESHIRE, J. A. 1969. *The Geology of the Middle Teign Valley, South-East Devon*. PhD thesis, University of Exeter.

EDMONDS, E. A., WRIGHT, J. E., BEER, K. E., HAWKES, J. R., WILLIAMS, J. R., FRESHNEY, E. C. & FENNING, P. J. 1968. *Geology of the country around Okehampton. Memoirs of the Geological Survey of Great Britain*. Explanation to Sheet 324 (New Series). HMSO, London.

FLETCHER, W. K. & LOH, C. H 1996. Transport of cassiterite in a Malaysian stream: implications for geochemical exploration. *Journal of Geochemical Exploration*, **57**, 9–20.

FOX, A. 1957. Excavations on Dean Moor in the Avon Valley 1954–56. *Transactions of the Devonshire Association*, **98**, 18–77.

—— 1995. Tin ingots from Bigbury Bay, South Devon. *Devon Archaeological Society Proceedings*, **53**, 11–24.

GERRARD, S. 1992. The Beckamoor Coombe streamwork survey. *Dartmoor Tin Research Group Newsletter*, **3**, 6–8.

—— 1997. *English Heritage book of Dartmoor: landscapes through time*. Batsford, London.

GREEVES, T. A. P. 1981. *The Devon tin industry 1450–1750: an archaeological and historical survey*. PhD thesis, University of Exeter.

HARRIS, H. 1992. *The Industrial Archaeology of Dartmoor*. Peninsula Press, Newton Abbot.

HITCHENS, F. & DREW, S. 1824. *History of Cornwall — from the earliest records and traditions to the present time*. W. Penaluna, Helston.

HOSKING, K. F. G. & CAMM, G. S. 1982. Summary of the present views of the nature and genesis of the Cornish stanniferous placers of SW England. *In*: WAUSCHKUHN, A., KLUTH, C. & ZIMMERMAN, R. A. (eds) *Syngenesis and Epigenesis in the Formation of Mineral Deposits*. Springer, Berlin, 260–274.

JAMES, J. A. 1991. Incision and morphologic evolution of an alluvial channel recovering from hydraulic mining sediment. *Geological Society of America Bulletin*, **103**, 723–736.

KNIGHTON, A. D. 1989. River adjustment to changes in sediment load: the effects of tin mining on the Ringarooma River, Tasmania, 1875–1984. *Earth Surface Processes and Landforms*, **14**, 333–359.

MACKLIN, M. G. 1985. Floodplain sedimentation in the upper Axe valley, Mendip, England. *Transactions of the Institution of British Geographers*, **10**, 235–244.

——, RIDGWAY, J., PASSMORE, D. & RUMSBY, B. T. 1994. The use of overbank sediment for geochemical mapping and contaminant assessment: results from selected English and Welsh floodplains. *Applied Geochemistry*, **9**, 689–700.

——, HUDSON-EDWARDS, K. A. & DAWSON, E. J. 1997. The significance of pollution from historic metal mining in the Pennine orefields on river sediment contaminant fluxes to the North Sea. *Science of the Total Environment* **194/195**, 391–397.

MILES, H. 1975. Barrows on the St. Austell Granite, Cornwall. *Cornish Archaeology*, **14**, 5–81.

PENHALLURICK, R. D. 1986. *Tin in Antiquity*. Institute of Metals, London.

PEARCE, S. 1979. The distribution and production of Bronze Age metalwork. *Proceedings of the Devonshire Archaeological Society*, **37**, 136–145.

PIRRIE, D., CAMM, G. S., SEAR, L. G. & HUGHES, S. H. 1997. Mineralogical and geochemical signature of mine waste contamination, Tresillian River, Fal Estuary, Cornwall, UK. *Environmental Geology*, **29**, 58–65.

SHARPE, A. 1992. Footprints of former miners in the far west. *Cornish Archaeology*, **31**, 35–40.

# Provenancing iron ore from the Bristol Channel Orefield: the cargo of the Medieval Magor Pill Boat

TIMOTHY P. YOUNG[1] & GARY R. THOMAS[2]
[1]*GeoArch, 54 Heol-y-Cadno, Thornhill, Cardiff CF14 9DY, UK*
[2]*Department of Earth Sciences, Cardiff University, PO Box 914, Cardiff CF1 3YE, UK*

**Abstract:** A boat (built *c.*1240) foundered with a cargo including iron ore, close to the settlement of *Abergwaitha*, seaward of the modern Magor Pill (Gwent). Excavation in 1995 recovered 180 kg of mixed powder and lump ores. A source within the Bristol Channel Orefield may readily be determined from the mineralogy and texture of the lump ores. Provenancing within the orefield is more problematic. Various lines of evidence constrain the likely source of the ore as Glamorgan; including textural evidence that the ore was emplaced within substantial cavernous porosity, petrological evidence that the ore was within the Carboniferous limestone, and the presence of quartz. This raises the intriguing question of why a cargo of ore was apparently travelling towards the major ore sources in the Forest of Dean. An explanation is suggested by the likely date for the cargo of 1250-1280, during the northward expansion of the de Clare Lordship of Glamorgan, into Meisgyn (including most orebodies west of the Taff Valley) in 1246, and Is Caiach (including those east of the Taff Valley) in 1267. The de Clares are known to have undertaken large-scale iron smelting in Trelech (Gwent) in the period *c.* 1240–1290. It is possible that ore from the newly secured sources was shipped to Trelech for smelting during this period of insecurity.

The circumstances of the discovery in 1995 and lifting in 1996 of the Magor Pill boat, together with a full description of the boat and its cargo, have recently been published (Nayling 1998). The vessel had foundered close to the settlement of *Abergwaitha*, seaward of the current mouth of Magor Pill (Gwent, South Wales; Fig. 1). On its final voyage, the boat had been carrying a cargo of iron ore. The ore had been placed on a hurdle, and comprised a mixture of coarse lump ore and powder grade material. Initial expectations that the cargo would have originated within the Forest of Dean (known to be a major ore producing region in the 13th century) soon proved to be incompatible with the petrology and mineralogy of the ore recovered. Allen (1996) argued for a possible origin in the Mendip or Bristol area, but after an extensive sampling of ore outcrops, Young & Thomas (1998) demonstrated the the most likely source for the cargo was in Glamorgan. Redknap & Young (1998) have described the place of the Magor boat in the context of 13th century trade and iron-making. The purpose of this contribution is to illustrate, and to amplify the description of, the cargo given by Young & Thomas (1998), and to place the cargo within the detailed context of the Glamorgan orefield, both geologically and with respect to the 13th century political geography.

*From:* POLLARD, A. M. (ed.) 1999. *Geoarchaeology: exploration, environments, resources.* Geological Society, London, Special Publications, **165**, 103–121. 1-86239-053-3/99/$15.00

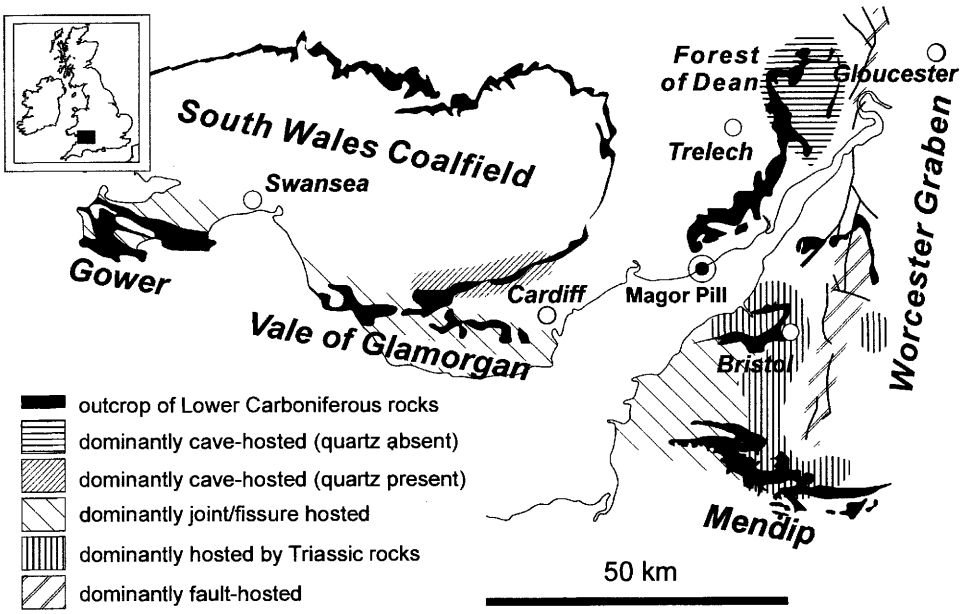


**Fig. 1.** The Bristol Channel orefield, showing the distribution of the main orebody types and the location of Magor Pill

**Fig. 2.** (a)–(d) Layered facies ore from the Magor Pill boat. (e)–(g) Stalactitic facies ore from the Magor Pill boat. (f) Botryoidal facies ore. (h) Replacement facies ore. (a) Radial growths of goethite needles (bright) nucleated on the ghosted outlines of former carbonate crystals and overgrowing euhedral quartz crystals. Scale bar 200 μm. Backscattered electron (BSEM) image of polished block. Sample M48. (b) Quartz (grey) to left overgrowing radial growths of acicular goethite. Scale bar 200 μm. BSEM image of polished block. Sample M47. (c) Goethite-rich layer, below, overgrown by botryoidal goethite (above) partially occluding inter-layer void (filled by grey resin). Margin of goethite rich layer marked by thin layer of haematite, revealing the outline of carbonate grains replaced by goethite. Scale bar 1 mm. Reflected light photomicrograph of polished block. Sample M14. (d) Goethite-rich layer bearing an enclosed void (filled incompletely by resin appearing grey). Haematized surface layer and inner zones of replaced carbonate crystals reveals the replacive nature of the goethite. Scale bar 500 μm. Reflected light photomicrograph of polished block. Sample M113. (e) Longitudinal section through stalactites formed of acicular goethite crystals. Inter-stalactite porosity filled by resin (grey) which has been scratched during specimen preparation (dark lines). Scale bar 500 μm. Reflected light photomicrograph of polished block. Sample M43. (f) Transverse section through goethite stalactites, which have been overgrown by botryoidal goethite. Inter-stalactite porosity filled by resin (grey) which has been scratched during specimen preparation (dark lines). Scale bar 1 mm. Reflected light photomicrograph of polished block. Sample M43. (g) View of central region of a dominantly goethite (grey) stalactite, showing radial structures of haematite (white) in the core of the denser goethite clusters. 6-fold symmetry of the haematite can be clearly seen (compare Fig. 3). Scale bar 50 μm. BSEM image of polished block. Sample M82. (h) Replaced dolomite host rock. Outlines of dolomite crystals marked by voids. Interior filled largely by fine grained goethite, but also bear geopetal (gravity controlled) fill of radial clusters of haematite crystals. Scale bar 1 mm. Reflected light image of polished block. Sample M54.

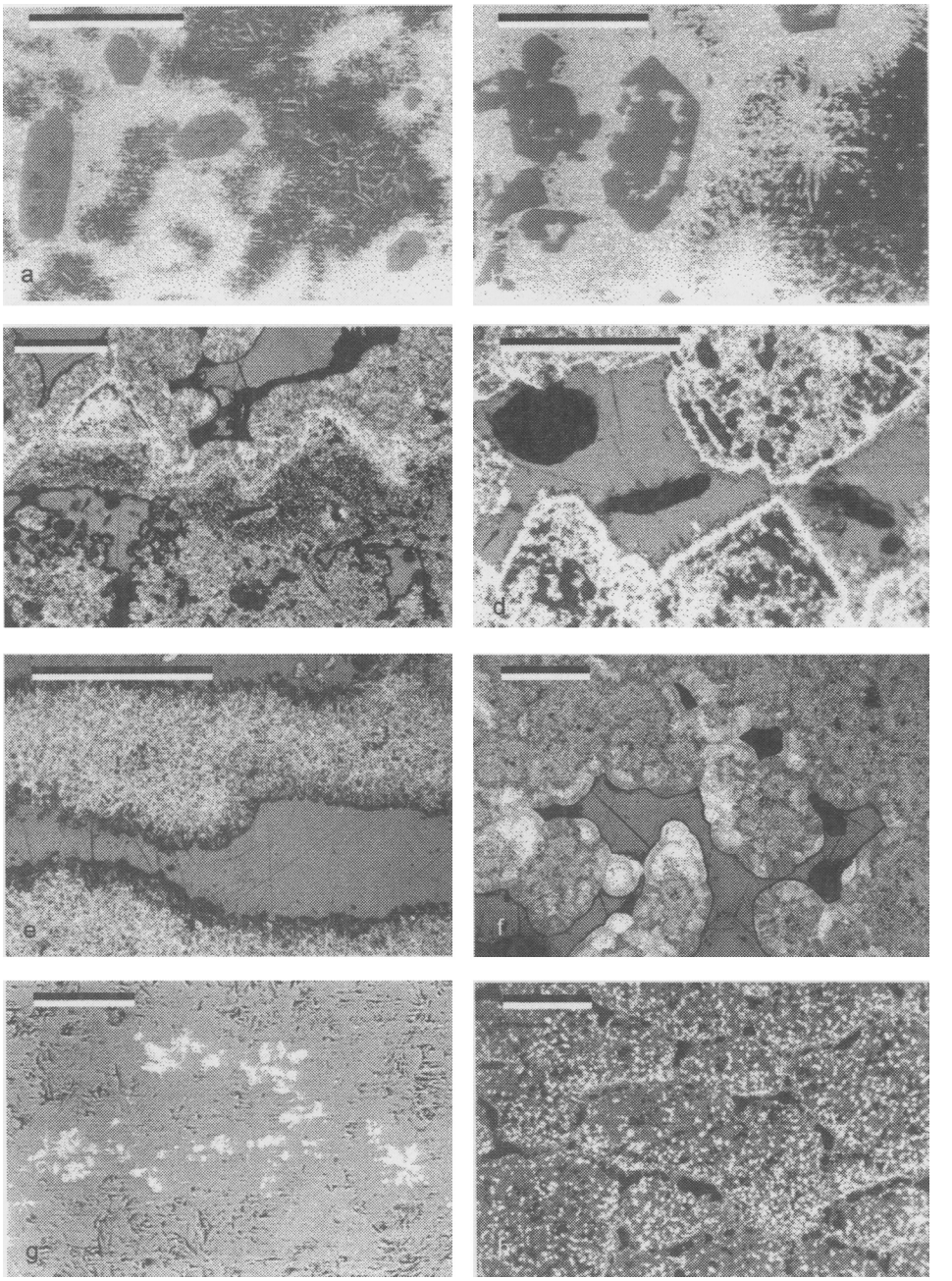
a
d
e
f
g

## Description of the ore

The nature of the ore comprising the cargo of the vessel has been described briefly by Young & Thomas (1998). The cargo included two components, which occurred mixed together. The main component (129 kg recovered) is a yellow ochreous powder, containing small fragments of broken iron ore and host dolomitic limestone, whereas the second component comprises discrete blocks of lump ore ranging up to 4.3 kg. The lump ore can be divided into four facies, which occur in intimate association.

### *1. Layered facies (Fig. 2a–d)*

This ore type comprises alternating layers (0.6–6 mm thick) of high-density goethite/haematite ore, with low-density layers (<2 mm) and open voids (<20 mm). The dense layers are richer in haematite (typically 10–20%) than the porous layers (<10%). The porosity of the low density layers is often surrounded by, and smaller pores may occur within, the ghosted outlines of former carbonate crystals (Fig. 2c, d). The surfaces of the former carbonate crystals are often particularly haematite-rich. This facies generally bears small quartz crystals (<200 μm), which are usually intimately associated with goethite needles. Generations of goethite are often seen to both pre- and post-date quartz precipitation.

### *2. Stalactitic facies (Fig. 2e–g)*

The stalactitic facies comprises thin (<3 mm diameter) stalactites of crystalline goethite. The cores of the stalactites may be dense, and these dense areas may bear radial groups of haematite needles, often showing a six-fold symmetry (each arm up to 6 μm long and 0.5 μm wide) and which are probably twinned (Fig. 2g). The low-density areas (Fig. 2e) show crude radial clumps of goethite needles. The stalactites reach up to at least 180 mm in length. The stalactitic facies is almost always overgrown by the botryoidal facies (Fig. 2f), sometimes to the almost total occlusion of the inter-stalactite porosity.

### *3. Botryoidal facies (Fig. 2f)*

The botryoidal facies occurs as coatings (usually <500 μm) which overgrow the stalactitic and layered facies ores. Some specimens show overgrowth of the botryoids by a layer of goethite crystals up to 150 μm in length and 5 μm in diameter. The crystalline overgrowths are often dark in colour, and may have given rise to some of the earlier reports of manganese minerals being present in the ores.

### *4. Replacement facies (Fig. 2h)*

A few specimens show complete replacement of coarse dolomite rock by goethite and haematite. In the illustrated specimen, the outlines of the former dolomite rhombs are marked by porosity, and the main goethite replacement carries geopetal accumulations of haematite within each former carbonate grain.

The powder ore component bears small fragments of the various lump ore types, as well as abundant small fragments of a replacement facies lithology, in which goethite

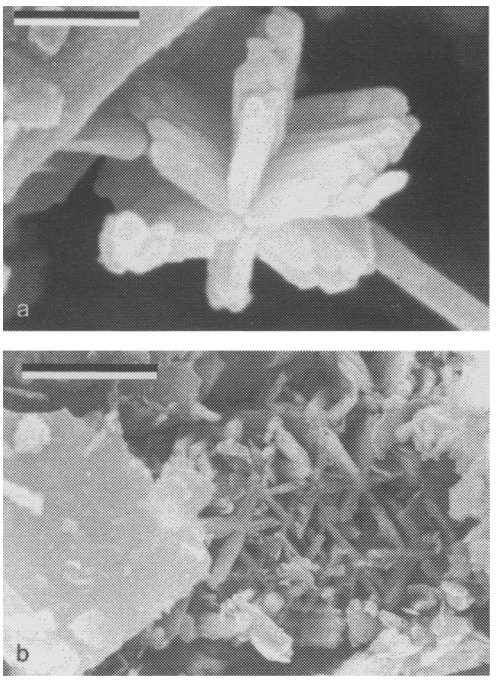


**Fig. 3.** Powder ores from the Magor Pill boat. (a) Stacked '6-pointed stars' of goethite. Secondary electron image of strew mounted ochre. Scale bar 1 μm. Sample M117. (b) Lattice of '6-pointed stars' of goethite, together with other goethite grains. Secondary electron image of strew mounted ochre. Scale bar 5 μm. Sample M115.

is often subordinate to fine-grained quartz. The quartz distribution is variable on a lamina scale, imparting a crude fissility to the distinctive yellow rock. Much of the sand-grade component of the powder ore is formed of degraded stalactitic facies material. The dominant fine-grained component of the powder ore is of clay grade, and is typified by six-pointed goethite 'stars' (<5 mm diameter). These 'stars' may be linked together axially (Fig. 3a) or laterally to form a lattice-like structure (Fig. 3b). Impurities in the powder ore include quartz and clay minerals, together with some barite and relict carbonate grains. These features indicate that the powder ore is largely relict material deposited after dissolution of host dolomitic limestone, freeing microscopic goethite particles, pieces of silicified host and larger blocks of adhering goethitic ore.

The ores are all of high grade, with the lump ores having a goethite + haematite content of 97–99% (Table 1). The powder is of slightly lower grade, but still has a bulk goethite content of around 83%. Trace element contents (Tables 2 and 3) of the lump ores are extremely low (ΣREE <16 ppm and usually <10 ppm, U average 2.0 ppm, P typically <0.025%).

The cargo appears to have been derived from a single deposit, indeed the features of the ore and the demonstrably close relationship between the various facies, means that the cargo was probably derived from mining of a single karstic chamber. The volume of material is small, so the chamber might have been little more than a metre across, but equally the material could have been derived from part of a larger cavity.

**Table 1.** *Major element analysis of selected specimens from Magor by XRF quoted as weight% oxide.*

| Sample | Texture | $SiO_2$ | $Al_2O_3$ | $Fe_2O_3$ | MnO | MgO | CaO | $Na_2O$ | $K_2O$ | $TiO_2$ | $P_2O_5$ | LOI |
|---|---|---|---|---|---|---|---|---|---|---|---|---|
| M1 | spongy stalactitic | 1.54 | 0.48 | 87.19 | 0.02 | 0.30 | 0.03 | < | 0.05 | 0.02 | 0.04 | 10.34 |
| M6 | spongy stalactitic | 1.11 | 0.20 | 88.13 | 0.02 | 0.27 | 0.04 | < | < | < | 0.05 | 10.16 |
| M7 | massive replacement? ore | 0.25 | < | 89.30 | 0.01 | 0.13 | 0.01 | < | < | < | 0.03 | 10.27 |
| M14 | layered | 1.54 | 0.28 | 87.56 | 0.02 | 0.27 | 0.08 | < | 0.02 | 0.01 | 0.05 | 10.18 |
| M43 | stalactitic | 1.15 | 0.12 | 88.06 | 0.02 | 0.25 | 0.04 | < | < | < | 0.03 | 10.34 |
| M47 | layered | 2.94 | 0.04 | 86.94 | 0.02 | 0.21 | 0.04 | < | < | < | 0.02 | 9.80 |
| M48 | stalactitic on layered ore | 0.87 | 0.10 | 88.68 | 0.03 | 0.20 | 0.04 | < | < | 0.01 | 0.02 | 10.05 |
| M54m | replaced dolomite | 0.40 | 0.10 | 86.84 | 0.02 | 0.30 | 0.03 | < | < | < | 0.03 | 12.29 |
| M54b | stalactitic | 1.07 | 0.29 | 88.18 | 0.03 | 0.26 | 0.04 | < | 0.03 | 0.01 | 0.02 | 10.09 |
| M71 | layered | 1.51 | 0.35 | 87.78 | 0.02 | 0.30 | 0.11 | < | 0.05 | 0.03 | 0.04 | 9.82 |
| M75 | layered | 1.42 | 0.33 | 88.58 | 0.02 | 0.25 | 0.06 | < | 0.03 | 0.01 | 0.06 | 9.25 |
| M82 | stal. with botryoidal, massive | 1.53 | 0.26 | 87.43 | 0.02 | 0.30 | 0.04 | < | 0.03 | 0.02 | 0.05 | 10.33 |
| M87 | stal. with botryoidal | 1.72 | 0.10 | 87.36 | 0.02 | 0.31 | 0.05 | < | < | < | 0.10 | 10.33 |
| M90 | stalactitic | 1.28 | 0.13 | 87.75 | 0.02 | 0.26 | 0.17 | < | < | < | 0.05 | 10.32 |
| M91 | layered | 1.22 | 0.19 | 88.27 | 0.02 | 0.22 | 0.09 | < | 0.02 | 0.01 | 0.03 | 9.94 |
| M110 | calcite cemented replacement | 3.92 | 0.28 | 53.28 | 0.05 | 0.31 | 20.81 | < | 0.01 | 0.01 | 0.02 | 21.30 |
| M113 | layered | 1.02 | 0.16 | 89.92 | 0.01 | 0.20 | 0.05 | < | < | 0.01 | 0.04 | 8.57 |
| M115 | powder (lump) | 10.28 | 1.75 | 75.81 | 0.05 | 0.56 | 1.23 | < | 0.35 | 0.11 | 0.08 | 9.78 |
| M117 | powder | 10.45 | 1.68 | 74.79 | 0.05 | 0.73 | 1.58 | < | 0.33 | 0.10 | 0.09 | 10.21 |
| M116 | powder (lump) | 9.15 | 1.70 | 76.74 | 0.05 | 0.55 | 1.34 | < | 0.32 | 0.10 | 0.08 | 9.97 |

All iron quoted as $Fe_2O_3$.
< indicates value below detection limits.

**Table 2.** *Trace element analysis of selected specimens from Magor by ICP-MS quoted as ppm.*

| Sample | Be 4 | Sc 21 | V 23 | Cr 24 | Co 27 | Cu 29 | Zn 30 | Ga 31 | Rb 37 | Sr 38 | Y 39 | Zr 40 | Nb 41 | Mo 42 | Cd 48 | Cs 55 | Ba 56 | Ta 73 | Tl 81 | Pb 82 | Bi 83 | Th 90 | U 92 |
|---|---|---|---|---|---|---|---|---|---|---|---|---|---|---|---|---|---|---|---|---|---|---|---|
| M1 | 12.24 | < | 10.51 | < | 31.68 | 20.28 | 266.8 | 1.457 | 1.886 | 12.82 | 3.837 | 3.026 | 0.383 | 12.348 | < | 0.0542 | 9.7017 | 0.2585 | < | 4.234 | < | 0.2239 | 2.2584 |
| M6 | 8.38 | < | 6.774 | 1.925 | 37.09 | 10.45 | 35 | 1.265 | < | 3.635 | 2.058 | 1.64 | 0.282 | 9.9102 | < | < | 2.0581 | 0.5953 | < | 2.7724 | < | 0.106 | 1.6616 |
| M7 | 3.367 | < | 4.753 | < | 31.14 | 3.894 | 23.63 | 0.587 | < | 1.401 | 0.522 | 1.329 | 0.153 | 10.297 | < | < | 0.8858 | 0.2162 | < | 1.2047 | < | < | 0.6077 |
| M14 | 13.23 | < | 7.588 | 3.432 | 20.47 | 12.91 | 258.6 | 0.541 | 0.768 | 7.368 | 3.484 | 2.499 | 0.31 | 13.709 | < | < | 6.8937 | 0.1961 | < | 8.2533 | < | 0.185 | 1.421 |
| M43 | 14.06 | < | 5.489 | 1.761 | 20.34 | 5.404 | 47.14 | 0.402 | < | 4.831 | 2.911 | 1.659 | 0.199 | 12.396 | < | < | 2.4925 | 0.1627 | < | 2.7584 | < | < | 1.3492 |
| M47 | 7.062 | < | < | 5.134 | 31.11 | 5.261 | 37.15 | 0.314 | < | 4.36 | 1.214 | 2.296 | 0.243 | 8.3614 | < | < | 1.9732 | 0.2809 | < | 2.1623 | < | < | 1.6082 |
| M48 | 7.093 | < | 4.03 | 2.363 | 36.41 | 16.87 | 12.19 | 0.465 | < | 3.33 | 2.064 | 2.975 | 0.344 | 4.5838 | < | < | 6.0405 | 0.3752 | < | 2.0085 | < | 0.1462 | 1.0412 |
| M54m | 6.521 | < | 4.963 | < | 40.23 | 4.896 | 14.5 | 1.199 | < | 3.598 | 2.979 | 2.448 | 0.135 | 11.439 | < | < | 1.195 | 0.172 | < | 2.7596 | < | < | 1.6861 |
| M54b | 4.966 | < | < | 2.273 | 29.43 | 16.79 | 67.46 | 0.944 | 0.861 | 5.397 | 3.092 | 2.626 | 0.287 | 6.2242 | < | < | 5.361 | 0.2378 | < | 3.6134 | < | 0.1265 | 1.6626 |
| M71 | 9.671 | < | 6.738 | 5.658 | 16.45 | 6.557 | 75.15 | 0.649 | 0.759 | 12.96 | 3.892 | 8.572 | 0.604 | 2.348 | < | < | 9.5926 | 0.1534 | < | 6.1978 | < | 0.5413 | 2.4954 |
| M75 | 46.39 | < | 11.4 | 5.743 | 34.39 | 4.729 | 29.65 | 1.326 | < | 12.27 | 5.644 | 2.911 | 0.421 | 11.846 | < | < | 12.416 | 0.1946 | < | 9.7757 | < | 0.2501 | 3.2491 |
| M82 | 19.23 | < | 8.114 | 4.261 | 30.33 | 7.631 | 141.8 | 0.613 | < | 6.772 | 4.24 | 3.908 | 0.412 | 24.227 | < | < | 5.0657 | 0.2302 | < | 6.4706 | < | 0.1954 | 1.9298 |
| M87 | 25.4 | < | 2.277 | < | 16.55 | 4.229 | 89.99 | 0.399 | < | 6.498 | 4.449 | 1.578 | 0.16 | 32.486 | < | < | 2.3002 | 0.1185 | < | 4.1995 | < | < | 1.0687 |
| M90 | 20.04 | < | 8.299 | 2.551 | 18.14 | 3.934 | 77.13 | 0.715 | < | 8.578 | 4.063 | 1.655 | 0.19 | 23.569 | < | < | 4.5199 | 0.1682 | < | 4.9802 | < | 0.1589 | 2.577 |
| M91 | 3.752 | < | 14.6 | 9.384 | 23.12 | 9.707 | 47.6 | 0.556 | < | 7.103 | 1.346 | 3.249 | 0.3 | 2.8893 | < | < | 6.2708 | 0.1365 | < | 4.6508 | < | 0.1515 | 2.3803 |
| M110 | 7.639 | < | 8.431 | 3.383 | 43.85 | 6.406 | 36.87 | 0.841 | 0.418 | 48.43 | 6.327 | 2.299 | 0.282 | 3.8684 | < | < | 4.2824 | 0.1512 | < | 5.53 | < | 0.1345 | 1.8765 |
| M113 | 6.035 | < | 9.552 | 6.188 | 21.81 | 5.847 | 29.67 | 0.663 | < | 8.958 | 2.968 | 3.314 | 0.311 | 4.7128 | < | < | 5.1942 | 0.1677 | < | 15.019 | < | 0.096 | 5.1044 |
| M115 | 8.479 | 1.069 | 49.39 | 14.32 | 26.3 | 18.42 | 281.5 | 3.518 | 13.48 | 32.14 | 6.399 | 16.2 | 1.659 | 10.436 | < | 0.8462 | 43.779 | 0.2147 | < | 13.759 | < | 1.1407 | 3.4753 |
| M117 | 8.727 | 0.972 | 44.05 | 13.37 | 16.92 | 5.701 | 100.3 | 3.507 | 11.96 | 30.92 | 6.629 | 16.24 | 1.471 | 10.903 | < | 0.744 | 41.092 | 0.181 | < | 10.009 | < | 1.1517 | 3.9297 |
| M116 | 9.136 | 1.051 | 46.46 | 15.38 | 21.52 | 35.4 | 56.82 | 3.575 | 12.19 | 32.28 | 6.289 | 16.94 | 1.561 | 11.47 | < | 0.7304 | 45.575 | 0.1583 | < | 9.8109 | < | 1.054 | 3.9681 |

< indicates value below detection limits.

**Table 3.** *Rare earth element analysis of selected specimens from Magor by ICP-MS quoted as ppm.*

| Sample | La 139 | Ce 140 | Pr 141 | Nd 143 | Sm 147 | Eu 151 | Gd 157 | Tb 159 | Dy 161 | Ho 165 | Er 167 | Tm 169 | Yb 172 | Lu 175 | *Σ REE* |
|---|---|---|---|---|---|---|---|---|---|---|---|---|---|---|---|
| M1 | 1.508 | 3.4394 | 0.4621 | 1.8014 | 0.5416 | 0.1708 | 0.7872 | 0.1186 | 0.5736 | 0.1079 | 0.3467 | 0.0571 | 0.3202 | 0.0439 | *10.2785* |
| M6 | 0.6732 | 1.4689 | 0.2265 | 1.0596 | 0.3303 | 0.1102 | 0.4714 | 0.0661 | 0.3736 | 0.0709 | 0.1835 | 0.0353 | 0.1924 | 0.0234 | *5.2853* |
| M7 | 0.1553 | 0.3778 | 0.0605 | 0.2764 | < | 0.0229 | < | < | 0.0839 | < | 0.0679 | < | 0.0676 | < | *1.1123* |
| M14 | 1.1919 | 2.7765 | 0.3653 | 1.8122 | 0.5464 | 0.1454 | 0.7061 | 0.1139 | 0.6465 | 0.1094 | 0.2953 | 0.0431 | 0.2927 | 0.0425 | *9.0872* |
| M43 | 0.8520 | 1.9792 | 0.2921 | 1.3698 | 0.3993 | 0.1417 | 0.6475 | 0.0914 | 0.4959 | 0.0818 | 0.2589 | 0.0304 | 0.1878 | 0.0233 | *6.8511* |
| M47 | 0.4421 | 0.9407 | 0.1308 | 0.5804 | 0.1570 | 0.0617 | 0.2083 | 0.0298 | 0.2046 | 0.0486 | 0.1124 | < | 0.0727 | < | *2.9891* |
| M48 | 0.8357 | 1.5819 | 0.3205 | 1.5307 | 0.4664 | 0.1106 | 0.4302 | 0.0733 | 0.4297 | 0.0636 | 0.1921 | < | 0.1739 | < | *6.2086* |
| M54m | 0.9704 | 2.3456 | 0.3433 | 1.6981 | 0.4677 | 0.1575 | 0.7451 | 0.1125 | 0.5542 | 0.1001 | 0.2432 | 0.0278 | 0.1683 | < | *7.9338* |
| M54b | 1.1845 | 2.7227 | 0.4182 | 2.0135 | 0.5170 | 0.1712 | 0.7572 | 0.1192 | 0.6054 | 0.1096 | 0.2754 | 0.0348 | 0.1948 | 0.0247 | *9.1482* |
| M71 | 2.2998 | 4.5882 | 0.7082 | 3.0960 | 0.7745 | 0.1997 | 0.8954 | 0.1419 | 0.8293 | 0.1350 | 0.4120 | 0.0638 | 0.3563 | 0.0458 | *14.5459* |
| M75 | 2.0666 | 4.4003 | 0.7238 | 3.6772 | 1.2042 | 0.3002 | 1.4905 | 0.2299 | 1.1922 | 0.1828 | 0.5441 | 0.0653 | 0.3426 | 0.0391 | *16.4588* |
| M82 | 1.4342 | 3.0074 | 0.4855 | 2.2087 | 0.7127 | 0.1998 | 0.9788 | 0.1455 | 0.7442 | 0.1379 | 0.3699 | 0.0537 | 0.2861 | 0.0369 | *10.8013* |
| M87 | 1.1048 | 2.5496 | 0.4064 | 1.8779 | 0.7043 | 0.1910 | 1.0290 | 0.1418 | 0.7372 | 0.1409 | 0.3787 | 0.0512 | 0.3801 | 0.0463 | *9.7392* |
| M90 | 1.1506 | 2.5711 | 0.4243 | 1.9894 | 0.6293 | 0.1782 | 0.8891 | 0.1504 | 0.6712 | 0.1246 | 0.3936 | 0.0427 | 0.3661 | 0.0401 | *9.6207* |
| M91 | 0.7746 | 1.3625 | 0.2239 | 0.8749 | 0.2407 | 0.0527 | 0.2823 | 0.0566 | < | 0.0344 | 0.1161 | < | < | < | *4.0187* |
| M110 | 2.3141 | 3.203 | 0.6961 | 2.8458 | 0.7970 | 0.2282 | 1.0977 | 0.1615 | 0.8704 | 0.1808 | 0.4251 | 0.0584 | 0.3184 | 0.052 | *13.2485* |
| M113 | 1.8195 | 3.7926 | 0.5323 | 2.3632 | 0.6674 | 0.1969 | 0.734 | 0.1342 | 0.6624 | 0.1131 | 0.2949 | 0.0483 | 0.2428 | 0.0316 | *11.6332* |
| M115 | 5.6823 | 11.345 | 1.5099 | 5.9587 | 1.3876 | 0.3167 | 1.3675 | 0.2275 | 1.2163 | 0.1978 | 0.5862 | 0.0738 | 0.5059 | 0.0582 | *30.4333* |
| M117 | 5.2612 | 10.383 | 1.3994 | 5.6341 | 1.3436 | 0.3265 | 1.5075 | 0.2353 | 1.1795 | 0.2207 | 0.6527 | 0.0755 | 0.4960 | 0.0664 | *28.7813* |
| M116 | 5.0098 | 9.8518 | 1.296 | 4.8543 | 1.1605 | 0.3328 | 1.2549 | 0.2209 | 1.0418 | 0.1940 | 0.5601 | 0.0828 | 0.4623 | 0.0674 | *26.3894* |

< indicates value below detection limits.

## Provenance of the iron ores

The arguments for an origin of the iron ores in Glamorgan have been presented in detail by Young & Thomas (1998). The evidence included the REE contents, the U content, the quartz-bearing mineralogy, the ore textures and the associated host-rock fragments. Since preparation of the specialist report for the Magor boat monograph, the authors have had the opportunity for further investigation of the Glamorgan ores and the discussion of a more precise provenance is now appropriate.

## Geology of the Glamorgan orefield

The Glamorgan iron orefield comprises a series of areas with mineralization in cavernous porosity. Most of the significant deposits lie within the Lower Carboniferous limestones of the South Crop of the South Wales coalfield (Fig. 4), but other lesser deposits are known from elsewhere in the Vale of Glamorgan. The major ore occurrences of the South Crop (Llanharry, Miskin, Lesser Garth and Fforest Fawr) lie within pre-existing karstic voids. These caves have been interpreted to be of mid-Triassic (Norian) age (Simms 1990). In the western part of the Glamorgan orefield, at Llanharry and Miskin, the caves lie in the uppermost Dinantian limestones (the Oxwich Head Limestone at Llanharry and the Hunts Bay Oolite Group at Miskin), immediately below the seal provided by the unconformably overlying impermeable Namurian mudrocks. To the east, at Lesser Garth and Fforest Fawr, the major orebodies lie lower in the succession (within the Gully Oolite), and are capped by the dolomitized High Tor Limestone.

Study of the Glamorgan iron ores is hampered by the lack of extant exposure. Llanharry Mine closed over twenty years ago; Trecastell, Bute, Mwyndy and Lesser Garth Mines closed over a century ago. The Bute Mine opencast pit is backfilled, the Mwyndy opencast pit is flooded, the Lesser Garth Mine is worked out at the depths to which it is currently accessible (the lower parts are flooded) and the Fforest Fawr workings are also flooded. Iron ore is visible at a few localities, but these are

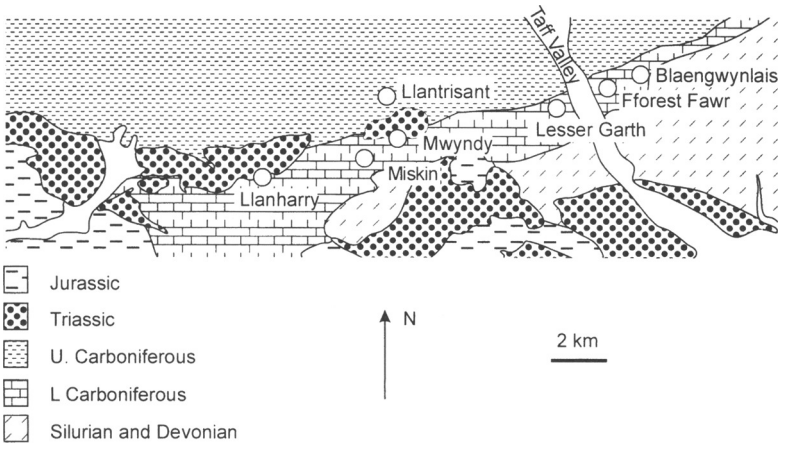


**Fig. 4.** Simplified geological sketch map of the area northwest of Cardiff, showing the principal localities mentioned in the text.

probably unrepresentative of the major deposits. On Lesser Garth poor examples of ores can be seen, both in the underground workings and in the adjacent Taff's Well Quarry. Perhaps the best current exposures are in Blaengwynlais Quarry where relatively small-scale mineralization can be seen within what is probably the Gully Oolite.

There is a limited literature on the Glamorgan iron ores. Some accounts of the ores were published when the mining was in its heyday during the last century (Vivian 1885, 1872, 1876, 1877; Watson 1859), and these subsequently formed the basis for later accounts (Sibly 1919; Sibly & Lloyd 1927; Strachan 1899, 1909; Strachan & Cantrill 1902, 1904, 1912). More recent work includes studies of the Llanharry deposit by Gayer & Criddle (1970), Rankin & Criddle (1985) and Williams (1958). Recently revised geological sheet memoirs (Waters & Lawrence 1987; Wilson *et al.* 1990) contain little modern addition to the description of the orefield beyond clarification of the stratigraphy of the host strata.

Studies of the iron ores of other sectors of the Bristol Channel Orefield are equally sparse. The 'Special reports on the Mineral Resources of Great Britain', published as Memoirs of the Geological Survey, provide an overview of the Forest of Dean (Sibly 1919; Sibly & Lloyd 1927). Similarly Cantrill *et al.* (1919) provided a summary of the deposits of the Bristol and Somerset area.

## Detailed provenance of the Magor Pill cargo

### *Geological evidence*

Clearly, many of the problems surrounding the interpretation of context, ownership and destination of the cargo might become clearer if a more precise origin of the cargo could be determined. The features of the cargo described above strongly suggest that ore was mined from within an open cave system, containing *in situ* ores on the walls and ceiling of the cave and a cave-fill comprising the ochreous material with reworked lump ore clasts. Minor ore accumulations at Blaengwynlais Quarry have these features on a small scale, and resemble the Magor material in having a low quartz content, and a lack of major subsequent carbonate precipitation. Higher quartz contents in the larger ore accumulations, and significant amounts of later carbonate minerals in open voids, seem to be more characteristic of the Glamorgan ore field. Significant accumulations of ochre were recorded during mining at Mwyndy, and some quartz-poor layered ores can be found in the surviving spoil dumps.

The small amount of material in the cargo, compatible with derivation from a small cavity, means that it is impossible to ascertain how representative this material is of its parent system. The Blaengwynlais Quarry orebodies include small cavities (<1 m diameter) with very variable fill: some are dominated by haematite, some by goethite; some show significant post-ore calcite precipitation, while others contain no carbonate phases. This inhomogeneity of the ore deposit hampers provenancing studies.

A spectrum of ore types has been recovered from the area of the former Bute Mine, near Miskin. Unpublished excavation of an early, probably Roman, smelting site 100 m south of the site of the Bute Mine has yielded a substantial quantity of ore (Table 4), as have nearby later smelting sites. Provisional interpretation of slag chemistry (authors' unpublished data) suggest that this early site smelted ores of up to 20% $SiO_2$, whereas probable 16th century bloomeries in the same area appear to have been smelting ore with less than 10% $SiO_2$. A small group of recent analyses of ores from

**Table 4.** *Major element analysis of selected specimens from archaeological sites near Miskin by XRF quoted as weight% oxide.*

| Sample | Locality | Description | $SiO_2$ | $Al_2O_3$ | $Fe_2O_3$ | MnO | MgO | CaO | $Na_2O$ | $K_2O$ | $TiO_2$ | $P_2O_5$ | LOI |
|---|---|---|---|---|---|---|---|---|---|---|---|---|---|
| MIS O1 | Site 1 | Red silty | 21.48 | 0.14 | 79.36 | 0.05 | 0.16 | 0.07 | < | 0.02 | 0.02 | 0.05 | 0.88 |
| MIS O2 | Site 1 | Yellow-brown quartz-rich layered | 49.91 | 0.08 | 50.71 | 0.01 | 0.07 | 0.01 | < | < | 0.01 | 0.02 | 4.39 |
| MIS O3 | Site 1 | Siliceous haemaite | 17.61 | 0.10 | 83.63 | 0.02 | 0.07 | 0.02 | < | < | < | 0.01 | 0.69 |
| MIS O4 | Site 1 | Yellow-brown quartz-rich layered | 19.03 | 0.15 | 80.93 | 0.06 | 0.20 | 0.04 | < | < | < | 0.02 | 8.72 |
| MIS O5 | Site 1 | Yellow-brown layered | 12.85 | 0.01 | 88.53 | 0.05 | 0.22 | 0.03 | < | < | < | 0.03 | 9.36 |
| MIS O6 | Site 1 | Yellow-brown stalactitic with quartz | 16.01 | < | 82.78 | 0.03 | 0.16 | 0.02 | < | < | < | 0.02 | 7.77 |
| MIS O7 | Site 1 unstr | Quartz-poor layered | 1.15 | 0.24 | 102.39 | 0.04 | 0.27 | 0.04 | < | < | 0.02 | 0.04 | 10.19 |
| MIS O8 | Site 1 unstr | Quartz-poor layered | 1.46 | 0.20 | 99.69 | 0.02 | 0.23 | 0.04 | < | < | 0.01 | 0.04 | 10.37 |
| MIS O9 | Site 1 unstr | Brown Quartz-rich | 16.17 | 0.02 | 85.47 | 0.03 | 0.19 | 0.02 | < | < | < | 0.02 | 8.93 |
| MIS O10 | Hendy Isaf | Red fine quartz-rich | 36.02 | 0.05 | 65.23 | 0.05 | 0.15 | 0.04 | < | < | < | 0.03 | 0.45 |
| MIS O11 | Hendy Isaf | Yellow-brown quartz-poor layered | 9.80 | 0.06 | 92.11 | 0.04 | 0.16 | 0.04 | < | < | < | 0.05 | 9.75 |
| MIS O12 | Rhiwsaeson | Yellow-brown massive | 22.43 | 0.09 | 78.01 | 0.04 | 0.13 | 0.02 | < | < | < | 0.03 | 8.93 |

All iron quoted as $Fe_2O_3$.
< indicates value below detection limits.Site 1 is Roman smelting site near Bute Mine, Hendy Isaf and Rhiwsaeson are post-Medieval bloomery sites.

**Table 5.** *Major element analysis of selected specimens from other Glamorgan outcrops by XRF quoted as weight% oxide.*

| Sample | Locality | Notes | $SiO_2$ | $Al_2O_3$ | $Fe_2O_3$ | MnO | MgO | CaO | $Na_2O$ | $K_2O$ | $TiO_2$ | $P_2O_5$ | LOI |
|---|---|---|---|---|---|---|---|---|---|---|---|---|---|
| LL1 | Llanharry | brush-textured specular haematite + quartz | 19.25 | 0.16 | 80.48 | < | 0.08 | 0.03 | < | < | < | 0.01 | 0.61 |
| LL3 | Llanharry | layered goethite ore | 0.48 | < | 99.22 | 0.02 | 0.14 | 0.12 | < | < | < | 0.01 | 9.789 |
| LL4 | Llanharry | layered goethite ore | 0.41 | 0.05 | 99.35 | 0.02 | 0.15 | 0.02 | < | < | < | 0.01 | 9.31 |
| LL5B | Llanharry | yellow botryoidal ore | 1.04 | 0.08 | 94.03 | 0.03 | 0.25 | 4.47 | < | < | 0.01 | 0.10 | 12.58 |
| FF1 | Fforest Fawr | | 16.51 | 0.03 | 83.26 | 0.02 | 0.15 | 0.02 | < | < | < | 0.02 | 8.37 |
| TF13 | Lesser Garth | | 12.05 | 0.16 | 86.07 | 0.03 | 0.73 | 0.92 | < | < | < | 0.04 | 7.87 |
| TF14 | Lesser Garth | | 11.93 | 0.38 | 87.48 | 0.04 | 0.10 | 0.04 | < | 0.01 | 0.01 | 0.02 | 0.889 |
| BQ3 | Blaengwynlais | | 0.69 | 0.12 | 91.22 | 0.02 | 0.26 | 7.65 | < | < | < | 0.03 | 12.19 |
| BQ7 | Blaengwynlais | | 0.92 | 0.07 | 98.51 | 0.04 | 0.34 | 0.07 | < | < | < | 0.04 | 10.44 |
| BQ9 | Blaengwynlais | | 6.21 | 0.34 | 59.21 | < | 0.31 | 0.09 | < | 0.01 | 0.04 | 0.05 | 9.63 |

All iron quoted as $Fe_2O_3$.
< indicates value below detection limits.

other Glamorgan outcrops is available (Table 5). The Llanharry deposits have been described by Gayer & Criddle (1970). The authors have collected over 100 kg of ore from the mine site for experimental smelting, permitting examination of a representative sample. The ores show a variation from a very high quartz content (sometimes >50%), down to ores with no quartz present at all. Unfortunately, there is no evidence as to how these extremes fit within the overall orebody system. Farther east, the range of lithologies for which there is evidence for working at Lesser Garth and Fforest Fawr is much more restricted: track surfaces near the 'Slide Pit' in Fforest Fawr yield dropped ore fragments which are dominantly siliceous, and siliceous material is found on Lesser Garth (although admittedly only on waste dumps). Sibly (1919) quotes $SiO_2$ and iron contents of ores from Llanharry (5.9% and 56% respectively), Trecastle (3.9% and 52%) and Mwyndy (18.4% and 49%) and comments that the average iron content of ores from Lesser Garth was <40%. It is not clear, however, how representative these analyses are of the ore raised in the nineteenth century from these mines.

## *The trace element geochemical evidence*

Although the major element geochemistry is compatible with an origin in Glamorgan, it does not assist with a more detailed provenance. Since the geological setting of the various ore deposits in Glamorgan is different, it was hoped that the trace element geochemistry might offer additional evidence.

The rare earth element data from the Magor specimens was summarized in Fig. 111 of Young & Thomas (1998). Additional analyses from Glamorgan are now available and are presented, together with facies information in Fig. 5. The new data confirm

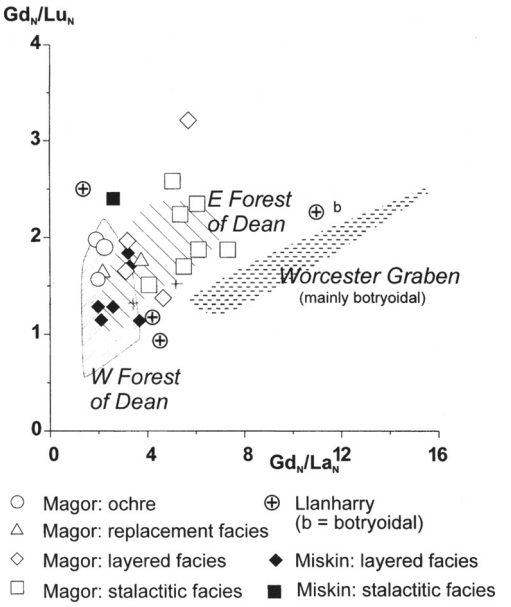


**Fig. 5.** Diagram of $Gd_N/Lu_N$ v. $Gd_N/La_N$ (normalised against upper crust; Taylor & McLennan 1981), showing analyses from the Magor cargo together with comparative data from elsewhere in the Bristol Channel Orefield.

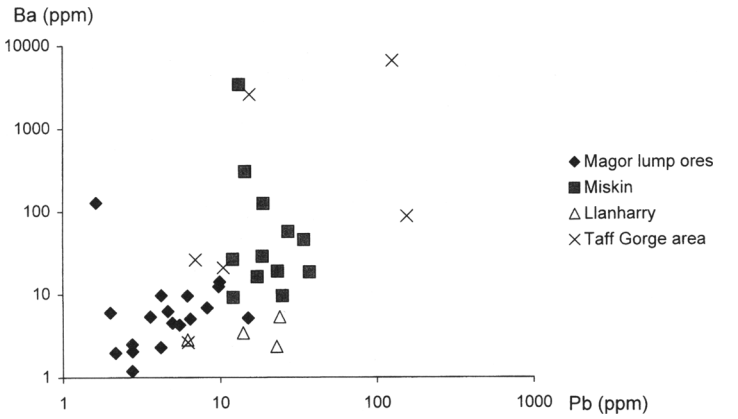


**Fig. 6.** Log Ba (in ppm) v. log Pb (in ppm) for lump ores from the Magor cargo, and from comparative locaities in Glamorgan.

earlier suspicions that the REE profiles are closely correlated with ore facies. Extreme LREE depletion is seen in botryoidal facies examples from Llanharry and the Worcester Graben faults. Layered and replacement facies ores plot much closer to a normal upper crust profile, suggesting that their REE contents may be determined by their sedimentary precursors. The stalactitic facies from Magor plots with a moderate LREE depletion, probably reflecting the large proportion of botryoidal facies overgrowth present in these rocks. A similar range of values is suggested by the data from Llanharry and Miskin.

The U content of the ores varies considerably across the orefield, and may in due course prove a valuable provenancing tool. At present the rather sparse data from Glamorgan show high U values in most samples from the Taff Gorge area (Lesser Garth, Fforest Fawr, Blaengwynlais), but the low-quartz goethite void fill at Blaengwynlais was also low U. The Llanharry data are mostly low U, as are those from Miskin, and resemble the values from the Magor cargo.

The South Crop of the South Wales coalfield hosts small-scale lead/zinc/barium mineralization both near Miskin and to the east near Rudry. The Pb and Ba contents of the Glamorgan ores are correspondingly variable (Fig. 6). The Magor cargo analyses are strikingly low in both these elements, and contrast strongly with most of the Miskin and Taff Gorge area samples, but are close to the Llanharry specimens.

The geochemical evidence is thus ambiguous. The major problem appears to be the high degree of local variation within the orefield. There are relatively few analyses from ores from the eastern part of the Glamorgan sector (Blaengwynlais, Fforest Fawr, Lesser Garth), but these appear slightly different from the Magor material. The existence at Blaengwynlais of the small goethite orebody with a mineralogy and geochemistry close to that of the Magor material warns against dismissal of this area as a possible source. In general the Magor material more closely resembles the western areas of Llanharry and Miskin, but the Pb/Ba data argue against Miskin. The possible existence of orebodies in the Miskin area without high Pb and Ba cannot be ruled out, and none of the analysed material comes from the area east of Mwyndy (Llwynsaer - Brofiskin), at a greater distance from the known Pb mineralization.

### *Exploitation evidence*

There is considerable doubt that the ores of the western end of the orefield around Llanharry would have been exploited at this early period. The late onset of 19th century mining at Llanharry (apart from near Patch Cottages) would argue that there was little if any early exploitation in this area. Accounts of the geology of the main Llanharry and Trecastell mine sites make it clear that the solid geology was overlain by considerable depths of Quaternary gravels. It is likely therefore that the main orebodies were not exploited early on, although exploitation of minor occurrences to the south of the main belt cannot be ruled out.

To the east of the River Ely the ores did crop out. There is documentary evidence that the Bute Mine cut through earlier workings, and there is ample evidence for early (Roman and Medieval) iron-making around the later open pits of the Bute and Mwyndy mines. To the west smaller orebodies may have cropped out on Cefn-yr-hendy, although most of the visible workings here are probably late 19th century. The siting of the probable early post-medieval bloomery at Hendy-isaf may have been influenced by proximity to these occurrences. Sixteenth century mining in this general area is described by contemporary sources (John Leland, 1506?–1552: Smith 1906). The Cefn-yr-hendy area together with the later Bute Mine lay within the bounds of the Medieval deer park of Clun or Gelynog, within which the 16th century mining was recorded, as did the Hendy-isaf site. Early mining outside the deerpark is less easy to demonstrate. There is no field or documentary evidence for early mines on the Mwyndy/Llwynsaer mining area, but the major early bloomery at Mwyndy, apparently ouside the deerpark, together with another possible bloomery at Rhiwsaeson, are strongly suggestive of activity in this area. The (trial?) workings north of Brofiscin are probably younger.

Three km ENE of Brofiskin lie the next ore workings, at Pen-y-garn (Pentyrch), but these are minor. The next major ore occurrences are a further 2 km ENE on Lesser Garth Hill. As with Mwyndy, the likely areas of early exploitation are largely masked by later mining, but the siting of 16th century ironworks (in existence by 1565, Riden 1992) at the foot of this hill, implies exploitation by this date.

On the opposite side of the Taff Gorge, there are numerous workings in Fforest Fawr, of which the Slide Pit is the largest. Trackways, with abundant ore fragments, lead downslope from the Slide Pit towards Tongwynlais, where another extremely early blast furnace was situated (in existence by 1564, and therefore one of the earliest blast furnaces in Wales; Riden 1992). One km northeast of Fforest Fawr lies Blaengwynlais Quarry, with its outcrops of orebodies, but with no evidence yet for exploitation. Evidence for substantial mineralization is generally lacking east of Blaegwynlais, but minor ores were encountered when the Caerphilly Railway tunnel, 3 km ENE of Blaengwynlais, was cut, and a further 3 km ENE a small mine was operated near Maenllwyd, Rudry in the 19th century.

Thus there are three areas in which medieval exploitation of iron is likely to have occurred: firstly in the Cefn-yr-hendy to Llwynsaer tract, near Miskin, secondly on Lesser Garth Hill and thirdly in Fforest Fawr. The available geological data do not permit distinction of the ores from these areas.

## Genesis of the ore

Somewhat ironically, the Magor cargo represents the most intensively studied and analysed ore deposit from the Bristol Channel orefield. Despite the fact that the

material is obviously not *in situ*, the cargo does offer evidence for the nature of ore genesis. The textural evidence indicates a paragenetic sequence from layered to stalactitic to botryoidal ore facies. The layered facies shows carbonate crystal terminations into open voids, including substantial cracks. Such cracks, with linings of calcite and dolomite crystals, are typical of the boxwork structure associated with the Crease Limestone in the Forest of Dean, and are particularly well developed where the host is not particularly mineralized. They are therefore interpreted as having developed as part of the process of cavernous porosity generation. The generation of the large-scale porosity is probably not a single event (Lowe 1993), but started with palaeokarst associated with the palaeosols in the roof of some orebodies (see above), reworked with major fluid flow during Variscan orogenesis, having a major phase of karstification during the Triassic (Simms 1990), and continuing with karstification following uplift in the Teriary to Recent. The emplacement of iron and silica may have occurred more or less simultaneously with the major void generation, but they post-date dolomitization and this, in part at least, is itself spatially associated with the voids (Sibly 1919). The generation of the stalactitic and botryoidal facies may represent reworking of this iron under different groundwater conditions.

## Historical context

Identification of the source of the Magor Pill cargo as the Glamorgan orefield immediately raises important questions about the political context of the boat. The major orebodies at outcrop within the orefield west of the Taff fall into the commote of Meisgyn and those east of the Taff within the commote of Is Caiach (part of the cantref of Senghenydd; Fig. 7). These two commotes lay immediately to the north of the lands held by Earl Gilbert, Lord of Glamorgan 1218–1230. Earl Richard

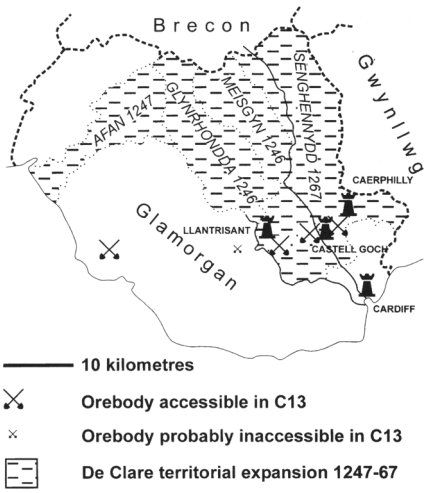


**Fig. 7.** Map showing the territorial acquisitions of the de Clare Lordship of Glamorgan during the 13th century, in relation to the iron ore deposits of the Glamorgan part of the Bristol Channel orefield.

was a minor at the time of Gilbert's death, but held the Lordship 1243–1262. He soon expanded his territory, first dispossessing the Lord of Meisgyn and Glynrhondda in 1246 and that of Afan the following year. He is believed to have established or enlarged Llantrisant Castle (just 2 km north of the Mwyndy orebodies) in around 1250. His son, Earl Gilbert the Red continued the dynastic expansion of the de Clares, at least in part as a response to the Treaty of Montgomery (1267) in which Henry III appeared to give control of the upland commotes to Llywelyn ap Gruffudd, ruler of Gwynedd. Gilbert seized Is Caiach in a series of actions, including the building of Castell Goch (1266), the imprisonment of the Lord of Senghenydd, Gruffudd ap Rhys in 1267 and building of Caerphilly Castle in 1268–1271. Thus during the period 1246–1266 the de Clares took control of the areas containing all the major Glamorgan iron orebodies.

A major industrial centre associated with the de Clares has been identified at Trelech, Gwent (Howell 1989, 1995*a*,*b*). The earliest record of a castle at Trelech, dates from 1231, but by 1288 it had 378 burgages, making it the second largest town in Wales at the time. Trelech appears to have declined during the early 14th century. The borough therefore had a relatively short-lived importance, coinciding with the period of the de Clare Lordship of Glamorgan (1218–1314). Excavations at Trelech have demonstrated the enormous scale of iron-making in and around the town, particularly concentrated in the period 1240–1290. Trelech is mentioned specifically in 'The Book of Dennis' the 'Miners Lawes and Priviledges' as a location (together with Monmouth, Caerleon, Newport and Berkeley) at which iron-making was undertaken by smiths with particular suppliers within the Forest of Dean. The earliest printed version of the book dates from 1678 (reproduced by Nicholls 1866), although there are extant manuscript copies dating from as early as 1610. These versions of the book are generally believed to be based on a thirteenth century code, and identical statements of part of the laws are to be found in a 'regard' dated to 1282. It seems reasonable to interpret the foundation of such a major iron making borough in a somewhat 'artificial' location, as an attempt by the de Clares to utilize the Forest of Dean ore by building within their domains, but as close to the Forest as possible. Indeed, Trelech is only 6 km farther from the ore sources of the western Forest of Dean than the thirteenth century Royal forge and arsenal at St Briavels (albeit on the opposite side of the Wye Valley).

The date of the foundering of the Magor Pill vessel is difficult to determine, but an estimate for its age as 10–40 years seems most likely (M. Redknap, pers. comm.). This would place the likely date of foundering in the period 1250–1280, but the vessel is unlikely to have been more than 50 years old, so the date almost certainly lies within 1240–1290; the peak period of iron making at Trelech. This same period saw the de Clares subsume the ore-producing areas in Glamorgan within their holdings, so a likely scenario would be that ore from those areas would be shipped to the de Clare industrial base at Trelech for smelting. The route for such a shipment would most likely have been overland to Cardiff, and then by boat up the channel, up the Wye as close as possible to Trelech; a route passing *Abergwaitha*. It is possible that the Glamorgan orefields found other customers during this period, but it may be significant that the mines on the later Bute Mine site, at least, were on demesne land, and would therefore have been subject to direct seigneurial control. It is worth noting that the Tewkesbury Annals for 1262

record that 'Gilbert, Earl of Gloucester, found mines of silver, iron and lead in Wales'.

## Conclusions

Major features of ore texture, mineralogy and geochemistry allow reasonably confident provenancing to the major sectors of the Bristol Channel orefield. On current data it has not been possible to provenance the cargo more precisely within the Glamorgan sector. This level of attribution would require a very detailed understanding of local variability, as well as general properties. Such understanding is not likely to be achieved, because of the working-out of most of the superficial orebodies. In the case of the Magor cargo, other factors, such as the likely contemporary accessibility of particular deposits, assist with the provenancing debate. Similar difficulties are likely to be encountered when attempting to provenance material within the other major sectors (west Forest of Dean, East Forest of Dean, Worcester Graben, Bristol & Somerset). One approach to this problem would be the detailed recording of the chemistry of smelting slags, from archaeological sites very close to the ore outcrops, and the interpretation of ore geochemistry from these data (Thomas & Young 1999). Through accumulation of such data it may be possible to model the variation in chemistry of the ores utilized both geographically and through time.

## References

ALLEN, J. R. L. 1996. A possible medieval trade in iron ores in the Severn Estuary of south-west Britain. *Medieval Archaeology*, **40**, 226–230.

CANTRILL, T. C., SHERLOCK, R. L. & DEWEY, H. 1919. *Special Reports on the Mineral Resources of Great Britain. Vol. IX — Iron ores (contd.) — sundry unbedded ores of Durham, East Cumberland, North Wales, Derbyshire, The Isle of Man, Bristol District and Somerset, Devon and Cornwall.* Memoirs of the Geological Survey. HMSO, London.

GAYER, R. A. & CRIDDLE, A. J. 1970. Mineralogy and genesis of the Llanharry iron ore deposits, Glamorgan. *In:* JONES, M. J. (ed.) *Ninth Commonwealth Mining and Metallurgical Congress 1969.* Institution of Mining and Metallurgy, London, 605–626.

HOWELL, R. 1989. A report on the excavation of a Medieval industrial site in Trelech, Gwent. *Medieval and Later Pottery in Wales*, **11**, 62–80.

—— 1995*a*. Excavations at Trelech, Gwent 1991–93. *Monmouth Antiquary*, **11**, 71–86.

—— 1995*b*. Ironworking at the Medieval Borough of Trelech, Gwent. *In:* CREW, P. & CREW, S. (eds) *Iron for Archaeologists, a review of recent work on the archaeology of early ironworking sites in Europe.* Plas Tan y Bwlch Occasional Paper No. 2, 25–27.

LOWE, D. J. 1993. The Forest of Dean caves and karst: inception horizons and iron-ore deposits. *Cave Science*, **20**, 31–43.

NAYLING, N. 1998. *The Magor Pill Medieval Wreck*, CBA Research Report 115. Council for British Archaeology, York.

NICHOLLS, H. G. 1866. *Iron making in the olden times: as instanced in the ancient mines, forges and furnaces of the Forest of Dean.* Facsimile reproduction with introduction by I. J. Standing. The Forest Bookshop, Coleford 1981.

RANKIN, A. H. & CRIDDLE, A. J. 1985. Mineralizing fluids and metastable low-temperature inclusion brines at Llanharry iron deposit, South Wales. *Transactions of the Institute of Mining and Metallurgy (Section B, Applied Earth Science)*, **94**, 126–132.

REDKNAP, M. & YOUNG, T. P 1998. The iron industry of south-east Wales in the 13th century. *In:* NAYLING, N. *The Magor Pill Medieval Wreck*, CBA Research Report 115, Council for British Archaeology, York, 112–115.

RIDEN, P. J. 1992. Early ironworks in the Taff valley. *Morgannwg*, **36**, 69–83.

SIBLY, T. F. 1919. *Special reports on the mineral resources of Great Britain. Vol. X — Iron ores (contd.) — The haematites of the Forest of Dean and South Wales.* Memoirs of the Geological Survey. HMSO, London.

—— & LLOYD, W. 1927. *Special reports on the mineral resources of Great Britain. Vol. X — Iron ores (contd.) — The haematites of the Forest of Dean and South Wales. 2nd Edition.* Memoirs of the Geological Survey. HMSO, London.

SIMMS, M. J. 1990. Triassic Paleokarst in Britain, *Cave Science*, **17**, 93–101.

SMITH, L. T. 1906. *The Itinerary in Wales of John Leland in or about the years 1536–1539 extracted from his MSS.* George Bell, London.

STRACHAN, A. 1899. *The Geology of the South Wales Coalfield. Part I. The country around Newport.* Memoir of the Geological Survey. HMSO, London.

—— 1909. *The Geology of the South Wales Coalfield. Part I. The country around Newport (2nd edition).* Memoir of the Geological Survey. HMSO, London.

—— & CANTRILL, T. C. 1902. *The geology of the South Wales Coalfield. Part III. The country around Cardiff.* Memoir of the Geological Survey of Great Britain. HMSO, London.

—— & —— 1904. *The geology of the South Wales Coalfield. Part VI. The country around Bridgend.* Memoir of the Geological Survey of Great Britain. HMSO, London.

—— & —— 1912. *The geology of the South Wales Coalfield. Part III. The country around Cardiff (2nd edition).* Memoir of the Geological Survey of Great Britain. HMSO, London.

TAYLOR, S. R. & MCLENNAN, S. M. 1981. The composition and evolution of the continental crust: rare earth element evidence from sedimentary rocks. *Philosophical Transactions of the Royal Society*, **A301**, 381-399.

THOMAS, G. R. & YOUNG, T. P. 1999. The determination of bloomery furnace mass balance and efficiency. *This volume.*

VIVIAN, S. 1885. The haematite deposits of the southern outcrop of the Carboniferous Limestone of South Wales. *Proceedings of the South Wales Institute of Engineers*, **14,** 164 [discussion p. 211]

—— 1872. The Mwyndy Mines. *Transactions of the Cardiff Naturalists' Society*, **3**, 79.

—— 1876. Note on paragenetic formation of carbonate of lime and oxide of iron, at the Mwyndy Mines, Glamorgnashire. With note on the specimens by J. H. Collins. *Transactions of the Cardiff Naturalists' Society*, **4**, 70.

—— 1877. Further notes on the oxides of iron, enclosed in quartz, at Mwynydy, Glamorganshire. *Transactions of the Cardiff Naturalists' Society*, **4**, 117.

WATERS, R. A. & LAWRENCE, D. J. D. 1987. *The geology of the South Wales Coalfield. Part III. The country around Cardiff. Memoir for 1:50,000 geological sheet 263 (England and Wales) (Third edition).* Britsh Geological Survey. HMSO, London.

WATSON, J. J. W. 1859. The haematite deposits of Glamorganshire. *Geologist*, **2**, 241–256.

WILLIAMS, M. 1958. *Geology and mineralisation of the Llanharry hematite deposits, South Wales.* PhD thesis, University of London.

WILSON, D., DAVIES, J. R., FLETCHER, C. J. N. & SMITH, M. 1990. *The geology of the South Wales Coalfield. Part VI. The country around Bridgend. Memoir for 1:50,000 sheet 261 and 262 (England and Wales). (Second edition).* Britsh Geological Survey. HMSO, London.

YOUNG, T. P. & THOMAS, G. R. 1998. The cargo: iron ore analysis. *In:* NAYLING, N. *The Magor Pill Medieval Wreck*, CBA Research Report 115. Council for British Archaeology, York, 105–111.

# Geochemistry of ballast granites from Brouage and La Rochelle, France: evidence for medieval to post-medieval trade with Falmouth, Cornwall, and Donegal, Ireland

CLAIRE E. LAZARETH[1] &
JEAN-CLAUDE C. MERCIER
*Université de La Rochelle, CLDG, UFR Sciences, Avenue Marillac F-17042 La Rochelle cedex 1, France*
[1]*Present address: ANCH-VUB, Pleinlaan 2, B-1050 Brussels, Belgium*

**Abstract:** Determination of the geographical origin of exotic ballast boulders found in various archaeologically dated constructions of medieval and post-medieval age along European shores provides evidence for early commercial sea links. However, ballast often consists of common granites. Some are identified here by combining multiple geochemical tools which support a first-degree classification into two groups, muscovite-bearing (with or without biotite) or muscovite-free (with biotite as the only mica), each one showing a remarkably very narrow and distinct range in mineral compositions. This suggests a single locality for the origin of each type of granites. Indistinguishable muscovite-bearing facies are found in La Rochelle and Brouage, with one representative sample geologically dated at $274 \pm 6$ Ma. In agreement with the evidence from bulk-rock and phase chemistry which are similar to those of the Carnmenellis intrusion, Cornwall, this geological age strongly supports early commercial sea links with nearby Falmouth, at least from the end of the 14th to the middle of the 16th century. For the muscovite-free granites found in Brouage in a different site dated *c.* 1650, similar investigations and a $393 \pm 9$ Ma geological age, strongly suggest ballast loading north of Ros Eoghain Point, Ireland, and direct trade with nearby Donegal.

European-scale maritime trade was important in the Middle Ages and early modern times, though written records are no longer available to reconstruct routes and modes of trade with much confidence. Ballast boulders such as those found along a 300 km stretch of the French Atlantic coast on either side of La Rochelle may now provide useful constraints on such old sea links.

Flat-hull merchant ships sailing offshore on ballast usually carried boulders collected on bars or moraines near the ports of departure. When they arrived close to the merchandise loading place, boulders were often thrown overboard to reduce the draught and make space for the goods such as salt or wine. Charts show that unloading ballast at specific places was strictly enforced, which produced over the centuries a mixture of rocks from various origins. These deposits are usually seen as the source of the ballast boulders used as building material in cities and villages along the seashore.

*From:* POLLARD, A. M. (ed.) 1999. *Geoarchaeology: exploration, environments, resources.* Geological Society, London, Special Publications, **165,** 123–137. 1-86239-053-3/99/$15.00

This is however not supported by observations at several archaeologically dated sites we studied, which consist of wall foundations, walls in elevation, or other structures made of ballast boulders. In none of these sites did we find mixed exotic rock types. Specifically, in Brouage, the same types/facies are found at a scale of several metres (up to decametres), though different ones are observed at the scale of a whole wall or in walls built at different times.

To have such a distribution pattern (further documented below), the rocks had to be originally picked up in a natural geological environment, presumably near the home port, they were not dumped and reloaded at established unloading sites but rather brought directly to final destination and they were ultimately discharged directly on the docks to be used very shortly afterwards as building material. If any one of these conditions had not been fulfilled, a mixing of rock types should have occurred.

Carrying ballast in such a way may have been exceptional and should not be opposed to traditional views on ballast dumping. However, it provides a unique opportunity to reconstruct former commercial routes at specific dates. Indeed, mineralogical and geochemical data for boulders may be used to constrain their geographical origin which, in this case, corresponds to the home port (or main port of call) of individual ships since the rocks were brought directly. On the other hand, their time of unloading is given by archaeologically dating the structure, which yields either the same age if the boulders were used immediately as building material, or an upper age.

The major-element phase-chemistry data discussed here were obtained on a CAMEBAX microprobe (Camparis analytical center, University Paris-VI) under a 15 kV acceleration voltage, a 9.2 nA current and with a counting time of 10 s. In our study, diagrams appeared to be more discriminating when considering the elemental fraction for each crystallographic site (Lazareth 1998). Hence, the compositional data for micas are recalculated in atom numbers for 22 positive charges, subsequently abbreviated as 'at. per $22^+$ f.u.'. This convention also makes it easier to identify compositional correlations that are mere artefacts due to stoichiometry and/or charge compensation. The significant correlations observed between cations and the replicate analyses yield analytical uncertainties significantly less than 0.01 per $22^+$ f.u. for all analysed elements, with the exception of fluorine ($\pm 0.05$ per $22^+$ f.u.).

The sample selection for whole-rock analyses of each type of granite was based on the degree of alteration, the rock homogeneity, and the fresh-core volume available. Fist-sized fragments of the selected samples were analysed through inductively coupled plasma-atomic emission spectrometry (ICP-AES) at the Centre Régional de Mesures Physiques, University of Clermont-Ferrand. Analytical conditions and standards are given in Cantagrel & Pin (1994). Selected samples were geologically dated on separate minerals by the K/Ar method, with potassium contents measured by atomic absorption spectrometry and argon on a modified THN 205 E mass spectrometer, both at the Centre de Recherche Pétrographique et Géochimique, CNRS-Nancy.

## Sample environments

### *La Rochelle*

This city, 170 km north of Bordeaux on the west coast of France, grew out of a small medieval village and harbour after 1146, with the settling of heirs of the mighty feudal

lord of Chatelaillon expelled in 1130 from his château, 12 km to the south. Meanwhile, the English founded an important garrison fort beside it, the so-called Vauclair castle. Built in 1162 under Henri II Plantagenêt, Vauclair had full control of harbour activities which included trade with Southampton, Portsmouth and Dublin, as early as 1185 (Delafosse *et al.* 1991). This fortified place was taken and levelled to the ground in 1372 by the inhabitants of La Rochelle by authorization of the king of France. At this time, La Rochelle already had the privilege of making metal money and, soon after the dismantling of the garrison, the manufacture was moved to the former garrison grounds, in 1394.

The place where this new 'Hôtel de la Monnaie' used to stand was excavated in 1995. Among various structures illustrating all the steps of processing the metal, from ore to coins, there was also found the basal part of an important ore treatment complex made of local Jurassic limestone except for the internal faces of a furnace (Fig. 1a) entirely built of rounded granitic boulders (except for rare gneisses and for a few bricks used in repairs). These granites (0.2–0.8 m long, >0.1 m thick) are unknown regionally in natural geological environments and hence they are interpreted as ballast boulders used here for their (relative) refractory properties, as is also the case in back-chimney stews found in a medieval tower of La Rochelle.

As this structure was to be dug out, all the granites used as internal facing stones were numbered and collected (159 samples) and, in the absence of any spatial heterogeneity in petrological types, our further studies were arbitrarily limited to the 36 boulders of the eastern wall. Archaeological stratigraphic data (Bocquet & Mille 1995) suggest the very first years of the 15th century for the date of construction of the furnace and, considering the manufacture was moved in 1394, the intermediate date of *c.* 1400 will be used.

## *Brouage*

Brouage, a still fully fortified city about 30 km south of La Rochelle, was founded around 1550 (La Popelinière 1581) at the mouth of the main channel used to drain the furthest inland marshes and, at rising tides, to feed the lower salt marshes surrounding the area. Extraction of salt in these marshes began as early as the second century BC, but production increased tremendously between the end of the 8th and the early 9th centuries (Glénisson 1981). Soon after 1550, Brouage became the foremost port in Europe for salt exportation.

In Brouage, abundant exotic rounded ballast boulders (about 0.3 m in size, some up to 0.5 m) were sampled in three structures:

- a remnant of the oldest-dated city wall built by Italians in 1570 and which consists of the lower part of the internal facing of the northern wall named 'Courtine Royale'
- the foundation garnish (rock/lime filling between elements of a wood structure built on the marsh to support a wall) of the external doubling built under Richelieu in 1631 against the western city wall named 'Courtine de la Mer' (from here on, referred to as CM; Fig. 1b)
- a discontinuous sandy layer directly underneath an earth-made internal terrace built under Vauban in 1689 against the city wall named 'Courtine Richelieu' (henceforth referred to as CR)

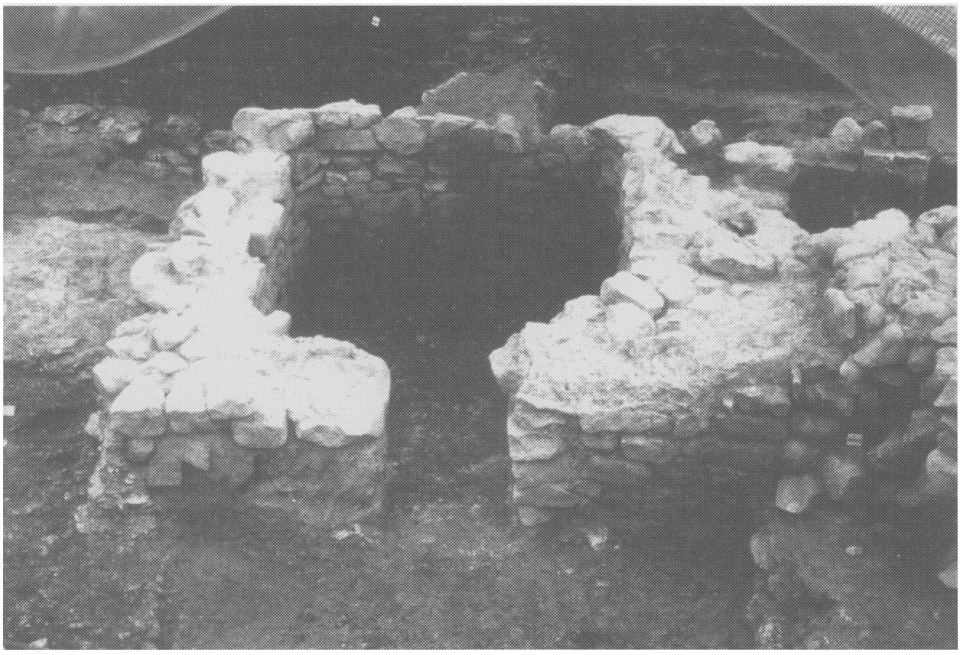

(a)

(b)

**Fig. 1.** Two of the structures providing archaeologically dated ballast boulders: (**a**) ore furnace (lower half) of the coin manufacture in La Rochelle (*c.* 1400); (**b**) wood structure used for building on the marsh, western wall, Brouage (1631).

## Rock type distribution as evidence for direct travel

In Brouage, the samples collected virtually all belong to a single rock-type or series at each site (Table 1) and are different from one site to another. The Italian wall is characterized by a particular type of syenites known to originate only in Norway where it is locally called larvikites, whereas most of the CM samples are muscovite-bearing granites (85%) and the CR ones, muscovite-free granites (90%). Moreover, a careful inspection of all ballast-made historic walls of Brouage failed to provide any evidence of mixing for the lithological types which could be identified *in situ*, such as larvikites, but also fresh olivine basalts and amphibolitized coarse gabbros, each one of these being strictly restricted to a very well defined part of a wall.

As for La Rochelle, the internal facing stones of the ore furnace were virtually all muscovite-bearing granites (96%) and the few gneisses described actually are the main parts of igneous natural polymict samples partly made of similar granites, hence pointing to a common geographical origin. This contrasts with the large variety of metamorphic rocks observed in the walls and towers of La Rochelle, including the medieval back-chimney stews in Tour de la Chaîne.

As stated earlier, this non-mixing of sample types at one site is a strong argument for direct travel from the geological source regions of the boulders, rather than cabotage, at least for the ships sailing on ballast which traded with Brouage and La Rochelle. Cabotage, that is trading with numerous port stops *en route*, would have indeed needed unloading and reloading of ballast at specific sites, with mixing of the rocks from various ships. Similarly, ballast picked up for construction at nearby earlier unloading sites would have also been mixed, according to the large variety of rock types observed in the various walls. This suggests that ballast was used immediately upon unloading, i.e. that it was taken to a dock (as would have been commercial goods) as building material for works in progress.

The above preliminary conclusion is further supported by the phase chemistry for the granites (Lazareth 1998). For instance, the muscovite-free and the muscovite-bearing facies must indeed be considered as two distinct populations. As an example, plotting the silicon (Si; all tetrahedral) versus octahedral aluminium ($^{VI}$Al) contents of biotites (Fig. 2) yields two groups with a compositional gap in between. Even if Al-saturated biotites of muscovite-bearing granites are likely to be richer in Al (formally, this would hold only under similar physical conditions of crystallization), a continuous change in liquid composition as expected from fractional crystallization could not result in such a gap. Thus, we are dealing with two genetically unrelated populations which we shall discuss independently. The restricted compositional domain for each group compared to various European granites will provide further evidence for the absence of mixing and therefore against the practice of cabotage.

## The muscovite-bearing granites

Muscovite-bearing granites have been found both in La Rochelle (furnace; *c.* 1400) and in Brouage (site CM, precisely dated 1631). They are described together since no significant difference has been found between them at any point during the study. A geological date could not be obtained for the samples from La Rochelle because of their long exposure to the very high temperatures reached in the furnace, whilst the date of furnace construction restricts their geographical origin to European shores.

**Table 1.** *Schematic description of the sites and samples*

| City | Structure | Date | Dominant rock type | Percent of dominant-type samples | Number of lab.-studied samples |
|---|---|---|---|---|---|
| La Rochelle | Inside of furnace, Hôtel de la Monnaie | *c.* 1400 | muscovite-**bearing** granites | 96 | 36 |
| Brouage | Italian's wall, Courtine Royale | 1570 | **larvikites** and related facies | ~95 | 5 |
| Brouage | Foundation garnish, Courtine de la Mer | 1631 | muscovite-**bearing** granites | ~90 | 45 |
| Brouage | Sands under terrace, Courtine Richelieu | *c.* 1650 | muscovite-**free** granites | 90 | 9 |

Percentages of rock types are given relative to large numbers (up to hundreds) of exotic rocks observed in the field, i.e. excluding eventual local silex and limestone. Note that many of the exotic rocks not included in the main type may be cognate and of the same geographic origin, sometimes even all of them (e.g. in La Rochelle).

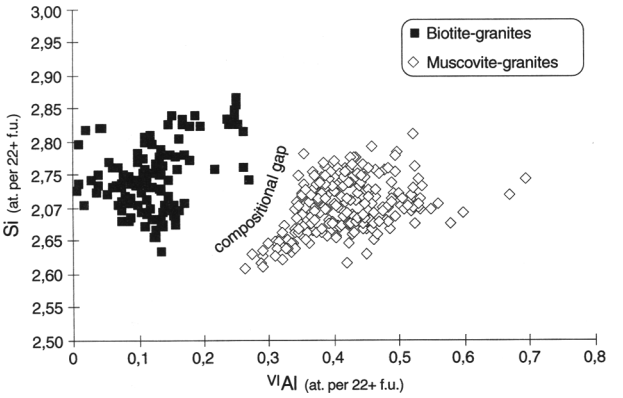


**Fig. 2.** Concentrations in Si and $^{VI}$Al for the biotites of all the granites from La Rochelle and Brouage (CM and CR sites). A significant gap exists between the biotites of the muscovite-bearing and muscovite-free granites, but overlaps between samples do not support further identification of subgroups.

## *Petrography*

The muscovite-bearing granites are mostly two-mica granites that can be ascribed to different facies according to their mineralogy. In addition to quartz, plagioclase and potassic feldspars (the three basic components of a granite) and, of course, to biotite and muscovite, the mineral assemblage may also include garnet, green tourmaline and blue tourmaline, the latter two never being found together. Biotite-free granites are always associated with the two-mica granites in our different sites and they share some common characteristics (same compositions or same compositional trends depending on the parameters). Accordingly, they will be described together under the generic name of muscovite-bearing granites.

According to the textures observed in thin sections, the two micas may have crystallized simultaneously or not. In the first case, biotite and muscovite are systematically associated (Fig. 3a); in the second, muscovites can be subdivided into two populations: early muscovites included in feldspars (Fig. 3b) and later ones occurring as isolated tablets in the 3D-mineral matrix (association of the two micas is then exceptional). Garnets are always small isolated crystals (0.25 to 0.80 mm), xenomorphic in most granites, sometimes subidiomorphic in the biotite-free granites. Green tourmaline occurs either as small isolated crystals or partly included in biotites (Fig. 3c). This contrasts with the behaviour of blue tourmaline that is either interstitial between crystals (Fig. 3d) or intermingled with feldspar, apparently filling hydraulic fractures in crystals of the latter phase. Unlike green tourmaline, blue ones are thus clearly late-crystallization phases and correspond to the last liquids.

## *A magmatic series*

The above characteristics can be used to define a large number of mineralogical types and subtypes of granites among the samples. In theory, this may result from the mixing of muscovite-bearing granites of different geographical origins. However, phase chemistry (compositions, Fe partitioning, etc.) rather suggests a continuous series resulting from magma differentiation.

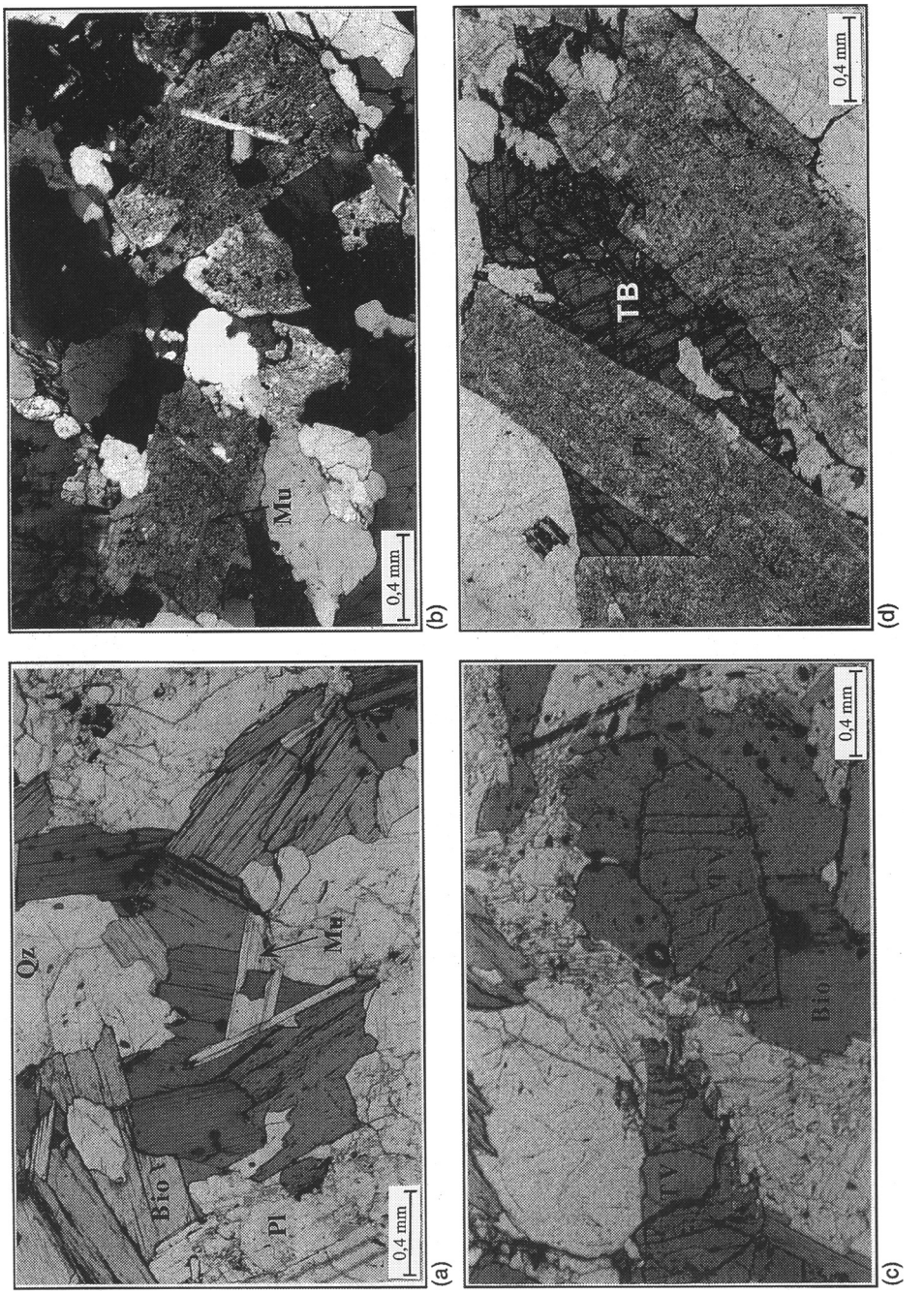
Qz
Bio 1
Pl
Mu
0,4 mm
(a)
Mu
0,4 mm
(b)
Mu
Bio
0,4 mm
(c)
TB
0,4 mm
(d)

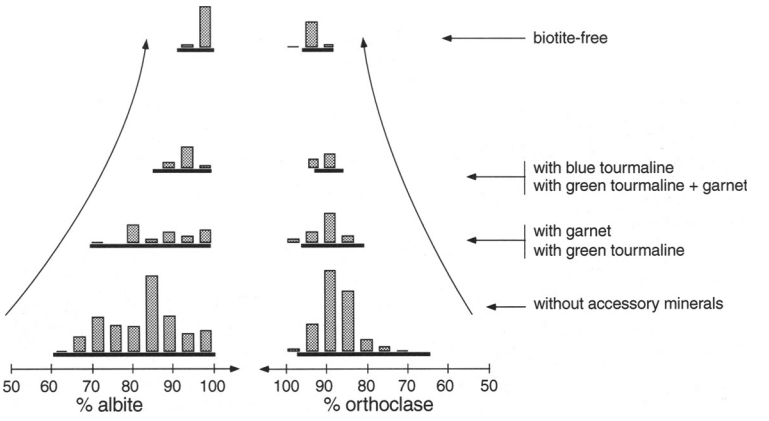


**Fig. 4.** Evolution of feldspar compositions for the muscovite-bearing granites, from assemblages without accessory mineral to the biotite-free granites. The order follows that of differentiation defined by the mineral assemblages and agrees with all chemical trends observed (Lazareth 1998). Solid lines under the histograms represent the actual compositional ranges, and the vertical dimension, the relative number of samples within each compositional bracket.

For example, feldspar compositions of the muscovite-bearing granite evolve with compositional ranges becoming narrower and average compositions more albitic (for plagioclases) and potassic (for potassic feldspars), when covering the series facies in the order: no accessories, green tourmaline or garnet, green tourmaline and garnet, blue tourmaline, biotite-free (Fig. 4). This pattern is consistent with all the muscovite-bearing granites deriving from a same primary magma by fractional crystallization with falling temperature, which is further supported by the relative physical conditions of crystallization estimated for the various facies (Lazareth 1998).

Other mineral phases also provide similar evidence for a single magmatic series. Very strong positive or negative correlations may even be observed as is the case for Mn and $Fe^{2+}$ v Mg in garnet or for Ti v Mn in muscovite (Fig. 5). Here, with increasing degree of differentiation, Ti first decreases to near nil values with Mn close to nil, then Mn increases while Ti virtually stays at zero. The compositional trend is in full agreement with the above conclusion on feldspars, though the presence of garnet, which has little effect on muscovite chemistry, would mainly be related to local bulk-system heterogeneities.

Finally, whole-rock ICP-AES analyses also yield trends consistent with differentiation. For example, Si, Na and Y increase from no-accessory to blue-tourmaline granites, whilst Al, K, Ti, Ce, Ba and Sr decrease. Simultaneously, the average slope of the rare-earth element patterns goes from negative to positive, while the europium anomaly is up to 50 times larger when blue tourmaline is present, with or without biotite (Lazareth 1998).

---

**Fig. 3.** Textural phase relations in some of the muscovite-bearing granites. Bio, biotite; Mu, muscovite; Qz, quartz; TV, green tourmaline; TB, blue tourmaline. (**a**) Cotectic-grown biotites and muscovites (BR.G9, Brouage; parallel Nicols). (**b**) Early muscovites in feldspars (BR.G38, Brouage; crossed Nicols). (**c**) Early to cotectic green tourmaline with biotite (BR.A13, Brouage; parallel Nicols). (**d**) Late interstitial blue tourmalines (VE.19E, La Rochelle; parallel Nicols).

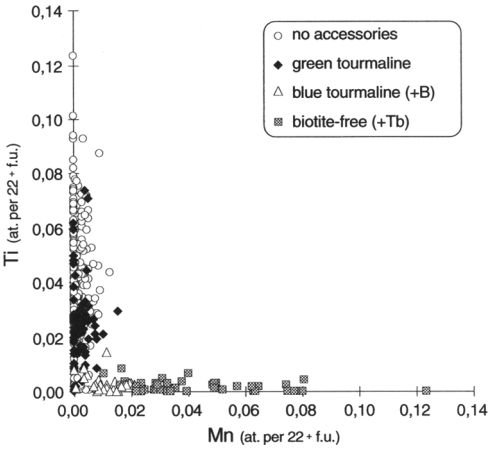


**Fig. 5.** Ti/Mn trend for the muscovites in granite boulders according to differentiation inferred from the mineral assemblages (arrow). All symbols include garnet-bearing and garnet-free granites as presence of this phase has no apparent effect on the chemical parameters used here. B and Tb stand for biotite and blue tourmaline, respectively.

In addition, the narrow ranges in phase compositions (both sampling sites combined) compared to those for European muscovite-bearing granites (Scandinavia, Scotland, Cornwall and Brittany; references in Fig. 6) is striking, and imply a common specific range of physical conditions for all the muscovite-bearing granites found as boulders. For the latter, the $^{VI}$Al values for biotites lie between 0.25 and 0.70 at. per $22^{+}$ f.u. (maximum range), with most samples between 0.30 and 0.55, in contrast to the 0.05 to 0.93 range recorded in the literature. Furthermore, the overall scatter for the boulders is even less than that for any of the localities described in the literature, when discarding the limited dataset for Brittany. It is thus highly probable that all the muscovite-bearing granites from both La Rochelle and Brouage have the same origin, at least at a regional level.

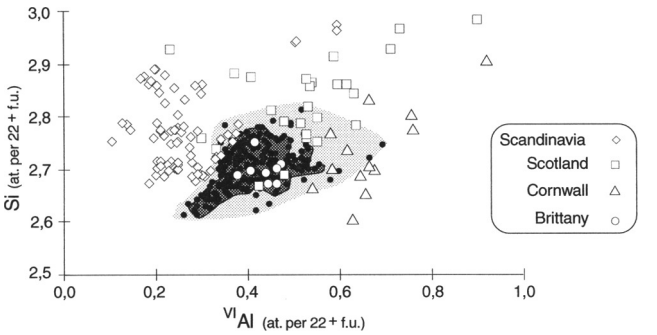


**Fig. 6.** Concentrations in Si and $^{VI}$Al for biotites of the muscovite-bearing granites from Brouage and La Rochelle (ballast: solid circles and patterns, the darker one including 95% of the samples) and from European localities: Scandinavia (Lazareth 1998), Scotland (Tindle & Webb 1990; Harrison 1990), Cornwall (Tindle & Webb 1990; Stone *et al.* 1988) and Brittany (Nachit 1986). Biotite compositions from the literature have been recalculated on $22^{+}$ charges for consistency.

## *Geographical origin*

We may first compare the petrochemical characteristics of our boulders to those of various European muscovite-bearing granites likely to have provided material for shore bars and moraines. Scandinavian muscovite-bearing granites can be excluded as a potential source as their biotites mainly have totally distinct compositions (Fig. 6). Though biotites from Scotland and Cornwall granites not only show a large scatter, but also a compositional distribution somewhat offset, such sources cannot be excluded because the sparse data in the literature may not be volumetrically representative. The Brittany granites would however appear as better candidates, still conforming to the biotite compositions. Other minerals such as accessory phases also provide some constraints. For instance, the tourmalines in Scandinavian granites have much higher Mg contents and about three times more X-site vacancies per structural formula than those from any ballast granite (Lazareth 1998), again excluding such a possible Scandinavian origin.

In addition to phase-chemistry criteria, whole-rock compositions may also be used. None of the binary plots (e.g. CaO v $SiO_2$, Ba v Sr, etc.; (Lazareth 1998)) appear to be sufficiently discriminating to indicate whether the granite boulders come from either Brittany or Cornwall (or even Scotland) by clearly excluding one (or two) of these regions. However, the granites from Cornwall have rare-earth element patterns quite similar to those for the ballast boulders, one of which, that for the Carnmenellis intrusion, near Falmouth, is virtually identical (Fig. 7).

It is thus clear that geochemical data, either for mineral phases or bulk rocks, may provide definite criteria to exclude some granites, but that the validity of the source identification depends on the quality of a European-scale database which is still very fragmentary. The geographical origin of the ballast granites can however be ultimately constrained by geochronological data, i.e. geological ages of formation.

Granites in shore bars and coastal moraines may be related to three major tectonic and age units: the Baltic-Fennoscandian shield (Precambrian, *c.* 3300–550 Ma), the North-Atlantic Caledonides (Caledonian, *c.* 500–400 Ma) and the Variscides (Hercynian, *c.* 400–240 Ma). As the age of formation obtained through K/Ar dating on muscovite for one representative muscovite-bearing granite from Brouage (BR.G5)

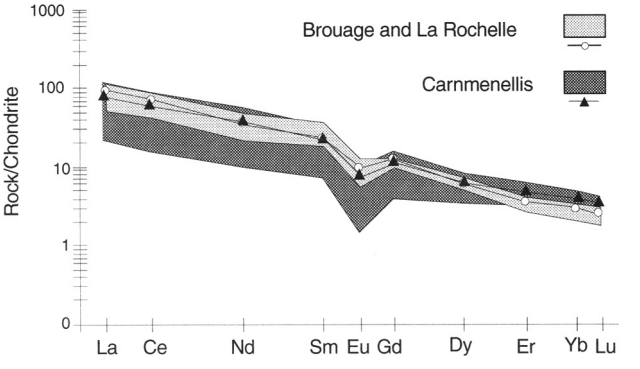


**Fig. 7.** Ranges and means of normalised rare-earth element concentrations for blue-tourmaline-free muscovite-bearing granites occurring as ballast boulders (Brouage, La Rochelle) and from the Carnmenellis intrusion, Cornwall (Jefferies 1985).

is 274 ± 6 Ma, that is of Hercynian age, the source locality should be looked for exclusively only along the coast of Brittany, Cornwall, Portugal or Galicia. The latter two can be readily discarded as being too old (>310 Ma) and/or hornblende-bearing (Julivert *et al.* 1980). As the granites of Brittany are always older than 300 Ma (Carron *et al.* 1994), the younger ones in Cornwall (268 to 290 Ma; London & Manning 1995) appear to be the only possible source for the muscovite-bearing granite ballast. The exact provenance can even be pinpointed as being the Carnmenellis intrusion, with an age ranging from 269 ± 2 Ma to 290 ± 2 Ma (Darbyshire & Shepherd 1985, 1987) which encompasses the BR.G5 age of 274 Ma ± 6 Ma. All the other intrusions are younger (268 ± 2 Ma) or older (from 280 to 287 ± 4 Ma) granite (London & Manning 1995). Thus, considering all the characteristics of the muscovite-bearing granite boulders (mineral chemistry, rock compositions and geological age), the only place from where they could have been picked up is along the Channel shore to the south of the Carnmenellis intrusion, by ships from the home port of Falmouth.

## The muscovite-free granites

Muscovite-free granites are the only plutonic type (except for one tonalite sample) found in the discontinuous sandy layer beneath the eastern wall earthwork built by Vauban in 1689 (site CR). Previous occupation and apparent sand removal before building the earth terrace justifies an earlier date for the ballast deposit, estimated to be *c.* 1650. Hence, a New World import would be historically possible if it were not that such granites are not identified at nearby ports then potentially trading with Brouage. Archaeological sites not yet sampled (e.g. the walls of the former hospital), however, show volcanic/plutonic rocks that could have a New World origin (Antilles, Canada).

### *Petrography*

The mineralogical assemblage of the muscovite-free granites is very homogeneous, with the four rock-forming phases: quartz, plagioclase, K-spar and biotite. A few rare samples also have some scattered amphibole, the only accessory phase found in this type of granite. Compared to the muscovite-bearing granites, the simplicity of the assemblages, the lack of specific textural relationships and the likeness of the samples (Lazareth 1998) do not justify further petrographic descriptions herein.

### *Geographical origin*

In terms of Si v $^{VI}$Al, the biotite compositions of the Scandinavian muscovite-free granites are mainly not consistent with the boulder biotite compositions (Fig. 8). The muscovite-free granites from England and Brittany show a large scatter, with only two analyses for Brittany plotting over the main field for the ballast granites. As for amphiboles, those from boulders plot somewhat to the lower side of a gross Mg/(Mg + Fe) v Na + K negative correlation found for European muscovite-free granites (Lazareth 1998), which does not support a source locality in England and virtually excludes an origin in Brittany (much lower Na + K). This conclusion is in agreement with hand-specimen observations, the muscovite-free granites from Brittany having a typical pink hue never observed for any boulder.

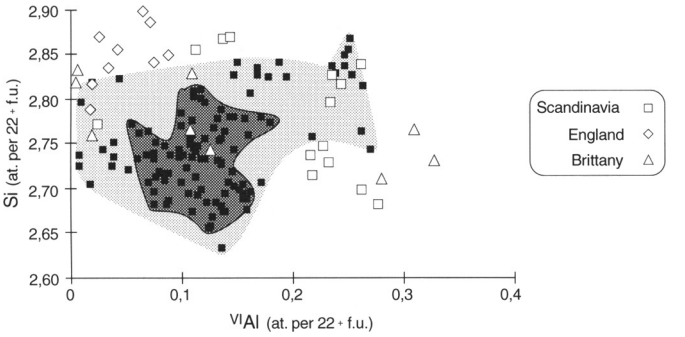


**Fig. 8.** Concentrations in Si and $^{VI}$Al for biotites of muscovite-free granites from Brouage and La Rochelle (symbols as in Fig. 6) and from European localities : Scandinavia (Brigatti *et al.* 1991; Lazareth 1998), England (Shap granite; Caunt 1986) and Brittany (Nachit 1986).

In terms of whole-rock compositions, the Si content, potentially significant as a differentiation index, also does not support a source locality in England for the ballast muscovite-free granites. Such an origin can be definitely discarded according to other parameters such as the Ba/Sr ratio, 1.6 for granites from England compared to 4.5 for the ballast samples (Lazareth 1998). Hence, the geochemical data strongly suggest that the boulders were loaded in Ireland inasmuch as amphibole-bearing facies are also known in this region.

As muscovite-free granites are Hercynian (*c.* 400–240 Ma) in Brittany, Caledonian (*c.* 500–400 Ma) in Ireland and Precambrian (*c.* 3300–550 Ma) in Scandinavia, the age of formation of the boulder granites again is a final and critical argument for establishing their geographic origin. Measurement of K/Ar isotopes on separate biotites from a representative muscovite-free sample from Brouage (BR.C10) yields an age of $393 \pm 9$ Ma, which unambiguously denotes it as a Caledonian granite. England and Scandinavia can thus be definitely excluded as potential source regions, as was already suggested above. The muscovite-free granites must, then, have been picked up in the British Caledonides and, even more precisely, along the shore of northwestern Ireland. Indeed, only the Donegal batholith, which is located along this shore, has whole-rock compositions similar to those of the ballast muscovite-free granites. Furthermore, the ages of formation for this granite range from 357 to 400 Ma. More specifically still, the oldest age of $392 \pm 8$ Ma is indistinguishable from that of the ballast sample. It is found to the north of Ros Eoghain Point, which ships coming from the city of Donegal (Dùn Na Gall) had to pass on their way to the Irish Sea and to France (Fiquet & Leblanc 1997).

## Conclusions

Two granite series are identified within the samples, the presence or absence of muscovite being the simplest discriminant criterion. Muscovite-bearing granites and muscovite-free granites are totally unrelated petrogenetically as shown by their phase chemistry (e.g. biotites), their whole-rock chemistry (e.g. rare-earth elements) and geological ages determined for two representative samples (Hercynian v

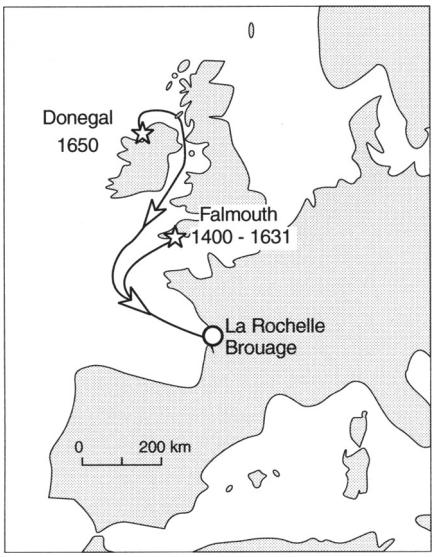


**Fig. 9.** The early commercial sea links reconstructed from the granite ballast study: Falmouth – La Rochelle, Falmouth – Brouage and Donegal – Brouage.

Caledonian). That they are found in separate sites with no mixing with each other or with other local ballast rock types (larvikites, basalts, gabbros rocks), shows the ballast studied was carried directly from near the home ports to Brouage or La Rochelle, without cabotage. This is also illustrated by the distribution of specific lithological types among the sealed archaeological sites and provides multiple evidence for a mode of trade previously assumed to have been minor relative to cabotage.

The petrochemical study of archaeologically sealed granite ballast from Brouage and La Rochelle has also proved effective for reconstructing early commercial sea links (Fig. 9) despite the limited chemical data base available in the literature. The muscovite-bearing granite ballast corresponds to direct commercial trade between Falmouth, Cornwall, and La Rochelle (*c.* 1400) and Brouage (1631), presumably related to wine and salt trade, respectively. As for the muscovite-free granite ballast, it documents direct commercial sea-links between Brouage and Ireland at a later period (*c.* 1650).

Though the present results fit in with the general pattern acknowledged for old trade, here, for the first time, the home port for three different series of ballast samples in the British Islands, twice for Falmouth and once for Donegal, are precisely identified at dates archaeologically established. Such exotic ballast boulders hence become as valuable as artefacts and their geochemical study may now be considered as a new tool for archaeology.

The Conseil Régional du Poitou-Charentes provided a 3-year stipend to C. E. Lazareth and the Conseil Général de la Charente-Maritime (Syndicat Mixte de Brouage) and Communauté de Ville de La Rochelle, the financial support for field work and analyses. Thanks are extended personally to N. Fiquet, T. Eliasson and A. Sylvester.

## References


BOCQUET, A. & MILLE, P. 1995. *La Rochelle, place de Verdun (Charente-Maritime), fouille préventive d'octobre 1994 à juillet 1995*. Direction régionale des Affaires Culturelles de Poitou-Charentes, Service régional de l'Archéologie, Poitiers, France, Document final de synthèse 17. 300. 027.

BRIGATTI, M. F., GALLI, E. & POPPI, L. 1991. Effect of Ti substitution in biotite-1M crystal chemistry. *American Mineralogist*, **76**, 1174–1183.

CARRON, J. -P., LE GUEN DE KERNEIZON, M. & NACHIT, H. 1994. Variscan granites from Brittany. *In*: KEPPIE, J. D. (ed.), *Pre-Mesozoic geology in France and related areas*. Springer, Berlin, 231–239.

CANTAGREL, F. & PIN, C. 1994. Major, minor and rare-earth element determinations in 25 rock standards by ICP-atomic emission spectrometry. *Geostandards Newsletter*, **18**, 123–138.

CAUNT, S. L. 1986. *Igneous and Metamorphic Processes in the Shap Granite and its Aureole*. PhD thesis, University of Leeds.

DARBYSHIRE, D. P. F. & SHEPHERD, T. J. 1985. Chronology of granite magmatism and associated mineralization, SW England. *Journal of the Geological Society of London*, **142**, 1159–1177.

—— & —— 1987. Chronology of granite magmatism in south-west England: the minor intrusions. *Proceedings of the Ussher Society*, **6**, 431–438.

DELAFOSSE, M., FAVREAU, R., PÉROUAS, L., SAINT-AFFRIQUE, O. & DE TROCMÉ, E. 1991. *Histoire de La Rochelle*, Privat, Toulouse, France.

FIQUET, N. & LEBLANC, F.-Y. 1997. *Brouage, ville royale*. Patrimoines & Médias, Niort, France.

GLÉNISSON, J. 1981. Le Moyen Age. *In*: COMBES, J. & LUC, M. (eds) *La Charente-Maritime, L'Aunis et la Saintonge des origines à nos jours*. Bordessoules, Saint-Jean-d'Angély, France, 101–114.

HARRISON, T. N. 1990. Chemical variation in micas from the Cairngorm pluton, Scotland. *Mineralogical Magazine*, **54**, 335–366.

JEFFERIES, N. L. 1985. The distribution of the rare-earth elements within the Carnmenellis Pluton, Cornwall. *Mineralogical Magazine*, **49**, 495–504.

JULIVERT, M., MARTINEZ, F. J., & RIBEIRO, A. 1980. The Iberian segment of the European Hercynian foldbelt. *Proceedings of the 26th International Geological Congress*. Bureau de Recherches Géologiques et Minières, Orléans, France, 132–158.

LA POPELINIÈRE, H. DE, 1581. *L'histoire de France, enrichie des plus notables occurances*. Abraham, La Rochelle, France.

LAZARETH, C. E. 1998. *Pierres de lest du littoral Poitou-Charentes: granites et larvikites; pétrologie, géochimie, typologie et provenance géographique; contraintes sur les voies de commerce maritime anciennes*. PhD thesis, Université de La Rochelle.

LONDON, D. & MANNING, D. A. C. 1995. Chemical variation and significance of tourmaline from southwest England. *Economic Geology*, **90**, 495–519.

NACHIT, H. 1986. *Contribution à l'étude analytique et expérimentale des biotites des granitoïdes, applications typologiques*. PhD thesis, Université de Bretagne Occidentale, Brest, France.

STONE, M., EXLEY, C. S. & GEORGE, M. C. 1988. Composition of trioctahedral micas in the Cornubian batholith. *Mineralogical Magazine*, **52**, 175–192.

TINDLE, A. G. & WEBB, P. C. 1990. Estimation of lithium contents in trioctahedral micas using microprobe data: application to micas from granitic rocks. *European Journal of Mineralogy*, **2**, 595–610.

# Geochemistry and the early alum industry

ANDREW R. MILLARD
*Department of Archaeology, University of Durham, South Road, Durham DH1 3LE, UK*

**Abstract:** One of the earliest chemical industries in Britain was the alum production industry. The early alum industry relied on a complex series of extractions from suitable shale deposits, until the rise of alternative methods in the 19th century, based on industrially produced sulphuric acid. Relatively little is known about the actual processes involved. This paper discusses the evidence that can be gleaned for the chemical processes involved and reports investigations on residues recovered from waste tips at the 17th–18th century alum works at Carlton Bank, North Yorkshire. For the first time it can be said that the sulphur content of the alum shale would have limited yields from the alum production process. Wide variability in the sulphur content of unworked shale implies variable yields in the alum production process, which may have contributed to the historically recorded boom and bust of individual alum works. Analyses of waste calcined shale were shown to be of limited value without experimental reconstruction of shale processing. Future investigations need to concentrate on waste residues recovered from alum works during excavations, and on reconstructions of the process.

This paper is an attempt to draw the attention of archaeological scientists and geochemists to some interesting problems relating to the archaeological investigation of early industrial chemistry.

An alum is a hydrated double sulphate of formula $XAl(SO_4)_2.12H_2O$, where X is commonly K, $NH_4$ or Na. Alum was widely used in the past as a mordant to bind dyes to cloth. In the post-medieval period its large-scale production gave rise to the first chemical industry. In England from *c.*1600 the alum industry developed based mainly on extraction from the Jurassic alum shales of North Yorkshire. There are thus a large number of former alum works in North Yorkshire and Cleveland that survive from the 17th to 19th centuries. There is some documentary evidence of these works, as well as excavated evidence from a few of them. The economic aspects of the industry have been fairly well studied, but the industrial process of converting shale to pure alum is known only in outline and not in detail (Marshall 1995). This is due in part to the complexity of the processes involved, a lack of study of the processes, and the fact that the historical accounts are often deliberately vague in order to prevent rivals from picking up in any local improvement to the process.

## The alum industry in the 16th to 19th centuries

Prior to the 15th century alum was imported into Europe from a number of sources, mostly in the Byzantine Empire. After the fall of Byzantium to the Turks in 1453, a shortage developed and European sources were sought. Vast deposits of alunite ($KAl_3(SO_4)_2(OH)_6$) were discovered at Tolfa, Italy, and became Europe's chief

*From:* POLLARD, A. M. (ed.) 1999. *Geoarchaeology: exploration, environments, resources.* Geological Society, London, Special Publications, **165,** 139–146. 1-86239-053-3/99/$15.00

source of alum. Tolfa lay within the Papal Territories and so the alum supply of Europe became virtually a Papal monopoly (Taylor & Singer 1956).

After the English Reformation this Papal control became a problem for supplies to the English cloth dyeing industry and Henry VIII initiated prospection for indigenous alum sources. After a series of unsuccessful attempts to establish an English alum industry in the second half of the 16th century, successful exploitation of the North Yorkshire alum shales began *c.* 1600. Until 1679, the right to produce alum remained a Crown monopoly that was farmed out to a small group of licensees. This early English production was probably also limited by the difficulty of perfecting the extraction process for this new source. Production appears to have first satisfied the home demand of about 1800 tons per annum by *c.* 1635, and by the 18th century production reached 4000–5000 tons per annum (Marshall 1995, Turton 1938). Although other areas of Britain developed alum works in the late 18th century, the North Yorkshire works continued to dominate the industry until 1850, when Peter Spence introduced a new production method based on sulphuric acid digestion of coal measure shales. One Spence process works could produce alum more rapidly than the entire North Yorkshire industry at its peak, and so by 1871 all the North Yorkshire works had closed (Marshall 1995).

## The alum production process

The North Yorkshire production process involved quarrying of the shale, calcining to oxidize sulphides to sulphates, extraction of aluminium sulphate, purification, conversion to alum by addition of an alkali, and further purification of the alum. Turton (1938) gives the best descriptions of the processes involved for the calcining, and Young (1817) and Marshall (1995) for the extraction and purification. The following analysis of the chemistry involved is based on these accounts. The Imperial units of the original accounts are given here, together with approximate metric equivalents. Figure 1 gives a diagrammatic summary of the process.

The shale was quarried after removal of the overburden and built into a clamp (calcining heap) composed of alternating layers of brushwood and shale. The largest clamps were as much as 200 feet (61 m) square and 80–90 feet (24–27 m) in height, though more typical dimensions may have been 90 feet (27 m) square. A clamp would be lit when it reached 4 feet (1.2 m) high and layers would continue to be added. The process of calcining would take 9–12 months to complete. For optimum production the temperature had to be high enough to convert ferric sulphate (formed from oxidation of the ferrous disulphide of the shale) to sulphur trioxide, but not high enough to decompose the aluminium sulphate that was formed by the reaction of the $SO_3$ with the aluminosilicate clays. This is achieved at 450–550°F (230–290°C). In order to regulate the temperature, slow the combustion and retain gaseous $SO_3$, the sides of the clamp were plastered with wet earth, clay or shale, particularly on the windward side. Additionally, a 'mellowing period' of slow cooling was allowed after calcining to aid the recombination of any decomposed aluminium sulphate.

Once the clamp had cooled it was opened and the bright red calcined shale was dug out. Extracting the aluminium sulphate and converting it to alum would have been relatively easy but for the fact that the product had to be of high purity. Iron salts co-extract from the calcined shale impart an orange or brown colour to the alum. If such alum is used to mordant dyes, it has the undesirable effect of darkening

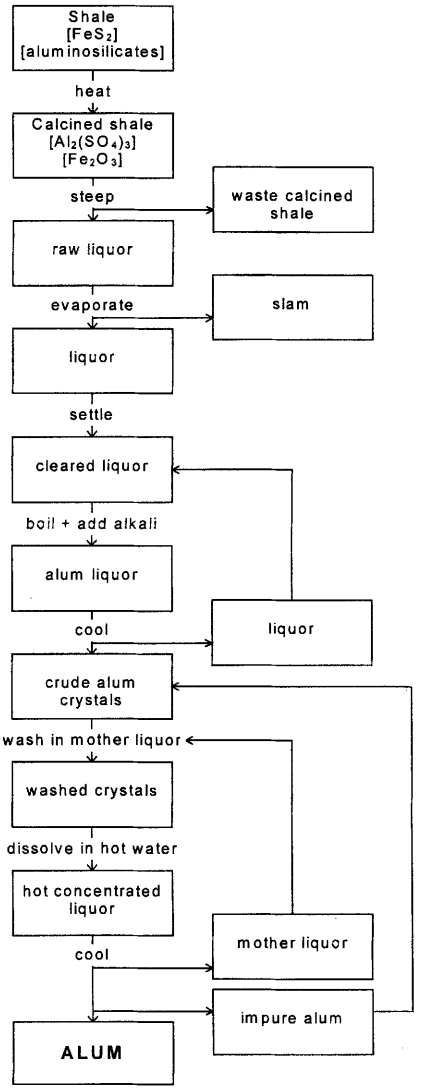


**Fig. 1.** Schematic representation of the alum extraction process.

their colour. Therefore the extraction process involved a series of purification steps in order to obtain colourless alum.

The calcined shale was steeped in water to extract the soluble aluminium sulphate as a 'raw alum liquor'. This was transported through a series of troughs to the alum house where it was heated to evaporate the water and concentrate the solution. Much of the iron impurity was removed at this stage as a yellow iron silicate crust known as 'slam'. After solid impurities had settled out, the 'cleared liquor' was moved on to a further set of evaporating pans where it was boiled to concentrate it, and an alkali was added. The main sources of alkali were urine for ammonia and potash (or muriate (chloride) of potash) for potassium. Upon cooling, crude alum crystals formed.

The crystals were collected and the solution recycled to the previous stage to be further concentrated. The crystals were then washed with 'mother liquor', a saturated solution of alum generated in the final stage, 'roached' (recrystallized) by dissolving them in hot water (or, in some later works, using steam) and then crystallized in barrels. The cask would be opened and a hole drilled to remove the 'mother liquor' from the centre of the mass of alum crystals. At the base of the cask would be impure alum, but the upper parts contained the purified product. Any of the alum not of suitable purity (as judged by its colour) would be roached again.

The scale of the industry, handling vast tonnages of shale and large volumes of 'liquor' means that there are numerous buildings and other remains at alum works sites, but few have been excavated and interpreting them in terms of the production process is difficult as the different evaporation or cooling operations produce similar remains. There are also large waste tip deposits of red calcined shale, and occasional excavated deposits of slam.

Whilst the above outline can be constructed from the historical sources, it is a composite account and, as such, cannot reflect variations in the process between different works and through time. There remain questions such as whether the optimum calcining temperatures were attained, and whether there were several steps within a stage, e.g. repeated evaporation of raw liquor and removal of slam. The efficiency of the extraction, both overall and in individual stages is also entirely unknown, although Young (1817; 814) states that between 50 and 130 tons of shale were required to produce 1 ton of alum, depending on the quality of both the shale and the calcining process.

## Geochemical studies at Carlton Banks Alum Works

Carlton Banks Alum Works, Carlton, North Yorkshire, (National Grid Reference NZ 520 027) was in operation *c.* 1680–1774 (Young 1817; 811), but little documentary evidence survives. The site consists of the abandoned quarry and waste tips on the hillside below its mouth. The first edition Ordnance Survey map indicates that there was an 'alum house' at the mouth of the quarry above the waste tips, which was presumably the location of alum processing. No detailed modern archaeological or historical study had been undertaken until recently when the North Yorkshire National Park commissioned a study from the Lancaster University Archaeological Unit ahead of reclamation and landscaping works. The waste tips of calcined shale were to be regraded to make them safer and, as part of mitigation works, samples were taken from an exposed section in an erosion gully.

The geochemical results presented here arise from an exploratory analysis of these samples and samples of fresh shale obtained from the abandoned quarry. The aim of the programme was to explore the potential for geochemical analysis of shale deposits to address questions relating to the industrial process of alum production. However the excavated samples proved limited and questions relating to temperature of firing, and changes in the process through time could not be tackled. The calcining of shale turns it bright red due to the oxidation of the iron compounds present and thus will result a very large increase in magnetic susceptibility. This allows samples of altered calcined shale to be distinguished from samples containing orange-red clays, which will not be so oxidized. This method for identifying deposits containing calcined shale was successful, and the chemical composition of fresh and calcined shales allows an initial evaluation of the efficiency of the extraction process.

Duplicate samples were taken from strata within the waste tip and fresh shale from three sites around the quarry. Elemental analysis by X-ray fluorescence was undertaken to examine extraction efficiencies; magnetic susceptibility was used to identify burning via iron mineral transformation.

## Methods

### *Magnetic susceptibility*

Samples were air dried and ground in a mortar to less than 2 mm particles. Low-frequency magnetic susceptibility and frequency dependence were determined as described by Clark (1996; 103–104) on samples of approximately 10 g using a Bartington MS2 magnetic susceptibility meter.

### *Energy dispersive X-ray fluorescence (EDXRF)*

Analysis for major and minor inorganic components was undertaken by energy dispersive X-ray fluorescence (EDXRF) on 0.5 g of dried, ground and pelletized sample. Quantitative analysis was undertaken for the elements Na, Mg, Al, Si, P, S, K, Ca, Ti, Mn, Fe and Sr, the results being calibrated using the United States Geological Survey Sco-1 shale standard.

## Results and discussion

### *Magnetic susceptibility*

High magnetic susceptibility values with high-frequency dependence are to be expected in calcined shale, due to the formation of maghaemite ($\gamma Fe_2O_3$) of small grain size during the calcination process, whilst the fresh shale is expected to show low values. This is borne out in the results (Table 1) where the fresh shale shows low values and the samples with a large proportion of visible red shale (CB97 3-A, J-A and J-B) show elevated values. Samples from layer K with less red shale show slightly elevated values. Other samples where burnt shale was not noted visually are shown to contain burnt material, or soil, by their magnetic susceptibility values (contexts 4, 5 and 13), some of which are elevated and show frequency dependence.

### *EDXRF*

In the elemental analyses, Si, Ca, Na, Mn and Sr were either not detected or showed very little variation: they are not reported or discussed here. Context 13 stands out from all the other samples in its composition, this is not surprising given its interpretation on-site as a buried soil rather than a shale deposit. The fresh shale samples show uniformity in their Al contents, but wide variation in their S contents. The waste tip samples overlap in their ranges of concentration with the fresh samples. Contexts 2 and K stand out as lower in Mg and Al and context 5 as lower in K and higher in Ti than the fresh shales. A reduction in Mg, Al and K and increase in Ti would be consistent with a leaching process, either natural or artificial. The wide variation in fresh shale composition precludes definite statements on the nature of this leaching, or whether other samples have been leached.

**Table 1.** *Results of analyses*

| Sample reference | Description | Magnetic susceptibility | | EDXRF results (%) | | | | | | |
|---|---|---|---|---|---|---|---|---|---|---|
| | | $\chi_{LF}/10^{-8}$ SI kg$^{-1}$ | % $\chi_{FD}$* | $Al_2O_3$ | MgO | $K_2O$ | $TiO_2$ | $P_2O_5$ | FeO | $SO_3$ |
| Unweathered shale 1 – A | Grey shale | 5.2 | ns | 22.7 | 1.26 | 3.83 | 1.16 | 0.17 | 4.01 | 0.89 |
| Unweathered shale 1 – B | Grey shale | 5.5 | ns | 22.0 | 1.23 | 3.86 | 1.12 | 0.15 | 4.75 | 0.74 |
| Unweathered shale 2 – A | Grey shale | 9.0 | 4.2 | 22.7 | 1.87 | 3.74 | 1.08 | 0.32 | 6.64 | 1.42 |
| Unweathered shale 2 – B | Grey shale | 9.8 | ns | 22.4 | 1.93 | 3.51 | 1.00 | 0.28 | 9.92 | 1.71 |
| Unweathered shale 3 – A | Grey shale | 6.7 | ns | 22.5 | 1.59 | 3.89 | 1.09 | 0.15 | 5.58 | 0.34 |
| Unweathered shale 3 – B | Grey shale | 5.0 | ns | 22.9 | 1.23 | 3.89 | 1.12 | 0.13 | 3.96 | 0.37 |
| CB97 1 – A | Grey shale in orange clay | 12.7 | 3.7 | 22.9 | 1.41 | 3.64 | 1.05 | 0.21 | 7.67 | 0.61 |
| CB97 1 – B | Grey shale in orange clay | 8.7 | ns | 23.0 | 1.20 | 3.55 | 1.08 | 0.23 | 8.11 | 0.43 |
| CB97 2 – A | Mostly yellow shale, small amount of orange clay and grey shale | 6.8 | ns | 20.1 | 0.92 | 3.40 | 0.97 | 0.19 | 9.52 | 0.78 |
| CB97 2 – B | Mostly grey shale, small amount of orange clay and yellow shale | 8.7 | ns | 20.3 | 1.01 | 3.48 | 1.00 | 0.17 | 10.50 | 0.91 |
| CB97 3 – A | Red shale in red/orange clay | 131 | 8.3 | 22.3 | 0.98 | 3.41 | 1.12 | 0.21 | 7.66 | 1.38 |
| CB97 4 – A | Small amount of grey shale in grey clay | 19.2 | 5.7 | 22.6 | 1.13 | 3.40 | 1.34 | 0.16 | 6.03 | 0.78 |
| CB97 4 – B | Small amount of grey shale in grey clay | 19.9 | 7.8 | | | | no data | | | |
| CB97 5 – A | Grey clay | 8.6 | ns | 21.7 | 1.31 | 3.20 | 1.37 | 0.15 | 5.76 | 0.57 |
| CB97 5 – B | Grey clay (lighter and slightly orange compared to 5A) | 12.1 | 4.7 | | | | no data | | | |
| CB97 13 – A | Very clayey loam (buried soil) | 18.4 | 5.7 | 18.3 | 0.00 | 3.11 | 0.98 | 0.21 | 12.05 | 0.59 |
| CB97 13 – B | Very clayey loam (buried soil) | 3.8 | ns | 18.7 | 1.00 | 3.27 | 1.07 | 0.35 | 3.66 | 0.53 |
| CB97 J – A | Red shale | 413 | 9.1 | 23.2 | 1.16 | 3.63 | 1.10 | 0.16 | 6.28 | 0.48 |
| CB97 J – B | Red shale | 58.1 | 6.3 | 22.9 | 1.10 | 3.64 | 1.10 | 0.21 | 7.38 | 0.50 |
| CB97 K – A | Orange clay with small pieces of yellow shale | 13.6 | 2.1 | 20.8 | 0.95 | 3.41 | 0.92 | 0.23 | 12.76 | 1.03 |
| CB97 K – B | Orange clay with small pieces of sandstone & pieces of grey and red shale | 11.9 | 2.8 | 20.8 | 0.92 | 3.50 | 0.94 | 0.24 | 11.73 | 0.80 |

* ns, not significant

The element of most interest, sulphur, shows more variation in the fresh shale than the waste shale, which means that definite conclusions on the efficiency of the process cannot be drawn. However, some useful deductions can still be made. The maximum sulphur content of the shale is 1.7% $SO_3$, which implies a maximum yield of potassium alum of 2.7% of the weight of shale used. This yield would reduce the alumina content of the shale by only 1.1%, which will be difficult to detect given an observed natural variation of 0.9%. The well calcined shale from context J, which has presumably been processed, has a $SO_3$ content of at least 0.48%, suggesting that a high yield may have only been 2.0% alum:shale. This matches closely the 1 ton of alum for 50 tons of calcined shale reported as a good yield by Young (1817; 814).

The low sulphur content of some shale here, at 0.34% $SO_3$, would give a yield of only 0.56% alum:shale. Such low yields may have meant that as certain parts of a quarry were worked productivity would have declined and the unit cost of production risen to a point where a works could become economically unviable. The price of alum is recorded as having fluctuated with production and various works went in and out of business as it did so (Young 1817; 816–817, Marshall 1995). Perhaps part of the fluctuation at individual works was due to variation in the quality of the alum shale.

It is also instructive to compare these analyses with those of Gad *et al.* (1969) on the coastal exposures of the alum shales. They report 1.55–2.55% S (i.e. 3.9 to 6.4% $SO_3$) which is much higher than at Carlton. Thus yields from the coastal works may well have been higher than at Carlton, hence the larger scale and more successful works on the coast.

## Conclusions

This work has shown that magnetic susceptibility can be a useful method of detecting burnt shale within a deposit, due to the high maghaemite content of calcined shale. However, elemental analysis of waste shale is not a particularly productive exercise, because there is unlikely ever to be a specific composition of fresh shale with which to compare it. Further understanding of the alum production process will require reconstructions of the various stages of production in order to generate reference materials against which excavated material can be compared. Excavated samples of waste calcined shale may be useful in investigation of the calcining process, but not for investigation of productivity. Slam and other impurities, especially if recovered from identifiable parts of the production process, are more likely to yield information. Samples collected from excavations targetted with the chemistry in mind will be the best way to gain greater insight into the methods of the Britain's first large-scale chemical industry.

I would like to thank Phil Clogg for conducting the EDXRF measurements, and Lancaster University Archaeological Unit who commissioned the analyses as part an archaeological evaluation of the Carlton Banks site funded by the North Yorkshire Moors National Park.

## References

CLARK, A. 1996. *Seeing Beneath the Soil: Prospecting Methods in Archaeology*. Batsford, London.

GAD, M. A., CATT, J. A. & LE RICHE, H. H. 1969. Geochemistry of the Whitbian (Upper Lias) sediments of the Yorkshire Coast. *Proceedings of the Yorkshire Geological Society,* **37,** 105–139.

MARSHALL, G. 1995. Redressing the balance - an archaeological evaluation of North Yorkshire's coastal alum industry. *Industrial Archaeology Review,* **18,** 39–62.

TAYLOR, F. S. & SINGER, C. 1956. Pre-scientific industrial chemistry. *In*: Singer, C., Holmyard, E. J., Hall, A. R. & Williams, T. (eds) *A History of Technology. II. The Mediterranean Civilizations and the Middle Ages c. 700 BC to c. AD 1500.* Oxford University Press, Oxford, 347–374.

TURTON, R. B. 1938. *The Alum Farm.* Horne & Son, Whitby.

YOUNG, G. 1817. *A History of Whitby and Streoneshalh Abbey; with a statistical survey of the vicinity to the distance of twenty five miles.* Clark and Medd, Whitby.

# Zinc isotope fractionation in liquid brass (Cu–Zn) alloy: potential environmental and archaeological applications

PAUL BUDD[1], PAUL LYTHGOE[2], RONA A. R. MCGILL[1], A. MARK POLLARD[1] & BRETT SCAIFE[1,3]

[1]*Department of Archaeological Sciences, University of Bradford, Bradford BD7 1DP, UK*

[2]*Department of Earth Sciences, The University of Manchester, Oxford Road, Manchester M13 9PL, UK*

[3]*Present address: Sub-Unit for Medical Statistics, Nuffield Institute, University of Leeds, Leeds LS2 9LN, UK*

**Abstract:** A preliminary study of zinc isotope fractionation in brass melting suggests that the process can be modelled by simple Rayleigh fractionation. Brass melting experiments at 1100°C followed by quadrupole ICP-MS isotope ratio measurements of the resulting alloys suggest that the model is appropriate and that a useful approximation of the fractionation factor ($\alpha$) is 1.0064. The data indicate that the change in isotope ratio of the residual liquid alloy would be measurable for zinc losses by evaporation of more than about 30 wt.%. It is unlikely that measurements at the precision of the current study ($\sim$0.55‰ amu$^{-1}$) would be sufficient to distinguish between the two principal historical brass-making processes, although more precise measurement using a multi-collector ICP-MS probably would be. The experimental data also suggest that zinc vapour evolving during the evaporation of the first few per cent of the metal will be significantly fractionated ($\sim$1.5‰ amu$^{-1}$) with respect to the liquid. This might provide a basis to distinguish between environmental zinc from high-temperature industrial processes and that derived from natural and manufactured product sources.

The current study was undertaken in order to examine the hypothesis that measurable isotopic fractionation would take place during the evaporation of zinc from liquid brass (Cu–Zn) alloys at elevated temperatures. If the magnitude of fractionation was sufficient to measurably alter the isotopic composition of the residual liquid, it could also be possible to use zinc isotope ratio measurements to distinguish the products of the two principal brass-making processes used in antiquity. Additionally, if established, such fractionation might provide a basis for discriminating between environmental zinc emitted by evaporation during various high-temperature processes and that originating from manufactured zinc products or natural mineral sources.

As the boiling point of zinc is only 906°C the metal cannot be produced simply by direct reduction without distillation. The first appearance of brass, however, in the Anatolian and Mediterranean Iron Age, results not from the development of zinc distillation, but from the discovery that copper-zinc alloys could be produced by

*From:* POLLARD, A. M. (ed.) 1999. *Geoarchaeology: exploration, environments, resources.* Geological Society, London, Special Publications, **165,** 147–153. 1-86239-053-3/99/$15.00

'cementation' (Pollard & Heron 1996, 201). The cementation process involves the preparation of ZnO which is placed in a sealed vessel with charcoal and granular copper and heated to ~1000°C. At this temperature, and in the highly reducing conditions produced by the burning charcoal, zinc vapour is produced which diffuses into the solid copper to form the brass alloy.

The cementation process is thought to have dominated European brass production until the eighteenth century when zinc distillation was introduced. This allowed brass to be made by the 'direct' process, in which metallic zinc is added to liquid copper. The maximum zinc content of brass alloys produced by cementation is kinetically constrained to ~31–33 wt.% (Werner 1970; Haedecke 1973). However, the high zinc content of some later medieval brasses suggests that zinc distillation and direct alloying may have a considerably longer history in Europe than previously thought (Pollard & Heron 1996, 205–232). As most medieval brasses have zinc contents of less than 31 wt.%, an independent method with which to assess their production process would be a useful aid in charting the introduction of zinc distillation and possibly also in the authentication of early brass artefacts.

If isotopic fractionation during evaporation were to prove significant, and greater than any natural variation between ore sources, it might be possible to use zinc isotope measurements to distinguish between the two brass making processes. Cementation is a gas-solid reaction in a sealed vessel allowing little scope for zinc evaporation and escape of the vapour. By contrast, direct production methods, especially the addition of volatile metallic zinc to liquid copper, are processes likely to result in considerable zinc evaporation with scope for a consequent enrichment of the heavier zinc isotopes in the residual liquid.

The paper sets out a theoretical model for zinc fractionation during evaporation. This is compared with experimental data to derive a fractionation factor for the particular process under consideration: brass melting at 1100°C. Although empirical and semi-quantitative, the resulting estimate of fractionation may be used to comment on the potential for zinc isotope measurement to be used in pollution source tracing and process reconstruction.

## Modelling zinc isotope fractionation during evaporation

The fractionation of zinc as a result of its evaporation from liquid metal at elevated temperature arises from the slight difference in vapour pressure between its isotopes. This ensures that, in equilibrium, the vapour will be marginally enriched in the lighter isotopes with respect to the liquid. In various industrial and metallurgical processes involving the manipulation of zinc at high temperature, vapour may be lost from the liquid to condense elsewhere. If vapour is progressively lost in this way there will be a systematic change in the isotopic composition of the residual liquid and, correspondingly, of the evolving vapour.

The zinc isotope composition of the remaining liquid after a proportion of it has evaporated can be modelled on the basis of the kinetic theory of 'Rayleigh fractionation'. This will be familiar to geochemists in the context of meteorological oxygen isotope fractionation (Faure 1986, 430–436) but has also recently been applied to the evaporation of metals such as lead (Budd *et al.* 1995*a*, Macfarlane in press) and tin (Budd *et al.* 1995*b*, Begemann *et al.* in press). According to this model, the change in zinc isotope ratio in a liquid from which the metal is being lost as vapour can be

estimated as:

$$R_{l_f} = R_{l_0} f^{[(1/\alpha)-1]} \tag{1}$$

where $R_{l_f}$ is the $^{68}Zn/^{64}Zn$ ratio of the residual liquid, $R_{l_0}$ is the $^{68}Zn/^{64}Zn$ ratio of the initial liquid, $f$ is the proportion of liquid remaining and $\alpha$ is the fractionation factor. A related expression gives the isotopic composition of the vapour evaporating at the same stage ($R_{v_f}$):

$$R_{v_f} = \frac{R_{l_0} f^{[(1/\alpha)-1]}}{\alpha}. \tag{2}$$

Although the model is essentially very simple there are a number of complicating factors. Most importantly, the fractionation factor ($\alpha$) for zinc in relation to particular processes cannot easily be determined. A *maximum* value for the fractionation factor can be derived from kinetic theory as the square root of the ratio of the masses of the isotopes of interest, so that:

$$\alpha < (M_2/M_1)^{1/2}. \tag{3}$$

For $^{68}Zn/^{64}Zn$ this gives a value of $\alpha < 1.0308$, but it is probably more realistic to consider the evaporation of ZnO rather than Zn, making $\alpha < 1.0247$.

In practice, for the process under consideration here, the value of $\alpha$ is likely to be significantly lower than this. The theory assumes instantaneous equilibrium, complete mixing within the liquid and entirely efficient separation of the vapour. In practice, equilibrium is not instantaneous. Incomplete mixing within the liquid, vapour–gas molecular collisions and re-condensation of the vapour can all reduce the efficiency of fractionation. Furthermore, the theory deals with evaporation from a pure element rather than an alloy. Although copper has a very much lower vapour pressure than zinc, the presence of copper molecules in both liquid and vapour would be expected to reduce the fractionation factor.

The value of $\alpha$ is therefore process-dependent, relating to factors such as temperature, pressure and the efficiency of vapour removal and hence can only be accurately determined empirically. An experiment was therefore undertaken to measure the magnitude of isotopic fractionation during brass melting at 1100°C. This has been used to make an estimate of $\alpha$ which, it is suggested, may be a useful first-order approximation for a number of similar processes.

## Experimental methodology

The experiment involved zinc evaporation from brass in the manner expected during the direct process of brass making and subsequent handling of the liquid alloy at high temperature. A small quantity of a homogenous pure brass standard (BNF C30.05; 29.99% Zn) was heated to 1100°C in a muffle furnace, under excess charcoal for variable periods between 5 to 30 minutes (Table 1). Zinc evaporation from the liquid alloy was monitored by weight loss on cooling. This was found to give a useful approximation for the loss of zinc as vapour as the vapour pressure of copper is insignificant at this temperature. Eight samples with zinc weight losses of between approximately 20 and 80% were selected for zinc isotope analysis by ICP-MS.

**Table 1.** *Change in zinc isotope composition of the residual brass for various losses of zinc by evaporation at 1100°C*

| Sample | Heating time (mins) | Zn loss wt.% | Measured $^{68}Zn/^{64}Zn$ | $\delta^{68}Zn$ ‰ amu$^{-1}$ | Error (2 SE) | $\alpha$ |
|---|---|---|---|---|---|---|
| Standard | 0 | 0.00 | 0.4114 | 0 | 0.55 | |
| 1100–19 | 5 | 19.38 | 0.4117 | 0.18 | 0.61 | 1.0034 |
| 1100–20 | 10 | 20.03 | 0.4117 | 0.19 | 0.58 | 1.0033 |
| 1100–33.6 | 10 | 33.60 | 0.4116 | 0.15 | 0.34 | 1.0012 |
| 1100–38.1 | 12 | 38.15 | 0.4120 | 0.35 | 0.86 | 1.0030 |
| 1100–51 | 15 | 50.95 | 0.4131 | 1.03 | 0.44 | 1.0058 |
| 1100–61.6 | 18 | 61.60 | 0.4137 | 1.39 | 0.92 | 1.0059 |
| 1100–69.7 | 23 | 69.77 | 0.4151 | 2.18 | 0.60 | 1.0075 |
| 1100–76.5 | 30 | 76.52 | 0.4153 | 2.36 | 0.40 | 1.0066 |

Measured $^{68}Zn/^{64}Zn$ ratios are tabulated together with the fractionation presented as $\delta^{68}Zn$ (in units ‰ amu$^{-1}$). Errors (2 SE) are calculated from the six replicate analyses for each sample (12 for the standard). The table also shows calculated values of the fractionation factor ($\alpha$) for each of the samples.

## *Sample preparation*

Samples of each alloy and the brass standard were collected to give a total Zn content of ~2 mg. The samples were dissolved in dilute aqua regia (all *Romil Ultrapure* acids), dried down and then re-eluted with 2M HCl to form a 2 mg (Zn) ml$^{-1}$ Cu–Zn solution. The samples were then treated to separate the zinc from the copper in order to eliminate potential isobaric interferences from $^{63}Cu$ and $^{65}Cu$. Separation of the two metals was carried out by ion exchange chromatography. *Poly-Prep* 2 ml columns were filled with 2 g of *Bio-Rad* AG1-X8 ion exchange resin (chloride form, 200–400 mesh). The resin was then washed with alternate column volumes of water and 2M HCl. The sample solution (1 ml) was then loaded on each column. Copper was eluted from the column by 15 column volumes of 2M HCl. Zinc is most strongly adsorbed on the resin with this concentration of acid, but copper (and many other divalent transition metals e.g. Ni and Fe) are not (Kraus & Moore 1953; Friel *et al.* 1996). Zinc was then eluted by 10 column volumes of 0.05M HCl. Final solutions contained approximately 0.1 mg ml$^{-1}$ of zinc (100 ppm) with no significant copper. Column performance was monitored by ICP-AES.

## *ICP-MS zinc isotope analyses*

Sample solutions were diluted to 50 ppb zinc in 2% $HNO_3$, minimizing $Cl_2$ isobaric interference from use of HCl, and bringing sample concentration into the optimum range for isotope ratio ICP-MS. All stable isotopes of zinc were measured, but results are given as the $^{68}Zn/^{64}Zn$ ratio maximizing mass difference and minimizing analytical error. $^{65}Cu$ was monitored in case of isobaric interference. Measurements were made using a VG Elemental PQ2+ ICP-MS at the Department of Earth Sciences, University of Manchester. The instrument was operated in rapid peak jumping mode (dwell time 10.24 ms, and 3 points per peak), sample uptake time was 115 seconds (acquisition time 60 seconds) with a 120 seconds wash of 2% $HNO_3$ (*Primar*) between samples. Six replicate measurements were made for each sample. No mass discrimination correction was applied and measured ratios were not normalized as no accepted value $^{68}Zn/^{64}Zn$ standards were available. Measured ratios were used directly in the

calculation of $\delta^{68}$Zn. Instrument drift was monitored by six replicate measurements of the standard at the end of the analytical run. No drift was observed.

## Experimental results

The results of the zinc isotope analyses are given in Table 1. Fractionation, expressed as $\delta^{68}$Zn, in the residual liquid brass may be calculated (in units ‰ amu$^{-1}$) as:

$$\delta^{68}\mathrm{Zn} = \frac{1}{(68-64)} \times \left( \frac{R_{l_f} - R_{l_0}}{R_{l_0}} \right) \times 10^3. \tag{4}$$

The relationship between $\delta^{68}$Zn and zinc weight loss is plotted in Fig. 1. The measurements showed variations between 0.18 and 2.36‰ amu$^{-1}$ with respect to the brass standard ($R_{l_0}$). The variation appears systematic, but is clearly close to the resolution of the quadrupole instrument. The errors (all reported here as 2 SE) are relatively large, ranging from 0.34 to 0.92 amu$^{-1}$ . Only the final two samples (1100–69.8–Zn and 1100–76.5–Zn) with values of $2.18 \pm 0.60$‰ amu$^{-1}$ and $2.36 \pm 0.40$‰ amu$^{-1}$ appear to be significantly fractionated from the brass standard (itself measured with a precision of ±0.55‰ amu$^{-1}$).

## Estimate of the fractionation factor in brass melting

Experimental values for the isotopic composition of the residual liquid may be used to calculate the fractionation factor ($\alpha$). Rearranging equation 1 gives:

$$\alpha = \ln f \Big/ \ln \left( \frac{R_{l_f}}{R_{l_0}} f \right). \tag{5}$$

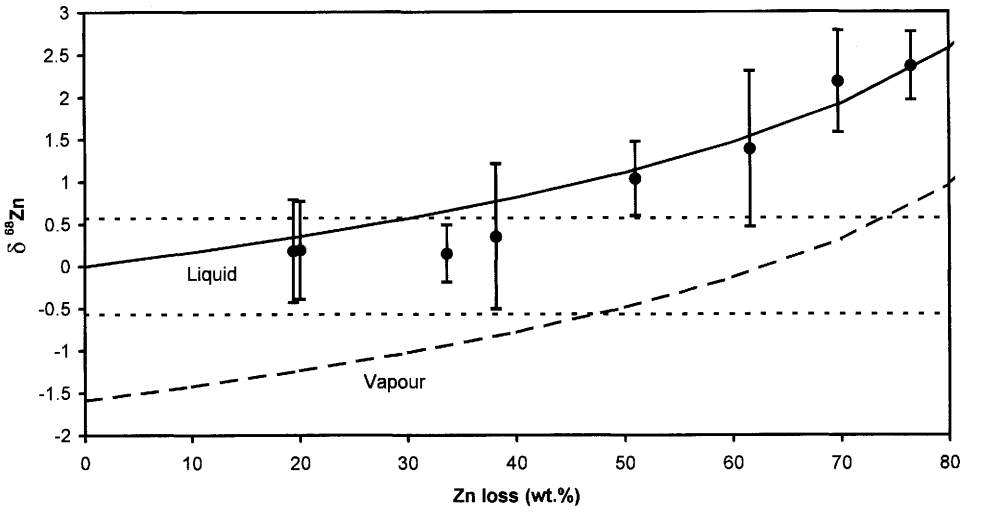


**Fig. 1.** The variation in zinc isotope fractionation (expressed as $\delta^{68}$Zn) with respect to the brass standard with zinc loss by evaporation from brass at 1100°C. Experimental brass samples are plotted with 2 SE measurement errors ($n = 6$). Short dashed lines represent the 2 SE measurement errors on the brass standard ($n = 12$). The solid black line represents the theoretical fractionation within the residual liquid according to the Rayleigh model with $\alpha = 1.0064$. Similarly, the dashed line represents the theoretical fractionation of the evolving vapour.

Values of $\alpha$ for each of the experimental samples are given in Table 1. Although all of the calculated values of $\alpha$ are estimates applicable to the brass melting process, the accuracy of those relating to relatively small zinc losses, where expected variations are likely to be lower than the measurement errors, are the least reliable. This is reflected in the data. The calculated values of $\alpha$ for those samples within measurement error of the standard are considerably more variable than those relating to zinc losses over ~50%. The mean of calculated values of $\alpha$ for the four samples with zinc losses over 50% is 1.0064 ($\sigma = 0.0008$) and this is considered the best estimate for the fractionation factor relating to brass melting at 1100°C.

Using equation (1) it is possible to calculate $\delta^{68}$Zn for the residual liquid using this estimate of the fractionation factor to give an approximation of the isotopic fractionation for any proportion of zinc loss (Fig. 1). This curve intersects the 2 SE error on the measurement of the brass standard at ~30% Zn loss, providing a rough estimate of the evaporation required to produce a measurable shift in the isotope ratio of the residual liquid using the quadrupole ICP-MS method. Similarly, equation (2) may be used to estimate the isotopic composition of the vapour (Fig. 1). This suggests that the initial vapour emitted will be fractionated by approximately $-1.5$‰ amu$^{-1}$ ($\delta^{68}$Zn) with respect to the liquid, approximately three times the 2 SE error on the measurement of the brass standard.

## Discussion

The data suggest that zinc has a large enough relative mass difference between its stable isotopes ($^{68}$Zn and $^{64}$Zn) and is sufficiently volatile to undergo isotopic fractionation during evaporation, even from a zinc-bearing copper alloy. It is suggested that the process can be usefully modelled by simple Rayleigh fractionation equations. Brass melting experiments, carried out under controlled conditions at 1100°C, have produced a series of samples for zinc isotope ratio analysis to test this hypothesis and to estimate the approximate value of the fractionation factor ($\alpha$). The results suggest that the Rayleigh model is appropriate and that a useful, although only approximate, estimate of $\alpha$ is 1.0064. It appears likely that similar values of $\alpha$ may apply to a wider range of industrial processes involving zinc evaporation from the liquid metal, or its alloys, at elevated temperatures.

The precision of the isotope ratio measurement technique (quadrupole ICP-MS) used in this preliminary study is relatively poor (~0.55‰ amu$^{-1}$, 2 SE). However, the data suggest that the change in isotope ratio of the residual liquid alloy would be measurable for zinc losses by evaporation of more than about 30 wt.%. Zinc losses in modern direct process brass making are only ~5% (Alexander & Street 1976, 61), but were probably very much higher in antiquity – for example, Chinese 17th Century texts document losses of 25% (Pollard & Heron 1996, 204). It seems unlikely that measurements at the precision of the current study would be sufficient to distinguish between cementation and directly produced brass given the range of losses (5–25%) that might be expected in the latter. However, higher precision stable isotope ratio measurement is possible using the magnetic sector, multi-collector technique. It seems likely that multi-collector measurement could be used for this application.

Perhaps the most significant prediction to arise from the investigation is the suggestion that the zinc vapour evolving during the evaporation of the first few percent of

the metal will be significantly fractionated ($\sim$1.5‰ amu$^{-1}$) with respect to the liquid. Although little information is currently available on the extent of natural zinc isotope variation, it is possible that this might provide a basis to distinguish between environmental zinc emitted as vapour during high-temperature industrial processes and that derived from natural sources and manufactured products.

This work was carried out as part of a NERC Research Grant (GR3/10057). One of the authors (PDB) wishes to acknowledge the support given by a NERC Advanced Fellowship.

## References

ALEXANDER, W. & STREET, A. 1976. *Metals in the Service of Man*. 6th Edn. Penguin, Harmondsworth.

BEGEMANN, F., KALLAS, K., SCHMITT-STRECKER, S. & PERNICKA, E. In press. Tracing ancient tin via isotope analysis. *In:* HAUPTMANN, A. & PERNICKA, E. (eds) *Proceedings of the International Symposium on the Beginnings of Metallurgy*, Bochum, April 1995.

BUDD, P., POLLARD, A. M., SCAIFE, B. & THOMAS, R. G. 1995*a*. The possible fractionation of lead isotopes in ancient metallurgical processes. *Archaeometry*, **37**, 143–150.

——, HAGGERTY, R., POLLARD, A. M., SCAIFE, B. & THOMAS, R. G. 1995*b*. New heavy isotope studies in archaeology. *Israel Journal of Chemistry*, **35**, 125–130.

FAURE, G. 1986. *Principles of Isotope Geology*. 2nd Edn. Wiley, New York.

FRIEL, J. K., ANDREWS, W. L., SIMMONS, B. S., MILLER, L. V. & LONGERICH, H. P. 1996. Zinc absorption in premature infants: comparison of two isotopic methods. *American Journal of Clinical Nutrition*, **63**, 342–347.

HAEDECKE, K. 1973. Gleichgewichtsverhältnisse bei der messingherstellung nach dem Glameiverfahren. *Erzmetall*, **26**, 229–233.

KRAUS, K. A. & MOORE, G. E. 1953. Anion exchange studies. VI. The divalent transition elements, manganese to zinc, in hydrochloric acid. *Journal of the American Chemical Society*, **75**, 1460–1462.

MACFARLANE, A. In press. The lead isotope method for tracing the sources of metal in archaeological artifacts: strengths, weaknesses and applications in the Western Hemisphere. *In:* YOUNG, S. M. M., BUDD, P. D., IXER, R. A. & POLLARD, A. M. (eds) *Metals in Antiquity*. Proceedings of the International Symposium, Harvard University, 10–13 September 1997. Archaeopress, Oxford.

POLLARD, A. M. & HERON, C. 1996. *Archaeological Chemistry*. Royal Society of Chemistry, Cambridge.

WERNER, O. 1970. Analysen Mittlealterlicher bronzen und messinge II und II. *Archäologie und Naturwissenschaften*, **2**, 106–170.

# The determination of bloomery furnace mass balance and efficiency

GARY R. THOMAS & TIMOTHY P. YOUNG[1]
*Department of Earth Sciences, Cardiff University, PO Box 914, Cardiff CF1 3YE, UK*
[1]*Current address: GeoArch, 54 Heol-y-Cadno, Thornhill, Cardiff CF14 9DY, UK*

**Abstract:** A technique for the graphical solution of the ore:furnace lining:fuel ash mixture in the melt and the yield of the reaction during bloomery iron smelting is presented. The technique focuses on the so-called immobile elements, particularly the rare earth elements, but employs a wide range of elements. Previous attempts to determine ore sources from iron slag chemistry have generally examined the major and minor elements of the slags, but are complicated both by the significant, but variable, concentrations of some of these elements in charcoal and by the mobility of some major elements during weathering. The new approach has been developed to aid the provenancing of slags from the smelting of iron-ores from the Bristol Channel Orefield, which is characterized by high purity goethite/haematite ores with extremely low trace element concentrations. It is thus particularly important to understand the involvement of furnace lining in the melt, for this material will have the dominant contribution to the trace element chemistry. The mass balance approach is illustrated using smelting slags, furnace lining and roasted ore fragments from the Roman iron making town of *Ariconium* (near Ross-on-Wye, Herefordshire) and a good degree of compatibility of these materials is demonstrated.

Modern analytical techniques such as thermal ionization mass spectrometry (TIMS) and inductively coupled plasma-mass spectrometry (ICP-MS) offer not only the ability to analyse rapidly for a larger range of elements (Young *et al.* 1997), but also to a greater degree of precision than previously. However, workers investigating the components of ancient iron smelting still place great reliance upon a small number of elements, and most attempts to solve furnace mass-balance equations (e.g. Serneels 1993) have employed the smallest number of simultaneous equations possible for a solution.

Tylecote (1986) noted that the silica content of a slag can be elevated by the assimilation of furnace lining. Likewise Fulford & Allen (1993) suggested that much of the non-ferrous material present in Roman slags from the smelting of Forest of Dean ores at Woolaston (in the northeast of the Bristol Channel Orefield) would have originated from the furnace lining and not from the ore. Serneels (1993) has, amongst others, discussed techniques of assessing the contribution of the furnace lining to the slag and described such a contribution as 'contamination'. However, it is clear from the work of Fulford & Allen (1993) as well as the authors' unpublished data, that the contribution from the lining in the Bristol Channel Orefield slags is extremely high.

The approach adopted in this study is to examine the ore: furnace lining mixing using as many elements as possible. A graphical technique allows easy inspection

*From:* POLLARD, A. M. (ed.) 1999. *Geoarchaeology: exploration, environments, resources.* Geological Society, London, Special Publications, **165,** 155–164. 1-86239-053-3/99/$15.00

for 'goodness of fit' of any particular ore–lining–fuel ash system. This technique can be employed, as it is here, to assess whether ore samples are compatible with the slags generated from a furnace made of a particular material, or to model the ore composition capable of generating a particular slag in a furnace built of a given material. The basic idea of the graphical approach was introduced by Thomas & Young (forthcoming), in which we considered a simple ore-lining mixture without influence from charcoal ash. One component of this contribution is to justify this simplification for the smelting of the high purity Bristol Channel ores. However, it should be emphasized that the smelting of other ores, or the utilization of other furnace types, may involve a much greater degree of incorporation of the fuel ash than observed here.

The provenance of ore fragments located at archaeological sites within the UK tends to rely heavily upon a proximity to a local ore source, (e.g. Ruddock 1961) as, unlike copper, the widespread availability of iron ore was thought to make long distance transport unlikely (Salter 1987). There exists a great variability in the major element chemistry of iron ore bodies (Salter 1987). However, the greatest obstacle to provenancing ore material is the lack of good geological and geochemical data on UK iron sources, particularly the bog ores, because of their current economic unimportance.

Slags are readily abundant at smelting sites, and although the remains of furnaces are rare, small quantities of lining can frequently be found attached to slag samples. Charcoal samples, if not forthcoming from excavations, can be produced from wood samples collected from the modern-day site, as the bulky nature of charcoal suggests that transportation would be limited. Fragments of iron ore from smelting sites are rare and when they do occur they should not automatically be assumed to represent the material actually smelted, as these could equally represent material discarded as unsuitable for smelting.

In this study 21 slag samples consisting of both tap and furnace slags (total weight 5 kg) along with 3 lining samples (0.4 kg) and 2 ore fragments (52 g) were obtained from 220 kg of material excavated by the Hereford and Worcester County Council Archaeology Service during their 1993 excavation at the major Roman iron working site of *Ariconium*. These were subjected to geochemical analysis using X-ray fluorescence of fused beads (major elements) and powdered pellets (minor and trace elements) along with Inductively Coupled Plasma–Mass Spectrometry of solutions (minor and trace elements).

## Geological background

The iron ores of the Bristol Channel Orefield generally occur within cavernous porosity in the Carboniferous Limestone, close to the post-Variscan unconformity. Towards the south of the region, in the Bristol and Mendip areas, the ores are found within the Triassic 'Dolomitic Conglomerate'. The largest orebodies occur in the Forest of Dean and Glamorgan, and are hosted by karstic features of probable Triassic age (Simms 1990). The age of the mineralization is poorly constrained, but is probably Triassic to early Jurassic, although it is possible that some of the quartz-rich iron mineralization in the Vale of Glamorgan may be slightly older. The ores are dominated by the anhydrous iron oxide, haematite and the hydrated oxide, goethite, these being characterized by their high levels of purity (goethite + haematite typically in excess of 97%). It is the low detrital content of the ores from

the Bristol Channel region that results in them possessing a relatively low total REE (ΣREE) value, typically <40 ppm.

There has been a long tradition of iron mining within the Bristol Channel Orefield from the pre-Roman Iron Age to relatively recently; the last mine in Glamorgan, at Llanharry, closed in 1978. The Forest of Dean was, in particular, a major centre for iron production in Roman and Medieval times, with a reduced importance during the industrial period.

## Mass balance of smelting components

It is possible to construct a mass balance description of the reaction in the bloomery furnace. For each element the input to the reaction must be equal to the output. Some of these values will be relatively easy to measure (e.g. elemental composition of the ore, furnace lining and charcoal), others may be more difficult (e.g. elemental composition of the gas and ash particles lost through the top of the furnace to the atmosphere). If, however a few basic criteria are met, then the mass balance equations become manageable:

- For all elements involved in the analysis, the system must be closed (i.e. there must be no additional sources or losses). This means that the elements must not be lost from the system via routes such a volatilization, or incorporation in the metallic iron phase of the bloom.
- Incorporation of fuel ash and lining is assumed to be complete; no partial melting of these phases to generate the slag may occur.
- The slag composition in the calculation is the overall composition of the entire slag production of the smelt. Slags produced in smelting may be extremely heterogeneous. Only when a process is producing relatively large volumes of slag (and therefore usually with that slag being tapped) will individual slag samples be likely to approach the mean composition of slag for the smelt. Alternatively, the slag values used can be averaged from the range of slag types generated at the furnace.

A graphical technique can be used to solve simultaneously the mass balance equations for each element. The concentration of species N in phase P is expressed as $c_N^P$, and in our calculations is measured by weight% for major element oxides and ppm element for traces. All components are recalculated to be an anhydrous composition with all iron expressed as FeO. As iron is removed from the system the remaining elements respectively increase in concentration, thus the degree of enrichment ($E$) for any element N, other than iron, brought about by the removal of iron to produce the concentration observed in the slag can be calculated as:

$$E = c_N^{slag}/[(c_N^{ore}x) + (c_N^{lining}y) + (c_N^{fuel\ ash}z)]$$

where $x$, $y$ and $z$ are the proportions of ore, lining and fuel ash by weight incorporated into the melt and where $x + y + z = 1$.

The iron concentration in the slag is related to the components by the following equation:

Total concentration of FeO in the system (F):

$$F = (c_{FeO}^{ore}x) + (c_{FeO}^{lining}y) + (c_{FeO}^{fuel\ ash}z).$$

Proportion of system removed for bloom formation (expressed as FeO) = $B$

$$E = 1/(1 - B)$$
$$\Rightarrow B = 1 - (1/E).$$

The iron concentration in the slag will be:

$$c_{\mathrm{Fe}}^{\mathrm{slag}} = E(F - B)$$
$$\Rightarrow c_{\mathrm{Fe}}^{\mathrm{slag}} = E[F - (1 - 1/E)]$$
$$\Rightarrow E = (c_{\mathrm{Fe}}^{\mathrm{slag}} - 1)/(F - 1)$$
$$\Rightarrow E = (c_{\mathrm{Fe}}^{\mathrm{slag}} - 1)/[(c_{\mathrm{Fe}}^{\mathrm{ore}} x) + (c_{\mathrm{Fe}}^{\mathrm{lining}} y) + (c_{\mathrm{Fe}}^{\mathrm{fuel\ ash}} z) - 1].$$

Values of $E$ are calculated at 0.02 intervals for the ore:lining mixture ranging from 0 (lining + fuel ash only) to $1 - z$ (ore + fuel ash only) for particular values of the fuel ash component, $z$. The results of this are then plotted so that each element is represented by a line of ore-lining-fuel ash/enrichment factor solutions. If a perfect match between ore, charcoal, furnace lining and slag occurs then the respective lines will show a common intersection. Such a case will represent the situation where all elements in a slag can be produced at the appropriate concentrations from a single melt combination of ore, ash and lining by the single degree of enrichment ($E$). For such a solution to be possible all the various criteria expressed above must have been met.

In practice the graphical solution is rarely perfect, and a combination of the above criteria may not have been met. However, the greatest problem is the inhomogeneity of natural materials and the unlikelihood that it will be possible to sample ore, slag and lining that were actually involved in a particular smelt, rather than just being typical of the materials passing through the bloomery.

If the elemental lines demonstrate a close grouping of intersections, then a 'best-fit' solution to the smelting mass balance can be placed by eye. The mix and enrichment values obtained from the diagram can then be used to investigate the yield and efficiency of the process.

The proportion of the melt that will be removed as a bloom ($B$) will be represented by:

$$B = (1 - 1/E)$$

Thus 1 kg of reduced anhydrous ore will require $y/x$ kg of furnace lining ($L$) and $z/x$ kg of fuel ash ($A$) to give a yield (bloom), expressed as kg FeO ($I$), of:

$$(1 + L + A)M$$

equivalent to metallic iron yield, in kg, of:

$$I \times (\text{Atomic weight Fe/Molecular weight FeO}) = I \times 56/72$$

and produce

$$1 + L + A - I \text{ kg of slag } (S).$$

The concentration of iron in the bloom can then be compared to that of the ore to give an overall indication of the efficiency of the smelting process.

$$\text{Efficiency} = \text{weight of iron in bloom/weight of iron in ore.}$$

Since the oxidation and hydration state of the ore feed is rarely known, this can be standarized to:

$$\text{Efficiency}' = I \times (56/72)/\text{Fe}_{\text{ore}}$$

where $\text{Fe}_{\text{ore}}$ is the weight of iron in a quantity of ore, which would be equivalent to 1 kg of anhydrous material in which all iron is present as $\text{Fe}^{\text{II}}$ (i.e. core FeO, see p. 157).

For the Bristol Channel Orefield goethite ores being smelted at Ariconium, as an example, 1 kg of anhydrous reduced ore is equivalent to 1.25 kg of goethite or 1.1 kg of haematite. Therefore, the expression:

$$\text{Efficiency}' = I(56/72)/c^{\text{ore}}_{\text{FeO}}$$

will overestimate the true efficiency by about 20% if the material fed to the furnace was goethite and by about 10% if the feed was haematite. In practice the precise oxidation and hydration state of the ore entering the furnace is unlikely to be able to be determined with a high degree of certainty, unless positive evidence for ore roasting is found.

The consistency of the model gained from the mass balance approach with respect to any particular component can be investigated by comparing the values generated with those observed in the actual specimens. Thus, one might check that the model is satisfactorily close in predicting the concentration of key components (such as FeO and ΣREE), and has not been too biased towards elements of a lesser significance.

## Example: *Ariconium*

Recent excavations at the Romano-British iron working site of *Ariconium* have yielded a large quantity of slag, but also samples of furnace lining and two ore fragments: three of the four components required for a mass balance approach to furnace operation. The fourth component, charcoal ash, has been derived by producing charcoal in the laboratory furnace from wood taken at various points within the study area. Major element chemical data for each of the smelting components are presented in Table 1.

The best-fit solution to the mass-balance graphs has been judged by eye. The proportion of fuel ash involved is very small, and its value is largely driven by the need to balance the calcium and magnesium lines. The fit of these lines is poor, as are those of some of the other 'major' elements. The calcium and magnesium lines are strongly influenced by the fuel ash composition, which has been found to be rather variable. Attempts to produce mass balance solutions for varying fuel ash proportions demonstrate that only a small range of values allow a reasonably close approach to a common intersection between calcium, magnesium and the other major elements. A fuel ash contribution of 1.8% (Fig. 1), produces the closest fit for these lines, so that value has been used for the graphs on which the fit for $E$ and for the ore contribution has been based. Phosphorus and manganese solutions are poor; in both cases the lines are lower than the expected fit position, indicating that the elements are too rich in the mixture to allow for the observed slag composition. The likely

**Table 1.** *Major element compositions of smelting components normalized for the purpose of the model*

| | Sample number | $SiO_2$ | $Al_2O_3$ | FeO | MnO | MgO | CaO | $Na_2O$ | $K_2O$ | $TiO_2$ | $P_2O_5$ |
|---|---|---|---|---|---|---|---|---|---|---|---|
| Slag | Average tap slag | 21.83 | 4.40 | 67.09 | 0.17 | 1.20 | 2.72 | 0.50 | 1.50 | 0.23 | 0.36 |
| Lining | A13 | 77.00 | 12.25 | 5.96 | 0.09 | 0.84 | 0.53 | 0.00 | 2.62 | 0.47 | 0.23 |
| Ore | A26 | 2.06 | 1.17 | 95.34 | 0.49 | 0.34 | 0.22 | 0.00 | 0.12 | 0.05 | 0.22 |
| Fuel ash | A29 | 5.39 | 1.09 | 0.69 | 0.16 | 7.07 | 69.63 | 3.26 | 7.40 | 0.04 | 5.25 |

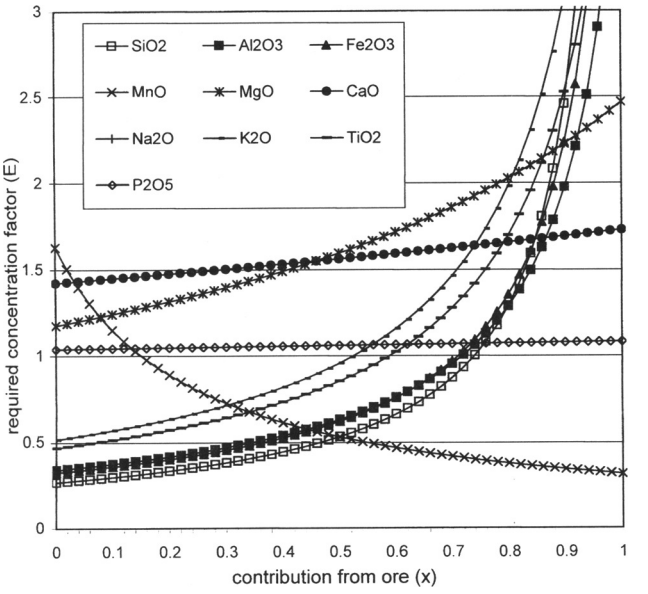


**Fig. 1.** Required concentration factor ($E$) against proportion of contribution from the ore ($x$) for mass balance calculation for major elements of material from *Ariconum*. Ore, sample A26; lining, sample A13; slag, average of tap slags from site; fuel ash, sample A29 (charcoal produced from oak wood growing near site). Model assumes fuel ash concentration of 0.018 (i.e. 1.8% of total mix).

solution to this is that both are present in the metallic iron phase, and not just the slag. The likely fit position lies between $E = 1.3$ (80% ore contribution and $E = 2.2$ (90% ore contribution).

The trace element graph (Fig. 2) shows a wide spread of solutions, mostly incompatible with a sensible solution. The elements appearing too low on the diagram include Pb, Cu, Mo and Cr. The Pb and Cu are likely to have been lost through volatilization, whilst Mo and Cr may be in the metallic iron. The elements with lines which are too high (i.e. indicating they are more abundant in the slag than the raw materials should permit) include Be, Zn, Ba, V, Zr. The fuel ash composition may be a strong influence on the Ba content, and may be strongly locally variable. The cause of variation in the other elements is not known, but it should be noted that V was below detection in the ore sample. The remaining elements give a very close zone of intersection between $E = 1.6$ (80% ore contribution) and $E = 2.2$ (87% ore contribution).

The intersection of the REE lines (Fig. 3) suggests an $E$ value of between 1.25 (67% ore contribution) and 1.8 (82% ore contribution).

Several components are particularly useful in estimating the fit position. These include iron (because it dominates the system), uranium (because it is the only element other than iron commonly more abundant in the ore than in the furnace lining), thorium and the sum of the REE (both immobile, and typically in very low concentrations in the ore). Solutions for these taken alone give possible solutions between $E = 1.65$ (for an ore contribution of 82%) and $E = 2.2$ (ore contribution 88%) (Fig. 4).

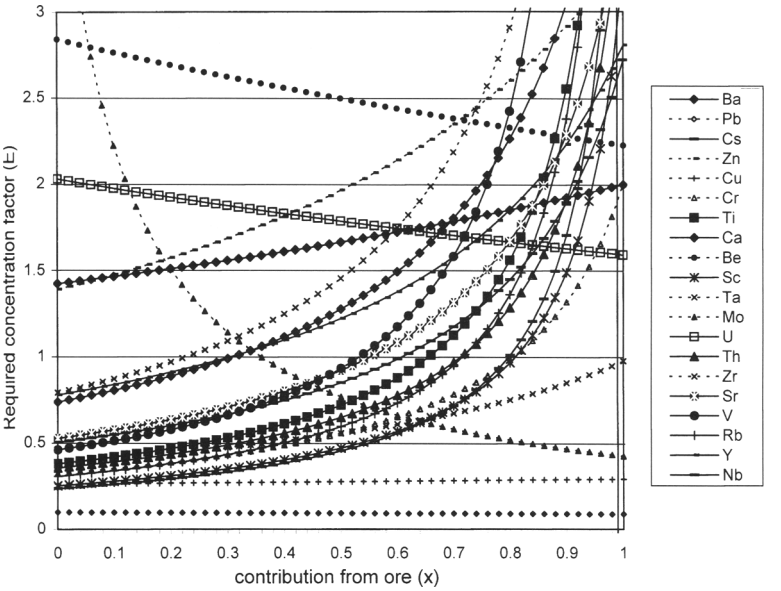


**Fig. 2.** $E$ against $x$ for minor and trace elements. Model and sample details as Fig. 1.

It is readily apparent that there is considerable 'noise' in the data; there are various problems inherent in this example. Most obvious is the poor control on fuel ash composition, but also important is the fact that the materials analysed were not those involved in a single smelt, and that the slag analysis is not that of the total slag from a single smelt, but is based only on the average tap slag composition. It is possible however, to take a value ($E = 1.8$ and ore contribution = 83%) which is a 'best fit' to the solutions discussed above.

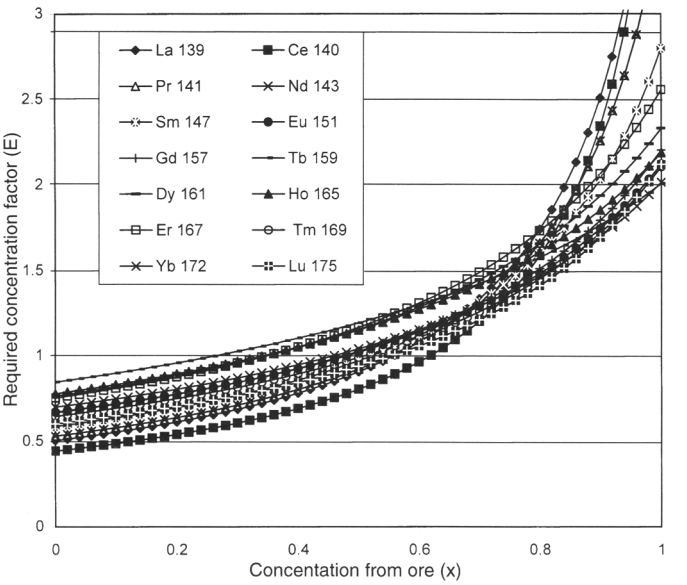


**Fig. 3.** $E$ against $x$ for rare earth elements. Model and sample details as Fig. 1.

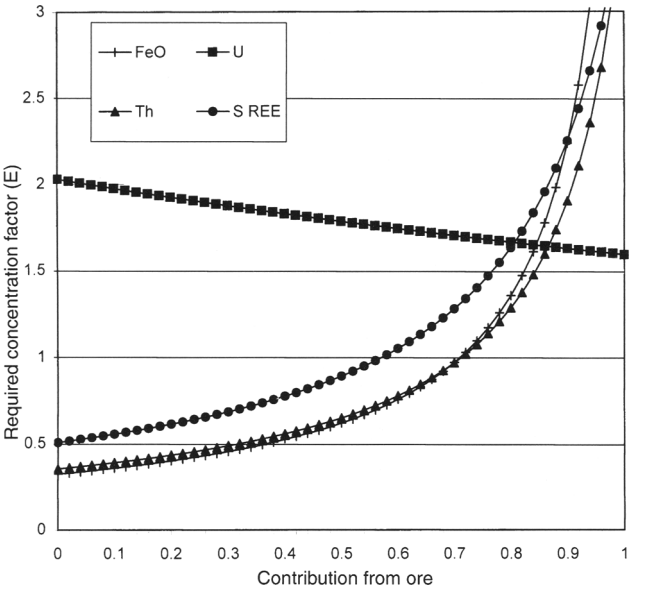


**Fig. 4.** *E* against *x* for 'key' components. Model and sample details as Fig. 1.

Because this is a 'best fit' there are resulting errors; the overall model slag composition would have the concentration of FeO = 64.1% (observed average tap slag has 67.1%) and ΣREE = 69.0 ppm (observed average tap slag has 72.6 ppm). Adjusting the model to remove these discrepancies (i.e. taking a solution solely at the intersection of the Fe and ΣREE lines) would necessarily introduce greater errors with other elements.

Putting this 'best fit' solution into the yield equations discussed above gives the following results: *1 kg of anhydrous ore* would react with *0.18 kg of reduced anhydrous lining* and *0.02 kg of fuel ash,* and will produce *0.42 kg of metallic iron* and *0.67 kg of slag*. The *efficiency'* (weight of iron in bloom/weight of iron in reduced anhydrous ore) = *56%*.

It is worth noting that 0.02 kg of fuel ash would correspond to approximately 0.4 kg of charcoal (based on a typical ash content of charcoal of 5%). Fuel usage is reported by Crew (1991; Experiment 27 has fuel to ore ratio of 3.5), Tylecote *et al.* (1971; average fuel:ore ratio for later experiments 2.3) and in our own unpublished experiments (fuel to ore ratio 3–3.5). This implies that only a small fraction (approximately 12% in this case) of fuel ash becomes incorporated into the slag phase.

## Conclusion

Mass balance calculations of the smelting components recovered from *Ariconium* produce a reasonably tightly grouped set of intersections. This indicates that the ore samples recovered by the excavators are compatible with the composition of the material smelted at this site in antiquity. The imprecision of the solution reflects the nature of the materials on which the mass balance has been based, which do not constitute components and products from a single smelt. There are additional problems associated with poor constraint on the composition of the charcoal ash.

The composition of slags formed from the smelting of the high purity (low ΣREE) ores found in this region are subject to an over-riding dominance by the assimilation of small quantities of furnace lining. In assessing the compatibility of slags and ore fragments recovered from ancient iron working sites in this area, it is thus also essential to study the chemistry of the furnace lining.

The authors would like to thank the Hereford and Worcester County Council Archaeology Service for providing the materials used in this study.

## References

CREW, P. 1991. The experimental production of prehistoric bar iron. *Journal of the Historical Metallurgy Society*, **25**, 21–36.

FULFORD, M. G. & ALLEN, J. R. L. 1993. Iron making at the Chesters villa, Woolaston, Gloucestershire: Survey and excavation 1987-1991. *Britannia*, **23**, 159–215.

RUDDOCK, F. A. 1961. Metalworking at Bagendon and finds of clay, metal, stone, flint and glass. *In:* CLIFFORD, E. M. *Bagendon: A Belgic Oppidum*. Heffer, Cambridge.

SALTER, C. J. 1987. The relevance of chemical provenance studies to Celtic ironwork in Britain. *Bulletin of the Institute of Archaeology University of London*, **19**, 73–81.

SIMMS, M. J. 1990. Triassic palaeokarst in Britain. *Cave Science*, **17**, 93–101.

SERNEELS, V. 1993. Archéometrie des scories de fer. Recherches sur la sidérurgie ancienne en Suisse occidentale. *Cahiers d'archéologie Romande, No. 61*, Lausanne.

THOMAS, G. R. & YOUNG, T. P. (forthcoming). The influence of furnace lining on the composition of iron making slags in Roman-British smelting of high purity iron ores (Bristol Channel Orefield, UK). *In:* YOUNG, S. M. M., BUDD, P. D., IXER, R. A. & POLLARD, A. M. (eds) *Metals in Antiquity*. Archaeopress, Oxford.

TYLECOTE, R. F. 1986. *The Prehistory of Metallurgy in the British Isles*. The Institute of Metals, London.

——, AUSTEN, J. N. & WRAITH, A. E. 1971. The mechanism of the bloomery process in shaft furnaces. *Journal of the Iron & Steel Institute*, **209**, 342–363.

YOUNG, S. M. M., BUDD, P., HAGGERTY, R. & POLLARD, A. M. 1997. Inductively coupled plasma-mass spectrometry for the analysis of ancient metals. *Archaeometry*, **39**, 379–392.

# Geoarchaeological research into the historical relics of the South Urals: problems, results, prospects

V. V. ZAYKOV[1], A. P. BUSHMAKIN[1], A. M. YUMINOV[1], E. V. ZAYKOVA[1], G. B. ZDANOVICH[2], A. D. TAIROV[2] & RICHARD J. HERRINGTON[3]

[1]*Institute of Mineralogy, Urals Branch of Russian Academy of Sciences, 456301 Ilmen Nature Reserve, Chelyabinsk District, Russia*

[2]*Chelyabinsk State University, 454136 Chelyabinsk, Bratçya Kashiriny street, 129, Russia*

[3]*Natural History Museum, Cromwell Road, London SW7 5BD, UK*

**Abstract:** A description is given here of the major geoarchaeological research undertaken in the Southern Urals region between 1991 and 1998. General petrographic characteristics of the stone material used for the manufacture of tools in the settlements of Arkaim and Alandskoe are discussed, together with their possible raw material sources. Research has indicated that Bronze Age settlements in the region used at least nine types of copper ore. One of these, the ancient mine 'Vorovskaya Yama', is described. Chemical analysis of metal objects from the settlements of Arkaim, Sintashta and Kuisak show that three types of copper (pure, arsenical and argentiferous) and three kinds of bronze (arsenical, stanniferous, and nickeliferous) are used for the artefacts. Buried objects show evidence of corrosion with formation of the minerals atacamite, paratacamite, nantokite, malachite, cuprite, and tenorite. The process of corrosion in the presence of organic material has been studied and malachite, azurite and sampleite have been shown to form. Microprobe analysis of gold objects from eight burial mounds shows that, in the Bronze Age, pure native gold was used to make jewellery. The use of binary artificial alloys of gold and silver is characteristic of the Early Iron Age; in the Early Middle Ages ternary artificial alloys of gold, silver and copper were used. The composition of lead wire found in the Kuisak settlement has also been determined.

Recently the scientific direction of the Institute of Mineralogy has been focused on the geological and mineralogical study of archaeological relics in the South Urals (Yushkin 1990). The research was prompted by the creation in 1991 of the Arkaim Cultural Reserve, which highlighted the need to study the territory and the historical relics located on it. The objects are evidence of the material development of the Palaeolithic, Neolithic, Bronze and Early Iron Age cultures (Fig. 1). The main areas of study are proto-towns or settlements of 18th–15th centuries BC, grouped by G. B. Zdanovich and I. M. Batanina into the so-called 'Country of towns' (Zdanovich 1996; Zdanovich & Batanina 1995).

*From:* POLLARD, A. M. (ed.) 1999. *Geoarchaeology: exploration, environments, resources.* Geological Society, London, Special Publications, **165**, 165–176. 1-86239-053-3/99/$15.00

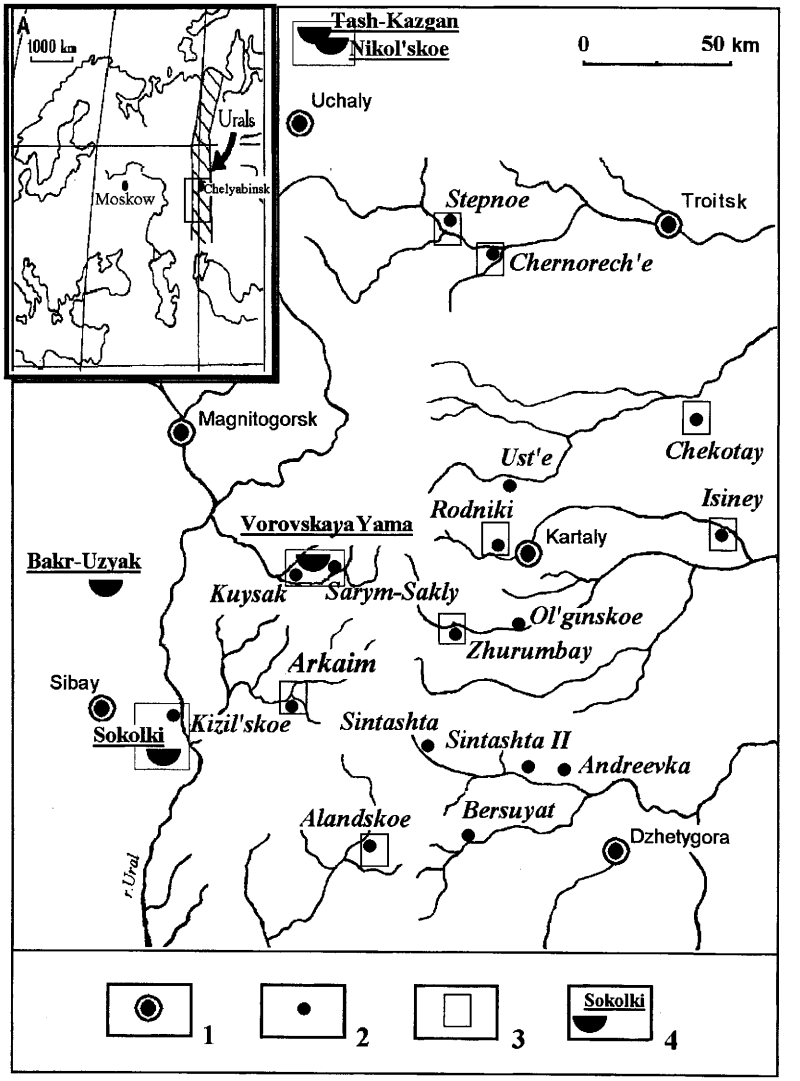


**Fig. 1.** Map of 'the Country of towns' showing settlements and ancient copper mines locations: 1, the modern settlements; 2, large settlements of the Bronze Age; 3, areas of geoarchaeological research; 4, ancient surveyed copper mines.

## Scope of research

The research covers the fields of petrography, mineralogy and economic mineralogy. Results have contributed to an understanding of patterns of ancient mineral utilization and economies. Additional effort has been put into creating a computer database system. The programme can be described under six headings:

1. Research into the raw material sources for the lithic industry of the ancient communities, devising petrographic maps of the ancient stone buildings and the determination of rock sources regionally from geological investigation of possible quarries in the region.

2. Mineralogical, geochemical and petrological investigation of ores, slags, and metals from excavated proto-towns and burial mounds in order to determine the raw material sources and types of metallurgical technology used.
3. The prospection for ancient mines, study of their geological setting and ore composition, and reconstruction of technologies used in mining.
4. The study of the composition of jewellery products and paints together with the determination of possible raw material sources and manufacturing technologies.
5. The conservation of corroded and altered artefacts, determination of environmental conditions since burial and the estimation of the long-term stability of artefacts in museum displays.
6. The creation of a geological–mineralogical data bank for the purposes of archaeology.

## Material sources of the stone industry

Definition of raw material sources for the ancient stone industry is based on the study of rocks from which ancient artefacts were made. This was carried out for artefacts found at Arkaim and Kuisak. Recently, similar work has been carried out in the Altai and Orenburg districts. Our work was based on a study of the compositions and properties of rocks. The main parameters defined were: mineral composition, texture, structure, density, porosity, durability, abrasion resistance and ductility. These properties were defined as those which would have determined whether Bronze Age settlers would use them. Durability is mainly influenced by the hardness and elasticity of the component minerals and how these combine together with the degree of jointing. Tools for striking were mainly made from fine-grained rocks, for which the combined properties are highly favourable. Cherts, red-coloured jaspers, diabases, gabbro, epidosites and dacites are the main rocks with suitable properties. The most important single factor in the choice of material for the manufacture of striking tools is the bulk density of rock. More dense lithologies such as diabase with a density of about $3.0\,g\,cm^{-3}$ are highly favoured.

### *Arkaim*

A petrographic study of 192 objects collected by S. Ya. Zdanovich was carried out. They comprised 18 types of objects made from 26 different types of rocks. This study resulted in three major conclusions. Firstly, all the artefacts are made of rocks sourced from the area of study. Secondly, there are strict rules about which rocks are used for which type of object. For example, arrow-heads and drilling tools were only made from siliceous rocks which take a sharp edge. Only clastic rocks with grains of quartz are used as abrasives. Tools used for metal foundry work are made from talcose rocks, which have a high heat resistance. Striking tools are produced from rocks with a high durability and strength, namely epidosites, silica-rich sediments, and jaspers. Thirdly, the utilization of the rocks is determined not only by their physical–mechanical properties, but also by the orientation and degree of jointing. For this reason, epidosites with a distinctive prismatic jointing was used for the manufacture of hammers, whereas basaltic and rhyolitic lavas, which have a wedge-shaped interlocking fracture system, were made into mattocks.

## *Kuisak*

From Kuisak, 84 artefacts, made from 25 types of rocks and minerals, have been investigated. The most numerous types are percussive tools of some description (hammers, anvils, picks, pestles, etc.). The next most numerous are abrasive tools (grinders, abraders and polishers), followed by cutting and piercing tools (scrapers, knifes, arrow-heads), then foundry tools, special tools (fishing sinkers and spinning weights) and ritual objects which simulated tools but which were made from soft material incapable of working. Cherts, diabase and red-coloured jasper are by far the most frequently used lithologies for the manufacture of instruments on the site of the ancient town. These rocks are the most common universal raw material for the manufacture of stone tools of varying types. Outcrops of siliceous rocks and diabases are located in the immediate vicinity of the ancient town. Fragments of jaspers are found in talus deposits to the east of the ancient town and in alluvial deposits of the rivers Kuisak and Zingeika. Talc-containing rocks served as raw material for the foundry tools. Use of other rocks such as sandstone, dacite, granite and serpentinite is uncommon at Kuisak. To date, only rarely have tools made of gabbro, basalt, aleurolites and quartzites been found, despite these lithologies being common in the region. Ritual objects (e.g., hatchets, maces) are made from easily polished rocks such as serpentinites and talc-schist. A number of exotic finds include fragments of fossil belemnites, characteristic organisms in Mesozoic limestones of the region. However, the nearest finds of belemnites in the Urals lie some 150 km to the southwest, near to the Akchyar settlement.

As distinct from Arkaim, the Kuisak inhabitants used a limited number of rocks for manufacturing tools and were more conservative in their choice of stone for these products. They used no more than three lithologies, whilst the Arkaim inhabitants used up to eight kinds of rock. This may have been due to the poorer choice of stone available in the Kuisak area. However, in comparison with Arkaim, at Kuisak the inhabitants used stone to build the walls of the settlement. The excavations revealed two defensive walls made from boulders of siliceous rocks, sandstones and basalts, which can be found in outcrop on the east bank of the Zingeika river.

## *Alandskoe*

Among the proto-towns of the South Urals, the settlement of Alandskoe is distinguished by the abundance of rocks used in building the settlement. Excavations carried out in 1997 have revealed two strong defensive walls with a height of the order of 5–6 m. The walls are covered by plates and blocks of various lithologies, which are dominated by granites and amphibolites. Sources of this stone were outcrops of granitoids of the Suunduk massif and metamorphic rocks in scarps of the Solonchanka river valley. In burial mounds flanking the settlement, stone is also common.

This petrological work is only preliminary in nature. Only a broad regional picture of the stone used in the settlements and possible sources of this material is defined. Further work is needed to answer questions about sources of raw materials. Such preliminary work is limited in scale to areas such as Isiney, Rodniki, Kuisak, Sarym-Sakly and Alandskoe.

## Bronze Age copper mines

The study of ancient mines on the Southern Urals began at the end of the 18th century, carried out by the classical Russian geologists I. I. Lepyekhin, P. S. Pallas and N. P. Rychkov. In 1884, I. P. Aspelin systematized the collected the data on ancient open pit mines. In the first half of the 20th century, M. V. Malachov, D. Kashintsev, L. P. Levitcky and A. A. Iessen researched the origins of ancient metallurgy in the Urals (Iessen 1948), the sources of ore, and the connections between adjacent mining and metallurgical operations. Before this, ancient open pits had been located at Bakr-Uzyak (A. Kh. Ivanov), Elenovka (A. S. Novichenko and I. L. Rudnitsky), and Ush-Kattyn (A. I. Rybalkin and S. K. Nechitailo). The basis of our modern understanding of ancient mining and metallurgy in the Urals was defined by B. G. Tikhonov¢s and O. N. Bader¢s. Long-term research on ancient metallurgy of the region, particularly the geochemistry of copper ores, was carried out by E. N. Chernykh (see Chernykh (1992) for an English translation which includes this work). Chernykh studied about 30 ancient copper deposits on the eastern side of the Urals. The most prolific work on the metal products of the Bronze Age is by G. B. Zdanovich, who introduced the term 'metalliferous layers' due to the abundance of bronze artefacts in horizons excavated at Petrovskaya. The most recent information about copper-mining production in the South Urals is found in work by S. A. Grigor¢ev, E. V. Zaykova, V. V. Zaykov, and A. F. Bushmakin concerning the mining and recycling technologies of copper ores in 'the country of towns'. One important result from this work is the discovery of the Bronze Age mine 'Vorovskaya Yama' near the Zingeisky settlement (see Fig. 2). The work also links the discovery of tourmaline-containing copper ores found at the excavations at Arkaim with the Elenovka ore deposit.

Raw material sources for ancient copper production in the South Urals are the numerous deposits of oxidized sulphide ores, many of them small, in which copper carbonates (malachite and azurite) are the dominant ore minerals. Ore assemblages can be classified into the following types:

1. Zones of oxidation of disseminated sulphide ores hosted in ultra basic and basic igneous rocks that are in crust of oceanic affinity. The mineralization is present as veinlets and films of malachite and azurite, forming stringers and networks. The thickness of such zones varies from a few to tens of metres.
2. Oxidation zones of cupriferous massive sulphide ores of volcano-sedimentary origin in Devonian-age strata. These deposits formed in island arc settings, at the margins of the Palaeozoic Urals Ocean. These ores are dominated by brown iron oxide ores in which are masses of copper carbonates, which formed during weathering. Ore bodies are sheet or lens shaped, with a maximum thickness of some tens of metres. At the base of the oxide zone, primary sulphide ores are usually found.
3. Oxidation zones of copper-bearing hematite-quartz ores which formed as low-temperature precipitates on the seafloor. One of these sites (Bugodak), where ancient mining is evident, occurs west of the Magnitogorsk zone near the Aslaevsky settlement.
4. Oxidation zones of irregular disseminated ores in granitoid and gabbroid massifs of Devonian age, which are cut by porphyry intrusives. The primary ores comprise copper sulphides. Ore bodies are isometric, linear or annular, from a few hundred metres to a few kilometres in diameter. Evidence of Bronze Age mining of these deposits is not yet demonstrated.

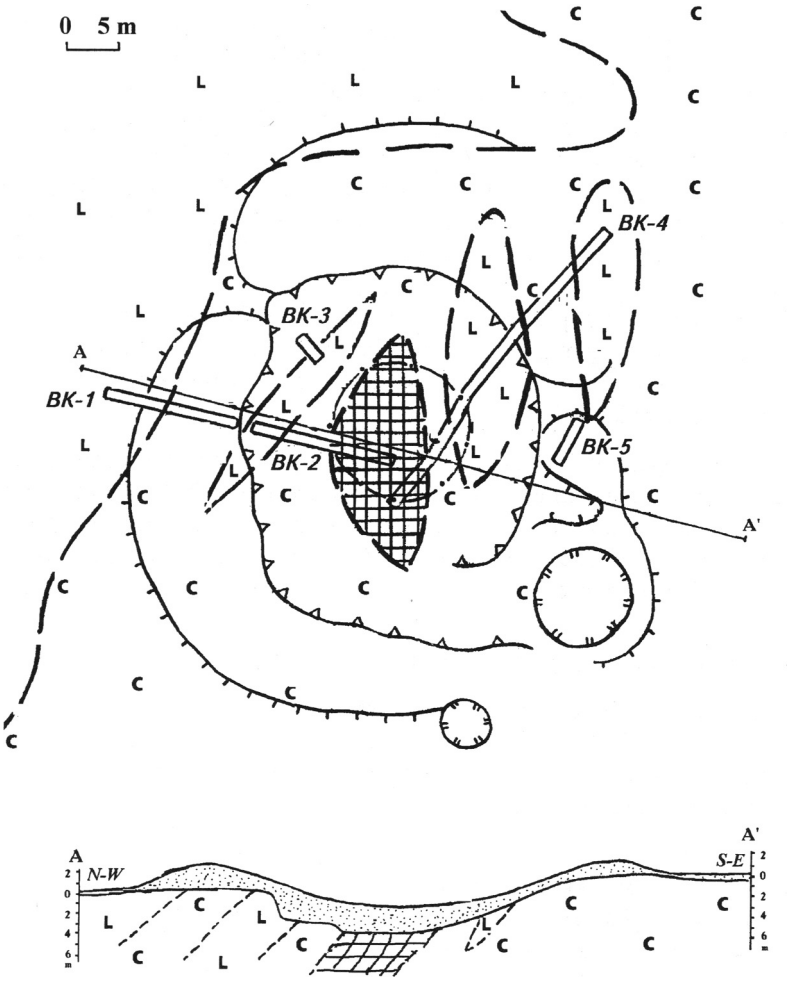


**Fig. 2.** Geological sketch of the 'Vorovskaya Yama' mine.

5. Oxidation zones in basaltic lavas with irregular disseminated copper mineralization associated with zeolites and native copper.
6. Oxidation zones of irregular disseminated sulphide ores in tourmaline-bearing rocks close to the contacts of granitoid massifs. Elenovka deposit (Orenburg district) is a typical example. It has a rarer mineralogical assemblage of molybdenite-chalcopyrite-tourmaline. Because of this rather unique mineralogy, it has been found that ores from or similar to the Elenovka deposit, were one of the sources of raw material for metallurgical manufacture in Arkaim. This was demonstrated by the identical mineral compositions and similar mineral textures and associations of some samples of copper ore found in archaeological excavations compared to Elenovka ores. In foundry slags recovered from Arkaim, the presence of high levels of boron (one of the main components of tourmaline of schorl-dravite series) is demonstrated (Bushmakin & Zaykov 1996).

7. Oxidation zones of sulphide-quartz and sulphide-carbonate-quartz veins and stockworks, usually associated with granitoid bodies of more alkaline affinity. Such deposits are rather small and low in tenor but are very numerous. Apart form copper, these veins contain gold, silver, tungsten, molybdenum and other metals. The presence of the mineral arsenopyrite in the veins is significant, since this may be the source of arsenic found in the arsenical bronze artefacts.
8. Oxidation zones of garnetiferous skarns at the contacts of granitoid bodes, and also of rodingites. The Vorovskaya yama mine, 40 kms to the north of Arkaim is one such deposit (Zaykov *et al.* 1995) where rodingites are host to rich copper carbonate deposits
9. Oxidation zones of cupriferous sandstones which formed in shallow sedimentary basins. The Kargala group of deposits in the west of Orenburg district was the source of large quantities of copper in the Bronze Age and are classical examples of this type (Chernykh 1970).

Linking geological with archaeological researches shows that in the South Urals it is quite possible to determine the ancient mines from which the ores are sourced. The mines are found as anomalies in the relief of the terrain, often as depressions or rounded knolls and unusual elongate mounds. These are often flanked by overgrown dumps on which there are fragments of rocks with secondary copper minerals.

## The composition of copper and bronze artefacts

Significant data on the composition of copper and bronze artefacts from historical relics of the South Urals has been obtained. On the basis of the study of the chemical composition of ancient artefacts made from copper and copper alloys, the following types of metals are distinguished:

Types of copper:
- pure (where As, Sn, Ag <0.1 wt%)
- arsenical (where As contents are in the range 0.1–1 wt%)
- argentiferous (content of Ag 0.1–1 wt%)

Types of bronze:
- arsenical (content of As 1–4 wt%)
- stanniferous (content of Sn 1–7 wt%)
- nickeliferous (content of Ni 1–5 wt%)

### *Arkaim*

Research shows the composition of the metal artefacts is mainly of pure copper with alloying metals less than 0.5 wt%. However, some specimens of awls and knives are made from arsenical bronze where As is between 1.1 and 2.8 wt%, arsenical copper where As is between 0.13 and 0.88 wt%, and one specimen of nickeliferous bronze with a Ni content of 1.10 wt%. Slag material found here contains inclusions of nickeliferous bronze, German silver and pure copper. S. A. Grigor¢ev, A. F. Bushmakin and E. V. Zaykova have shown (by composition of slags and fragments of ores) that at Arkaim, ores from serpentinites, brown iron ore (oxidation zone of massive sulphide deposits?), quartz veins, and chlorite-tourmaline rock were used. During the smelting of the ores, quartz and limonite were added to the charge.

## *Sintashta*

In the Institute of Archeology, Russian Academy of Sciences, the collection of 70 metal artefacts from Sintashta has been analysed to define the geochemical types of the metals. Around half (48%) of the specimens are bronze, mainly arsenical, whilst the remainder are arsenical copper (34%) and 'pure' copper. There are some rare finds made of stanniferous bronze that are mainly ornamental objects. This testifies to the fact that only arsenic-bearing ores were used, or that copper in some way was alloyed with arsenic-containing minerals. Only more detailed research can answer this question. In respect of the stanniferous bronze, the source of this metal must be some other mining and metallurgical centres, with the Altai region being the most probable.

## *Kuisak*

Two artefacts examined from this settlement are made respectively from pure copper and stanniferous bronze (content of Sn between 4.49 and 6.11 wt%). Investigation of slag from here showed them to be composed of pure copper.

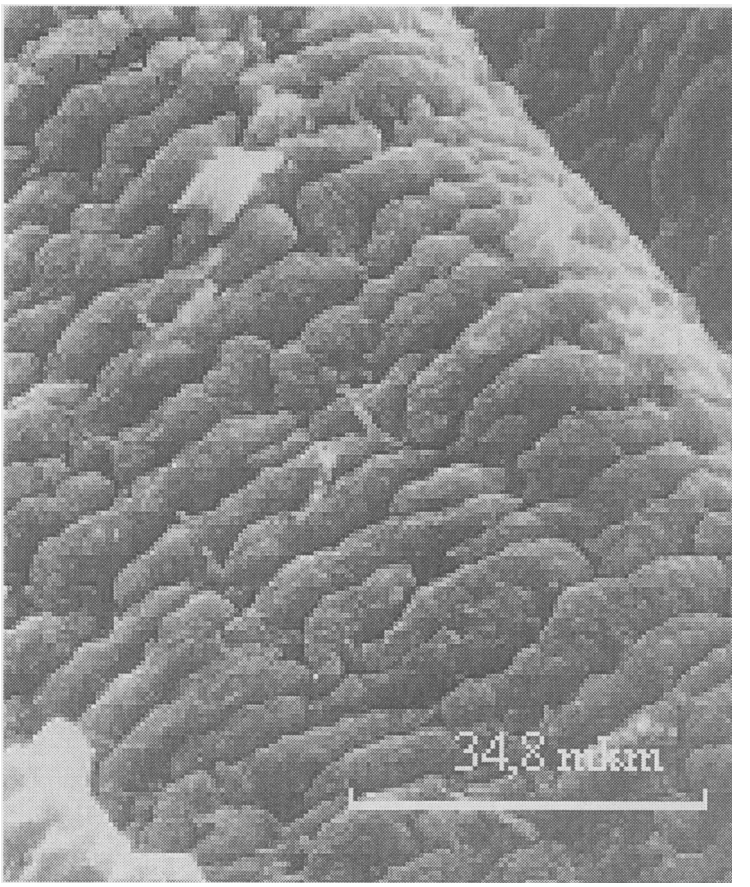


**Fig. 3.** Pseudomorph of sampleite after lambswool (photomicrograph obtained with electron microscope).

The preliminary conclusions are that the investigated sites yielded objects made from pure copper, arsenical copper and arsenical bronze. The few specimens found made from stanniferous bronze are rare and were apparently imported from elsewhere.

## Minerals formed by the corrosion of copper artefacts and their pseudomorphs

The ancient copper and bronze artefacts are susceptible to alteration when buried and the following minerals have been found as products of this alteration: atacamite, paratacamite, nantokite, cuprite, tenorite, brochantite, antlerite, malachite and azurite. Metal objects found in contact with buried corpses or with other phosphatic objects of organic origin give rise to the light-blue copper phosphate sampleite $NaCaCu_5(PO_4)_4 \cdot Cl \cdot 5H_2O$. This mineral was first suggested as a product of corroded artefacts by Bridge *et al.* (1978). Sampleite, and sometimes malachite, replaces both the metal and the organic material in contact with it. In some cases, this results in extremely good preservation of structural details of the objects (see Fig. 3). This replacement also includes the organic material involved. For example, a copper awl

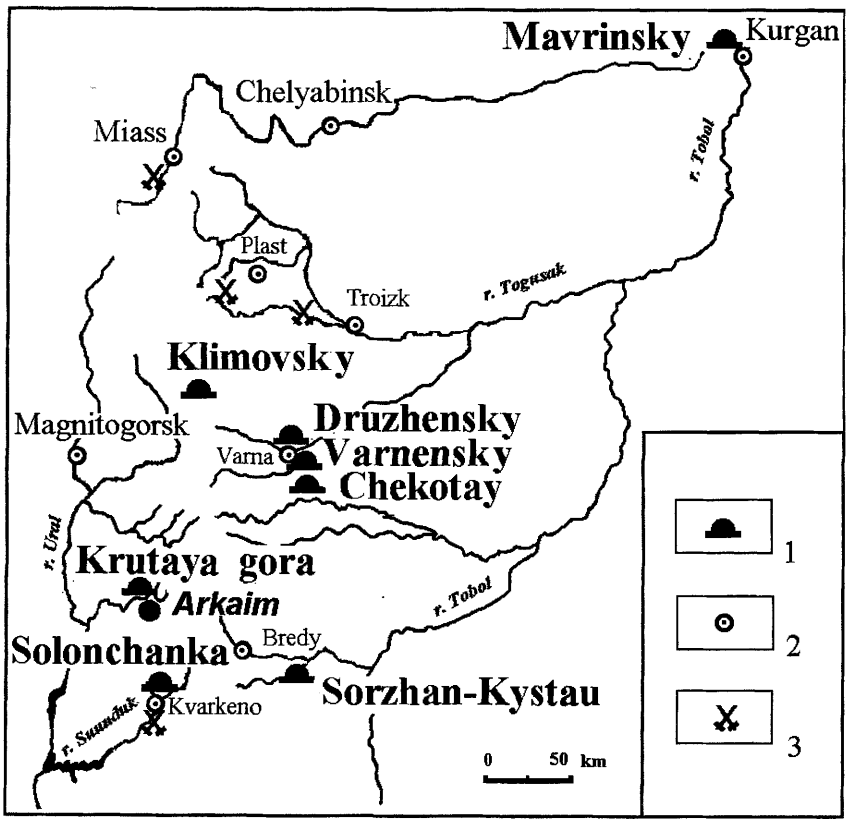


**Fig. 4.** The scheme of burial mounds setting: 1, burial mounds; 2, modern settlements; 3, places of possible ancient gold mining.

**Table 1.** *Composition of the gold artefacts from the South Urals burial mounds*

| No. | Artefacts | Burial mound | Age | Number of analyses | Average contents, wt% | | |
|---|---|---|---|---|---|---|---|
| | | | | | Au | Ag | Cu |
| 1 | foil from the copper ring | Chekotay | XV BC | 3 | 59.75 | 36.30 | 0.13 |
| | foil from the copper ring | | | 1 | 57.29 | 38.86 | 0.10 |
| 2 | object for plait | Varnensky | VII–VI BC | 5 | 88.16 | 13.77 | 0.95 |
| | object for plait | | | 4 | 86.18 | 13.63 | 0.90 |
| 3 | foil | B. Klimovsky | VI BC | 7 | 76.55 | 17.68 | 4.29 |
| | ear-ring | | | 3 | 9.56 | 15.00 | 2.53 |
| 4 | ear-ring | Sorzhan-Kystau | IV–III BC | 4 | 69.69 | 28.82 | 2.51 |
| | ear-ring | | | 3 | 83.36 | 15.09 | 2.50 |
| 5 | temple's pendants | Mavrinsky | III–II BC | 3 | 83.99 | 15.27 | 1.56 |
| 6 | pendent with carnelian | Druzhensky | III–V BC | 3 | 87.61 | 10.48 | 3.59 |
| | foil from quiver's lap | | | 6 | 37.08 | 56.05 | 4.66 |
| | foil from the facing of a saddle-tree | | | 5 | 41.51 | 49.52 | 6.28 |
| 7 | foil from bridle plate | Solonchanka-I | V–VI AD | 4 | 37.00 | 55.98 | 5.49 |
| | foil from plate | | | 3 | 38.04 | 55.11 | 5.02 |
| | foil from the facing of a horse statuette | | | 6 | 48.73 | 43.18 | 6.01 |
| 8 | foil from a plate | Krutaya Gora | ? | 6 | 65.18 | 31.24 | 1.38 |

Analysis parameters using electron microprobe JCXA-733 Jeol; 15 kV, 25 nA standards used : Au, Ag, artificial alloys; Cu, chalcopyrite.

found at the Bol'shekaragan burial site was adjacent to the chitinous covers of a fly pupa (0.5–2 mm in length), which became replaced by azurite. The mineral forms moulds that exactly reproduce most of the fine detail of the pupa form.

## Composition of lead

Lead was found during excavations in the Kuisak settlement, as a bent section of thick wire weighing 8.7 g with a greyish-brown to brown coloration. From the centre of the sample, a section analysed by microprobe shows that the specimen consists of practically pure lead. From this analysis and the morphology of the object, it is concluded that the material is part of a rod-like ingot, in its foundry form. The described part was separated from rod by untwisting a small section. The lead was probably obtained from pure galena, the normal source for the metal in ancient cultures.

## Composition of the gold artefacts

Composition of the gold objects from eight burial mounds ranging in age from the Bronze Age up to the Early Middle Ages has been determined (Fig. 4) using the collections of A. D. Tairov, S. G. Botalov, N. A. Polushkin and D. G. Zdanovich.

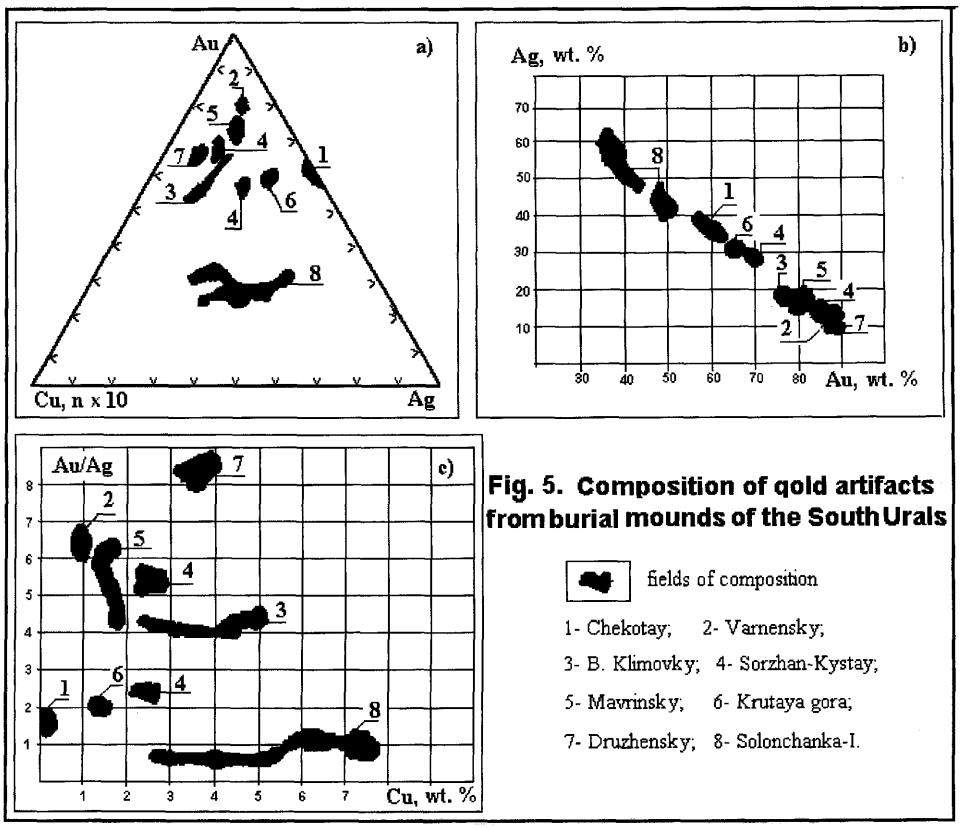


**Fig. 5.** Composition of gold artefacts from burial mounds of the South Urals.

The dates, brief description and composition of alloys are shown in Table 1. For the analyses, representative sections of metal with thickness of 0.5–2 mm have been made. After careful polishing, the analysis of each section was carried out at several points. Gold composition is shown graphically in Fig. 5. The analyses show distinctive variations in the compositions of the objects. Au and Ag, as well as Cu are quite variable, a testament to the changing technologies for manufacture of the artefacts. The highest gold contents are found in jewellery where fineness reaches 800–860‰. For the manufacture of gold foils, middle to low-grade alloys were used.

The authors wish to thank E. V. Belogub, I. G. Zhukov, V. A. Muftakhov, V. A. Popov, I. V. Sinyakovskaya, O. S. Telenkov, Eu. I. Churin, I. M. Batanina, D. G. Zdanovich, S. Ya. Zdanovich, A. I. Levit, I. E. Lubchansky, M. V. Kuznetsova, T. S. Malutina and F. N. Petrov for help in writing this article.

## References

BRIDGE, P. J., PRYCE, M. W., CLARKE, R. M. & COSTELLO, M. B. 1978. Sampleite from Jingemia Cave, Western Australia. *Mineralogical Magazine*, **42**, 369–371.

BUSHMAKIN, A. PH. & ZAYKOV, V. V. 1996. Copper-tourmaline Elenovka deposit is probable source of the ore for copper-smelting Arkaim production. *Ural's Mineralogical Collections. Miass,* **5**, 221–232. (in Russian).

CHERNYKH, E. N. 1970. *Ancient Metallurgy of the Urals and Povolzhia.* Nauka, Moscow. (in Russian).

—— 1992. *Ancient Metallurgy in the USSR: the Early Metal Age.* Cambridge University Press, Cambridge.

IESSEN, A. A. 1948. About ancient production of gold in the Urals. 200 years of gold industry of the Urals. *Sverdlovsk*, 5–34. (in Russian).

YUSHKIN, N. P. (ed). 1990. *Mineralogy of the Urals: Elements, Carbides, Sulphides.* Urals Branch RAS USSR, Sverdlovsk. (in Russian).

ZAYKOV, V. V., ZDANOVICH, G. B. & YUMINOV, A. M. 1995. "Vorovskaya yama" copper mine of bronze century (the Southern Urals). *Proceedings of the 3th International Scientific Conference 'Russia and East: the Problems of Interaction'.* Chelyabinsk university, Chelyabinsk, 2, 157–162. (in Russian).

ZDANOVICH, G. B. 1996. Arkaim is cultural complex of middle bronze epoch of the Southern Transurals. *Domestic Archeology*, **7**, 47–62. (in Russian).

—— & BATANINA, I. M. 1995. "Country of towns" is consolidation settlement of bronze epoch (XVIII–XVII B.C.) in the Southern Urals. *Arkaim: Researches, searches, discoveries. Chelyabinsk,* 54–62. (in Russian).

# Index

Note: page numbers in *italic* type refer to illustrations and tables

# Geoarchaeology: exploration, environments, resources

*edited by*

A. M. Pollard
(Department of Archaeological Sciences, University of Bradford, UK)

Geology and archaeology have a long history of fruitful collaboration stretching back to the early 19th century. Geoarchaeology - the application of the geosciences to solve research problems in archaeology - has now emerged as a recognized sub-discipline of archaeology, especially in the USA. Traditionally, methods used include geomorphology, sedimentology, pedology and stratigraphy, reflecting the fact that most archaeological evidence is recovered from the sedimentary environment. As reflected in the sub-title, this volume embraces a broader definition, including geophysics and geochemistry.

Geophysical techniques, both terrestrial and remote, are now used routinely to locate and horizontally map buried features of archaeological interest. New developments include the use of georadar and other methods of giving vertical information. Geochemistry has long been used to give information about the exploitation, trade and exchange of mineral resources and finished products such as metals and pottery. Refinements, such as the use of isotopic measurements to define not only exploitation but also production techniques, are increasingly being applied. Perhaps most significantly of all, geoarchaeology can contribute to an understanding of the dynamic relationship between human society and the environment in that most significant (if brief) period of geological time when human activity dramatically modified the natural world.

The papers presented here exemplify the many and varied ways in which geology and archaeology can combine to the mutual benefit of both.

- 180 pages
- 72 illustrations
- 13 papers
- index



ISBN 1-86239-053-3